$^{40}Ar/^{39}Ar$ DATING OF MOUNT EREBUS VOLCANO, ANTARCTICA

by
Richard P. Esser

Submitted in Partial Fulfillment of the Requirements
for the Degree of Master of Science in Geochemistry
January, 1996

Department of Earth and Environmental Science
New Mexico Institute of Mining and Technology
Socorro, New Mexico

This dissertation is accepted on behalf of the faculty of the Institute by the following committee:

Philip R. Kyle
Adviser

William C McIntosh

1/30/96
Date

I release this document to New Mexico Institute of Mining and Technology.

Richard Essen Jan 29, '96

Students Signature Date

ABSTRACT

The $^{40}Ar/^{39}Ar$ dating technique reveals the analytical and volcanological complexities of Mt. Erebus, a 3794 meter high active polygenetic stratovolcano. Anorthoclase phenocrysts recently ejected by strombolian eruptions (year: 1984) have yielded K/Ar and $^{40}Ar/^{39}Ar$ ages in excess of 200 ka indicating the presence of a trapped argon component with a $^{40}Ar/^{36}Ar$ ratio greater than atmosphere (e.g. excess argon).

In this study of historically erupted anorthoclase there is a positive correlation between apparent age and Cl/K ratio suggesting that the excess argon is associated with melt inclusions (~1700 ppm Cl) in the anorthoclase (<50 ppm Cl). The degassing behavior of the feldspar and inclusions for multiple anorthoclase aliquots containing 1% and 30% melt inclusions indicate the most accurate apparent ages are yielded by those samples containing the smallest quantities of inclusions. In addition, the highest accuracy is achieved by furnace-extraction steps below 1200°C. Rigorous sample preparation (crushing and HF treatment) is able to remove many of the contaminating inclusions, thereby yielding geologically reasonable ages. However, due to the uncertainty of complete excess argon removal, all $^{40}Ar/^{39}Ar$ apparent ages from Mt. Erebus are considered maxima.

$^{40}Ar/^{39}Ar$ results indicate that anorthoclase-phyric activity characteristic of Mt. Erebus is predominantly less than 250 ka, significantly younger than previously believed. All Mt. Erebus flows between about 40 and 250 ka, with the exception of one phonolite flow (76±5 ka), are anorthoclase tephriphonolite in composition. An anorthoclase tephriphonolite flow in the southwest sector of the volcano (235±4 ka) represents the oldest dated stage of anorthoclase-phyric activity on Mt. Erebus. The youngest dated lava flows on Mt. Erebus are anorthoclase phonolite in composition and were emplaced at the summit and flanks (11 ka to 33 ka).

Pre-anorthoclase-phyric lavas, (basanite to phonotephrite) crop out on Fang Ridge, an eroded remnant of a proto-Erebus volcano and other sporadic locations on the flanks of

the Mt. Erebus edifice. Plagioclase-phyric phonotephrite from coastal and flank flows range in age from 368±9 ka to 531±19 ka. Dating of the Fang Ridge escarpment reveals an approximate eruptive interval for the proto-Erebus volcano. Plagioclase from a stratigraphically high flow at Fang Ridge yields an age of 758±10 ka while a groundmass separate from a stratigraphically low flow yields an age of 1070±90 ka. The oldest dated rock on Mt. Erebus is a basanite dike (1311±8 ka) exposed at Cape Barne that is next to and locally overlain by younger anorthoclase phonolite flows (89±1 ka).

ACKNOWLEDGMENTS

This thesis would not have been possible without the support of numerous people at New Mexico Tech. The illustrious members of my committee (Phil Kyle, Bill McIntosh and Matt Heizler) were not only advisers, professors and bosses these past three years, but were also trusted friends. I can thank each of them for where I am sitting today and look very much forward to working with them in the years to come.

Other friends at New Mexico Tech deserve no less thanks. Nelia Dunbar and Thom Wilch each shared considerable expertise, advice and time. Kurt Panter, Mike O'Keeffe, Ellen Wilch and countless others (you know who you are) must also be acknowledged for their friendship and assistance. And one can't forget those working "behind the lines" in the Department of Geoscience and Bureau of Mines.

Antarctic support was provided by friends and colleagues: Phil Kyle, Bill McIntosh, Nelia Dunbar, Thom Wilch, Ed Klimasauskas, Ken Simms, Alexei Ozerov and Ray Dibble. One can't forget the thankless helicopter pilots of Navy squadron VXE-6 and the support staff of McMurdo Station.

This work was partially funded by grants to Philip Kyle from the Office of Polar Programs, National Science Foundation.

TABLE OF CONTENTS

Section A

Excess Argon in Melt Inclusions in Young (<250 ka) Anorthoclase Feldspar from Mt. Erebus, Antarctica, as revealed by the $^{40}Ar/^{39}Ar$ Method

Section B

$^{40}Ar/^{39}Ar$ Dating of Mount Erebus, Antarctica:
Insights into the Evolution of a Polygenetic Volcano

APPENDICES

LIST OF TABLES

LIST OF FIGURES

INTRODUCTION

Mount Erebus is a 3794 meter high polygenetic stratovolcano located on Ross Island, Antarctica and is the largest and only active volcano on Ross Island, Mount Erebus contains a persistent summit lava lake of anorthoclase-phyric phonolite that experiences small strombolian eruptions (Kyle 1982). Distinctive anorthoclase phenocrysts found within the bombs and lavas are large (≤10 cm), abundant and contain many melt inclusions trapped during crystal growth (Dunbar et al. 1994). Anorthoclase phonolite and tephriphonolite lava flows fill the major summit caldera and are the dominant rock-type exposed on the flanks. Stratigraphically older and less differentiated lavas (basanite to *ne*-benmoreite) are principally exposed at Fang Ridge, an eroded remnant of an earlier volcanic edifice.

Over 20 years of scientific research on Mt. Erebus has concentrated on the eruptive activity and degassing behavior of the persistent summit lava lake (Caldwell, 1989, Zreda-Gostynska et al. 1993, Kyle 1994). Other studies have looked at the geologic and petrologic evolution of the volcano (Moore and Kyle 1987, Kyle et al. 1992). Isotopic dating of Mt. Erebus using the conventional K/Ar method was attempted, but proved too inaccurate and imprecise due to probable contamination by excess argon (Treves 1968, Armstrong 1978, Moore and Kyle 1987).

There are two main objectives in this study. The principle objective is to determine a comprehensive volcanic history for Mt. Erebus using the $^{40}Ar/^{39}Ar$ dating method. Dating samples gathered over several field seasons in conjunction with geological and geochemical data from various authors (Moore 1986, Moore and Kyle 1987, Caldwell 1989, Kyle et al. 1992) serve as a platform for the evolutionary interpretation. However, prior to the assignment of geologically meaningful $^{40}Ar/^{39}Ar$ ages, excess argon within Mt. Erebus anorthoclase samples must be identified and removed. Although identification of the excess argon component through the $^{40}Ar/^{39}Ar$ technique is an alternate incentive, it ultimately turned out to be the most important and influential element of this study.

This thesis is separated into two coherent sections which are submitted in manuscript form. The first paper examines historically erupted samples for the purpose of isolating and removing the excess argon component. The second paper employs the techniques of the first to derive accurate and precise $^{40}Ar/^{39}Ar$ ages for the rest of Mt. Erebus. These new $^{40}Ar/^{39}Ar$ ages infer a relatively detailed geological and geochemical volcanic history for Mt. Erebus. Appendices located in the back of this thesis contain all analytical and graphical data and sample locations.

REFERENCES

Armstrong, R. L. (1978). K-Ar dating: Late Cenozoic McMurdo Volcanic Group and dry valley glacial history, Victoria Land, Antarctica. N.Z. Journal of Geology and Geophysics 21: 685-698.

Caldwell, D. A. (1989). "Physical and geochemical properties of summit flows and recent volcanic ejecta from Mount Erebus, Ross Island, Antarctica." Unpublished Master's thesis, New Mexico Inst. of Mining and Tech.

Dunbar, N. W., Cashman, K. V., and Dupre, R. (1994). Crystallization Processes of Anorthoclase Phenocrysts in the Mount Erebus Magmatic System: Evidence from Crystal Composition, Crystal Size Distributions, and Volatile Contents of Melt Inclusions. *In* "Volcanological and Environmental Studies of Mount Erebus, Antarctica." (P. R. Kyle, Ed.), pp. 129-146. American Geophysical Union.

Kyle, P. R., Dibble, R. R., Giggenbach, W. F., and Keys, H. J. (1982). Volcanic Activity Associated with the Anorthoclase Phonolite Lava Lake, Mount Erebus, Antarctica. *In* "Antarctic Geoscience." (C. Craddock, Ed.), pp. 1172. The University of Wisconsin Press, Madison, Wisconsin, U.S.A.

Kyle, P. R., Moore, J. A., and Thirlwall, M. F. (1992). Petrologic Evolution of Anorthoclase Phonolite Lavas at Mount Erebus, Ross Island, Antarctica. Journal of Petrology 33: 849-875.

Moore, J. A. (1986). "Mineralogy, Geochemistry and Petrogenesis of the Lavas of Mount Erebus, Antarctica." Unpublished Master's thesis, New Mexico Institute of Mining and Technology.

Moore, J. A., and Kyle, P. R. (1987). Volcanic Geology of Mount Erebus, Ross Island, Antarctica. *In* "NIPR Symposium on Antarctic Geosciences.", pp. 48-65. National Institute of Polar Research, Tokyo.

Treves, S. B. (1968). Volcanic Rocks of the Ross Island area. Antarctica Journal of the US 3: 108-109.

Zreda-Gostynska, G., Kyle, P. R., and Finnegan, D. L. (1993). Chlorine, Fluorine, and Sulfur Emissions from Mt. Erebus, Antarctica and Estimated Contributions to the Antarctic Atmosphere. Geophysical Research Letters 20: 1959-1962.

Excess Argon in Melt Inclusions in Young (<250 ka) Anorthoclase Feldspar from Mt. Erebus, Antarctica, as revealed by the $^{40}Ar/^{39}Ar$ Method.

R.P. Esser
Department of Earth and Environmental Science,
New Mexico Institute of Mining and Technology,
Socorro, NM 87801

ABSTRACT

Historically erupted anorthoclase phenocrysts (ca. 1984) from Mt. Erebus yield K/Ar and $^{40}Ar/^{39}Ar$ apparent ages as old as 700 ka indicating the presence of excess argon. $^{40}Ar/^{39}Ar$ furnace step heating results from anorthoclase reveal a positive relationship between Cl/K ratio and apparent age. Because chlorine is present in melt inclusions (up to 1700 ppm) and absent in the anorthoclase, the positive correlation suggests that the excess argon is associated with glass melt inclusions trapped within the anorthoclase during rapid crystal growth.

Confirmation of the source of excess argon comes from two sample aliquots separated from single phenocrysts. One aliquot, prepared through crushing and HF treatment, contained less than 1% (by volume) melt inclusions. The second aliquot, crushed but not treated with HF, contained up to 30% melt inclusions. In both cases, those aliquots containing higher quantities of inclusions yielded higher Cl/K ratios and apparent ages.

Differences in the degassing behavior of the anorthoclase and their trapped melt inclusions allow the two to be distinguished and geologically reasonable ages to be obtained. Melt inclusions exposed on the outside of anorthoclase grains principally degas during furnace extraction at temperatures less than 1200°C. Inclusions on the inside of anorthoclase grains degas at temperatures greater than 1200°C. The latter degassing behavior is a result of the entrapment of melt inclusion gas by the anorthoclase lattice. Once the anorthoclase lattice begins to decrepitate (~1200°C) a pathway is created allowing

the melt inclusion argon to escape. Anorthoclase aliquots prepared with less than 1% inclusions can be fitted with a plateau for heating steps below 1200°C to yield ages as young as 8±2 ka, whereas steps above 1200°C yield ages in excess of 100 ka. Conversely, anorthoclase aliquots containing up to 30% melt inclusions yield ages in excess of 200 ka for heating steps below 1200°C.

Introduction

Recent studies have shown that young sanidine and anorthoclase can be accurately dated using the $^{40}Ar/^{39}Ar$ method (McDougall, 1981; McDougall, 1985; Deino and Potts, 1990; Turbeville, 1992; Hu et al., 1994; van den Bogaard, 1995). Improvements in argon gas extraction and mass spectrometry over the past decade have allowed smaller samples to be analyzed while also increasing the precision and accuracy of analytical data. Studies of young (<100 ka) volcanism have concentrated on anorthoclase-bearing silica-undersaturated intermediate lavas (e.g. tephriphonolites, phonolites and trachytes) due to the rarity of very young rhyolitic volcanism and the lack of sanidine or anorthoclase mineral phases in more mafic lavas. In many cases, stratigraphic control (Deino and Potts, 1990; Turbeville, 1992) and independent geochronometers (van den Bogaard, 1995) have been used to support $^{40}Ar/^{39}Ar$ results.

Traditionally, young sanidine and anorthoclase have been dated using the $^{40}Ar/^{39}Ar$ laser-fusion method (Deino and Potts, 1990; Turbeville, 1992; Hu et al., 1994; van den Bogaard, 1995). The biggest advantage of laser fusion is the ability to date small samples and individual crystals thereby allowing identification and elimination of older contaminant grains (i.e. xenocrysts). Disadvantages to laser analyses include: 1) poor temperature control, 2) crystal-to-crystal temperature inhomogeneity caused by differential laser coupling, and 3) limitations on larger sample sizes. These disadvantages become significant when attempting to characterize argon distribution within a sample. Furnace step heating, in contrast to laser fusion, is ideal for identifying anomalous argon components (e.g. excess argon) in $^{40}Ar/^{39}Ar$ analyses. Excess argon, a potentially large

problem when dating extremely young volcanic samples, is more likely to be identified by furnace step heating rather than by laser fusion.

Samples of independently determined age are useful for evaluating the fundamental assumptions of the $^{40}Ar/^{39}Ar$ method. Volcanic samples erupted less than 1,000 years ago are ideal in this regard, because the negligible amount of radiogenic ^{40}Ar ($^{40}Ar^*$) permits the $^{40}Ar/^{36}Ar$ ratio of the trapped component to be determined with confidence. Young samples which possess $^{40}Ar/^{36}Ar$ values greater than 295.5 (equivalent to present-day atmosphere) indicate contamination by excess ^{40}Ar ($^{40}Ar_E$). Small quantities of excess argon in young samples can significantly increase the apparent $^{40}Ar/^{39}Ar$ age.

Dating of recently erupted anorthoclase phenocrysts from the active Mount Erebus volcano by conventional K/Ar analyses have yielded ages as old as 400 ka (Armstrong, 1978), suggesting contamination by $^{40}Ar_E$ (Dalrymple and Lanphere, 1969). $^{40}Ar/^{39}Ar$ results from historically erupted anorthoclase, while analytically more precise, also indicate contamination by excess argon. The large (up to 10 cm in length) anorthoclase phenocrysts contain up to 30% (by volume) glass melt inclusions. The melt inclusions result from melt entrapment due to rapid growth of the anorthoclase within the Erebus magma chamber (Dunbar et al., 1994). The two morphological melt-inclusion end members are large (>200 μm), irregularly shaped inclusions and small (<20 μm), euhedrally shaped inclusions (Dunbar et al., 1994). Contraction bubbles, lining the anorthoclase/inclusion interface, are most common within the large inclusions, while the small inclusions typically contain only one or two contraction bubbles. Volatile contents (H_2O, Cl and F) of the melt inclusions are low and suggest entrapment depth of less than 400 meters (Dunbar et al., 1994).

Melt inclusions are common in most extrusive magmatic environments (Roedder, 1984) and may act as a host for $^{40}Ar_E$ in a mineral phase. Excess argon within melt inclusions will significantly affect the dating of young (<100 ka) volcanic samples, especially using $^{40}Ar/^{39}Ar$ laser fusion or conventional K/Ar dating.

Samples and Analytical Methods

This paper focuses on five sample aliquots prepared from a bomb erupted at the summit of Mt. Erebus in 1984. Four aliquots of anorthoclase were separated from two individual feldspar phenocrysts. One phonolitic glass sample was prepared from the bomb matrix. Sample preparation for the anorthoclase involved crushing to about 250 μm followed by removal of much of the glass using a Frantz magnetic separator. To assess the contribution of excess argon within melt inclusions, one aliquot per phenocryst was left intentionally contaminated with 10-30% melt inclusions while the second aliquot was concentrated by ultrasonic treatment in 15% hydrofluoric acid (HF) for up to 20 minutes yielding nearly pure (>99%) anorthoclase. This acid treatment removed any melt inclusions exposed on the outside of the grains. The inclusion-rich anorthoclase was treated in 15% HF for a maximum of 5 minutes. This shortened HF treatment preserved some exposed melt inclusions on the outside of the anorthoclase grains. The separates were finally hand-picked under a binocular microscope to remove any unwanted glass/minerals and to make a visual estimate of the percent glass contamination. Final grain size of most anorthoclase separates were 125-250 μm. Matrix glass from the bomb was crushed to ~500 μm, and hand-picked to remove any phenocrysts.

The anorthoclase samples were precisely weighed (40-200 mg), encapsulated in tin or copper foil and sealed in evacuated quartz vials along with interspersed Fish Canyon Tuff sanidine (FC-1) monitors. The vials were irradiated in known geometries for 1.0 hour in the L67 position at the University of Michigan's Ford Research reactor under fast neutron fluxes of approximately 7.0×10^{-5} J/hr.

All $^{40}Ar/^{39}Ar$ analyses were performed in the New Mexico Geochronology Research Laboratory at the New Mexico Institute of Mining and Technology. J-values for the separate irradiations were determined by total fusion of Fish Canyon Tuff sanidine

monitors (27.84 Ma) using a CO_2 laser. The standard deviation for the averaged results of four aliquots per monitor location was typically less than ±0.25% (1σ).

Argon was extracted from the anorthoclase by incremental heating in a molybdenum crucible using a double vacuum resistance furnace capable of 1750°C. Each heating step was typically 10 minutes long during which reactive (non-noble) gases were removed using a SAES AP-10 getter. A second stage cleaning of 5 to 8 minutes used a SAES GP-50 getter. System blanks were between 7×10^{-16} and 3×10^{-15} moles ^{40}Ar. The argon isotopes were measured using a Mass Analyzer Products (MAP) 215-50 mass spectrometer utilizing an electron multiplier with an effective gain of approximately 100 (sensitivity ≈ 2×10^{-17} moles/pA). All $^{40}Ar/^{39}Ar$ ages were determined using the decay constants recommended by Steiger and Jäger (1977). Uncertainties of the ages in this study are reported at one sigma (1σ) and include the error in the J-values, background, isotope measurements and correction factors. Apparent ages calculated from plateaus are weighted by the inverse of their variance.

Heating schedules for the anorthoclase separates were kept nearly uniform from sample to sample. Initial low temperature steps were used to degas any encapsulating tin foil and drive off atmospheric argon. Heating steps ≤ 600°C rarely contained greater than 1% $^{40}Ar^*$ and 5% cumulative ^{39}Ar. Six to nine subsequent temperature pairs increased in increments of about 100° beginning at 700°C and ending at 1650°C. The temperature pairs follow the contiguous isothermal heating approach used by Harrison et al. (1993).

Results

The results of furnace step heating on zero-age anorthoclase phenocryst and glass samples are given in Table 1 and Figures 1a-d and 2. Integrated (total gas) ages for the four anorthoclase samples range from 48±8 ka to 640±30 ka (±1 standard deviation). The integrated age for the matrix glass is 101±16 ka. For those aliquots containing ~1% melt inclusions "plateaus" fitted to the lower temperature (<1200°C) steps yielded apparent ages

Table 1. $^{40}Ar/^{39}Ar$ analytical data for the four samples of historically erupted anorthoclase and one sample of historically erupted bomb matrix glass from Mt. Erebus. Recalculated ages used the method of Harrison et al (1993). Errors on recalculated ages are largely controlled by uncertainty in J-value, isotopic peak heights, system blank and interference reactions and thus are the same as those in the original $^{40}Ar/^{39}Ar$ age calculation.

Lab#	Temp (°C)	$^{40}Ar/^{39}Ar$	$^{37}Ar/^{39}Ar$	$^{36}Ar/^{39}Ar$	$^{39}Ar_K$ (moles)	K/Ca	Cl/K	$^{40}Ar^*$ (%)	Cum. ^{39}Ar (%)	Age (ka)	Err (1σ)	Recalc. Age (ka)	Err (1σ)
Anorthoclase Phenocryst #1, 197.3 mg anorthoclase (~1% glass)					**J=0.0000698±0.0000002**			**Disc. = 288.0**					
1316-01A	600	3.04e+02	5.53e-01	1.02e+00	5.8e-16	0.9	2.3e-03	0.7	1.78	273 ±	151	107 ±	151
1316-01B	600	8.10e+00	5.22e-01	2.49e-02	3.2e-16	1.0	1.1e-03	9.5	2.77	97 ±	22	17 ±	22
1316-01C	700	3.42e+00	5.17e-01	1.06e-02	9.4e-16	1.0	5.1e-04	8.7	5.63	38 ±	8	1 ±	8
1316-01D	700	2.15e+00	5.10e-01	6.58e-03	9.1e-16	1.0	3.7e-04	10.4	8.41	28 ±	7	2 ±	7
1316-01E	800	1.23e+00	5.04e-01	3.53e-03	2.2e-15	1.0	4.1e-04	16.2	14.97	25 ±	3	-5 ±	3
1316-01F	800	1.45e+00	5.01e-01	4.20e-03	2.1e-15	1.0	4.7e-04	15.5	21.27	28 ±	3	-5 ±	3
1316-01G	900	7.49e-01	5.00e-01	2.07e-03	3.3e-15	1.0	2.5e-04	20.4	31.23	19 ±	2	1 ±	2
1316-01H	900	7.81e-01	4.98e-01	2.43e-03	3.1e-15	1.0	1.2e-04	10.2	40.60	10 ±	2	1 ±	2
1316-01I	1000	8.13e-01	5.04e-01	2.47e-03	3.2e-15	1.0	2.2e-04	12.1	50.29	12 ±	2	-3 ±	2
1316-01J	1000	8.86e-01	5.03e-01	2.63e-03	2.9e-15	1.0	1.5e-04	14.3	59.04	16 ±	3	5 ±	3
1316-01K	1100	1.14e+00	4.94e-01	3.02e-03	2.5e-15	1.0	5.5e-04	23.0	66.62	33 ±	3	-7 ±	3
1316-01L	1100	1.77e+00	4.92e-01	5.02e-03	1.5e-15	1.0	4.5e-04	17.2	71.14	38 ±	5	6 ±	5
1316-01M	1200	2.38e+00	4.85e-01	5.15e-03	1.4e-15	1.1	1.9e-03	36.9	75.54	111 ±	5	-29 ±	5
1316-01N	1200	4.86e+00	4.92e-01	1.44e-02	9.3e-16	1.0	1.3e-03	12.7	78.38	77 ±	8	-19 ±	8
1316-01O	1300	3.16e+00	4.74e-01	7.01e-03	1.9e-15	1.1	2.5e-03	34.9	84.16	139 ±	3	-42 ±	3
1316-01P	1300	6.56e+00	4.86e-01	2.06e-02	1.3e-15	1.1	1.5e-03	7.3	88.16	61 ±	7	-48 ±	7
1316-01Q	1400	5.19e+00	5.52e-01	1.39e-02	9.5e-16	0.9	2.2e-03	21.2	91.05	139 ±	11	-19 ±	11
1316-01R	1550	5.60e+01	5.36e-01	1.88e-01	2.9e-15	1.0	1.4e-03	0.9	100.00	66 ±	24	-36 ±	24
total gas age					3.3e-14				n=18	48 ±	8	-5 ±	8
plateau age							C-L		68.37	20 ±	3	-1 ±	1
Anorthoclase Phenocryst #1, 229.8 mg anorthoclase (~10% glass)					**J=0.0000701±0.0000002**			**Disc. = 288.0**					
1317-01A	600	2.26e+02	4.20e-01	7.53e-01	1.3e-15	1.2	1.1e-01	1.3	2.78	374 ±	96	-1399 ±	96
1317-01B	600	1.79e+01	4.02e-01	5.47e-02	7.4e-16	1.3	2.1e-02	10.0	4.40	227 ±	18	-110 ±	18
1317-01C	700	1.20e+01	3.78e-01	3.31e-02	2.1e-15	1.4	1.8e-02	18.2	8.93	275 ±	7	-17 ±	7
1317-01D	700	8.10e+00	3.65e-01	1.99e-02	2.0e-15	1.4	1.8e-02	27.4	13.30	281 ±	8	-11 ±	8
1317-01E	800	6.46e+00	3.72e-01	1.53e-02	4.1e-15	1.4	1.7e-02	30.1	22.27	246 ±	4	-23 ±	4
1317-01F	800	5.28e+00	3.68e-01	1.15e-02	3.6e-15	1.4	1.8e-02	36.0	30.16	240 ±	4	-40 ±	4

Table 1. continued...

Lab#	Temp (°C)	$^{40}Ar/^{39}Ar$	$^{37}Ar/^{39}Ar$	$^{36}Ar/^{39}Ar$	$^{39}Ar_K$ (moles)	K/Ca	Cl/K	$^{40}Ar^*$ (%)	Cum. ^{39}Ar (%)	Age (ka)	Err (1σ)	Recalc. Age (ka)	Err (1σ)
1317-01G	900	5.83e+00	3.75e-01	1.27e-02	5.3e-15	1.4	1.7e-02	35.7	41.74	263	± 3	-2	± 3
1317-01H	900	4.10e+00	3.79e-01	7.89e-03	4.3e-15	1.3	1.6e-02	43.3	51.20	225	± 3	-23	± 3
1317-01I	1000	5.77e+00	3.90e-01	1.40e-02	4.5e-15	1.3	1.4e-02	28.7	60.99	209	± 3	-8	± 3
1317-01J	1000	5.01e+00	4.23e-01	1.49e-02	3.0e-15	1.2	8.4e-03	12.2	67.63	78	± 5	-57	± 5
1317-01K	1100	7.93e+00	4.17e-01	2.43e-02	2.6e-15	1.2	1.0e-02	9.6	73.34	96	± 6	-64	± 6
1317-01L	1100	8.68e+00	4.68e-01	2.97e-02	1.1e-15	1.1	1.8e-03	-1.0	75.70	-11	± 11	-40	± 11
1317-01M	1200	1.20e+01	4.76e-01	3.95e-02	2.1e-15	1.1	4.0e-03	2.7	80.20	41	± 8	-23	± 8
1317-01N	1200	1.26e+01	5.17e-01	4.22e-02	1.4e-15	1.0	7.4e-04	1.0	83.21	15	± 13	4	± 13
1317-01O	1300	1.09e+01	6.52e-01	3.48e-02	3.0e-15	0.8	2.4e-03	5.7	89.80	78	± 6	40	± 6
1317-01P	1300	7.23e+00	5.97e-01	2.33e-02	1.1e-15	0.9	1.6e-03	5.2	92.16	48	± 13	22	± 13
1317-01Q	1400	5.38e+00	6.64e-01	1.68e-02	1.4e-15	0.8	1.7e-03	8.4	95.21	57	± 8	30	± 8
1317-01R	1550	1.33e+02	7.03e-01	4.46e-01	2.2e-15	0.7	3.3e-03	0.8	99.96	128	± 75	75	± 75
1317-01S	1550	1.95e+03	4.86e-01	6.62e+00	1.8e-17	1.0	6.5e-03	-0.4	100.00	-894	± 12960	-997	± 12960
total gas age					4.6e-14				n=19	179	± 16	-19	± 16
plateau age										N.A.			
Anorthoclase Phenocryst #2, 206.6 mg anorthoclase (~1% glass)					**J=0.0000700±0.0000002**			**Disc. = 288.0**					
1330-01A	550	4.51e+03	1.03e+00	1.52e+01	2.2e-17	0.5	3.0e-02	0.8	0.06	4371	± 16125	3372	± 16125
1330-01B	600	3.47e+03	6.17e-01	1.17e+01	6.0e-17	0.8	1.2e-02	0.1	0.21	507	± 6650	119	± 6650
1330-01C	600	6.05e+02	4.24e-01	2.04e+00	9.8e-17	1.2	-8.7e-04	0.1	0.45	86	± 745	115	± 745
1330-01D	700	8.11e+01	4.39e-01	2.70e-01	5.1e-16	1.2	9.6e-04	1.6	1.72	166	± 54	134	± 54
1330-01E	700	9.25e+00	4.27e-01	3.03e-02	9.5e-16	1.2	2.6e-04	3.5	4.10	41	± 12	32	± 12
1330-01F	800	1.43e+00	4.19e-01	3.99e-03	1.9e-15	1.2	3.4e-04	18.1	8.74	33	± 5	21	± 5
1330-01G	800	1.86e+00	4.28e-01	5.76e-03	2.5e-15	1.2	1.6e-04	9.0	14.88	21	± 3	16	± 3
1330-01H	900	7.54e-01	4.30e-01	2.17e-03	3.6e-15	1.2	2.2e-04	16.6	23.87	16	± 2	8	± 2
1330-01I	900	7.94e-01	4.23e-01	2.48e-03	4.3e-15	1.2	9.5e-05	9.0	34.75	9	± 2	6	± 2
1330-01J	1000	1.02e+00	4.27e-01	3.21e-03	4.5e-15	1.2	1.2e-04	8.1	45.99	10	± 2	6	± 2
1330-01K	1000	1.22e+00	4.23e-01	4.04e-03	4.8e-15	1.2	1.5e-04	3.0	57.95	5	± 2	0	± 2
1330-01L	1100	1.20e+00	4.17e-01	3.37e-03	3.6e-15	1.2	4.8e-04	18.1	67.02	28	± 2	11	± 2
1330-01M	1100	2.20e+00	4.13e-01	7.06e-03	2.2e-15	1.2	1.7e-04	5.6	72.63	15	± 4	10	± 4

Table 1. continued...

Lab#	Temp (°C)	$^{40}Ar/^{39}Ar$	$^{37}Ar/^{39}Ar$	$^{36}Ar/^{39}Ar$	$^{39}Ar_K$ (moles)	K/Ca	Cl/K	$^{40}Ar^*$ (%)	Cum. ^{39}Ar (%)	Age (ka)	Err (1σ)	Recalc. Age (ka)	Err (1σ)
1330-01N	1200	3.54e+00	4.07e-01	8.23e-03	1.9e-15	1.3	1.5e-03	31.6	77.35	142	± 4	90	± 4
1330-01O	1200	5.72e+00	4.04e-01	1.71e-02	1.1e-15	1.3	9.5e-04	12.0	80.05	86	± 9	54	± 9
1330-01P	1300	2.53e+00	4.05e-01	4.59e-03	2.9e-15	1.3	1.8e-03	46.6	87.38	149	± 2	89	± 2
1330-01Q	1300	4.48e+00	4.17e-01	1.30e-02	2.0e-15	1.2	1.0e-03	14.5	92.43	82	± 5	47	± 5
1330-01R	1400	7.78e+00	4.28e-01	2.44e-02	5.1e-16	1.2	1.3e-03	7.4	93.72	72	± 13	28	± 13
1330-01S	1400	3.40e+01	4.29e-01	1.13e-01	3.0e-16	1.2	1.4e-03	2.0	94.46	88	± 44	41	± 44
1330-01T	1500	6.03e+00	4.32e-01	1.81e-02	1.4e-15	1.2	8.5e-04	11.5	97.95	88	± 8	59	± 8
1330-01U	1650	3.86e+01	4.51e-01	1.27e-01	7.6e-16	1.1	1.0e-03	2.7	99.84	129	± 25	95	± 25
1330-01V	1650	5.78e+02	5.02e-01	1.94e+00	6.3e-17	1.0	3.9e-03	0.9	100.00	671	± 834	116	± 834
total gas age					4.0e-14				n=22	50	± 30	20	± 30
plateau age							I-K		34.08	8	± 2	7	± 1
Summit Phenocryst #2, 202.4 mg anorthoclase (~30% glass)					**J=0.0000690±0.0000002**			**Disc. = 288.0**					
1331-01A	550	4.21e+03	6.44e-01	1.41e+01	4.5e-17	0.8	3.5e-01	1.1	0.12	5867	± 11980	-19111	± 11980
1331-01B	600	1.45e+03	3.93e-01	4.79e+00	7.7e-17	1.3	6.9e-02	2.6	0.31	4716	± 2044	-151	± 2044
1331-01C	600	3.33e+02	3.44e-01	1.08e+00	9.2e-17	1.5	2.7e-02	4.3	0.55	1801	± 479	-121	± 479
1331-01D	700	4.29e+01	3.68e-01	1.15e-01	4.9e-16	1.4	1.7e-02	20.9	1.82	1120	± 39	-53	± 39
1331-01E	700	2.06e+01	3.66e-01	4.29e-02	1.0e-15	1.4	1.3e-02	38.4	4.49	984	± 17	65	± 17
1331-01F	800	1.64e+01	3.62e-01	2.82e-02	2.2e-15	1.4	1.2e-02	49.3	10.22	1010	± 9	162	± 9
1331-01G	800	1.34e+01	3.71e-01	1.96e-02	2.3e-15	1.4	1.1e-02	56.9	16.20	950	± 7	157	± 7
1331-01H	900	1.22e+01	3.84e-01	1.86e-02	3.6e-15	1.3	9.3e-03	54.9	25.38	834	± 5	174	± 5
1331-01I	900	1.05e+01	3.85e-01	1.33e-02	3.7e-15	1.3	8.9e-03	62.9	34.91	824	± 5	193	± 5

Table 1. continued...

Lab#	Temp (°C)	$^{40}Ar/^{39}Ar$	$^{37}Ar/^{39}Ar$	$^{36}Ar/^{39}Ar$	$^{39}Ar_K$ (moles)	K/Ca	Cl/K	$^{40}Ar^*$ (%)	Cum. ^{39}Ar (%)	Age (ka)	Err (1σ)	Recalc. Age (ka)	Err (1σ)
1331-01J	1000	1.46e+01	3.59e-01	1.46e-02	4.8e-15	1.4	1.3e-02	70.4	47.33	1278 ±	5	365 ±	5
1331-01K	1000	8.91e+00	3.92e-01	1.31e-02	3.5e-15	1.3	6.3e-03	56.6	56.48	628 ±	5	182 ±	5
1331-01L	1100	1.12e+01	3.89e-01	1.82e-02	3.2e-15	1.3	7.5e-03	52.3	64.84	732 ±	6	200 ±	6
1331-01M	1100	5.94e+00	4.40e-01	2.01e-02	1.3e-15	1.2	2.2e-04	0.1	68.20	1 ±	9	-15 ±	9
1331-01N	1200	7.97e+00	4.69e-01	2.41e-02	1.8e-15	1.1	1.6e-03	10.9	72.94	109 ±	7	-3 ±	7
1331-01O	1200	9.57e+00	5.18e-01	3.31e-02	1.0e-15	1.0	2.4e-04	-2.0	75.61	-24 ±	12	-41 ±	12
1331-01P	1300	6.15e+00	7.33e-01	1.67e-02	3.7e-15	0.7	3.4e-03	20.1	85.22	154 ±	5	-89 ±	5
1331-01Q	1300	6.07e+00	6.18e-01	1.84e-02	1.9e-15	0.8	1.7e-03	11.1	90.04	84 ±	6	-35 ±	6
1331-01R	1400	5.40e+00	6.23e-01	1.59e-02	1.5e-15	0.8	1.8e-03	13.3	93.89	90 ±	7	-40 ±	7
1331-01T	1500	1.08e+01	5.20e-01	3.52e-02	8.1e-16	1.0	1.3e-03	4.2	95.97	56 ±	11	-39 ±	11
1331-01U	1650	2.48e+01	5.93e-01	8.19e-02	1.2e-15	0.9	2.4e-03	2.3	99.04	71 ±	16	-97 ±	16
1331-01V	1650	1.12e+02	5.11e-01	3.71e-01	3.7e-16	1.0	1.7e-03	1.8	100.00	248 ±	93	126 ±	93
total gas age					3.9e-14				n=21	640 ±	30	117 ±	30
plateau age										N.A.			
151.0 mg Bomb matrix glass (100% glass)				**J=0.0000694±0.0000002**		**Disc. = 288.0**							
1332-01A	550	1.37e+03	4.88e-01	4.76e+00	3.6e-17	1.0	6.6e-02	-2.3	0.08	-4029 ±	3499	N.A.	
1332-01B	600	4.75e+02	1.91e-01	1.65e+00	1.8e-16	2.7	5.5e-02	-2.4	0.49	-1446 ±	367	N.A.	
1332-01C	600	1.44e+02	1.67e-01	4.91e-01	1.1e-16	3.1	5.4e-02	-0.5	0.73	-86 ±	194	N.A.	
1332-01D	700	1.32e+01	1.49e-01	4.34e-02	8.9e-16	3.4	5.0e-02	2.6	2.78	43 ±	14	N.A.	
1332-01E	700	2.21e+00	1.53e-01	6.80e-03	1.6e-15	3.3	4.8e-02	8.5	6.40	23 ±	6	N.A.	
1332-01F	800	1.80e+01	1.52e-01	6.01e-02	3.4e-15	3.3	4.8e-02	1.5	14.25	33 ±	10	N.A.	
1332-01G	800	3.01e-01	1.57e-01	3.09e-05	4.1e-15	3.3	4.9e-02	93.7	23.58	35 ±	2	N.A.	
1332-01H	900	8.10e+01	1.53e-01	2.67e-01	7.7e-15	3.3	4.8e-02	2.4	41.26	246 ±	27	N.A.	
1332-01I	900	1.61e+00	1.53e-01	3.69e-03	6.9e-15	3.3	4.9e-02	31.7	57.18	64 ±	1	N.A.	
1332-01J	1000	1.64e+00	1.53e-01	3.29e-03	6.0e-15	3.3	4.8e-02	40.0	70.85	82 ±	1	N.A.	
1332-01K	1000	1.77e+00	1.52e-01	3.12e-03	3.6e-15	3.4	4.8e-02	47.2	79.16	104 ±	2	N.A.	
1332-01L	1100	2.05e+00	1.52e-01	3.48e-03	5.1e-15	3.4	4.8e-02	49.3	90.89	126 ±	2	N.A.	
1332-01M	1100	2.97e+00	1.44e-01	6.61e-03	1.8e-15	3.5	4.9e-02	33.8	95.11	126 ±	5	N.A.	
1332-01N	1200	4.46e+00	1.70e-01	1.09e-02	1.6e-15	3.0	4.8e-02	27.4	98.71	153 ±	6	N.A.	
1332-01O	1200	1.34e+01	4.25e-01	4.09e-02	2.4e-16	1.2	4.9e-02	10.0	99.26	168 ±	42	N.A.	
1332-01P	1300	1.78e+01	2.45e+00	5.61e-02	1.8e-16	0.2	6.0e-02	7.7	99.67	172 ±	36	N.A.	

Table 1. continued...

Lab#	Temp (°C)	$^{40}Ar/^{39}Ar$	$^{37}Ar/^{39}Ar$	$^{36}Ar/^{39}Ar$	$^{39}Ar_K$ (moles)	K/Ca	Cl/K	$^{40}Ar^*$ (%)	Cum. ^{39}Ar (%)	Age (ka)	Err (1σ)	Recalc. Age (ka)	Err (1σ)
1332-01Q	1300	1.62e+02	6.41e+00	5.44e-01	3.2e-17	0.1	8.1e-02	1.3	99.74	263 ±	449	N.A.	
1332-01R	1400	1.67e+02	1.03e+01	5.76e-01	2.0e-17	0.0	9.3e-02	-1.6	99.79	-337 ±	609	N.A.	
1332-01S	1400	1.88e+03	2.88e+01	6.12e+00	3.8e-18	0.0	2.6e-01	3.9	99.80	9419 ±	22142	N.A.	
1332-01T	1650	4.64e+02	2.96e+00	1.55e+00	8.9e-17	0.2	4.0e-02	1.1	100.00	650 ±	491	N.A.	
total gas age					4.4e-14			n=20		101 ±	16	N.A.	
plateau age										N.A			

Errors are given at 1σ and include the uncertainty in J-values (±0.25%).
Plateau ages are weighted by the inverse of the variance whereas total gas ages are weighted by ^{39}Ar.
All isotopic ratios are corrected for sytstem blank, nuclear interference reactions and radioactive decay ($^{37}Ar_{Ca}$).
$(^{40}Ar/^{39}Ar)_K = 0.022$; $K/Ca = .510 \times (^{39}Ar_K/^{37}Ar_{Ca})$; $Cl/K = .277 \times (^{39}Ar_K/^{38}Ar_{Cl})$
Ages are calculated using the decay constants recommended by Steiger and Jagar (1977).

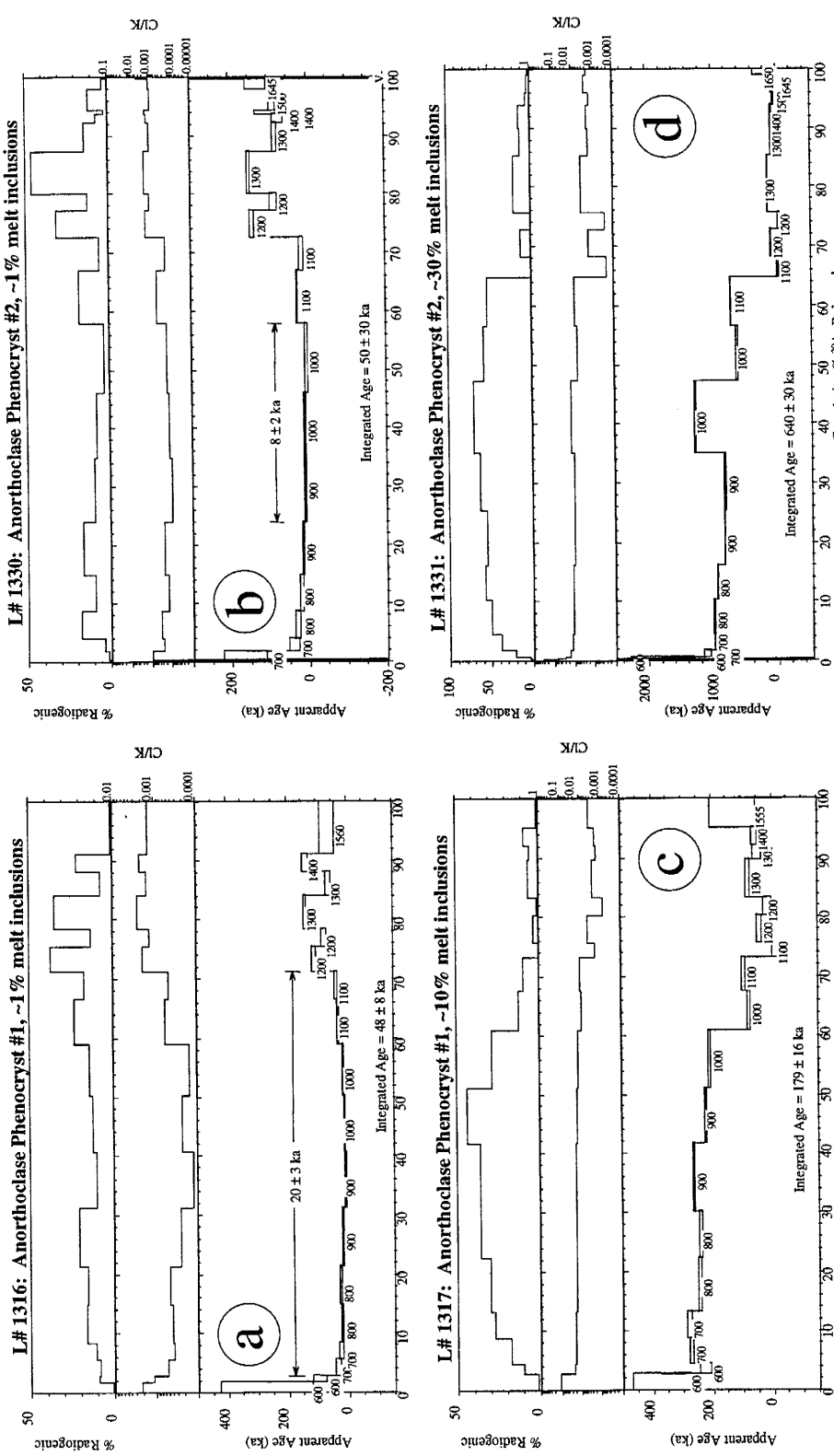

Figure 1a-d. $^{40}Ar/^{39}Ar$ age spectra results of four historically erupted Mt. Erebus anorthoclase samples containing various quantities of melt inclusions. All four anorthoclase aliquots show a clear positive correlation between Cl/K ratio, radiogenic yield and apparent age. The second step of the isothermal heating pairs consistently yields lower Cl/K ratios, radiogenic yields and younger apparent ages, but fails to achieve zero ages. The relative degassing behavior of the large and small melt inclusions is also apparent by the relative increase or decrease in Cl/K, radiogenic yield and apparent age at 1200°C. Errors on the apparent ages are presented at 1σ.

of 20±3 ka and 8±2 ka. The anorthoclase containing ~10% and ~30% melt inclusions have discordant age spectra with no apparent plateau (#1317 & #1331)(Fig. 1c and 1d). Individual steps below 1200°C have maximum ages of 263±3 ka (#1317, ~10% melt inclusions) and 1278±5 ka (#1331, ~30% melt inclusions). Unlike those aliquots with only about 1% melt inclusions, the higher temperature steps for the aliquots with ~10% and ~30% melt inclusions decrease in age with maxima of 78±6 ka and 154±5 ka, respectively. The bomb matrix glass (#1332) is essentially exhausted of argon by 1200°C and does not show any significant increase or decrease in apparent age except for an anomalously old age at the first 900°C step (figure 2). Of the 80 total steps performed on the four anorthoclase aliquots, only twelve individual steps achieve ages analytically equivalent to zero at 2 sigma (2σ). Inverse isochron analyses of the five zero-age samples are extremely discordant with MSWD values greater than 100.

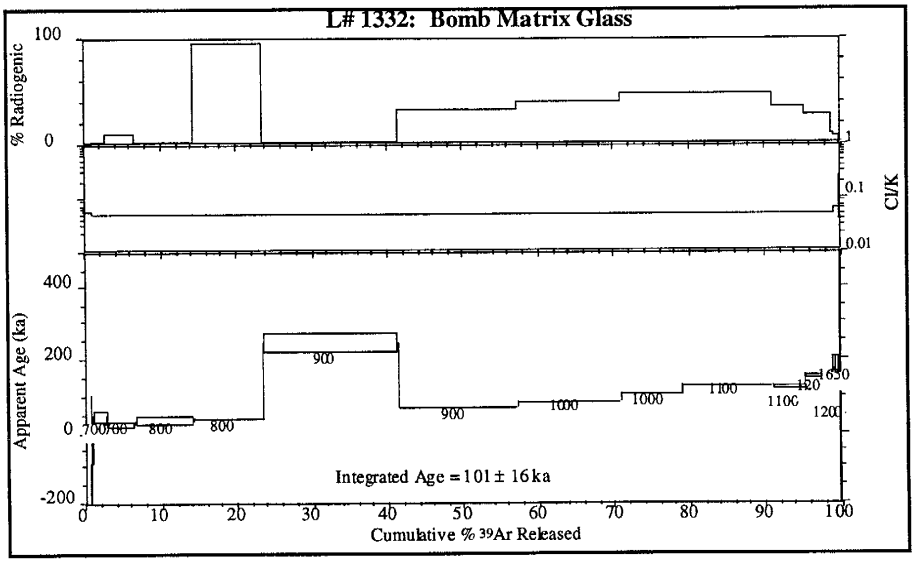

Fig. 2. $^{40}Ar/^{39}Ar$ age spectrum of matrix glass from a bomb erupted from Mt. Erebus in 1984. The degassing behavior of the glass is similar to that of the melt inclusions attached to the outside of anorthoclase grains.

Apparent yields of $^{40}Ar^*$ (measured ^{40}Ar not attributed to atmospheric argon or nuclear interference reactions) for the five analyses vary among the different samples. The lowest apparent $^{40}Ar^*$ yields are shown by the low-temperature release portions of

anorthoclase containing 1% inclusions. The highest apparent $^{40}Ar^*$ yields (approaching 70%) are achieved for the intermediate temperature steps of anorthoclase with the highest abundance of melt inclusions (#1331). Concentrations of apparent $^{40}Ar^*$ in the anorthoclase range from 1×10^{-18} to 1×10^{-15} moles per milligram and correlate positively with the melt inclusion concentrations in the anorthoclase. Trapped $^{40}Ar/^{36}Ar$ values calculated from individual heating steps for the four zero-age anorthoclase samples range from 324 to 459.

There is also a significant positive correlation between apparent radiogenic yield, age and Cl/K ratio for the anorthoclase samples. The Cl/K ratio, determined from $^{38}Ar_{Cl}/^{39}Ar_K$, is smallest for the low temperature steps of the two anorthoclase aliquots containing 1% melt inclusions. At temperatures above about 1100°C, the Cl/K ratio increases. For the two aliquots containing 10% and 30% melt inclusions, the observed pattern of temperature dependent Cl/K ratio is opposite, with the highest Cl/K ratios being achieved at the lower temperature steps (<1200°C). The highest Cl/K ratios are shown by the matrix glass and is constant across the entire spectrum (figure 2). K/Ca ratios do not vary with temperature and are not correlative with radiogenic yield and age.

The isothermal heating steps show differential release with respect to $^{40}Ar/^{39}Ar$ and Cl/K ratios. The first of the two isothermal heating steps consistently had a higher apparent $^{40}Ar^*$ yield, age and Cl/K ratio. However, the second of the two isothermal heating steps rarely achieved an age analytically equivalent to zero.

Temperature dependent release of $^{40}Ar_E$ and $^{38}Ar_{Cl}$ is confirmed by a plot of $^{40}Ar^*/^{39}Ar_K$ versus $^{38}Ar_{Cl}/^{39}Ar_K$, where argon extraction steps above and below 1200°C are plotted separately (figure 3). For the two anorthoclase aliquots containing only 1% melt inclusions (#1316 & #1330; figures 3a and 3b), the incremental heating steps above 1200°C contain the majority of $^{38}Ar_{Cl}$ and $^{40}Ar_E$. Although the steps below 1200°C contain over 70% of the total cumulative ^{39}Ar released they account for less than 50% of the total cumulative $^{40}Ar_E$ and therefore contribute less to the integrated age of the sample than do the

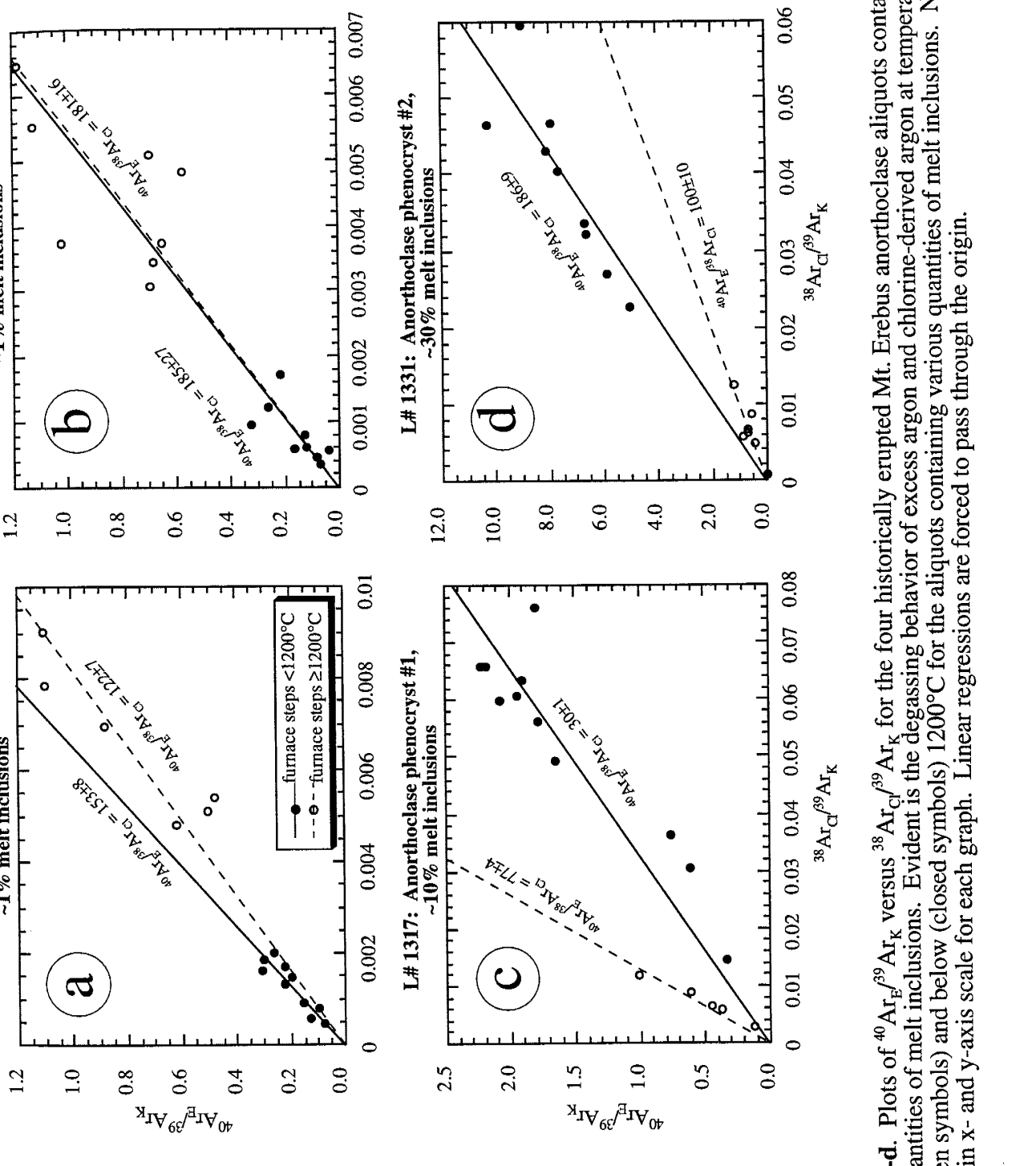

Figure 3a-d. Plots of $^{40}Ar_E/^{39}Ar_K$ versus $^{38}Ar_{Cl}/^{39}Ar_K$ for the four historically erupted Mt. Erebus anorthoclase aliquots containing various quantities of melt inclusions. Evident is the degassing behavior of excess argon and chlorine-derived argon at temperatures above (open symbols) and below (closed symbols) 1200°C for the aliquots containing various quantities of melt inclusions. Note the variations in x- and y-axis scale for each graph. Linear regressions are forced to pass through the origin.

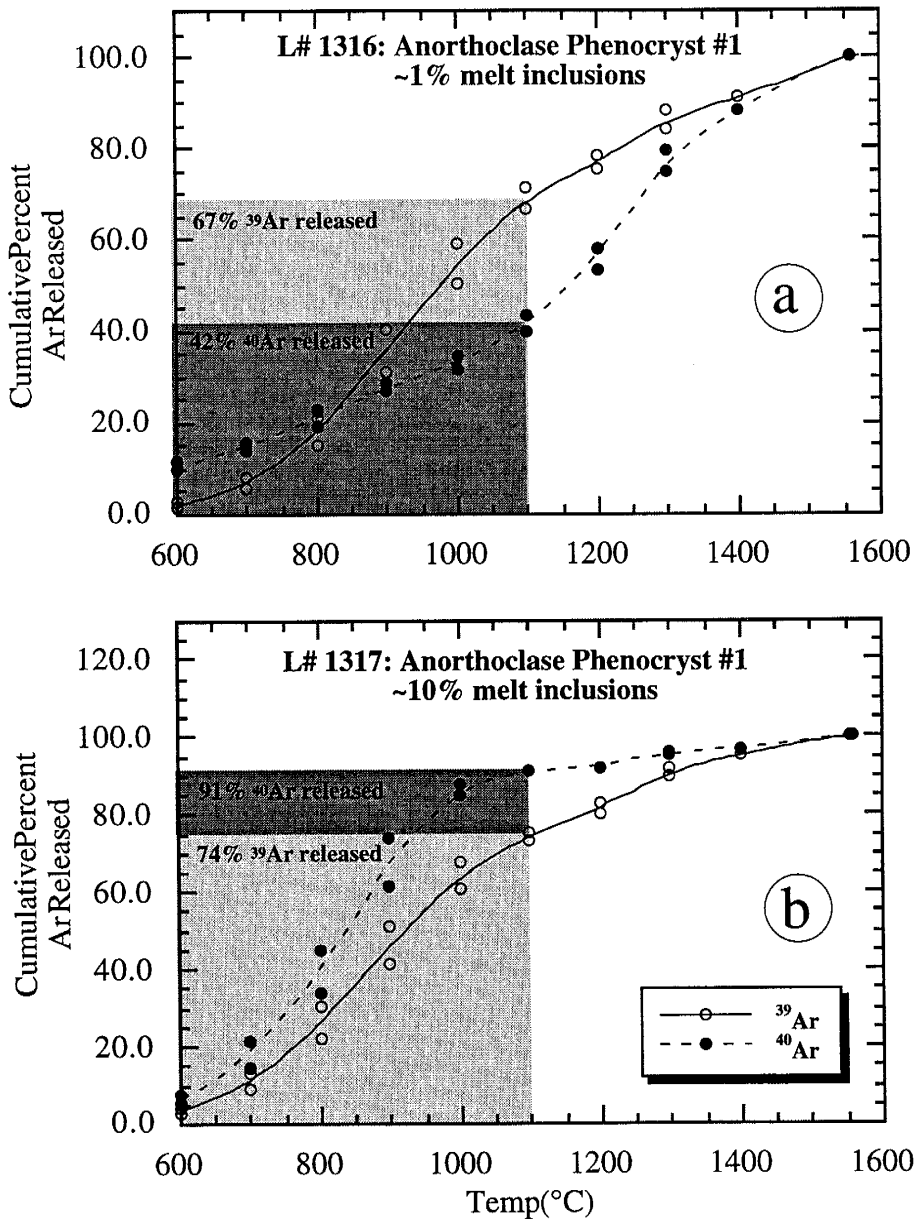

Figure 4a &b. Plots of cumulative percent ^{40}Ar and ^{39}Ar released versus temperature for samples 1316 and 1317. The degassing behavior of the pure and glassy anorthoclase is evident from the relative fractions of ^{40}Ar and ^{39}Ar released at or below 1100°C. Less than half of the total ^{40}Ar is released at ≤1100°C for sample 1316 (1% M.I.) whereas sample 1317 (10% M.I.) releases over 90% of its ^{40}Ar.

higher temperature steps (figure 4a). An opposite relationship is observed for the two aliquots containing 10% and 30% melt inclusions (figures 3c and 3d and figure 4b). Below 1200°C, release of $^{38}Ar_{Cl}$ and $^{40}Ar_E$ is greatest, resulting in high Cl/K ratios and anomalously old ages. Above 1200°C, quantities of $^{38}Ar_{Cl}$ and $^{40}Ar_E$ released from samples 1317 and 1331 are comparable to the high temperature steps in 1316 and 1330.

Attempts at using the method of Harrison et al (1993) to post-analytically subtract excess argon correlated with chlorine were able to derive ages approaching zero. However, re-calculated ages for the individual steps of the four anorthoclase aliquots (table 1) are variable in their accuracy and positively and negatively deviate from zero-age by more than two sigma. The most accurate re-calculated ages are calculated for the <1200°C steps of samples 1316 and 1330 which yield weighted-mean ages (steps C-L) of -1±1 ka and 7±1 ka, respectively. The <1200°C temperature steps for samples 1317 and 1331 yield re-calculated apparent plateaus of -23±4 ka and 205±12 ka, respectively. Re-calculated ages for steps above 1200°C in all four samples are 30-40 ka too old or too young and are not correlative to degree of glass contamination.

Discussion

The anomalously high trapped argon values found in Mt. Erebus anorthoclase can potentially be explained by: 1) xenocrystic contamination, 2) radiogenic argon or 3) excess argon. Extensive characterization of Mt. Erebus anorthoclase phenocrysts (Caldwell 1989; Kyle et al. 1992; Dunbar et al. 1994) has revealed no evidence for xenocrystic contamination. The prevalence of anomalously old ages for nearly all Mt. Erebus anorthoclase phenocrysts statistically excludes the possibility of xenocrysts. Radiogenic growth and retention of ^{40}Ar ($^{40}Ar^*$) within the anorthoclase while at magmatic temperatures is not plausible. Such a scenario would require the anorthoclase to reside in the magma chamber for several hundred thousand years at temperatures below which argon begins to diffuse out of the crystal lattice (i.e. closure temperature). On the basis of U and Th data, Reagan et al. (1992) suggested the anorthoclase were less than 2,400 years old,

much younger than the $^{40}Ar/^{39}Ar$ apparent ages for historically erupted phenocrysts. Even this small radiogenic ^{40}Ar growth would probably be degassed by the long residence times in the high temperature environment of the present Erebus magma chamber (~1000°C) (Kyle et al., 1982). The lack of support for either xenocrystic contamination or radiogenic argon retention leads to the conclusion that the exceptionally old ages are attributable to excess argon ($^{40}Ar_E$) as defined by Dalrymple and Lanphyre (1969) (i.e. ^{40}Ar that is not attributed to atmospheric argon or *in situ* radioactive decay of ^{40}K).

Zero-age anorthoclase phenocrysts display a positive correlation between chlorine content (Cl/K) and apparent age. Chlorine abundances in the anorthoclase are below detectable limits using an electron microprobe (~50 ppm; Dunbar et al. 1994). Electron microprobe measurements of Cl abundances in melt inclusions from Mt. Erebus anorthoclase average 1700 ppm (Dunbar et al. 1994). Because the melt inclusions are extremely small and abundant, significant quantities still persist following rigorous sample preparation. The large (>100 mg) samples used here combined with a best case, post-sample-preparation estimate of about 1% melt inclusions would yield at least 1 mg of melt inclusions containing approximately 0.17 mg of chlorine. Fast neutron irradiation of chlorine produces ^{38}Ar through the reaction $^{37}Cl(n,\gamma)^{38}Cl \rightarrow {}^{38}Ar$ ($t_{1/2}$ of $^{38}Cl \approx 37$ minutes) (McDougall and Harrison, 1988). Comparison of the degassing behavior of chlorine derived ^{38}Ar ($^{38}Ar_{Cl}$) with that of apparent $^{40}Ar^*$ (figure 3) reveals that most, if not all, of the excess argon is associated with the melt inclusions in the Erebus anorthoclase.

The location of excess argon within the anorthoclase samples and the degassing behavior of the $^{40}Ar_E$ and $^{38}Ar_{Cl}$, with respect to temperature, is controlled largely by the morphology of the melt inclusions and their respective bubbles (figure 5). The two anorthoclase containing 1% melt inclusions were crushed smaller (~200 μm) than many of the large melt inclusions, resulting in their truncation. The truncated inclusions and their coeval bubbles were subsequently removed by HF etching. In contrast, the interiors of

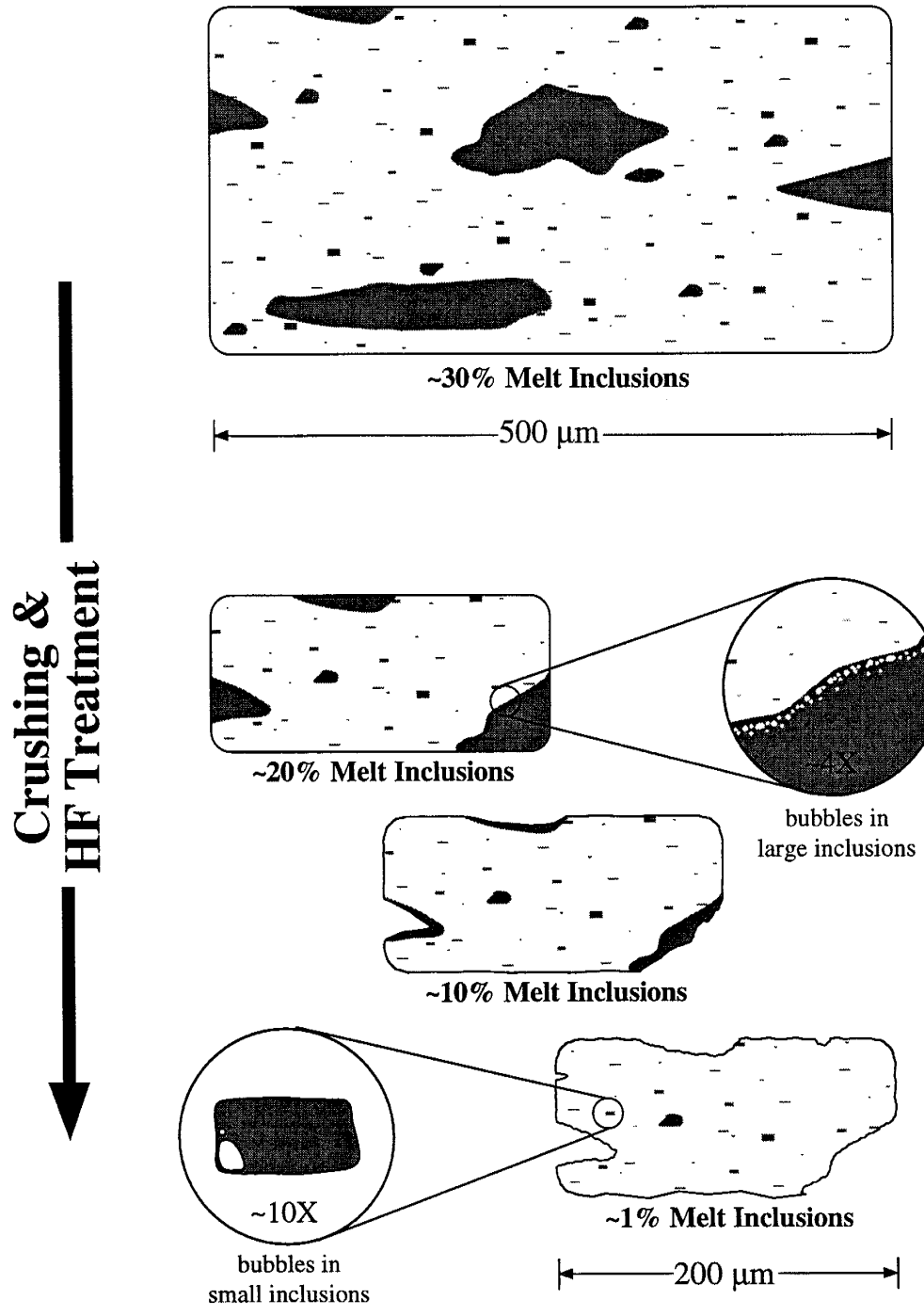

Figure 5. Cartoon showing placement of the two morphologically distinct melt inclusions and their co-eval bubbles within the anorthoclase grains. Percentages of melt inclusions within the anorthoclase decrease with smaller grain size (crushing) and hydrofluoric acid (HF) treatment.

200 μm anorthoclase grains still contain small melt inclusions that were not truncated and therefore not removed by crushing and HF treatment. However, for the two anorthoclase samples with larger quantities of melt inclusions, shorter periods of hydrofluoric acid treatment failed to remove all melt inclusions exposed on the exterior of the grains. This resulted in aliquots of "glassy" anorthoclase having grains with larger quantities of external rather than internal melt inclusions.

The morphologically controlled arrangement of melt inclusions within the anorthoclase grains becomes apparent during furnace extraction. Mt. Erebus phonolitic glass (i.e. bomb matrix glass) principally degasses at temperatures between 700° and 1100°C, with the majority being released at about 900°C (figure 2). Glass melt inclusions exposed on the outside of anorthoclase grains behave similarly and degas at ≤1100°C. Unlike the bomb matrix sample, $^{40}Ar_E$ and $^{38}Ar_{Cl}$ continue to degas from the anorthoclase samples at temperatures >1100°C. This gas represents excess argon and reactor induced $^{38}Ar_{Cl}$ from the smaller, internal melt inclusions and their respective bubbles. The argon associated with the internal inclusions remains trapped until a pathway within the anorthoclase is created. At ~1200°C the anorthoclase lattice begins to decrepitate resulting in the release of argon from melt inclusions trapped in the anorthoclase. Larger quantities of glass exposed on the outside of an anorthoclase grain, as in the case of #1317 and #1331, will result in an age spectrum with larger proportions of excess argon and ^{38}Ar being released at the lower temperature steps. For anorthoclase grains lacking large, external melt inclusions, the majority of excess argon and ^{38}Ar will be released at the higher temperature steps.

The technique of Harrison et al (1993) to post-analytically subtract excess argon correlated with chlorine reveals possible applicability toward correcting for melt inclusion excess argon. Originally formulated to correct for the excess argon contributed by *fluid* inclusions within plutonic potassium feldspar, the chlorine-correlation technique involves

isothermal heating steps to determine the differential rate of release of excess argon from the inclusions. The first of the two isothermal steps would decrepitate the fluid inclusions thereby releasing $^{40}Ar_E$ and $^{38}Ar_{Cl}$ in what is observed to be constant proportions. The mixture of excess argon from fluid inclusions and radiogenic argon from the K-feldspar would produce anomalously old age results. The second of the two isothermal heating steps would continue to degas the more retentive K-feldspar but not the fluid inclusions as they have been exhausted. The second step results in a higher $^{40}Ar^*/^{40}Ar_E$ ratio, yielding a better approximation to the true age of the sample. The difference in the two isothermal steps with respect to $^{40}Ar^*/^{39}Ar_K$ and $^{38}Ar_{Cl}/^{39}Ar_K$ is used to define an array whose slope is equal to the amount of excess argon per unit of chlorine (i.e. $^{40}Ar_E/^{38}Ar_{Cl}$). The amount of excess ^{40}Ar for each step can be calculated from its chlorine abundances ($^{38}Ar_{Cl}$) and subsequently subtracted from the total radiogenic ^{40}Ar. Using this application for igneous and metamorphic K-feldspars, Harrison et al. (1993) succeeded in correcting for excess argon which was obscuring the low-temperature portions of cooling-model-dependent age spectra.

Although the chlorine-correlation technique is able to improve the $^{40}Ar/^{39}Ar$ apparent ages for at least two out of the four zero-age anorthoclase aliquots, a number of factors will undoubtedly limit is application in very young feldspar samples with melt inclusions. The largest factor affecting the accuracy of the technique is the heterogeneous degassing of excess argon and reactor induced $^{38}Ar_{Cl}$ from melt-inclusions. Although the solubilities of argon in magma are poorly understand, it is conceivable that bubbles contained within the Mt. Erebus inclusions have a higher $^{40}Ar_E/^{38}Ar_{Cl}$ ratio than the surrounding glass. The relatively fragile (i.e. easily "popped") bubbles would likely degas their argon during the first of two isothermal heating steps. This phenomenon would result in an overestimation of the $^{40}Ar_E/^{38}Ar_{Cl}$ ratio. Too much $^{40}Ar_E$ being subtracted from the total (non-atmospheric) ^{40}Ar would produce re-calculated ages younger than the true age of the sample. This overestimation occurred in sample 1317. Conversely, an underestimation

of $^{40}Ar_E$ occurred in sample 1331 which resulted in re-calculated ages significantly older than zero. This underestimation is probably controlled by the incomplete degassing of ^{40}Ar between the two isothermal heating steps. It remains unclear why the degassing behavior of the two glassy aliquots (1317 and 1331) should be so different from one another. However, it is likely that small perturbations in the relative degassing of $^{40}Ar_E$ and $^{38}Ar_{Cl}$ for the two isothermal heating steps will greatly effect particularly young ages. These uncertainties in argon behavior with respect to melt inclusions require more attention before reliably accurate ages are produced by the chlorine-correlation technique for samples of unknown age.

Implications

The presence of excess argon in melt inclusions has profound implications for laser-fusion dating of young (<1 Ma) volcanic feldspars. The $^{40}Ar/^{39}Ar$ laser-fusion method relies on a bulk release of the argon from a sample and therefore is analogous to the conventional K/Ar method. Incremental laser heating has been attempted on young volcanic feldspar but has been primarily limited to degassing of low temperature fractions rich in atmospheric argon (Pringle et al., 1992). In cases where melt inclusions containing excess argon are present, imprecise laser-temperature control prevents consistent resolution of temperature dependent ^{40}Ar release. Homogenization of excess argon and radiogenic argon results in $^{40}Ar/^{39}Ar$ apparent ages older than the true age of the sample. It has been shown from Mt. Erebus anorthoclase that even rigorous sample preparation fails to remove all excess-argon-containing melt inclusions. In the case of Mt. Erebus zero-age anorthoclase, integrated ages (equivalent to laser-fusion ages) for the four samples in this study are at least 50 ka older than the true age of the sample (figure 1a-d).

The data from the zero-age anorthoclase samples can also be utilized to yield more accurate apparent ages for older anorthoclase samples from Mt. Erebus. Most anorthoclase from older tephriphonolites and phonolites contain large quantities of melt inclusions, similar to the historically erupted phenocrysts. Although older feldspar samples were

separated in a similar fashion and are >99% pure anorthoclase, their age spectra still show evidence of melt inclusions containing excess argon (see Section B). However, as is the case for the spectra from the historically erupted anorthoclase samples, apparent ages for individual heating steps below 1200°C are mostly isochronous (i.e. flat). Above 1200°C, ages increase to as much as three or four times those ages observed for lower temperature portions of the age spectra. As was the case with the samples focused on in this study, the most accurate $^{40}Ar/^{39}Ar$ apparent ages for older Mt. Erebus lava flows are determined from 'plateaus' fitted to the lower temperature portions of the age spectra (i.e. below 1200°).

Conclusions

The presence of excess argon in melt inclusions in Mt. Erebus anorthoclase presents challenges to high-precision, high-accuracy $^{40}Ar/^{39}Ar$ dating of young (<250 ka) samples. Crushed and non-HF treated historically erupted anorthoclase phenocrysts containing up to 30% melt inclusions yield $^{40}Ar/^{39}Ar$ integrated ages as old as 640±30 ka. Purified aliquots (containing about 1% melt inclusions) of the same anorthoclase phenocrysts yield $^{40}Ar/^{39}Ar$ integrated ages no older than 50±30 ka. Isotopic evidence for the excess argon/melt inclusion relationship comes from the similar degassing behavior of $^{38}Ar_{Cl}$ and $^{40}Ar_{E}$. Because the anorthoclase contains no measurable quantities of chlorine, the $^{38}Ar_{Cl}$ must be derived from the melt inclusions (chlorine ≈ 1700 ppm) (Dunbar et al 1995).

The bimodal degassing behavior, with respect to $^{38}Ar_{Cl}$ and $^{40}Ar_{E}$, during furnace extraction is a result of the morphological differences between Mt. Erebus melt inclusions. Melt inclusions exposed on the exterior of anorthoclase grains during crushing are easily exhausted of argon at temperatures below 1200°C. Melt inclusions trapped within the anorthoclase grains are not able to degas their argon until the crystal lattice of the anorthoclase begins to decrepitate (~1200°C). Depending on the relative proportions of

external versus internal melt inclusions, the low-temperature portion of the age spectrum will be older or younger than the high-temperature portion of the age spectrum.

Because melt inclusions are extremely common in feldspars, excess argon can be a significant problem when trying to date samples younger than 1 Ma. Conventional K/Ar and $^{40}Ar/^{39}Ar$ total-laser-fusion rely on bulk release of the argon isotopes to determine age. This bulk release, if melt-inclusion excess argon is present, is a combination of $^{40}Ar^*$ and $^{40}Ar_E$, resulting in apparent ages which are too old. Incremental heating is the only technique reliably able to discriminate between $^{40}Ar^*$ and $^{40}Ar_E$ from melt inclusions.

References

Armstrong, R.L., K-Ar dating: Late Cenozoic McMurdo Volcanic Group and dry valley glacial history, Victoria Land, Antarctica, *N.Z. Journal of Geology and Geophysics, 21*, 685-698, 1978.

Caldwell, D.A., Physical and geochemical properties of summit flows and recent volcanic ejecta from Mount Erebus, Ross Island, Antarctica, Master's thesis, New Mexico Inst. of Mining and Tech., 1989.

Dalrymple, G.B., and M.A. Lanphere, *Potassium-argon dating*, Freeman, San Francisco, 1969.

Deino, A., and R. Potts, Single-Crystal $^{40}Ar/^{39}Ar$ Dating of the Olorgesailie Formation, Southern Kenya Rift, *Journal of Geophysical Research, 55*, 8453-8470, 1990.

Dunbar, N.W., K.V. Cashman, and R. Dupre, Crystallization Processes of Anorthoclase Phenocrysts in the Mount Erebus Magmatic System: Evidence from Crystal Composition, Crystal Size Distributions, and Volatile Contents of Melt Inclusions, in *Volcanological and Environmental Studies of Mount Erebus, Antarctica*, vol. Antarctic Research Series, Volume 66, edited by P.R. Kyle, pp. 129-146, American Geophysical Union, 1994.

Harrison, T.M., M.T. Heizler, and O.M. Lovera, In vacuo crushing experiments and K-feldspar thermochronometry, *Earth and Planetary Science Letters, 117*, 169-180, 1993.

Hu, Q., P.E. Smith, N.M. Evensen, and D. York, Lasing in the Holocene: extending the ^{40}Ar-^{39}Ar laser probe method into the ^{14}C range, *Earth and Planetary Science Letters, 123*, 331-336, 1994.

Kyle, P.R., R.R. Dibble, W.F. Giggenbach, and H.J. Keys, Volcanic Activity Associated with the Anorthoclase Phonolite Lava Lake, Mount Erebus, Antarctica, in *Symposium on Antarctic Geology and Geophysics*, edited by C. Craddock, pp. 1172, The University of Wisconsin Press, Madison, Wisconsin, U.S.A., 1982.

Kyle, P.R., J.A. Moore, and M.F. Thirlwall, Petrologic Evolution of Anorthoclase Phonolite Lavas at Mount Erebus, Ross Island, Antarctica, *Journal of Petrology, 33*, 849-875, 1992.

Lippolt, H.J., M. Troesch, and J.C. Hess, Excess argon and dating of Quaternary Eifel volcanism, IV. Common argon with high and lower-than-atmospheric $^{40}Ar/^{36}Ar$ ratios in phonolitic rocks, East Eifel, F.R.G., *Earth and Planetary Science Letters, 101*, 19-33, 1990.

McDougall, I., $^{40}Ar/^{39}Ar$ age spectra from the KBS Tuff, Koobi Fora, Lake Turkana, northern Kenya, *Nature, 294*, 120-124, 1981.

McDougall, I., K-Ar and $^{40}Ar/^{39}Ar$ dating of the hominid-bearing Pliocene-Pleistocene sequence at Koobi Fora, Lake Turkana, northern Kenya, *Geol. Soc. Am. Bull., 96*, 159-175, 1985.

McDougall, I., and T.M. Harrison, *Geochronology and Thermochronology by the $^{40}Ar/^{39}Ar$ Method*, 212 pp., Clarendon Press, Oxford, 1988.

Pringle, M.S., M. McWilliams, B.F. Houghton, M.A. Lanphere, and C.J.N. Wilson, $^{40}Ar/^{39}Ar$ dating of Quaternary feldspar: Examples from the Taupo Volcanic Zone, New Zealand, *Geology, 20*, 531-534, 1992.

Reagan, M.K., A.M. Volpe, and K.V. Cashman, ^{238}U- and ^{232}Th-series chronology of phonolite fractionation at Mount Erebus, Antarctica, *Geochimica et Cosmochimica Acta, 56*, 1401-1407, 1992.

Roedder, E., *Fluid Inclusions*, 644 pp., Mineralogical Society of America, Washington, D.C., 1984.

Rothery, D.A., and C. Oppenheimer, Monitoring Mount Erebus by Satellite Remote Sensing, in *Volcanological and Environmental Studies of Mount Erebus, Antarctica*, vol. Antarctic Research Series, Volume 66, edited by P.R. Kyle, pp. 51-56, American Geophysical Union, 1994.

Steiger, R.H., and E. Jager, Subcommission on geochronology: Convention on the use of decay constants in geo- and cosmochronology, *Earth and Planet. Sci. Lett., 36*, 359-362, 1977.

Turbeville, B.N., $^{40}Ar/^{39}Ar$ Ages and Stratigraphy of the Latera caldera, Italy, *Bulletin of Volcanology, 55*, 110-118, 1992.

van den Bogaard, P., $^{40}Ar/^{39}Ar$ ages of sanidine phenocrysts from Laacher See Tephra (12,900 yr BP): Chronostratigraphic and petrologic significance., *Earth and Planetary Science Letters, 133*, 163-174, 1995.

$^{40}Ar/^{39}Ar$ Dating of Mount Erebus, Antarctica: Insights into the Evolution of a Polygenetic Volcano

R.P. Esser
Department of Earth and Environmental Science,
New Mexico Institute of Mining and Technology,
Socorro, NM 87801

ABSTRACT

Mt. Erebus, a 3794 meter high active polygenetic stratovolcano, is composed of voluminous anorthoclase-phyric lava (a.k.a. kenyte) overlying unknown volumes of poorly exposed, less differentiated lavas. The older basanite to phonotephrite lavas crop out on Fang Ridge, an eroded remnant of a proto-Erebus volcano and other sporadic locations on the flanks of the Mt. Erebus edifice. Anorthoclase-phyric lava flows are exposed around the flanks and fill the major summit caldera. Anorthoclase feldspars found within the bombs and lavas are large (≤10 cm), abundant (~30-40%) and contain many melt (glass) inclusions. Although excess argon is known to exist within the melt inclusions, rigorous sample preparation is able to remove the majority of the contaminant.

Results of $^{40}Ar/^{39}Ar$ dating indicate that anorthoclase-phyric activity characteristic of Mt. Erebus is predominantly less than 250 ka, nearly an order of magnitude younger than previously believed. All Mt. Erebus flows between about 40 and 250 ka, with the exception of one phonolite flow (76±5 ka), are anorthoclase tephriphonolite in composition. Dates on anorthoclase tephriphonolite flows at the caldera rim constrain the timing of caldera collapse. The truncated caldera wall, formed by caldera subsidence, contains flows as young as 87±7 ka while anorthoclase tephriphonolite flows locally spilling over the caldera wall (76±5 ka) suggest caldera collapse occurred sometime between 87 and 76 ka. Geochemical and age relationships of spatially separated flows suggest the present summit caldera may have collapsed due to the draining of a summit magma chamber which formed voluminous flows on the coast of Mt. Erebus (89±1 ka and 73±5 ka).

The youngest dated lava flows on Mt. Erebus are anorthoclase phonolite in composition and were emplaced at the summit and flanks (11 ka to 33 ka). Young (<11 ka?) to present-day strombolian activity responsible for building a pyroclastic cone at the summit has erupted chemically similar lava and pyroclastic rocks but dating is difficult due to contaminating excess argon.

Older eruptive activity reveals the petrologic evolution of Mt. Erebus. A short pulse of lavas with anomalously high degrees of crustal contamination occurred approximately 160 ky ago as indicated by at least two trachytic flows (157±3 ka and 166±5). Older anorthoclase tephriphonolite flows crop out principally in the southwest sector of the volcano (235±4 ka) and represent the oldest dated stage of anorthoclase-phyric activity on Mt. Erebus. Plagioclase-phyric phonotephrite from other coastal and flank flows yield ages between 368±9 ka and 531±19 ka.

Dates of lavas from Fang Ridge escarpment reveal an approximate eruptive interval for the proto-Erebus volcano. Plagioclase from a stratigraphically high flow at Fang Ridge yields an age of 758±10 ka while a groundmass separate from a stratigraphically low flow yields an age of 1070±90 ka. The oldest dated rock on Mt. Erebus is a basanite dike (1311±8 ka) exposed on the shores of Mt. Erebus at Cape Barne.

Introduction

Mt. Erebus (77°32'S, 167°10'E), Ross Island, Antarctica is the world's southern-most active volcano. Discovered in 1841 by James Ross, it is one of only a few volcanoes in the world with a persistent, convecting lava lake (Kyle et al. 1982). Over 20 years of scientific research, which began in the early 1970's, include studies of the eruptive activity and the degassing behavior of the lava lake and the petrology of the volcano (Moore and Kyle 1987; Kyle et al. 1992; Zreda-Gostynska et al. 1993; Kyle 1994) Lack of rock exposures and stratigraphic relationships have obscured the relative and absolute age control, allowing only a generalized eruptive history for Mt. Erebus (Moore and Kyle 1987).

Attempts at obtaining chronological control by radioisotopic dating have been limited. Treves (1968), Armstrong (1978) and Moore and Kyle (1987) obtained conventional K/Ar dates for samples from eleven separate locations on the volcano, including a recently erupted anorthoclase phenocryst from the summit. While many of the K/Ar dates possessed large analytical uncertainties, the apparent ages were tolerably within expected values for the active Erebus volcano. Armstrong (1978) obtained anomalously old apparent ages for the historically erupted anorthoclase and glass from summit bombs which he attributed to excess ^{40}Ar ($^{40}Ar_E$). The presence of $^{40}Ar_E$ in the historic samples called into question the geologic relevancy of all K/Ar apparent ages for lavas from Mt. Erebus. However, the conventional K/Ar technique in use at the time could not evaluate the extent of excess argon contamination within the Mt. Erebus anorthoclase.

The $^{40}Ar/^{39}Ar$ method is capable of revealing and, in many cases, resolving the excess argon and other complexities that conventional K/Ar could not. This study relies exclusively on the $^{40}Ar/^{39}Ar$ method to yield high precision apparent ages for more than 30 individual Mt. Erebus samples. Paleomagnetic data from previous workers (Funaki 1983; Mankinen and Cox 1988) and this study are used to test the accuracy of the $^{40}Ar/^{39}Ar$ apparent ages.

Geology

Mt. Erebus lies within a sequence of Cenozoic alkaline volcanoes that developed as a result of continental rifting along the western margin of the Ross Embayment (Kyle 1990a). A major graben, termed the Terror Rift (Cooper et al. 1987), is bounded at its northern and southern margins by two active volcanoes, Mt. Melbourne and Mt. Erebus, respectively. Kyle and Cole (1974) classified the alkalic volcanoes associated with the Terror Rift as the McMurdo Volcanic Group (MVG) which itself consists of three spatially and tectonically separate volcanic provinces (Hallett, Melbourne, and Erebus volcanic provinces) (Kyle 1990b). The Erebus volcanic province is composed of several large shield/stratovolcanoes of basaltic to phonolitic composition. Ross Island, within the

Erebus volcanic province, comprises at least three major volcanic centers with numerous smaller vents. Mt. Erebus is the central feature of Ross Island and is surrounded radially at 120° angles by Mt. Terror, Mt. Bird and Hut Point Peninsula. Kyle and Cole (1974) suggested crustal doming as the mechanism which contributed to the development Mt. Erebus and the three surrounding centers. Later, Kyle et al. (1992) explained Mt. Erebus and the radial structure as a result of a mantle plume. Mount Erebus remains the only active volcano on Ross Island. Mount Terror, Mount Bird and Hut Point Peninsula have probably been inactive for more than 300 ky (Armstrong 1978).

Mt. Erebus is a silica-undersaturated polygenetic stratovolcano composed predominantly of basanitic to phonolitic lavas. A significant proportion of exposed volcanic rock on the Mt. Erebus edifice, including its presently active summit cone, is composed of anorthoclase-phyric phonolite lava (a.k.a. kenyte). Anorthoclase phenocrysts within the phonolitic and tephriphonolitic bombs and lavas are large (up to 10 cm), abundant (~30%) and riddled with melt inclusions (up to 30%) (Kyle 1977; Dunbar et al. 1995). Anorthoclase phonolite and tephriphonolite lava flows are exposed principally on the upper slopes, probably accounting for the entire upper one quarter of the volcanic edifice (figure 1). Smaller volumes of anorthoclase phonolite are exposed on the lower flanks, primarily near the coast at Cape Evans, Cape Barne and Cape Royds. Much of the area in the southern half of the volcanic edifice is snow and ice covered, but is also assumed to be phonolitic in composition. Near the summit, numerous small anorthoclase phonolite lava flows fill and, in some cases, overflow a large caldera (~4 km in diameter) (Caldwell 1989). The summit cone is composed of lava flows and pyroclastic rocks which disintegrate forming a lag of anorthoclase crystals.

Stratigraphically older than the anorthoclase phonolite flows are unknown volumes of poorly exposed, less chemically differentiated lavas. Basanitic/tephritic lavas are primarily limited to the low, broad platform shield and to the north-northwest sector of the volcanic edifice. Slightly more evolved differentiates (phonotephrite to tephriphonolite),

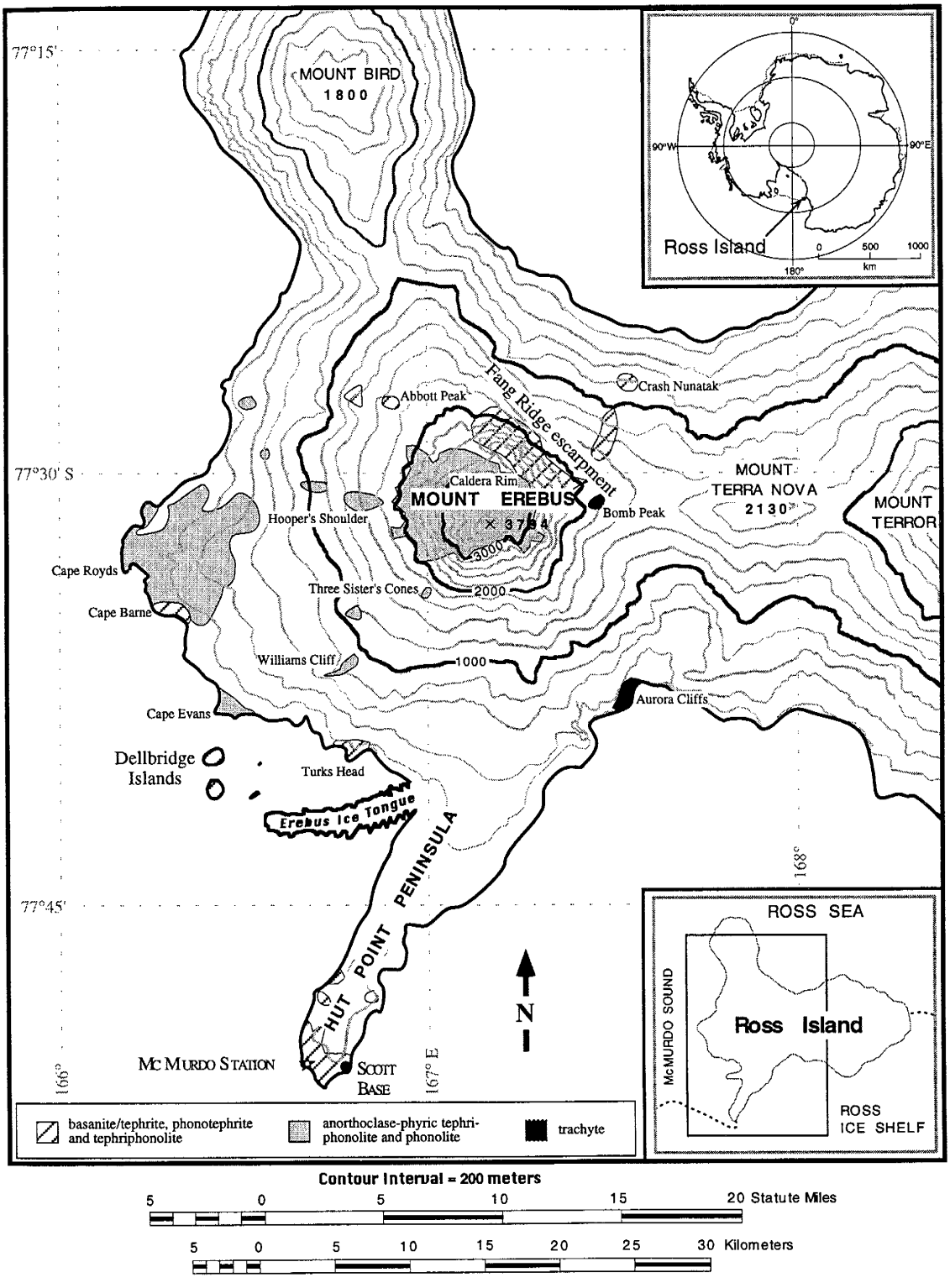

Figure 1. Generalized geologic map of Mt. Erebus and surrounding volcanic centers.

some containing large (~2 cm) laths of plagioclase, crop out principally at and around Fang Ridge, an eroded remnant of an older volcanic edifice and other scattered locations on the flanks of the Mt. Erebus edifice (fig. 1).

Mt. Erebus' basanitic to phonolitic lavas are referred to as the Erebus lineage (Kyle et al. 1992). Erebus lineage lavas evolved by fractional crystallization of olivine, clinopyroxene, feldspar, opaque oxides and apatite. Basanite/tephrite and phonotephrite commonly contain large phenocrysts of plagioclase whereas tephriphonolite and phonolite commonly contain large phenocrysts of anorthoclase. Basanite/tephrite is the least evolved lava exposed on Mt. Erebus and is presumed to be the parental melt from which subsequent, younger lavas are derived. Kyle et al. (1992) modeled the fractional crystallization of basanite and suggested phonotephrite, tephriphonolite and phonolite were 45%, 35% and 23% residual liquids, respectively.

Scattered exposures of trachyte containing less than 5% anorthoclase phenocrysts are also exposed on the Mt. Erebus edifice but are less common than less differentiated rocks. These trachytes represent the highest degree of differentiation achieved by Erebus lavas although the $^{87}Sr/^{86}Sr$ values for these rocks suggest they evolved by assimilation and fractional crystallization processes (Kyle et al. 1992).

Previous Work

The first geochronological studies of Mt. Erebus used the conventional K-Ar dating method (Table 1). Treves (1968) reported a date of 698±140 ka for an "anorthoclase trachyte" at Cape Royds; Moore and Kyle (1987) published a K/Ar whole-rock age of 860±200 ka for a trachybasalt flow at Turks Head. Armstrong (1978) dated whole-rock and anorthoclase separates from the summit of Mt. Erebus, Fang Ridge and Cape Barne. At Cape Barne a K-feldspar from an anorthoclase phonolite flow was 965±50 ka whereas a whole-rock from a basaltic dike was 821±200 ka. Two plagioclase basalts, one fine-grained, the other porphyritic, from Fang Ridge produced apparent ages of 832±20 and 750±70 ka, respectively. Feldspar and glass age determinations for summit samples had

Table 1. Published conventional K/Ar dates of Mt. Erebus samples.

Location	Sample type	†Age (ka) ± Error (1σ)	Source
Cape Barne	anorthoclase	965 ± 50	Armstrong (1978)
Cape Barne	whole rock basalt	821 ± 20	Armstrong (1978)
Mt. Erebus summit	anorthoclase	565 ± 150	Armstrong (1978)
Mt. Erebus summit	phonolite glass	462 ± 200	Armstrong (1978)
Mt. Erebus summit	anorthoclase	452 ± 90	Armstrong (1978)
2nd Mt. Erebus crater	phonolite glass	154 ± 50	Armstrong (1978)
2nd Mt. Erebus crater	anorthoclase	205 ± 70	Armstrong (1978)
Fang Ridge	whole rock-phonotephrite	832 ± 20	Armstrong (1978)
Fang Ridge	plagioclase-phonotephrite	750 ± 70	Armstrong (1978)
Cape Royds	anorthoclase	698 ± 140	Treves (1968)
Turks Head	whole rock-phonotephrite	860 ± 200	Moore and Kyle (1987)

† Ages of Armstrong and Treves are re-calculated to decay constants proposed by Steiger and Jager (1977) using the procedure of Dalrymple (1979)

K/Ar ages of between 565±150 and 154±50 ka. Glass and anorthoclase from recent eruptive activity were both dated to test for excess ^{40}Ar. According to Armstrong, excess argon was present in the Mt. Erebus samples but the similar apparent ages for the glass and anorthoclase indicate a uniform distribution of excess argon within his separates, eliminating the possibility of contamination by xenocrystic material. Because of the probability of excess argon, Armstrong (1978) recognized that his conventional K/Ar apparent ages were maxima.

Paleomagnetic investigations of Ross Island and Mt. Erebus were undertaken by Funaki (1983) and Mankinen and Cox (1988). However, paired paleomagnetic and K-Ar analyses are only available at Cape Barne and Cape Royds. For Cape Barne, the anorthoclase phonolite flow revealed normal polarity whereas the basaltic dike is reversely polarized (Mankinen and Cox 1988). The authors suggest that, based on the K/Ar results by Armstrong (1978), the reversed polarity of the Cape Barne dike is pre-Bruhnes (>780 ka; Cande and Kent 1992) whereas the normal polarity of the anorthoclase phonolite records the Jaramillo Subchron. The normal polarity of Cape Royds (Funaki 1983) also is in agreement with the 698±140 ka date given by Treves (1968).

Methods

Sample Preparation

Anorthoclase was separated from phonolite, trachyte and tephriphonolite samples collected from the summit and flanks of Mt. Erebus. Standard techniques were used to separate the anorthoclase from the groundmass. Removal of the ubiquitous glass melt inclusions was accomplished by further crushing and ultrasonic treatment in 15% hydrofluoric (HF) acid for up 20 minutes. Following these procedures, anorthoclase separates were commonly greater than 99% pure. Final grain size for the 'pure' anorthoclase separates were approximately 150-250 μm.

Plagioclase feldspar samples separated from basanites/tephrites and phonotephrites were prepared using similar procedures as for the anorthoclase. However, because of their

comparative lack of glass inclusions, plagioclase separates were cleaned in HF for only 3-6 minutes. Final grain size for pure plagioclase separates was 300-500 μm.

Where anorthoclase or plagioclase phenocrysts were lacking, groundmass samples were analyzed. Groundmass concentrates were prepared by removing the highly magnetic and non-potassium bearing phenocryst phases. Any carbonate present was removed by a solution of 5% nitric acid. Final grain size range of the groundmass samples was 300-500 μm.

Analytical Procedures

Samples were irradiated in five batches over a two year period. In each case, weighed samples (40-200 mg) were encapsulated in tin or copper foil and sealed in evacuated quartz vials. The mineral and whole-rock sample packets along with interspersed Fish Canyon Tuff sanidine (FC-1) monitors were irradiated in known geometries for 0.5 to 1 hours in the L67 position at the University of Michigan's Ford Research reactor under fast neutron fluxes of approximately 7.0×10^{-5} J/hr.

All $^{40}Ar/^{39}Ar$ analyses were performed in the New Mexico Geochronology Research Laboratory at the New Mexico Institute of Mining and Technology. J-factors for the separate irradiations were determined by total fusion of Fish Canyon Tuff sanidine monitors (age = 27.84 Ma) by resistance furnace (irradiation number - NM-2) or CO_2 laser (subsequent irradiations). Precision for the averaged J-factor results of up to four aliquots per monitor location was typically less than ±0.25% (1σ).

Argon extraction for Mt. Erebus samples was accomplished using a resistance furnace (NM-2, 10, 14 and 28) or CO_2 laser (NM-4). Laser extraction used up to two steps of differing wattages followed by 2-15 minutes of one-stage reactive gas clean-up by a SAES GP-50 getter. System blanks for both unknown and monitor laser analyses were typically 1×10^{-16} moles ^{40}Ar (2 minute getter for cleaner Fish Canyon Tuff sanidine gas) to 2×10^{-15} moles ^{40}Ar (15 minute getter for comparatively dirty Mt. Erebus anorthoclase gas). Furnace extraction was accomplished by incremental heating in a tantalum or molybdenum

crucible using a double vacuum resistance furnace capable of 1750°C. Time at temperature for each step was typically 10 minutes during which reactive gases were removed simultaneously by a SAES AP-10 getter. Further gas cleansing was accomplished in a second stage between the furnace and mass spectrometer using a GP-50 getter. Depending on quantities of reactive (non-argon) gas within a sample, second stage times ranged from 5 to 8 minutes. System blanks for furnace analyses were between 7×10^{-16} and 3×10^{-15} moles ^{40}Ar. The argon was analyzed using a Mass Analyzer Products (MAP) 215-50 mass spectrometer using an electron multiplier with an approximate gain of 1000 (sensitivity ≈ 2×10^{-17} moles/pA).

Results

Figure 2 and Table 2 show the $^{40}Ar/^{39}Ar$ apparent ages for Mt. Erebus samples. Figure 3 through Figure 6 and Table 3 show $^{40}Ar/^{39}Ar$ age spectra and analytical data from four representative samples (Appendices C1 and C2 contain the comprehensive analytical and graphical data, respectively, for all samples analyzed in this study). The four spectra show characteristics exhibited by the three types of samples analyzed: anorthoclase, plagioclase and groundmass separates.

The majority of anorthoclase samples have age spectra that behave similarly to sample #2645 (figure 3). Following a low temperature step with high analytical error, the age spectra remain relatively uniform until about 1100°C. At temperatures of 1200°C and above the apparent age, Cl/K ratio and radiogenic yield increase. The high temperature gas is interpreted to be excess argon degassing from melt inclusions within the anorthoclase (Esser et al. 1996), and result in an anomalously old integrated or total gas age. The steps from 900° to 1100°C yield lower Cl/K ratios and younger apparent ages with the plateau giving apparent ages for the anorthoclase. This plateau segment usually represents greater than 50% of the cumulative ^{39}Ar released. The plateaus fitted to the low temperature portions of the age spectra are weighted means and commonly do not fulfill traditional plateau requirements (two or more contiguous incremental heating steps containing greater

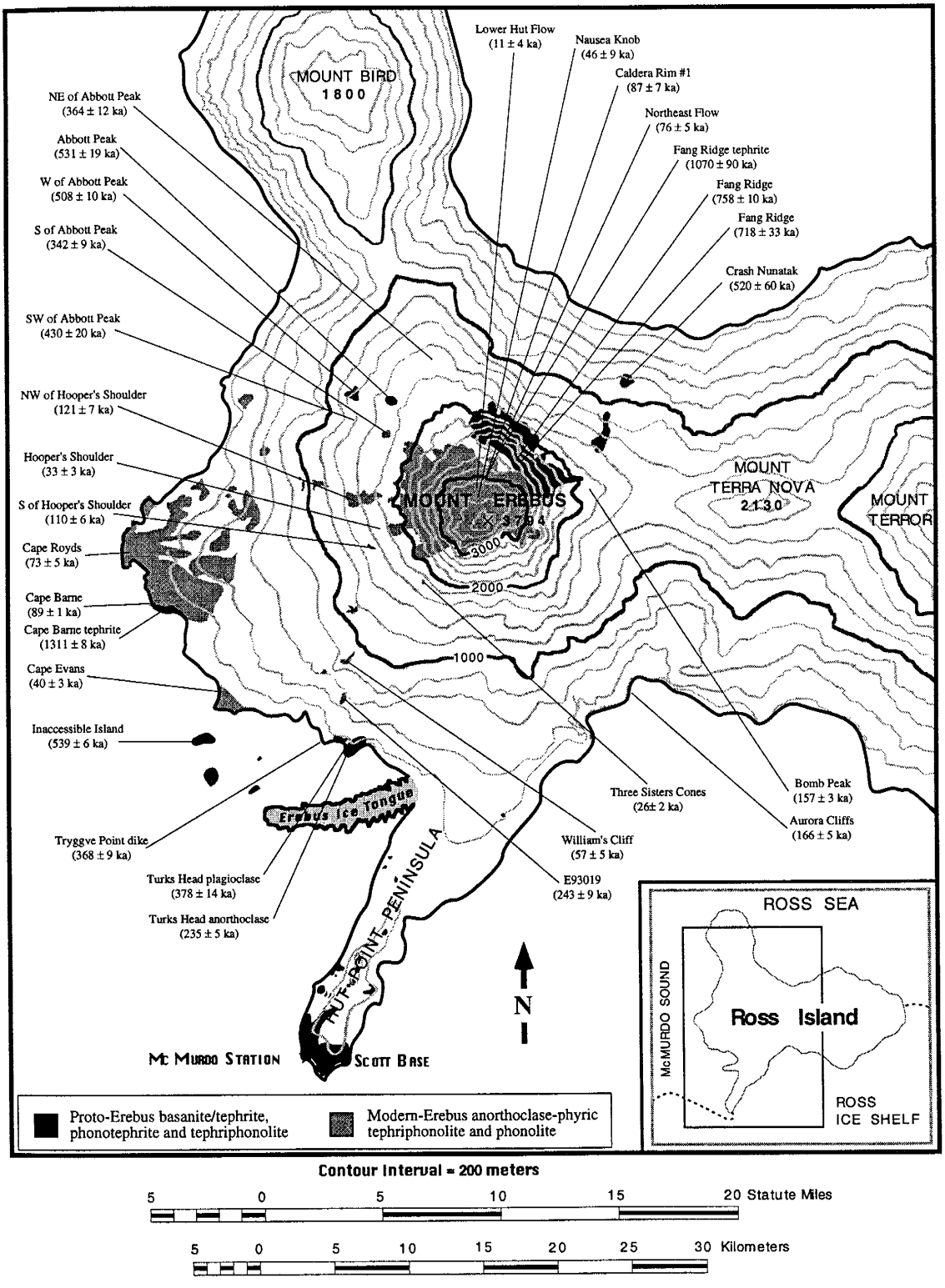

Figure 2. Generalized geologic map of Mt. Erebus with the 29 new $^{40}Ar/^{39}Ar$ dates from this study.

Table 2. $^{40}Ar/^{39}Ar$ apparent ages for 29 Mt. Erebus sites

Location/Rock Type	Rock Type	Lab ID	Sample #	Material	Method	Age (ka) ± Err. (1σ)
Lower Hut Flow	A.P.	842	E87034	an	plat.	11 ± 4
Three Sister's Cone	A.P.	1329	E80020	an	plat.	26 ± 2
Hooper's Shoulder Cone	A.P.	841	E81001	an	plat.	36 ± 4
Hooper's Shoulder Cone	A.P.	843	E81001	an	plat.	28 ± 5
Hooper's Shoulder Cone	A.P.	1318	E81001	an	plat.	32 ± 5
Mean Age (weighted)						33 ± 3
Cape Evans	A.T.	427	E83400	an	plat.	37 ± 7
Cape Evans	A.T.	1313	E83400	an	plat.	42 ± 4
Cape Evans	A.T.	1320	E83400	an	plat.	32 ± 6
Cape Evans	A.T.	54	E83400	an	plat.	53 ± 11
Mean Age (weighted)						40 ± 3
Nausea Knob	A.T.	2642	E87035	an	plat.	46 ± 9
William's Cliff	A.T.	2648	E93020	an	plat.	57 ± 5
Cape Royds	A.T.	1314	E83448	an	plat.	73 ± 5
Northeast Flow	A.P.	2643	E86026	an	plat.	87 ± 16
Northeast Flow	A.P.	2650	E86026	an	plat.	75 ± 5
Mean Age (weighted)						76 ± 5
Caldera Rim#1	A.T.	2646	E93013	an	plat.	87 ± 7
Cape Barne	A.T.	836	E83433	an	plat.	89 ± 2
Cape Barne	A.T.	838	E83433	an	plat.	90 ± 6
Cape Barne	A.T.	839	E83433	an	plat.	89 ± 2
Cape Barne	A.T.	840	E83433	an	plat.	87 ± 4
Mean Age (weighted)						89 ± 1
S of Hoopers Shoulder	A.T.	2645	E93021	an	plat.	110 ± 6
NW of Hoopers Shoulder	A.T.	2644	E93011	an	plat.	121 ± 7
Bomb Peak	TR.	1327	E82405	an	plat.	157 ± 3
Aurora Cliffs	TR.	1321	E83454	an	plat.	166 ± 5
Btwn Williams Cl. & Turks Hd	A.T.	2647	E93019	an	plat.	243 ± 9
Turks Head	A.T.	1315	AW82015	an	plat.	243 ± 5
South of Abbott Peak	P.T.	2655	E93024	gm	iso.	342 ± 9
NE of Abbott Peak	P.T.	2653	E93023	gm	iso.	364 ± 12
Tryggve Point dike	P.T.	1536	E77012	pl	plat.	368 ± 9
Turks Head	B.	1422	AW82038	pl	plat.	378 ± 14
SW of Abbott Peak	PH.	1865	E83453	gm	plat.	430 ± 20
West of Abbott Peak	PH.	2656	E93010	gm	iso.	508 ± 10
Crash Nunatak	PH.	2657	E93008	gm	plat.	520 ± 60
Abbott Peak	P.T.	1326	E81002	pl	plat.	531 ± 19
Inaccessible Island	P.	1537	E83407	gm	plat.	539 ± 6
Fang Ridge	P.P.	2651	E93005	pl	iso.	718 ± 33
Fang Ridge	P.P.	2652	E93007	pl	iso.	758 ± 10
Fang Ridge	TE.	2654	E93012	gm	plat.	1070 ± 90
Cape Barne dike	B.	1528	E83432	gm	plat.	1310 ± 8
Cape Barne dike	B.	2658	E93032	gm	plat.	1330 ± 30
Mean Age (weighted)						1311 ± 8

Rock Type: A.P. = anorth. phonolite, A.T. = anorth. tephriphonolite, P.T. = plag. tephriphonolite, P.P. = plag. phonotephrite, PH. = phonotephrite, P. = phonolite, TR. = trachyte TE. = tephrite, B. = basanite

Material: an = anorthoclase, pl = plagioclase, gm = groundmass

Method: plat. = plateau, iso. = isochron

Mean Ages are weighted according to the inverse of the analytical variance for duplicate samples

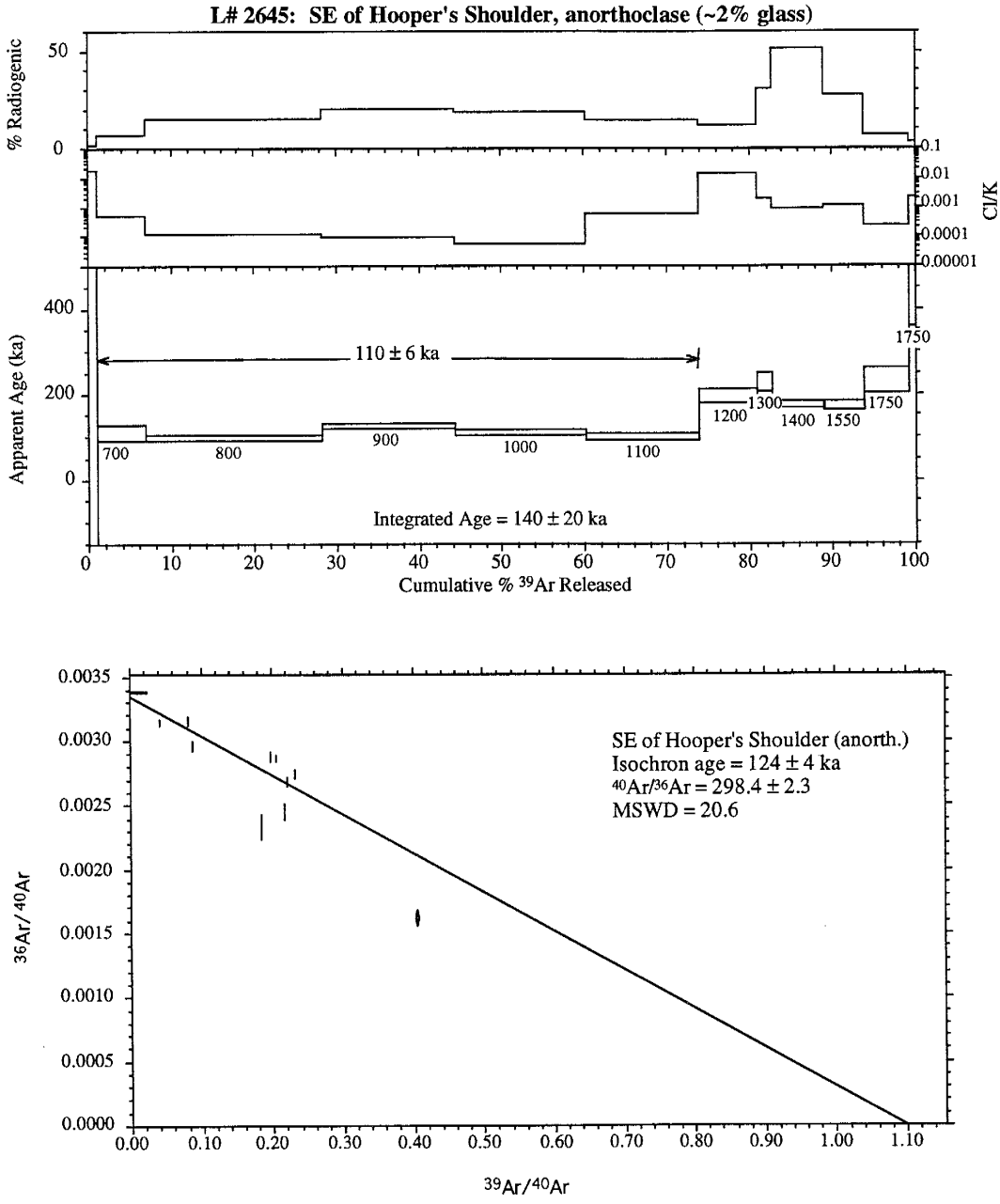

Figure 3. $^{40}Ar/^{39}Ar$ age spectrum and inverse isochron from anorthoclase separated from a lava flow southeast of Hooper's Shoulder. An increase in apparent age at 1200°C correlates with an increase in Cl/K ratio. The isotope correlation diagram does not define a meaningful isochron and therefore is not geologically relevant.

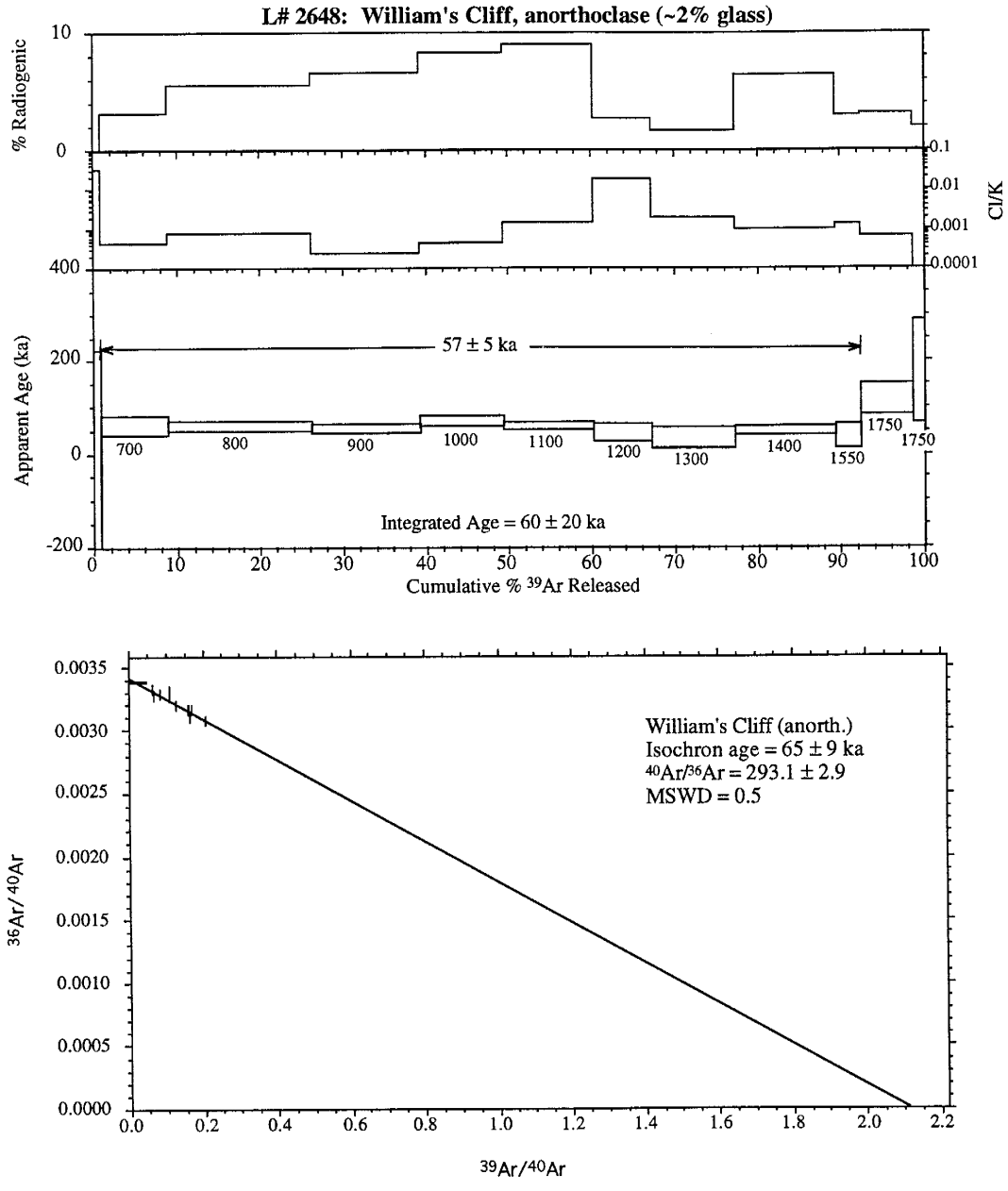

Figure 4. $^{40}Ar/^{39}Ar$ age spectrum and inverse isochron from anorthoclase separated from a lava flow near Williams Cliff. Unlike the spectrum in figure 3, an increase in Cl/K ratio is not correlated with an increase in apparent age. The isotope correlation diagram is analytically equivalent to the plateau age at one sigma. However, due to the samples low radiogenic yield (<10%) the isochron yields a less precise date.

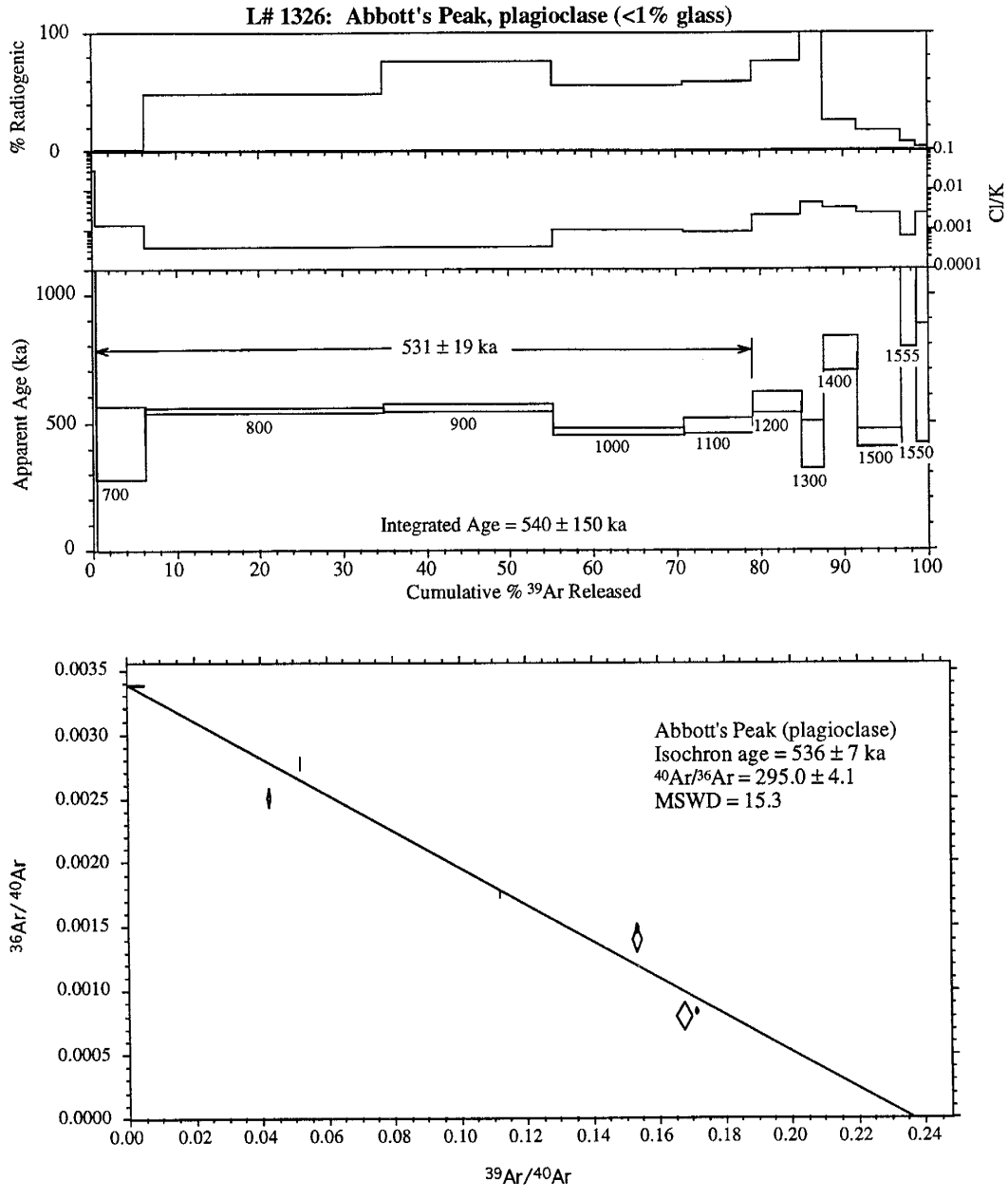

Figure 5. $^{40}Ar/^{39}Ar$ age spectrum and inverse isochron from plagioclase separated from a lava flow near Abbott Peak. Note that the apparent ages derived from the plateau and isochron are analytically equivalent at one sigma although the MSWD is greater than 15.

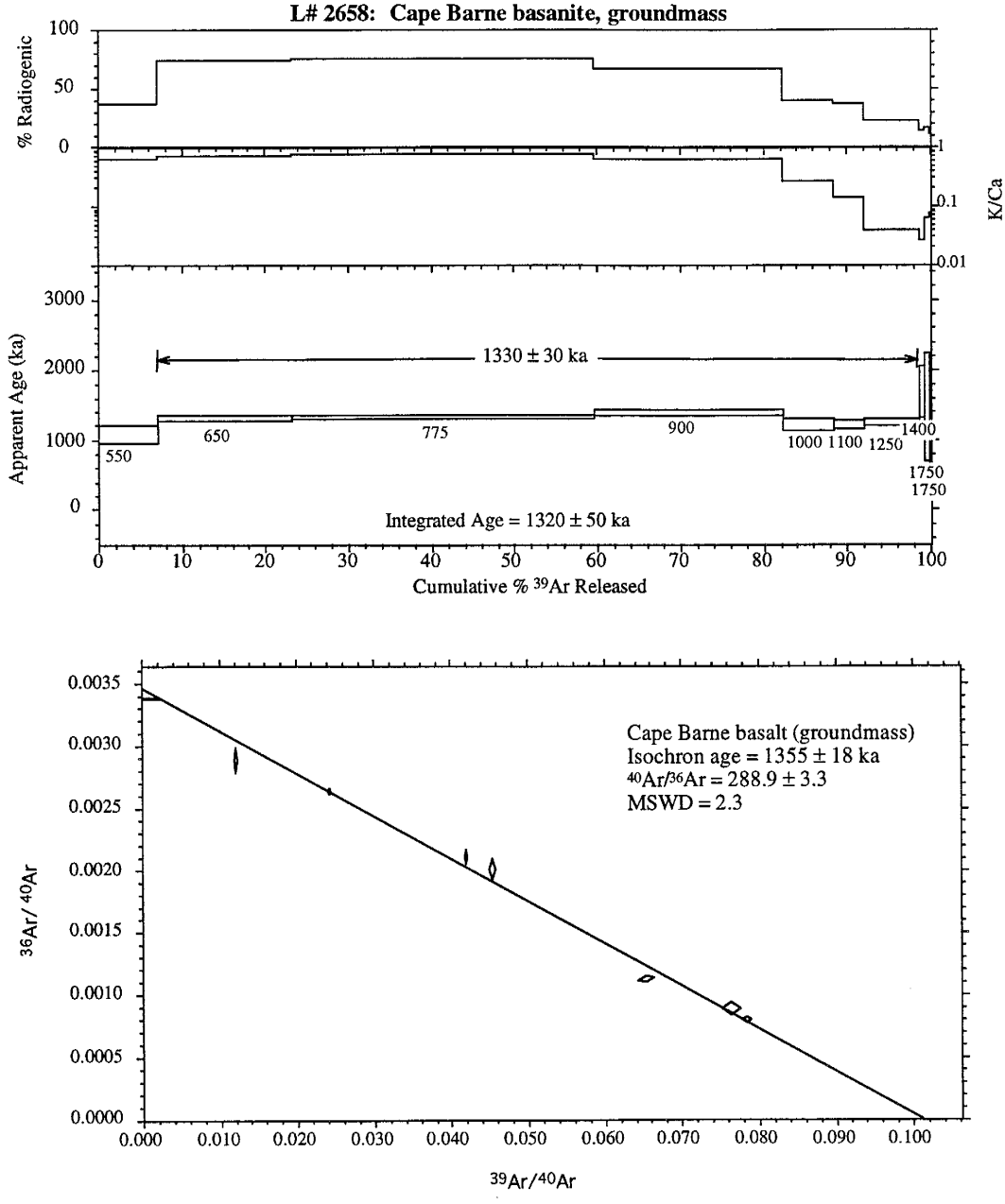

Figure 6. $^{40}Ar/^{39}Ar$ age spectrum and inverse isochron from groundmass separated from a basanite dike near Cape Barne. Again, plateau and isochron ages are analytically equivalent at one sigma.

Table 3. Representative $^{40}Ar/^{39}Ar$ analytical data for the anorthoclase, plagioclase and groundmass samples shown in figures 3 through 6.

Lab#	Temp (°C)	$^{40}Ar/^{39}Ar$	$^{37}Ar/^{39}Ar$	$^{36}Ar/^{39}Ar$	$^{39}Ar_K$ (moles)	K/Ca	Cl/K	$^{40}Ar^*$ (%)	Cum. ^{39}Ar (%)	Age (ka)	Err (1σ)
E93021: SE of Hooper's Shoulder Cone, 115.5 mg anorth. (~2% glass) J=0.0000755±0.0000002 Disc. = 286.2											
2645-01A	550	2.00e+02	2.84e-01	6.64e-01	3.9e-16	1.8	1.8e-02	1.8	0.87	502 ±	1294
2645-01B	700	1.23e+01	5.96e-01	3.89e-02	2.7e-15	0.9	5.6e-04	6.6	6.81	111 ±	18
2645-01C	800	4.85e+00	5.72e-01	1.40e-02	9.6e-15	0.9	1.2e-04	15.1	28.15	100 ±	6
2645-01D	900	4.52e+00	5.67e-01	1.22e-02	7.2e-15	0.9	1.0e-04	20.6	44.28	127 ±	7
2645-01E	1000	4.31e+00	5.66e-01	1.19e-02	7.1e-15	0.9	5.7e-05	18.9	60.06	111 ±	6
2645-01F	1100	5.07e+00	5.59e-01	1.47e-02	6.2e-15	0.9	6.2e-04	14.7	73.91	102 ±	7
2645-01G	1200	1.15e+01	5.52e-01	3.41e-02	3.1e-15	0.9	1.5e-02	12.4	80.78	194 ±	16
2645-01H	1300	5.44e+00	5.24e-01	1.28e-02	8.6e-16	1.0	2.0e-03	30.8	82.71	228 ±	22
2645-01I	1400	2.48e+00	5.68e-01	4.15e-03	2.8e-15	0.9	9.0e-04	51.5	88.91	174 ±	7
2645-01J	1550	4.62e+00	5.77e-01	1.14e-02	2.2e-15	0.9	1.1e-03	27.5	93.79	173 ±	11
2645-01K	1750	2.44e+01	5.62e-01	7.69e-02	2.4e-15	0.9	2.5e-04	6.9	99.21	230 ±	29
2645-01L	1750	1.28e+02	5.53e-01	4.18e-01	3.5e-16	0.9	2.2e-03	3.2	100.00	559 ±	202
total gas age					4.5e-14				n=12	140 ±	20
plateau age							B-F		73.04	110 ±	6
isochron age				$^{40}Ar/^{36}Ar$ = 298.4 ± 2.3			MSWD = 20.6			124 ±	4
E93020: William's Cliff, 109.0 mg anorth. (~2% glass) J=0.0000758±0.0000002 Disc. = 286.2											
2648-01A	550	1.88e+02	6.96e-01	6.52e-01	2.3e-16	0.7	3.3e-02	-2.7	0.67	-703 ±	926
2648-01B	700	1.48e+01	8.19e-01	4.86e-02	2.8e-15	0.6	4.5e-04	3.1	8.71	63 ±	19
2648-01C	800	7.86e+00	8.07e-01	2.53e-02	6.1e-15	0.6	8.2e-04	5.5	26.18	60 ±	10
2648-01D	900	6.25e+00	8.30e-01	1.99e-02	4.6e-15	0.6	2.3e-04	6.6	39.27	56 ±	10
2648-01E	1000	6.15e+00	8.37e-01	1.92e-02	3.5e-15	0.6	4.6e-04	8.3	49.32	70 ±	11
2648-01F	1100	4.87e+00	8.30e-01	1.51e-02	3.8e-15	0.6	1.4e-03	9.0	60.19	60 ±	9

Table 3. continued...

Lab#	Temp (°C)	$^{40}Ar/^{39}Ar$	$^{37}Ar/^{39}Ar$	$^{36}Ar/^{39}Ar$	$^{39}Ar_K$ (moles)	K/Ca	Cl/K	$^{40}Ar^*$ (%)	Cum. ^{39}Ar (%)	Age (ka)	Err (1σ)
2648-01G	1200	1.22e+01	8.11e-01	4.01e-02	2.4e-15	0.6	2.0e-02	2.8	67.14	46 ±	19
2648-01H	1300	1.57e+01	7.87e-01	5.24e-02	3.5e-15	0.6	1.9e-03	1.7	77.28	36 ±	21
2648-01I	1400	5.90e+00	8.36e-01	1.88e-02	4.2e-15	0.6	1.0e-03	6.4	89.25	52 ±	9
2648-01J	1550	9.18e+00	8.30e-01	3.03e-02	1.0e-15	0.6	1.3e-03	3.0	92.25	38 ±	25
2648-01K	1750	2.74e+01	8.29e-01	9.00e-02	2.2e-15	0.6	6.8e-04	3.1	98.67	118 ±	32
2648-01L	1750	6.53e+01	8.17e-01	2.17e-01	4.6e-16	0.6	-7.0e-04	2.0	100.00	178 ±	111
total gas age					3.5e-14				n=12	60 ±	20
plateau age							B-J		91.58	57 ±	5
isochron age				$^{40}Ar/^{36}Ar$ = 293.1 ± 2.9			MSWD = 0.5			65 ±	9
E81002: Abbott Peak tephriphonolite, 107.6 mg plag. (<1% glass) J=0.0000702±0.0000002 Disc. = 288.0											
1326-01A	550	3.67e+03	3.16e+00	1.23e+01	1.6e-17	0.2	3.4e-02	0.6	0.36	2826 ±	31565
1326-01B	700	2.03e+02	4.65e+00	6.77e-01	2.5e-16	0.1	1.4e-03	1.6	6.22	420 ±	143
1326-01C	800	8.91e+00	5.04e+00	1.68e-02	1.2e-15	0.1	3.9e-04	48.3	34.77	546 ±	8
1326-01D	900	5.84e+00	5.26e+00	6.23e-03	8.7e-16	0.1	3.7e-04	75.0	55.13	556 ±	10
1326-01E	1000	6.52e+00	4.42e+00	1.08e-02	6.7e-16	0.1	9.7e-04	55.9	70.85	463 ±	13
1326-01F	1100	6.52e+00	4.77e+00	1.03e-02	3.6e-16	0.1	9.0e-04	58.7	79.12	486 ±	30
1326-01G	1200	5.98e+00	4.00e+00	5.80e-03	2.5e-16	0.1	2.4e-03	76.1	84.86	578 ±	38
1326-01H	1300	2.93e+00	3.52e+00	-2.47e-04	1.1e-16	0.1	4.6e-03	111.0	87.52	412 ±	93
1326-01I	1400	2.35e+01	4.54e+00	6.01e-02	1.7e-16	0.1	3.4e-03	25.7	91.50	767 ±	67
1326-01J	1500	1.93e+01	3.96e+00	5.47e-02	2.3e-16	0.1	2.6e-03	17.8	96.88	437 ±	34
1326-01K	1550	1.25e+02	5.39e+00	3.98e-01	7.1e-17	0.1	7.2e-04	6.6	98.53	1044 ±	251
1326-01L	1550	1.46e+02	3.90e+00	4.79e-01	6.3e-17	0.1	2.6e-03	3.5	100.00	647 ±	232
total gas age					4.3e-15				n=12	540 ±	150
plateau age							B-F		78.76	531 ±	19
isochron age				$^{40}Ar/^{36}Ar$ = 295.0 ± 4.1			MSWD = 15.3			536 ±	7

Table 3 continued...

Lab#	Temp (°C)	$^{40}Ar/^{39}Ar$	$^{37}Ar/^{39}Ar$	$^{36}Ar/^{39}Ar$	$^{39}Ar_K$ (moles)	K/Ca	Cl/K	$^{40}Ar^*$ (%)	Cum. ^{39}Ar (%)	Age (ka)	Err (1σ)
E93032: Cape Barne basanite 103.7 mg groundmass				**J=0.0000759±0.0000002**			**Disc. = 286.2**				
2658-01A	550	2.16e+01	7.91e-01	4.61e-02	2.3e-15	0.6	8.4e-02	37.0	7.02	1096 ±	119
2658-01B	650	1.31e+01	7.11e-01	1.18e-02	5.2e-15	0.7	6.4e-02	73.7	22.64	1322 ±	41
2658-01C	775	1.28e+01	6.43e-01	1.03e-02	1.2e-14	0.8	7.6e-02	76.3	59.24	1338 ±	22
2658-01D	900	1.53e+01	8.19e-01	1.75e-02	7.6e-15	0.6	6.4e-02	66.6	82.04	1401 ±	33
2658-01E	1000	2.20e+01	1.85e+00	4.48e-02	2.0e-15	0.3	5.4e-02	40.4	88.09	1219 ±	79
2658-01F	1100	2.38e+01	3.77e+00	5.13e-02	1.2e-15	0.1	4.0e-02	37.5	91.72	1227 ±	60
2658-01G	1250	4.08e+01	1.28e+01	1.11e-01	2.3e-15	0.0	1.3e-01	22.2	98.61	1253 ±	48
2658-01H	1400	8.20e+01	1.85e+01	2.41e-01	2.1e-16	0.0	1.4e-01	14.8	99.23	1685 ±	363
2658-01I	1750	6.38e+01	8.24e+00	1.81e-01	1.8e-16	0.1	2.6e-02	16.9	99.76	1483 ±	771
2658-01J	1750	5.51e+01	6.64e+00	1.66e-01	7.9e-17	0.1	1.6e-03	11.9	100.00	903 ±	437
total gas age					3.3e-14				n=10	1320 ±	50
plateau age							A-G		98.61	1330 ±	30
isochron age				$^{40}Ar/^{36}Ar$ = 288.9 ± 3.3			MSWD = 2.3			1355 ±	18

Errors are given at 1σ and include the uncertainty in J-values (±0.25%).
Plateau ages are weighted by the inverse of the variance whereas total gas ages are weighted by ^{39}Ar.
All isotopic ratios are corrected for sytstem blank, nuclear interference reactions and radioactive decay ($^{37}Ar_{Ca}$).
$(^{40}Ar/^{39}Ar)_K = 0.022$; $K/Ca = .510 \times (^{39}Ar_K/^{37}Ar_{Ca})$; $Cl/K = .277 \times (^{39}Ar_K/^{38}Ar_{Cl})$
Ages are calculated using the decay constants recommended by Steiger and Jagar (1977).

than 50% of the ^{39}Ar, where the steps are analytically indiscernible at 2σ (Fleck et al. 1977)). Isotope correlation diagrams plotted for the younger anorthoclase samples are commonly discordant with MSWD's greater than 10 although apparent ages yielded by the 'errorchrons' usually agree with plateau ages at 1σ (figures 3 and 4).

The spectrum for an anorthoclase separate from Williams Cliff (Fig. 4) differs from other Mt. Erebus anorthoclase samples. Unlike most other anorthoclase spectra, the sample from Williams Cliff does not show an increase in apparent with an increase in Cl/K ratio. This suggests that melt inclusions are present within the anorthoclase but do not contain significant quantities of excess argon. Similar behavior was noted for anorthoclase samples from a Cape Barne tephriphonolite (e.g. #836). Multiple samples (#836, 838, 839, 840) yielded similar plateau and total fusion ages regardless of the quantities of melt inclusions.

A somewhat discordant or irregular spectra is typical for the plagioclase and groundmass. This reflects the young ages and low potassium content in the plagioclase as well as the multiple potassium-bearing phases likely still within the groundmass (McDougall and Harrison 1988). For most plagioclase and groundmass samples Cl/K and K/Ca ratios are not correlative with increases in apparent age and do not aid in the interpretation of the age spectra. In most cases, mean ages for plagioclase and groundmass samples were derived from the flattest and youngest portions of the age spectra (figures 5 and 6).

Isotope correlation diagrams or inverse isochrons were used for those plagioclase and groundmass samples displaying extreme age spectrum variability. Age spectra are calculated using an assumed trapped $^{40}Ar/^{36}Ar$ ratio of 295.5. However, an inverse isochron ($^{39}Ar/^{40}Ar$ vs. $^{36}Ar/^{40}Ar$) can be used to independently determine the $^{40}Ar/^{36}Ar$ value of the trapped gas. For those samples in which an inverse isochron was used, $^{40}Ar/^{36}Ar$ ratios indicate a trapped component greater than 295.5. The mean square of the

weighted deviates (MSWD) for the inverse isochron samples were mostly between 1.0 and 6.0, with the higher values probably reflecting a heterogeneity in trapped argon compositions.

Discussion

$^{40}Ar/^{39}Ar$ apparent ages for Mt. Erebus samples are as much as one order of magnitude younger and more precise than samples dated previously by the conventional K/Ar method (Treves 1968; Armstrong 1978; and Moore and Kyle 1987). Conventional K/Ar results from anorthoclase at Cape Barne and Cape Royds yielded results of 965±50 ka and 698±140 ka, respectively (Treves 1968; Armstrong 1978), whereas the $^{40}Ar/^{39}Ar$ ages are 89±1 ka and 73±5 ka, respectively (Table 4). The discrepancy between K/Ar ages and $^{40}Ar/^{39}Ar$ ages can largely be explained by the affect of melt-inclusion excess argon although there is evidence that some Mt. Erebus anorthoclase melt inclusions contain only minimal amounts of excess argon. $^{40}Ar/^{39}Ar$ apparent plateau ages for four samples of a Cape Barne anorthoclase (two glassy and two 'pure') are identical at 1σ regardless of their individual Cl/K ratios. By comparison, a $^{40}Ar/^{39}Ar$ plateau age for 'pure' anorthoclase from the upper flank outcrop of Hooper's Shoulder was 32±5 ka, whereas the mean age for the 'glassy' Hooper's Shoulder anorthoclase over the same temperature interval was 84±12 ka.

For samples with both paleomagnetic data and $^{40}Ar/^{39}Ar$ age data there is good agreement to the geomagnetic polarity time scale (figure 7). Of the seven paleomagnetic directions determined for samples dated in this study, only two are reversed: the Cape Barne dike and the Fang Ridge tephrite. The $^{40}Ar/^{39}Ar$ apparent ages for these two samples fall within the Matuyama reverse polarity interval (1757-1049 ka; Cande and Kent 1992). The two Fang Ridge samples (normal polarity) fall near the beginning of the Brunhes normal polarity event (780-0 ka; Cande and Kent 1992). The remaining three samples are significantly less than 700 ka ($^{40}Ar/^{39}Ar$) and have normal polarity.

Table 4. Comparison of conventional K/Ar dates from previous authors and $^{40}Ar/^{39}Ar$ dates from this study.

		Conventional K/Ar ages (previous workers)	**$^{40}Ar/^{39}Ar$ ages** (this study)
Location	Material	Age (ka) ± Error (1σ)	Age (ka) ± Error (1σ)
Cape Barne	anorthoclase	965 ± 50	89 ± 1
Cape Barne	groundmass	821 ± 20	1311 ± 8
Fang Ridge	groundmass	832 ± 20	1070 ± 90
Fang Ridge	plagioclase	750 ± 70	758 ± 10
Cape Royds	anorthoclase	698 ± 140	73 ± 5
Turks Head	gm/plagioclase	860 ± 200	378 ± 14

† All ages are calculated to decay constants proposed by Steiger and Jager (1977) using the procedure of Dalrymple (1979)

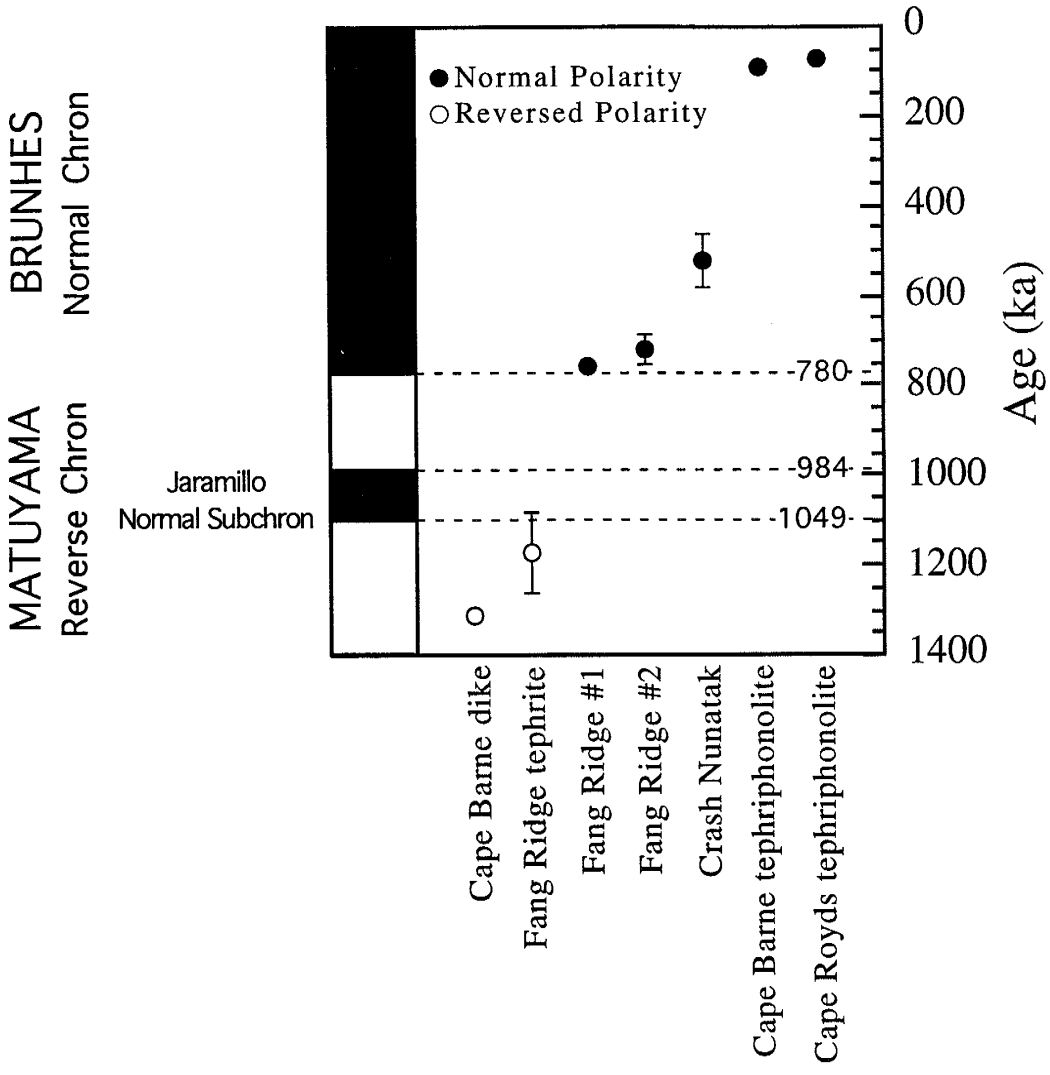

Figure 7. $^{40}Ar/^{39}Ar$ apparent age/paleomagnetic correlations for Mt. Erebus lava flows where magnetic directions are known. Cape Royds paleomagnetic samples are from Funaki (1983) while Cape Barne tephriphonolite and dike are from Mankinen and Cox (1988). All other data are from this study. Errors on ages are one sigma and in some cases are smaller than the symbol.

It is important to stress that all of the $^{40}Ar/^{39}Ar$ apparent ages from Mt. Erebus are maxima. Based on the accuracy of the zero-age anorthoclase analyses (Esser et al. 1996), a general geological error may be added to the analytical error of the non-zero-age samples from Mt. Erebus. Assuming the non-zero age anorthoclase samples are as pure as the purest zero-age anorthoclase samples, an uncertainty of ±20 ka may be appended to the apparent ages of all anorthoclase samples. However, this added uncertainty is probably not appropriate for some anorthoclase samples which show little or no evidence of excess argon (e.g. Cape Barne and possibly William's Cliff). Regardless, the $^{40}Ar/^{39}Ar$ apparent ages of this study represent a significant increase in the overall precision of dating young anorthoclase from Mt. Erebus and therefore allow a more comprehensive volcanic evolutionary model to be derived.

Volcanic Evolution

An evolutionary model for the Mt. Erebus volcanic edifice combining all of the geologic and geochemical data with the $^{40}Ar/^{39}Ar$ age data is presented in this study. Several stages or periods of eruptive activity can be inferred from the $^{40}Ar/^{39}Ar$ apparent ages. The highlights of eruptive activity from these stages are presented in this section and incorporate inferences where geological, geochemical or geochronological data is lacking. A generalized cartoon of the volcanic evolution based on the data from this study is presented in figure 8 through figure 13.

>1311-1000 ka: Shield Building Phase

Initial eruptive activity at Ross Island and Mt. Erebus probably involved the extrusion of basanitic pillow lava onto the floor of the Ross Sea. However, as is the case with most volcanoes, these earliest eruptive products have been buried by subsequent activity. The current Ross Sea depth is greater than 700 meters less than 10 km off shore (1:250,000 USGS Map of Ross Island). Although water depths have presumably been affected by sea level fluctuations and isostatic subsidence, the initial eruptive environment at Ross Island was certainly submarine. Unequivocal evidence for subaqueously erupted

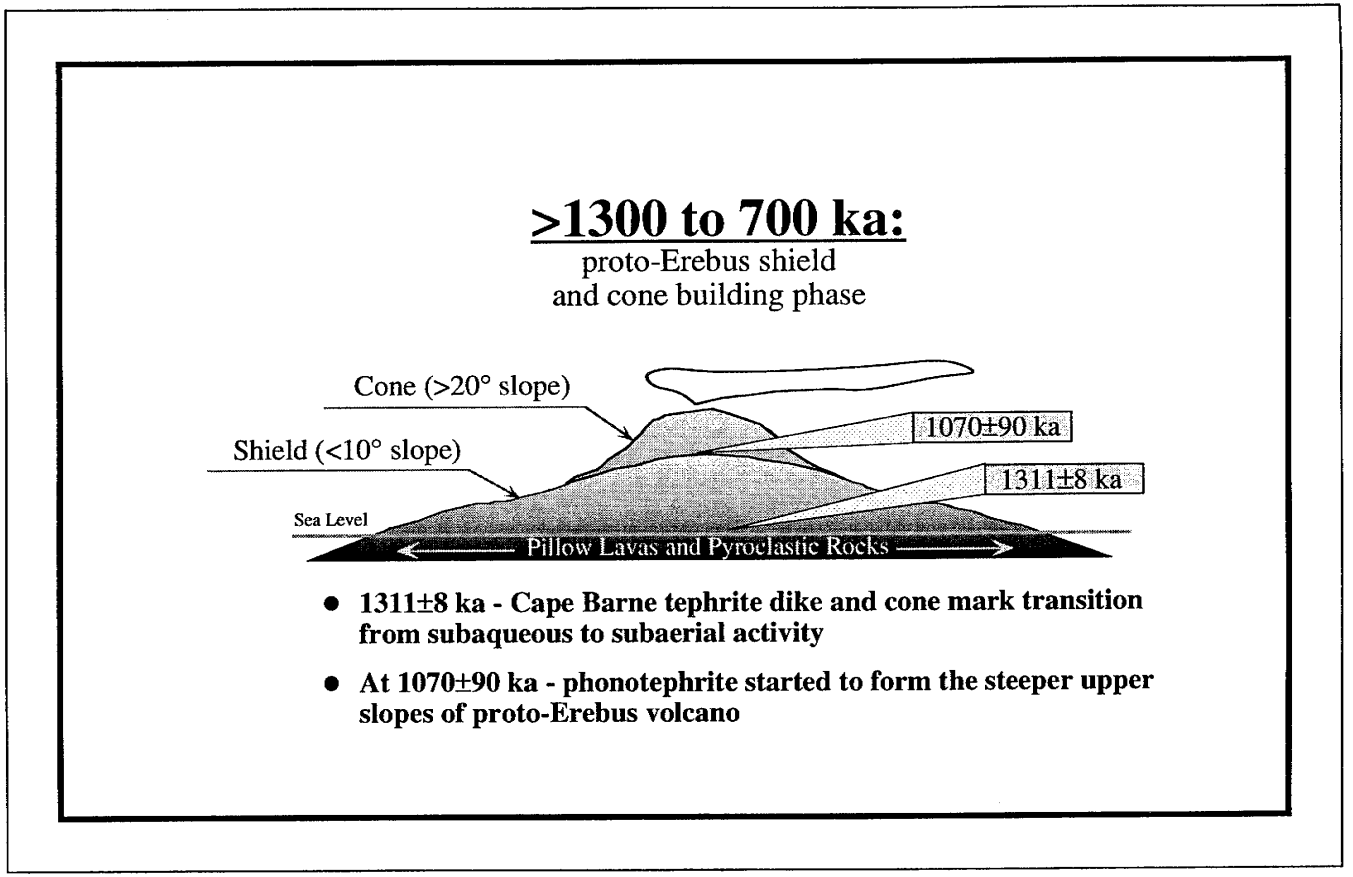

Figure 8. Evolutionary cartoon for Mt. Erebus from greater than 1300 to 700 ka.

Ross Island volcanic rocks was recovered by the Dry Valley Drilling Project (DVDP) cores 1, 2 and 3 at Hut Point Peninsula (Kyle 1981a). K-Ar dates on drill core basanitic hyaloclastites (1340±230 ka) (Kyle 1981a) are contemporaneous with the earliest dated activity on Mt. Erebus.

The oldest dated volcanic rock (1311±8 ka) is from a highly fractured and weathered tephritic dike intruding a cone of palagonitized hyaloclastite tuff at Cape Barne. The tuff cone has characteristics of both subaerial and subaqueous volcanic activity (Moore and Kyle 1987). This exposure apparently marks a transition from subaqueous to subaerial activity at this location at 1300 ka.

Alternatively, the Cape Barne dike may be a parasitic or lateral eruption which occurred after the extrusion of a subaerial proto-Erebus foundation. The earliest dated activity on Ross Island is a trachyte on Mount Bird of 4.5 Ma (Armstrong 1978). Assuming Ross Island represents the center of a mantle plume where the centers are controlled by associated crustal doming (Kyle et al. 1992), it is difficult to invoke a model whereby Mount Bird and possibly Mount Terror could have erupted large volumes of lava (~470 km^3 and ~1700 km^3, respectively) without contemporaneous activity occurring in the center of Ross Island (i.e. Mt. Erebus). Even without a mantle plume controlling the volcanism on Ross Island, overlap of Armstrong's K/Ar dates for Mount Terror, Hut Point Peninsula and, to a lesser extent, Mount Bird suggest approximately simultaneous activity. It may be assumed that early activity at Mount Erebus was also simultaneous. Accordingly, significant volumes of Mt. Erebus may have been extruded prior to the eruption of the tephrite at Cape Barne. However, as with most volcanoes, this earliest history of Mt. Erebus remains ambiguous with respect to timing and duration and may only be resolved with the aid of scientific drilling similar to that of the Dry Valley Drilling Project.

Following the emplacement of the Cape Barne cones and associated dike at 1311±8 ka, subaerial vents probably continued to erupt undifferentiated basanitic/tephritic lava.

These relatively low viscosity lavas likely formed the broad shield-like platform (slope≈9°) visible today at elevations between 0 and 1,600 meters above sea level. The basanite/tephrite shield reached a final elevation of at least 2,600 meters above sea level approximately one million years ago, as revealed by the current elevation of a 1070±90 ka basanite/tephrite flow at Fang Ridge that is presumed to be one of the last flows of this composition on Mt. Erebus.

~1000-350 ka: Proto-Erebus Cone Building Phase

Between approximately 1150 and 950 ka, the basanitic/tephritic activity on Mt. Erebus gave way to slightly more differentiated lavas including phonotephrite and tephriphonolite. The presumably more viscous phonotephrites and tephriphonolites rest immediately on top of the older, less differentiated lavas and apparently contributed to the construction of the steeper upper slopes of proto-Erebus which are currently preserved at Fang Ridge. Slopes in excess of 35°, above elevations of 2,000 meters, contrast sharply to the shallow 9° slopes of the lower shield. Although stratigraphic and $^{40}Ar/^{39}Ar$ age relationships verify the relative petrologic development at Fang Ridge (Moore and Kyle 1987), large uncertainties in the apparent ages for those samples (e.g. 1070±90 ka) hamper the formulation of a detailed geologic history. According to $^{40}Ar/^{39}Ar$ results, a minimum of 210 ky elapsed between the eruptions of the Fang Ridge basanite and tephriphonolite. This relatively large time span indicates the emplacement of less than 200 meters of vertically stacked flows, significantly less than what is presumed for earlier (and observed for later) Mt. Erebus activity. Alternatively, the halt in tephrite activity could mark a period of repose whereby magma chamber differentiation occurred producing the phonotephrites and tephriphonolites.

Following the eruption of the youngest Fang Ridge tephriphonolites at 758±10 and 718±33 ka, a caldera forming event created a large escarpment from the upper flank area of proto-Erebus. This escarpment today manifests itself as Fang Ridge, a prominent NW to SE striking ridge with a steep (>35°), northeast facing slope and a vertical, southwest

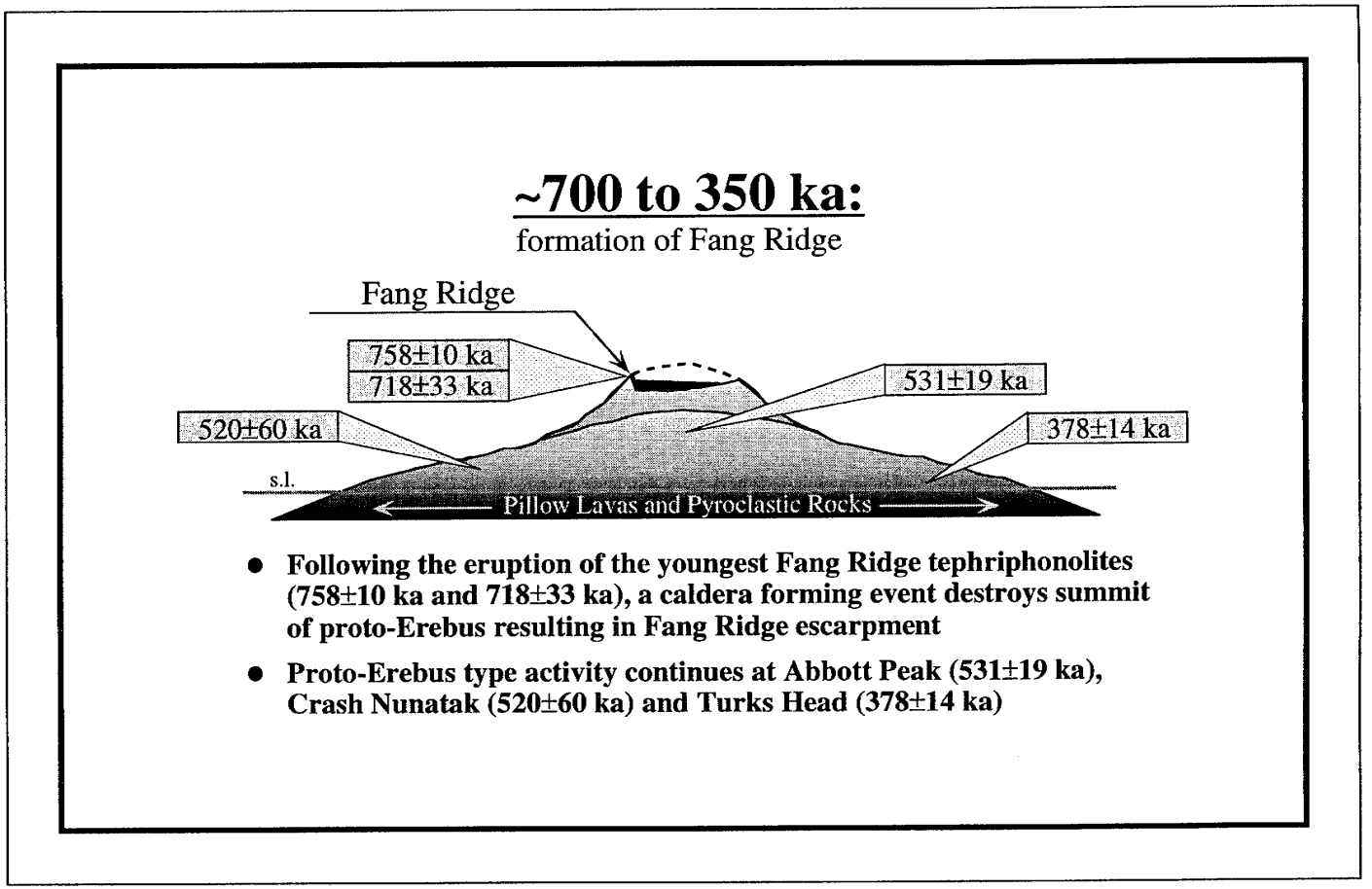

Figure 9. Evolutionary cartoon for Mt. Erebus from about 700 to 350 ka.

facing cliff greater than 150 meters tall. Fang Ridge is a roughly linear feature less than 7 km in length, situated 2,000 to 3,000 meters above sea level and at least 1,000 meters northeast of the steep upper slopes of the anorthoclase phonolite part of Mt. Erebus (figure 1). Although the middle of Fang Ridge achieves a topographic high of greater than 3,000 meters, the southeast and northeast ends of the scarp are about 200 and 400 meters lower in elevation, respectively. These topographically lower margins, especially in the northwest sector, may indicate a breach in the caldera wall either contemporaneous with or subsequent to caldera formation. Both ends of Fang Ridge begin to curve around to the southwest although later anorthoclase phonolite flows obscure the true outline of the caldera. Although a large proportion of the proto-Erebus caldera is buried beneath later anorthoclase phonolite flows, extrapolation of the existing scarp at Fang Ridge suggests a depression approximately 5 km in diameter with an unknown depth (fig. 14).

The two most probable scenarios to account for the large caldera at Fang Ridge are sector collapse or subsidence, however, evidence for either is incomplete. Volcanic sector collapse occurs when interdigitating unconsolidated pyroclastic material and lava result in the gravitational instability of a slope (Siebert 1984). The steep upper slopes and pyroclastic material of proto-Erebus would be sufficient to generate sector collapse. A mass movement occurrence may have been directed to the southwest, leaving Fang Ridge relatively intact (figure 14). Although a large volume of anorthoclase phonolite (modern-Mt. Erebus) lies directly southwest of Fang Ridge, no identifiable remains of the collapse feature are found down slope of what would have been the proto-Erebus summit. While it is possible that the younger anorthoclase phonolite flows (e.g. Hooper's Shoulder, Three Sister's Cones, William's Cliff, etc.) conceal the majority of the flank deposits, the long run-out distances typical of volcanic collapse features (Siebert 1984) may mean that any collapse deposits are concealed beneath McMurdo Sound. To date, no deposits resembling collapse breccia have been identified anywhere on Mt. Erebus.

Subsidence, rather than sector collapse, may have created Fang Ridge and its associated caldera. Caldera subsidence occurs 1) when large quantities of magma evacuate a magma chamber or dike system leaving the overlying crust unsupported (Macdonald 1965) or 2) when shallow intrusions cause crustal loading (Walker 1988). Both mechanisms result in the collapse of the overlying roof material. However, physical evidence for either mechanism is incomplete. Although volcanoes comparable in composition to Mt. Erebus are known to erupt explosively and non-explosively (Chester et al. 1985; Guest et al. 1988; Johnson 1989; Ancochea et al. 1990; van den Bogaard 1995), the absence of large quantities of primary pyroclastic material at Mt. Erebus likely constrains subsidence to either "passive" magma withdrawal or crustal loading. Passive magma withdrawal is usually characterized by eruptions at non-summit vents (Macdonald, 1965). No lateral or parasitic vents from the presumed time of collapse (circa 700 ka) have been identified on Mt. Erebus. However, concealment by snow, ice, erosion and/or younger flows may make recognition impossible. Similarly, subsidence due to shallow dike and sill loading cannot be confirmed due to the undissected nature of the volcano. Lack of evidence confirming the three caldera-forming scenarios prevents unequivocal interpretation. However, unequivocal evidence for caldera subsidence at the modern-Erebus summit about 90 ka suggests a similar event at proto-Erebus about 700 ka.

$^{40}Ar/^{39}Ar$ dates on the stratigraphically highest Fang Ridge flows indicate that the proto-Erebus collapse occurred after 718±33 ka. Subsequent summit flows would either be ponded or channeled within the caldera margins or through a proposed breach in the northwest sector, respectively (figure 14). However, no post-collapse lavas older than ~550 ka indicative of this scenario have been identified on the summit or flanks of proto-Erebus. Alternatively, the ca. 700 ka tephriphonolite lava flows may mark the beginning of a relatively dormant period in the activity of proto-Erebus. The roughly 100 ky of little to no extrusive activity may have enhanced the chemical differentiation of proto-Erebus lavas resulting in the slightly more evolved tephriphonolites of Abbott Peak and surrounding

areas which range in age from 531±19 to 508±10 ka. At least one flow, Crash Nunatak (520±60 ka), indicates non-summit activity. Had Crash Nunatak originated from the summit, it would have had to have flowed over the top of Fang Ridge or around either side of it to cool in its present location (northeast of Fang Ridge). In each case, the local topography prohibits such flow reaching the location of Crash Nunatak (figure 14). However, burial and erosion by later anorthoclase phonolite flows, as well as glaciation, has obscured the geology necessary for the clarification of events leading up to, and following, the collapse of the Fang Ridge caldera, making any interpretation speculative.

Flank activity more characteristic of proto-Erebus continued after another relative lull between 500 ka and 400 ka with the eruption and emplacement of lavas primarily southwest (430±20 ka), northeast (364±12 ka) and south of Abbott Peak (342±9 ka). The eruptive vents for these flows are unknown but they may have originated from a summit vent (intracaldera) or lateral vent (extracaldera). The phonotephritic chemistry of these flows, as represented by the sample southwest of Abbott Peak, indicates less differentiation than previous tephriphonolitic flows at Abbott Peak (i.e. 536±7 ka). This may suggest the injection of significant quantities of new, undifferentiated basanitic(?) melt into the proto-Erebus plumbing system.

Eruptive activity of unequivocally non-summit origin is found near the southwestern coast at the Dellbridge Islands (figure 1). The Dellbridge Islands consist of sequences of pillow lavas, pyroclastic breccia and individual flows dipping significantly (2-40°) in directions non-normal to the axis of flow from the summit of Mt. Erebus. The islands are interpreted to be the result of remnant cones formed early in the activity at Mt. Erebus (Moore and Kyle 1987). A $^{40}Ar/^{39}Ar$ date on a phonolite from one of the Dellbridge Islands, Inaccessible Island (527±8 ka), and the seemingly accelerated petrologic evolution of the stratigraphically oldest to youngest flows (Moore and Kyle 1987) compared to the rest of the Erebus edifice suggest that the Dellbridge Islands were active for a comparatively

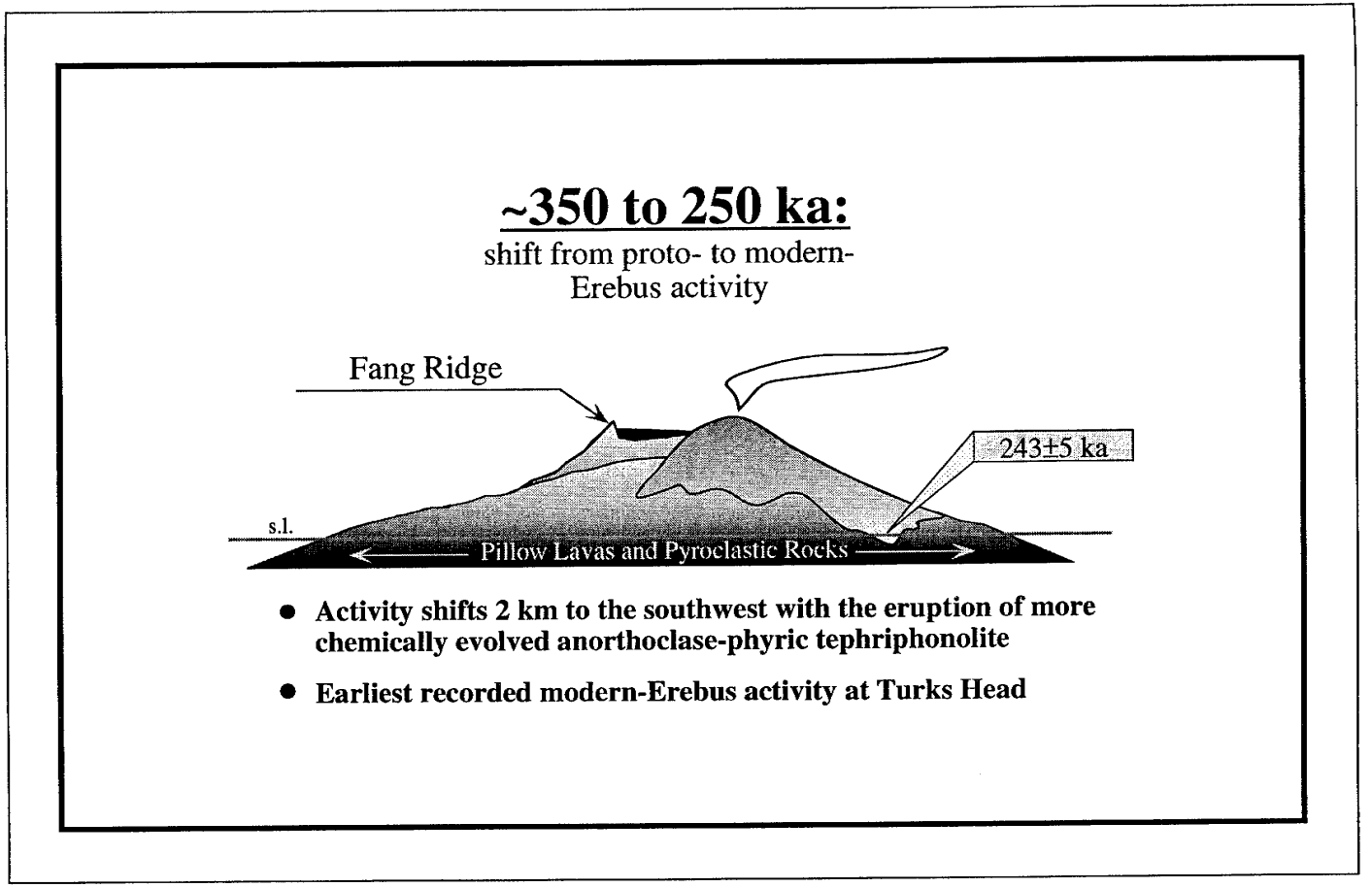

Figure 10. Evolutionary cartoon for Mt. Erebus from about 350 to 250 ka.

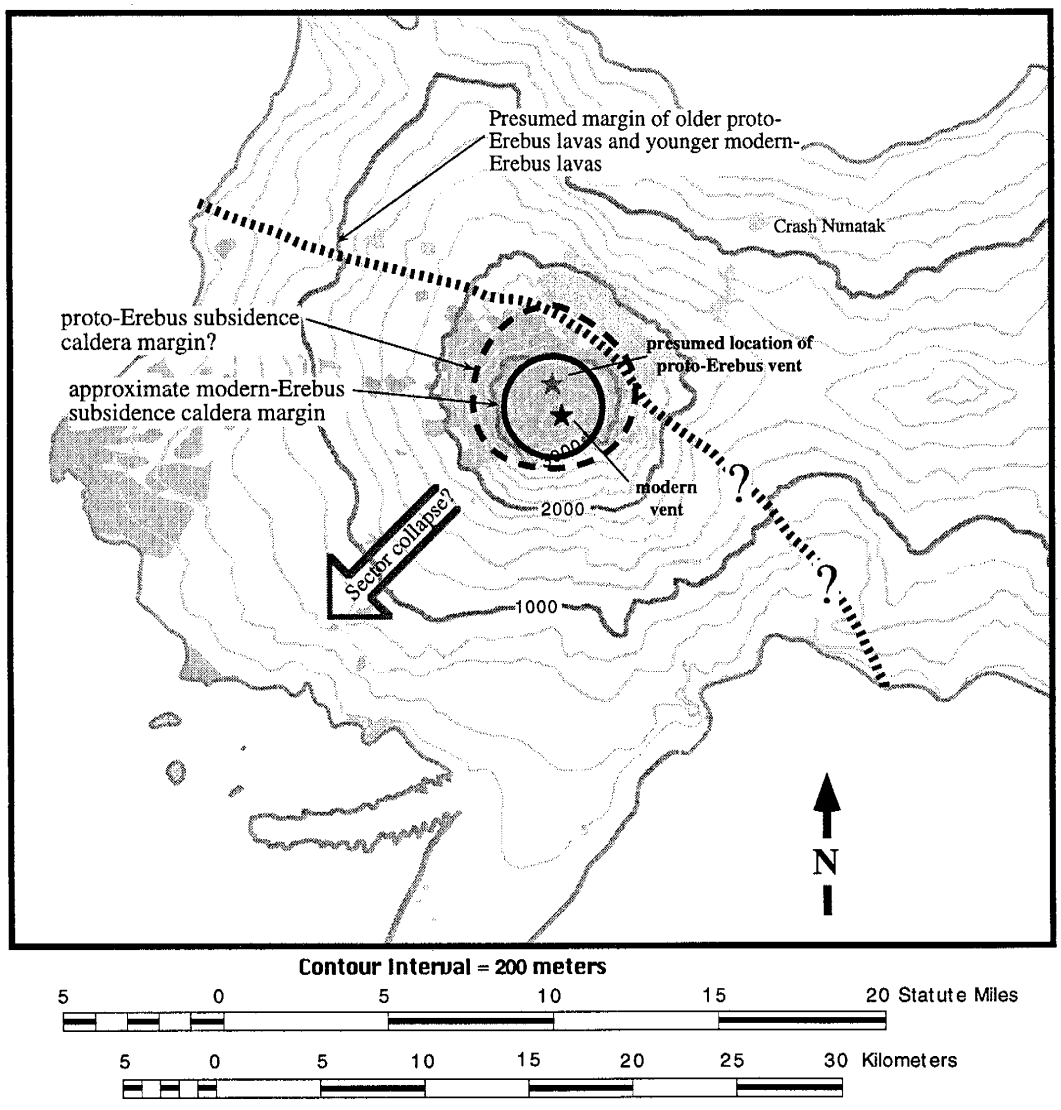

Figure 11. Topographic map of Mt. Erebus showing approximate locations of proto-Erebus (large arrow shows direction of mass movement necessary for sector collapse scenario) and modern-Erebus calderas. Dotted margin separates older, more mafic lavas from the young, anorthoclase-phyric lavas.

short period of time and were erupted from a magma chamber separate from that of Mt. Erebus proper.

The Inaccessible Island phonolite is geochemically more differentiated and mineralogically distinct from contemporaneous proto-Erebus lavas and is stratigraphically overlain by less evolved tephriphonolite (Moore and Kyle 1987). Younger tephriphonolite sequences displaying subaqueous and subaerial activity similar to that at Inaccessible Island have been identified at Turks Head and Tryggve Point, 5 kilometers east of the Dellbridge Islands (Moore and Kyle 1987). Based on the similarities between the Turks Head/Tryggve Point succession and the Dellbridge Island succession, Kyle (1976) and Moore and Kyle (1987) interpret the two locations to be parts of the same eruptive center. Two tephriphonolites at Turks Head and Tryggve Point yield $^{40}Ar/^{39}Ar$ ages of 378±14 and 368±9 ka, respectively. These tephriphonolites at Turks Head and Tryggve Point are geochemically similar to tephriphonolites found at Inaccessible and Tent Island (Moore 1986) and suggest the Dellbridge Islands center was active for over 150 ky.

~250 ka -present: Modern-Erebus Cone Building Phase

Following the cessation of the activity at the Dellbridge Islands, a younger flow (235±4 ka) of slightly more evolved anorthoclase-phyric tephriphonolitic composition unconformably overlies the ca. 375 ka tephriphonolites at Turks Head (Moore and Kyle 1987). Although the 235 ka flow is geochemically similar to the stratigraphically highest flows at Inaccessible and Tent Island (Moore 1986), its source is probably higher up on the slopes (summit?) of the Erebus edifice as suggested by a flow of analytically indistinguishable age (243±9 ka) and similar petrology found 850 meters above sea level at Turks Head. These tephriphonolites may indicate the approximate time when eruptive activity shifted from proto-Erebus flank vents to summit vents marking the cone building phase of modern-Erebus. The presumed morphology of the proto-Erebus caldera relative to the present summit indicates a lateral shift in vent location at least 2 kilometers to the south-southwest.

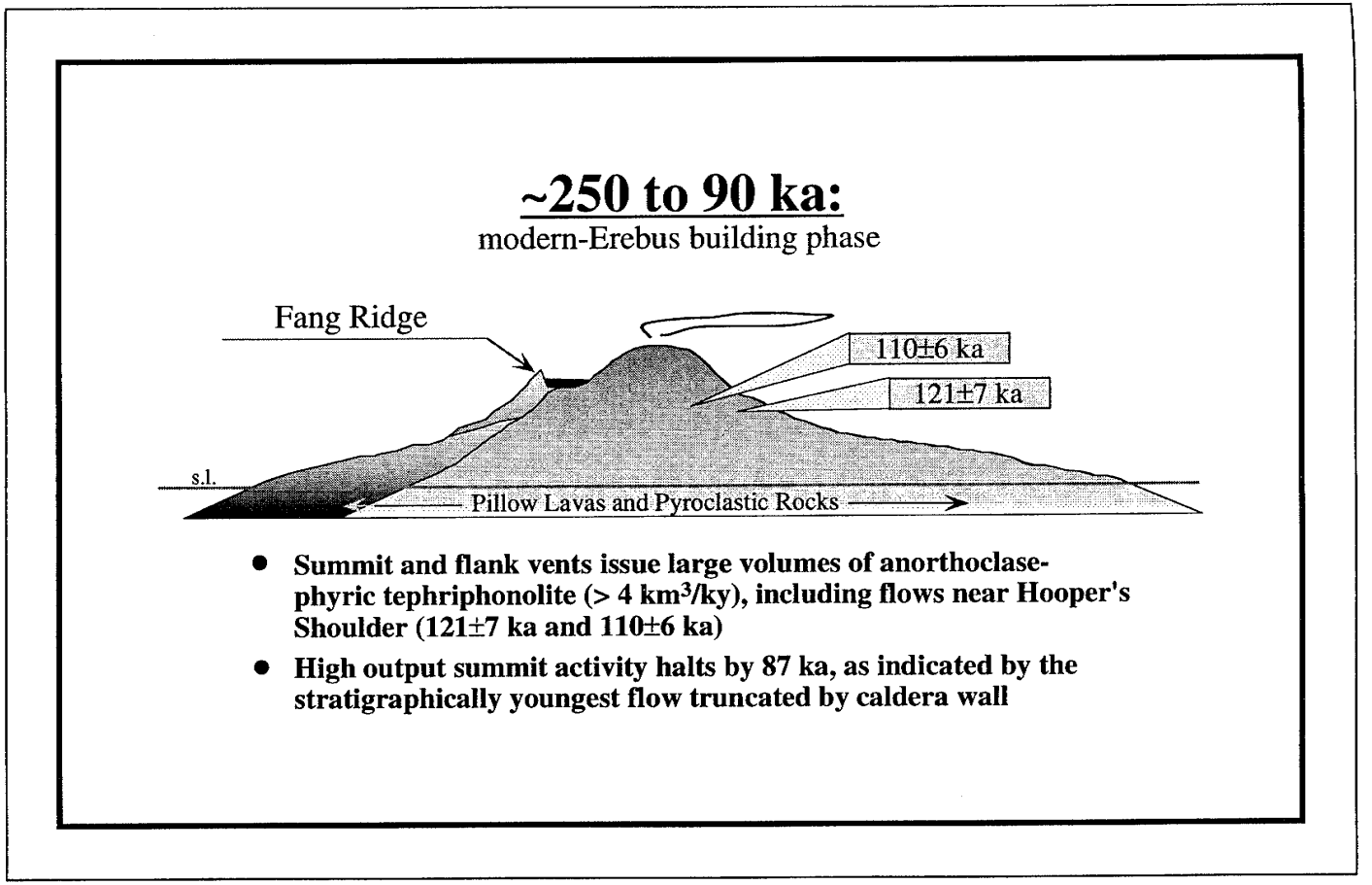

Figure 12. Evolutionary cartoon for Mt. Erebus from about 250 to 90 ka.

Following the eruption and emplacement of the ca. 230 ka tephriphonolite(s) at and above Turks Head, sporadic trachytic activity occurred on the upper and lower flanks of the Erebus edifice (west and southwest sector). Bomb Peak (157±3 ka) is a small (100 meter high) endogenous dome approximately 5 km east and 1,500 meters below the currently active Mt. Erebus summit. Aurora Cliffs (166±5 ka) is a sequence of possibly subglacial to subaerial trachyte on the present shore of Ross Island approximately 15 km south of Bomb Peak (Moore 1986). Both Bomb Peak and Aurora Cliffs are geochemically suggestive of contamination by crustal material (Kyle et al. 1992) and therefore are not representative of the evolution of the Erebus lineage lavas. Due to the similarity in $^{40}Ar/^{39}Ar$ apparent ages and chemical composition, it is conceivable that the trachytes of Bomb Peak and Aurora Cliffs, termed the enriched iron series (EFS) by Kyle et al (1992), evolved by assimilation and fractional crystallization (AFC) of tephriphonolites similar to those found at Turks Head (ca. 250 ka) (Kyle et al. 1992).

After eruption of the trachytes, large volumes of anorthoclase-phyric tephriphonolite continued to issue from vents located at the Mt. Erebus summit and upper flanks. Tephriphonolite sampled from exposures between 1600-1800 meters above sea level on the western flanks of the volcano yield $^{40}Ar/^{39}Ar$ ages of 121±7 and 110±6 ka. While these flows may have erupted from a proposed lateral or flank vent near Hooper's Shoulder (Moore and Kyle 1987), the majority of lava flows during this time period (120-90 ka) likely originated from the summit. This is supported by a large quantity of long (up to 5 km) and large (up to 50 meters wide) flows and flow levees of tephriphonolitic composition exposed on the steep upper slopes of Mt. Erebus. The radiating pattern of these flows indicate their source area was a central summit vent. The radiating lava flows at the summit are truncated by an escarpment whose stratigraphically highest flow has a $^{40}Ar/^{39}Ar$ age of 87±7 ka. The 87±7 ka exposure probably marks the end of these high volume tephriphonolitic lava flows from the summit region as no flows of similar morphology are observed spilling over the escarpment. The time interval between 250 ka

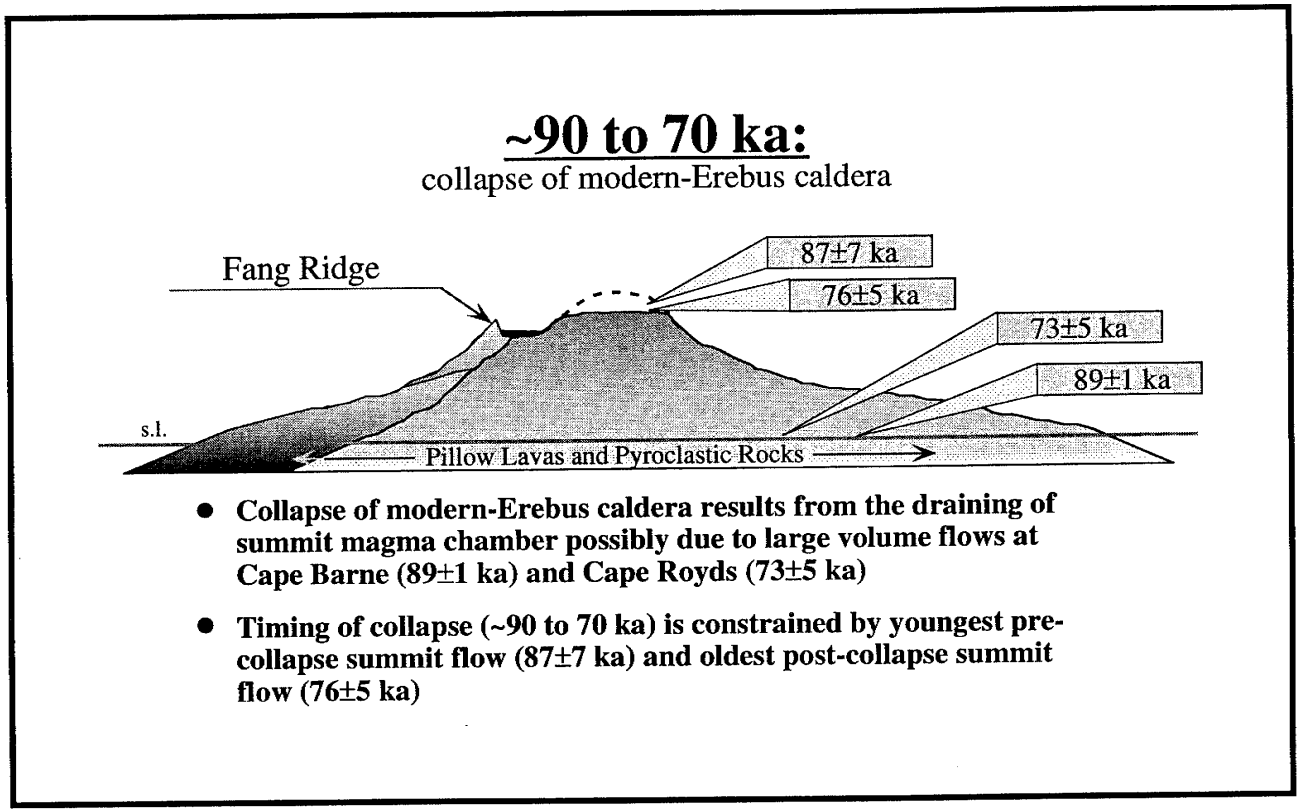

Figure 13. Evolutionary cartoon for Mt. Erebus from about 90 to 70 ka.

and about 90 ka marks an significant increase in Mt. Erebus activity. It is likely that the bulk of the Mt. Erebus volcanic edifice was built during this period.

The escarpment surrounding the present Erebus summit formed by caldera subsidence. Timing of the modern-Erebus caldera formation is constrained by the youngest pre-collapse summit flow (Caldera Rim #1 at 87±7 ka) and the oldest post-collapse summit flow (Northeast Flow at 76±5 ka) which locally spills over the caldera wall. Subsidence by magmatic withdrawal is supported by flows of similar age found on the present shores of Mt. Erebus at Cape Barne (89±1 ka) and Cape Royds (73±5 ka). The large areal extent and large volume of these flows may have emptied the summit magma enough to result in the collapse of the modern-Erebus caldera. Flank and coastal flows of equal or greater volume to those at Capes Barne and Royds also are exposed on Mt. Erebus. However, William's Cliff (57±5 ka), Cape Evans (40±3 ka), Hooper's Shoulder Cone (33±3 ka) and Three Sister's Cones (26±2 ka) are all substantially younger than the proposed time of caldera collapse.

There are 11 mappable anorthoclase phonolite lava flows within the present summit caldera (Caldwell 1989). In addition to the Northeast Flow, two other intra-caldera flows were dated in this study: Nausea Knob (46±9 ka) and Lower Hut Flow (11±4 ka). The Lower Hut Flow is currently the youngest dated lava flow from Mt. Erebus. Although still active, Mt. Erebus eruptions are limited to daily strombolian-type explosions which are responsible for building the pyroclastic cone at the present Erebus summit (Kyle et al 1982). However, because of their undoubtedly young age (less than 11 ka?) and contaminating excess argon, initiation and history of this strombolian activity on Mt. Erebus is currently beyond the ability of $^{40}Ar/^{39}Ar$ to decipher.

Petrologic Evolution

The petrologic evolution of Mt. Erebus lavas has been discussed by Kyle et al. (1992). Combining the geochemical data with the $^{40}Ar/^{39}Ar$ data of this study, a relationship between apparent age and petrologic evolution can be observed.

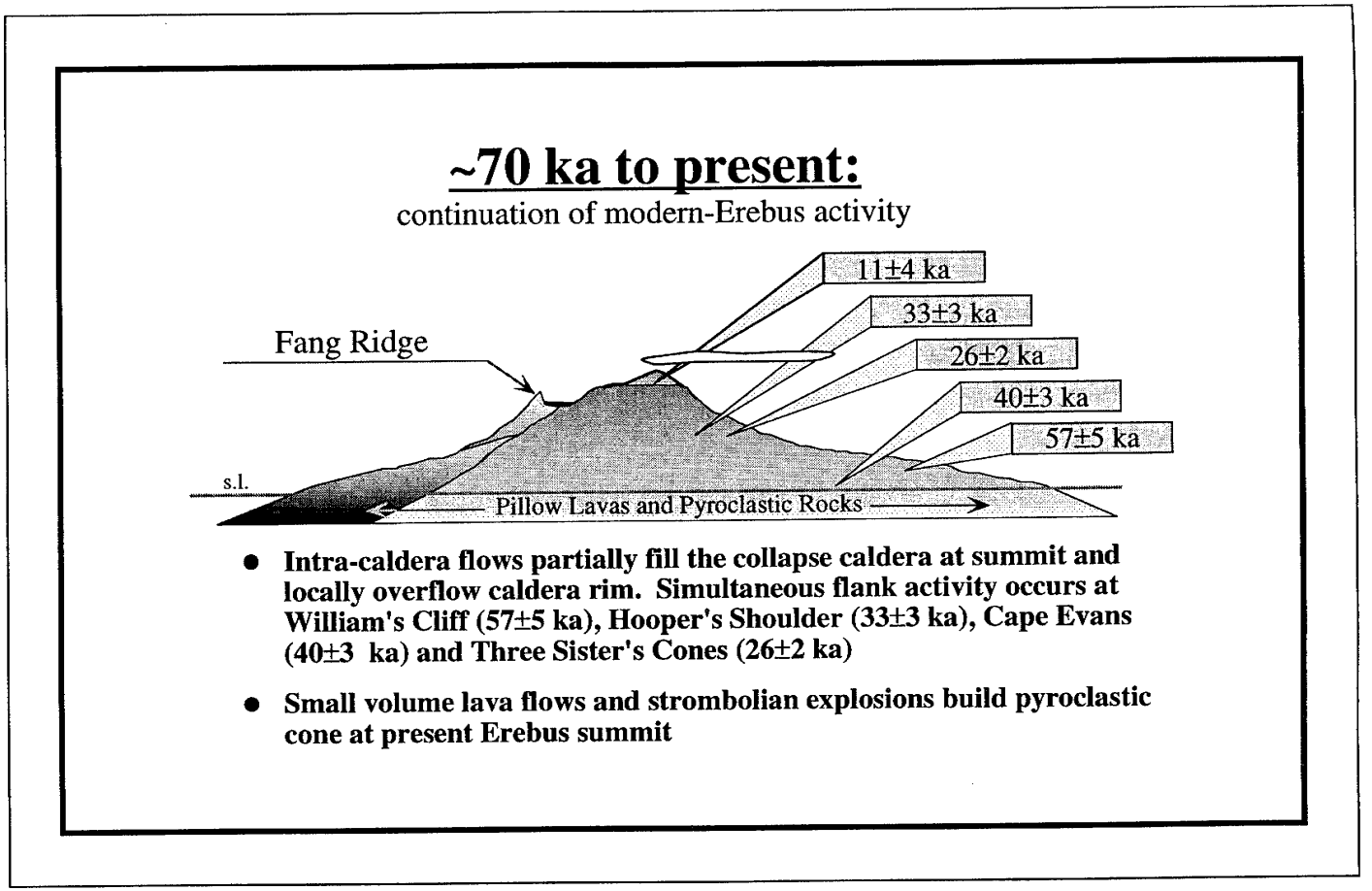

Figure 14. Evolutionary cartoon for Mt. Erebus from about 70 ka to present.

Figure 15 shows a total alkali/silica (TAS) plot for the Mt. Erebus lavas dated in this study, and figure 16 shows the Mg number [100(MgO/(MgO+FeO*)] versus $^{40}Ar/^{39}Ar$ apparent age. Evident is the progression of Erebus lineage rocks from the oldest, least differentiated lavas (basanite/tephrite) of Cape Barne and Fang Ridge to the youngest, most differentiated lavas (anorthoclase phonolite) of the intra-caldera series of modern-Erebus. The petrologic significance of the TAS and Mg# versus age relationships is that Mt. Erebus required approximately one million years to evolve from a basanite magma system to a phonolitic magma system with very few deviations. Volcanoes of similar chemistry have evolved contrasting magma compositions over time spans of only a few hundred thousand years (Anonchea et al. 1990; Panter et al. 1994).

Using the TAS nomenclature (Fig. 15), anorthoclase-phyric phonolite (sensu stricto) does not appear until approximately 75 ka. All lavas older than approximately 33 ka, with the exception of the intra-caldera Northeast Flow (76±5 ka), are tephriphonolite in composition although they petrographically resemble present-day anorthoclase phonolite. This geochemical versus age relationship may indicate that the Northeast Flow is younger than its $^{40}Ar/^{39}Ar$ apparent age suggests, possible due to excess argon. The impact of uncertainty arising from excess argon is the timing of caldera collapse on modern-Erebus. Instead of occurring between 90 and 75 ka, collapse would now be constrained by the ~90 ka date of the Caldera Rim #1 sample and the 46±9 ka date of Nausea Knob. Alternatively, the Northeast Flow may have differentiated to the phonolitic field while an injection of primitive basanitic melt formed the tephriphonolitic magmas of later eruptions (e.g. Cape Evans). However, in the absence of more reliable age data, the date of 76±5 ka for the Northeast Flow is used for the geological interpretations of this study.

Other geochemical deviations are observable on the Mg# versus $^{40}Ar/^{39}Ar$ apparent age plot, especially around 400-500 ka (figure 16). The Abbott Peak tephriphonolite (531±19 ka) has an 'evolved' Mg# of 19 while the phonotephrite SW of Abbott Peak

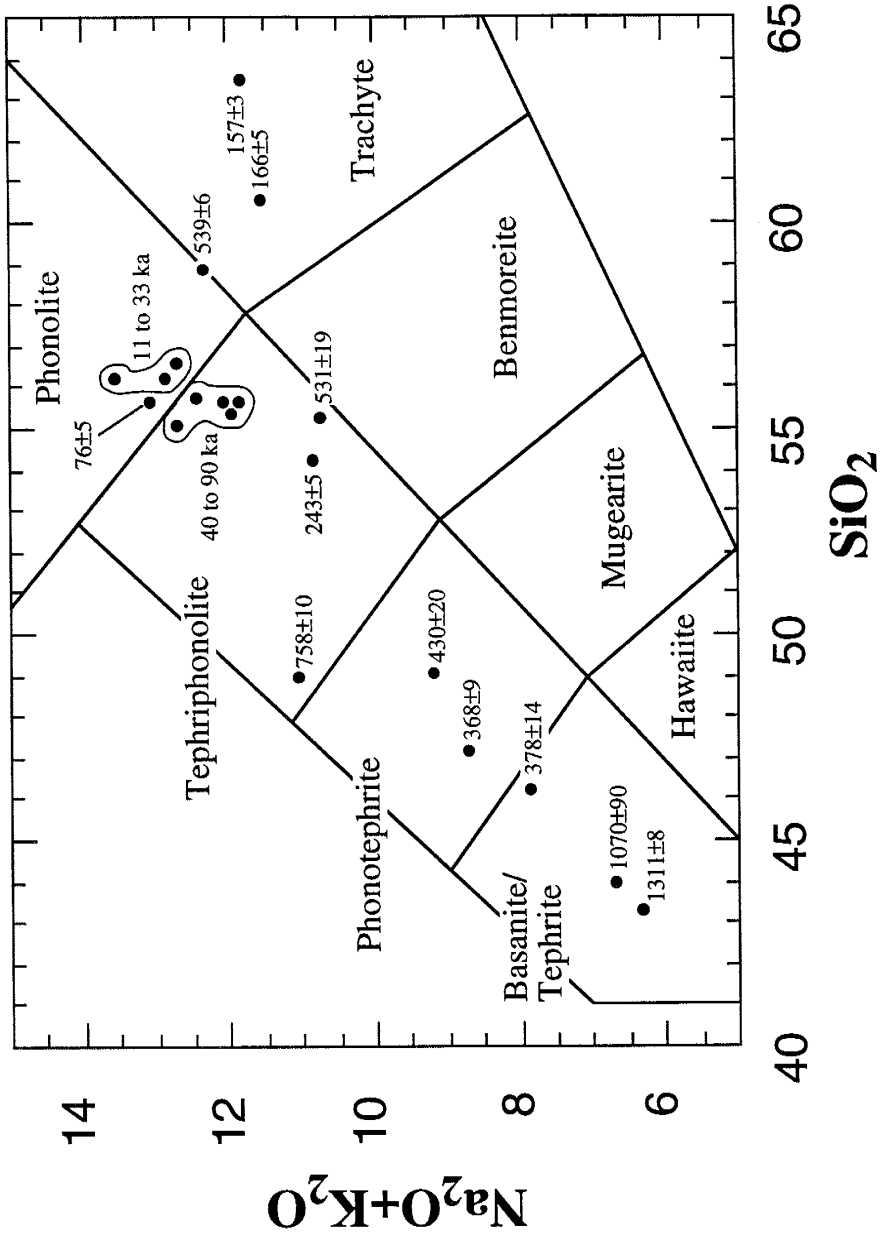

Figure 15. A total alkali-silica (TAS) diagram plotted with Mt. Erebus samples dated in this study. Note the general younging in samples as differentiation increases.

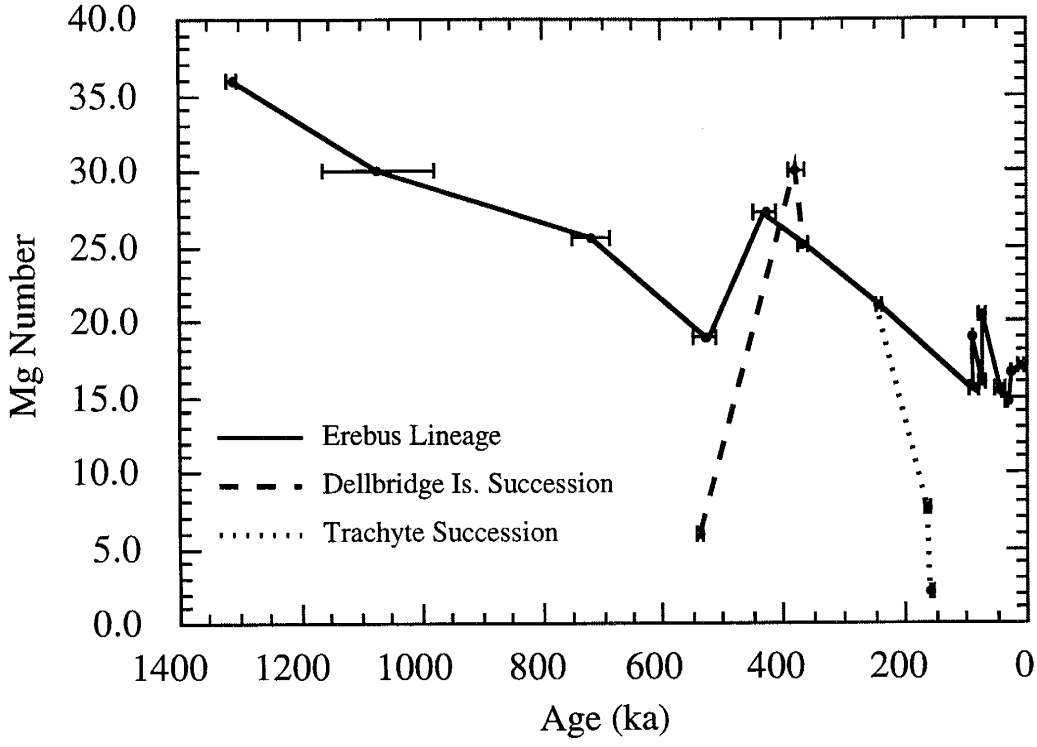

Figure 16. $^{40}Ar/^{39}Ar$ apparent age plotted against Mg number [100(MgO/(MgO+FeO*))] where increasing differentiation is represented by decreasing Mg #. Again, a general younging is apparent as differentiation increases. The Dellbridge Island and trachyte successions are noticeably different than that of the Erebus lineage.

(430±20 ka) has a less 'evolved' Mg# of 27.2, possibly indicating that a large volume of primitive parental basanite was injected into the Erebus magma chamber about 500 ka.

The Dellbridge Island and Bomb Peak/Aurora Cliffs trachytic successions differ from the straightforward evolution of Erebus lineage lavas from Mt. Erebus (figure 16). The Tryggve Point and older Turks Head samples, presumed to be from the Dellbridge Islands succession, are geochemically comparable to Erebus lineage lavas of similar age, but the phonolite from Inaccessible Island is significantly more differentiated than other contemporaneous Erebus lavas. On the Mg# vs. $^{40}Ar/^{39}Ar$ apparent age plot, an independent array can be assigned to the Dellbridge Island succession indicating that these lavas evolved in a magma chamber separate from that of Mt. Erebus. Likewise, the trachytic lavas of Bomb Peak and Aurora Cliffs form another independent array. The origin of this array is suggestive of assimilation and fractional crystallization (AFC) of a melt of similar composition to that of the tephriphonolite from Turks Head (243±5 ka).

Implications

Several implications for the new, younger $^{40}Ar/^{39}Ar$ apparent age data from Mt. Erebus are important. For example, dating of anorthoclase phonolite erratics in Ross Sea drift along the west side of McMurdo Sound (Kyle 1981b) may confirm their derivation from glacially scoured terrains at Capes Barne, Royds and Evans (89-40 ka) thereby better constraining the timing of Ross Sea glaciation. Other fields, such as climatology, may benefit from geochemical/age correlations of Mt. Erebus tephra found within south polar ice cores. Magma generation models of Mt. Erebus can be compared with other similar volcanic regions, possibly improving the understanding of source areas and evolution of alkaline volcanoes.

Eruption Rates and Volumes

Volcanic eruption rates and source output rates for Mt. Erebus have been calculated. Using the duration of volcanism at Mt. Erebus deduced from $^{40}Ar/^{39}Ar$ data, and generalized volumes, eruption rates may be estimated for the proto-Erebus and modern-

Erebus volcanoes. However, several assumptions are involved in these calculations. Most importantly, the volume of the proto-Erebus volcano can easily be calculated only if the shape of the edifice is assumed to be a symmetrical cone. The altitude of Fang Ridge, taken as the height of proto-Erebus, is approximately 3,000 meters above sea level. However, the total volume considers an average depth of 500 meters below sea level as the starting point for initiation of eruptive activity. Using this model height of the generalized cone of proto-Erebus (~3,500 meters), a volume of 1160 km^3 is calculated. Using a model height of 4,300 meters and the same equation for the entire Mt. Erebus edifice, a volume of 2170 km^3 is calculated. Subtracting the proto-Erebus volume from the whole-Erebus volume results in a modern-Erebus volume of 1010 km^3. These model volumes must also assume that there has not been a significant loss of volume due to explosive eruptions. While Mt. Erebus tephra has been discovered in ice sampled ~200 kilometers away from Ross Island (Dunbar et al. 1995) its total volume is probably not significant enough to affect eruption rate calculations.

Initiation of eruptive activity, both for proto-Erebus and modern-Erebus, require some additional assumptions. The tephritic dike at Cape Barne (~1300 ka) will be assumed to represent the initiation of all eruptive activity at Mt. Erebus. Likewise, the tephriphonolite south of Abbott Peak (342±9 ka) will be assumed to represent the cessation of eruptive activity of proto-Erebus. Initiation of modern-Erebus activity likely occurred around 250 ka as suggested by the anorthoclase-phyric tephriphonolite of Turks Head.

Using the model volume data for proto- and modern-Erebus combined with the $^{40}Ar/^{39}Ar$ apparent ages needed for respective life spans, resultant eruption rates for each edifice are distinctly different. The eruptive rates for proto-Erebus, over its ~950,000 year life span, are approximately 1.2 cubic kilometers per 1000 years (km^3/ky). Eruptive rates for modern-Erebus, over its 250,000 life span, are approximately 4.0 km^3/ky. The eruption rate for the entire Mt. Erebus edifice is 1.7 km^3/ky. These differing eruption rates for Mt. Erebus argue against a steady state output rate over the life of the volcano, as

defined for polygenetic volcanoes by Wadge (1982) (i.e. constant rate of magma supply and eruption over a given time period). Although steady state volcanism may have separately occurred for either the proto-Erebus volcano or the modern-Erebus volcano, lack of dates and representative volumes prevent confirmation.

Long-term eruption rates from Mt. Erebus can be compared to the eruption rates of other volcanoes of similar composition. Based on the older K/Ar dates from Armstrong (1978) and generalized model volumes (following those used in this study), Mount Terror, Ross Island has an eruption rate of 1.8 km^3/ky, only slightly higher than that calculated for the entire Mt. Erebus edifice (1.7 km^3/ky). Mount Bird, Ross Island, has a moderate eruption rate of 0.3 km^3/ky. Figure 17 shows a cumulative volume curve for the volcanoes of Ross Island and their respective eruption rates. Mt. Etna, a subduction related volcano of similar size and composition, has a steady state eruption rate of 8.2 km^3/ky (Wadge 1980). Tenerife Island, in the Canary Islands, is an oceanic-island alkaline volcano with an eruption rate for the subaerial portions of the island of 0.2 to 1.8 km^3/ky (Ancochea et al. 1990). Other intraplate volcanoes have eruption rates which are significantly higher than those calculated for Mt. Erebus (e.g. Mauna Loa at 20.8 (Wadge 1980)). The only two intracontinental volcanoes with available data are based on relatively short term eruption records (<200 years), extrapolated here to 1000 years. The resultant eruption rates for Vesuvius (Italy) and Nyamuragira (Africa) are 9.2 and 12.0 km^3/ky, respectively (Wadge 1980). Indications from these data are, that while Mt. Erebus grew at an accelerated rate beginning about 250 ka with eruptions of anorthoclase-phyric tephriphonolite lavas, its eruption rates are significantly lower than those of other volcanoes of similar geochemical composition.

Implications for the calculated eruption rates of Mt. Erebus include the calculation of plume rise rate. Using a simplified equation, Kyle et al. (1992) derived a plume rise rate for Mt. Erebus of approximately 65 mm/year. This rise rate however was determined using conventional K/Ar data of approximately 1 million years (Armstrong 1978). Using

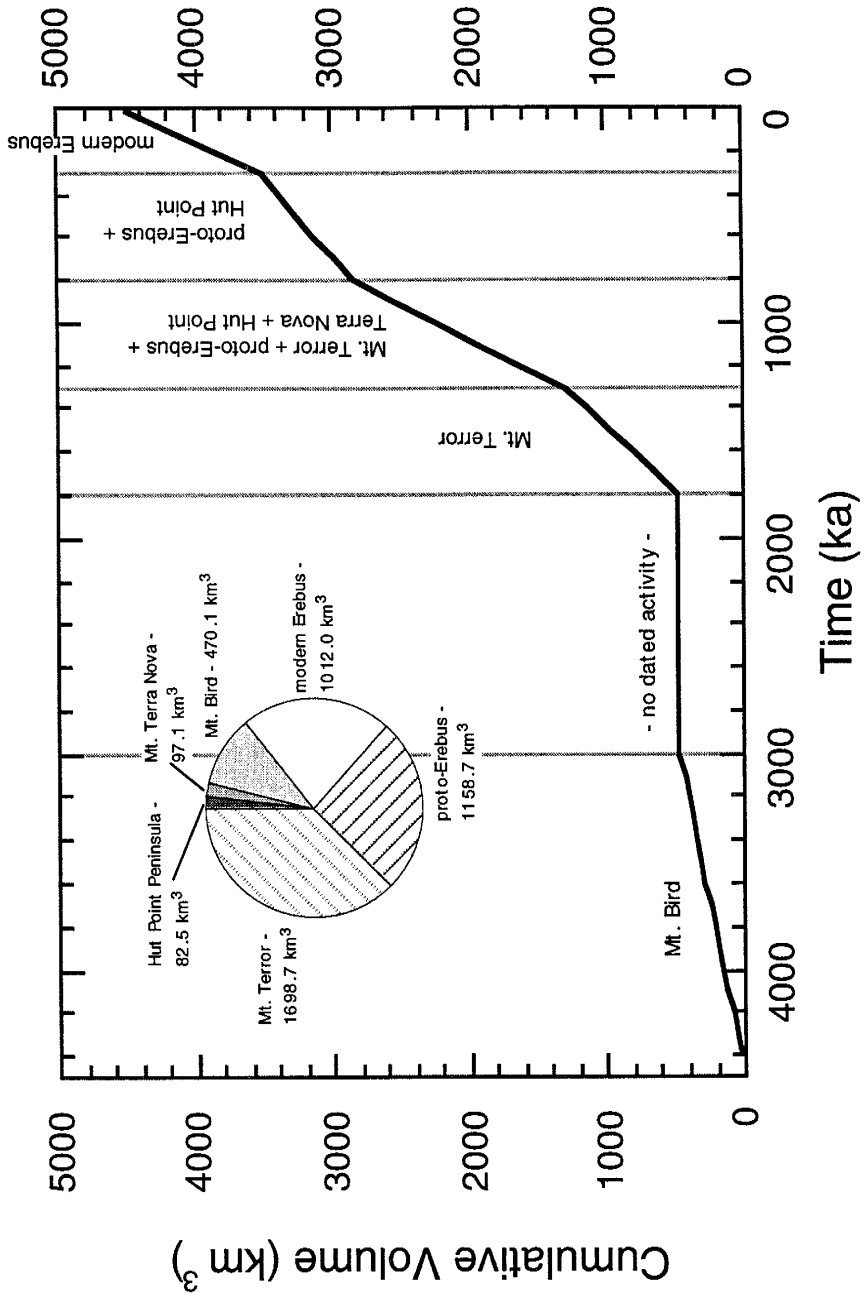

Figure 17. Cumulative volume curve for Ross Island. Overlap occurs (using the K/Ar dates of Armstrong (1978)) from approximately 1250 to 250 ka when multiple centers are contributing to the total volume of Ross Island. Volumes for the individual eruptive centers are shown on the inset pie chart.

the same methods employed by Kyle et al. (1992) with the new $^{40}Ar/^{39}Ar$ apparent ages of this study, a mantle rise rate can be determined for both proto- and modern-Erebus.

Kyle et al. (1992) used values for the extent with which a partial melt of basanite would produce phonolite (25% residual liquid) or phonotephrite (45%) based on the presumed volumes of those respective magma types on Mt. Erebus. These values were then used to calculate the volume of basanite and mantle material necessary to yield the volumes of lava presently observed at Mt. Erebus. Based on the above values, the calculated volumes of parental basanite required to account for the model volumes of proto- and modern-Erebus are 1270 km^3 and 3238 km^3, respectively. Assuming basanite resulted from garnet lherzolite, a 5% degree of partial melting of 25,402 km^3 and 64,768 km^3 of mantle is required to produce the basanite of proto- and modern-Erebus, respectively. Kyle et al. (1992) assumed a plume diameter of 40 km. If the same diameter is used here, cylinders of length 20.2 km (proto-Erebus) and 36.8 km (modern-Erebus) would be necessary to accommodate the large volumes of mantle calculated above. Using the same life spans calculated in the section on eruption rates, plume rise rates for proto-Erebus would be 21.2 mm/yr while modern-Erebus would be 147.3 mm/yr. These high source rise rates, especially for the modern-Erebus lavas (<250 ka), support the conclusion reached by Kyle et al. (1992) that a mantle plume is necessary to account for the large volumes of differentiated lavas found on Mt. Erebus.

Conclusions

For anorthoclase separates believed to contain minimal amounts of contaminating melt inclusions and excess argon, a one order of magnitude increase in analytical precision is observed compared to similar samples analyzed using conventional K/Ar. A similar *decrease* is observed for the apparent ages yielded by the $^{40}Ar/^{39}Ar$ method when compared to the conventional K/Ar results. This is undoubtedly due to the removal of significant quantities of the excess argon contained in melt inclusions through rigorous sample preparation.

Together with the larger number of samples dated, the increase in analytical precision yields a more comprehensive history of the Mt. Erebus edifice. Beginning with the building of a broad, mafic shield volcano at about 1300 ka, the edifice termed proto-Erebus continued to issue tephrites, basanites and phonotephrites until approximately 350 ka. During this time, a caldera forming event occurred after 718 ka, resulting in a remnant escarpment (Fang Ridge). By ~250 ka, activity probably shifted a few kilometers to the southwest and became slightly more differentiated. This was the birth of modern-Erebus activity, characterized by anorthoclase-phyric tephriphonolite and phonolite. A collapse event, similar to the one which occurred about 600 ky ago on proto-Erebus, formed the present modern-Erebus caldera about 75-90 ka. Activity over those 250 ky averaged 4 cubic kilometers of material erupted every 1000 years. This compares to the 1.2 km^3/ky erupted for proto-Erebus over its lifetime. These cone building rates for the two Mt. Erebus edifices are smaller than volcanoes of similar geochemistry and tectonic setting.

References

Ancochea, E., Fuster, J. M., Ibarrola, E., Cendrero, A., Coello, J., Hernan, F., Cantagrel, J. M., and Jamond, C. (1990). Volcanic evolution of the island of Tenerife (Canary Islands) in the light of new K-Ar data. Journal of Volcanology and Geothermal Research 44: 231-249.

Armstrong, R. L. (1978). K-Ar dating: Late Cenozoic McMurdo Volcanic Group and Dry Valley glacial history, Victoria Land, Antarctica. N.Z. Journal of Geology and Geophysics 21: 685-698.

Caldwell, D. A. (1989). "Physical and geochemical properties of summit flows and recent volcanic ejecta from Mount Erebus, Ross Island, Antarctica." Unpublished Master's Independent Study Project, New Mexico Inst. of Mining and Tech.

Cande, S. C., and Kent, D. V. (1992). A New Geomagnetic Polarity Time Scale for the Late Cretaceous and Cenozoic. Journal of Geophysical Research 97: 13,917-13,951.

Chester, D. K., Duncan, A. M., Guest, J. E., and Kilburn, C. R. J. (1985). "Mount Etna, the Anatomy of a Volcano." Chapman and Hall, London.

Coombs, D. S., and Wilkinson, J. F. G. (1969). Lineages and fractionation trends in undersaturated volcanic rocks from the East Otago Volcanic Province (New Zealand) and related rocks. J. of Petrology 10: 440-501.

Cooper, A. K., Davey, F. J., and Behrendt, J. C. (1987). Seismic stratigraphy and structure of the Victoria Land basin, western Ross Sea, Antarctica. *In* "The Antarctic Continental Margin: Geology and Geophysics of the Western Ross Sea." (A. K. Cooper, and F. J. Davey, Eds.), pp. 27-65. Circum-Pacific Council for Energy and Resources, Houston, TX.

Dunbar, N. W., Cashman, K. V., and Dupre, R. (1994). Crystallization Processes of Anorthoclase Phenocrysts in the Mount Erebus Magmatic System: Evidence from Crystal Composition, Crystal Size Distributions, and Volatile Contents of Melt Inclusions. *In* "Volcanological and Environmental Studies of Mount Erebus, Antarctica." (P. R. Kyle, Ed.), pp. 129-146. American Geophysical Union.

Dunbar, N. W., Kyle, P. R., McIntosh, W. C., and Esser, R. P. (1995). Tephra Layers in blue ice, Allan Hills, Antarctica: A new source of glacial tephrochronological data. *In* "IUGG XXI General Assembly, Abstracts", p. A303.

Esser, R., McIntosh, W., Kyle, P., and Heizler, M. (1996). Excess Argon in Melt Inclusions in Young (<250 ka) Anorthoclase Feldspar from Mt. Erebus, Antarctica, as revealed by the $^{40}Ar/^{39}Ar$ Method. (in prep.) .

Fleck, R. J., Sutter, J. F., and Elliot, D. H. (1977). Interpretation of discordant $^{40}Ar/^{39}Ar$ age spectra of Mesozoic tholeiites from Antarctica. Geochimica et Cosmochimica Acta 41: 15-32.

Guest, J. E., Duncan, A. M., and Chester, D. K. (1988). Monte Vulture Volcano (Basilicata, Italy): an analysis of morphology and volcaniclastic facies. Bulletin of Volcanology 50: 244-257.

Johnson, R. W. (1989). Intraplate Volcanism in Eastern Australia and New Zealand, pp. 408. Cambridge University Press, Cambridge.

Kyle, P. R. (1976). "Geology, mineralogy, and geochemistry of the Late Cenozoic McMurdo Volcanic Group, Victoria Land, Antarctica." Unpublished Ph.D. thesis, Victoria University at Wellington.

Kyle, P. R. (1977). Mineralogy and glass chemistry of recent volcanic ejecta from Mt. Erebus, Ross Island, Antarctica. N.Z.J. Geol. Geophys. 20: 1123-46.

Kyle, P. R. (1981a). Mineralogy and Geochemistry of a Basanite to Phonolite Sequence at Hut Point Peninsula, Antarctica, based on Core from Dry Valley Drilling Project Drillholes 1, 2 and 3. Journal of Petrology 22: 451-500.

Kyle, P. R. (1981b). Glacial history of the McMurdo Sound area as indicated by the distribution and nature of McMurdo Volcanic Group rocks. *In* "Dry Valley Drilling Project." (L. D. McGinnis, Ed.). AGU, Washington, D.C.

Kyle, P. R. (1990a). McMurdo Volcanic Group-Western Ross Embayment: Introduction. *In* "Volcanoes of the Antarctic Plate and Southern Oceans." (W. LeMasurier, and J. Thomson, Eds.), pp. 18-25. Antarctic Research Series. American Geophysical Union, Washington, D.C.

Kyle, P. R. (1990b). Erebus Volcanic Province: Summary. *In* "Volcanoes of the Antarctic Plate and Southern Oceans." (W. LaMasurier, and J. Thomson, Eds.), pp. 81-88. Antarctic Research Series. American Geophysical Union, Washington, D.C.

Kyle, P. R. (1994). Volcanological and Environmental Studies of Mount Erebus, Antarctica. *In* "Antarctic Research Series.", pp. 162. AGU, Washington, D.C.

Kyle, P. R., and Cole, J. W. (1974). Structural Control of Volcanism in the McMurdo Volcanic Group, Antarctica. Bulletin of Volcanology 38: 16-25.

Kyle, P. R., Dibble, R. R., Giggenbach, W. F., and Keys, H. J. (1982). Volcanic Activity Associated with the Anorthoclase Phonolite Lava Lake, Mount Erebus, Antarctica. *In* "Antarctic Geoscience." (C. Craddock, Ed.), pp. 1172. The University of Wisconsin Press, Madison, Wisconsin, U.S.A.

Kyle, P. R., Meeker, K., and Finnegan, D. (1990). Emission rates of sulfur dioxide, trace gases and metals from Mount Erebus, Antarctica. Geophysical Research Letters 17: 2125-2128.

Kyle, P. R., Moore, J. A., and Thirlwall, M. F. (1992). Petrologic Evolution of Anorthoclase Phonolite Lavas at Mount Erebus, Ross Island, Antarctica. Journal of Petrology 33: 849-875.

Le Maitre, R. W. (1984). A proposal by the IUGS Subcommission on the Systematics of Igneous Rocks for a chemical classification of volcanic rocks based on the total alkali silica (TAS) diagram. Australian Journal of Earth Science 31: 243-255.

Macdonald, G. A. (1965). Hawaiian calderas. Pacific Science 19: 320-334.

Mankinen, E. A., and Cox, A. (1988). Paleomagnetic Investigation of Some Volcanic Rocks From the McMurdo Volcanic Province, Antarctica. Journal of Geophysical Research 93: 11,599-11,612.

McDougall, I., and Harrison, T. M. (1988). "Geochronology and Thermochronology by the $^{40}Ar/^{39}Ar$ Method." Clarendon Press, Oxford.

Moore, J. A. (1986). "Mineralogy, Geochemistry and Petrogenesis of the Lavas of Mount Erebus, Antarctica." Unpublished Master's thesis, New Mexico Institute of Mining and Technology.

Moore, J. A., and Kyle, P. R. (1987). Volcanic Geology of Mount Erebus, Ross Island, Antarctica. *In* "NIPR Symposium on Antarctic Geosciences.", pp. 48-65. National Institute of Polar Research, Tokyo.

Panter, K. S., McIntosh, W. C., and Smellie, J. L. (1994). Volcanic History of Mount Sidley, a major alkaline volcano in Marie Byrd Land, Antarctica. Bull. of Volc. 56: 361-376.

Siebert, L. (1984). Large Volcanic Debris Avalanches: Characteristics of Source Areas, Deposits, and Associated Eruptions. Journal of Volcanology and Geothermal Research 22: 163-197.

Steiger, R. H., and Jager, E. (1977). Subcommission on geochronology: Convention on the use of decay constants in geo- and cosmochronology. Earth and Planet. Sci. Lett. 36: 359-362.

Treves, S. B. (1968). Volcanic Rocks of the Ross Island area. Antarctica Journal of the US 3: 108-109.

van den Bogaard, P. (1995). $^{40}Ar/^{39}Ar$ ages of sanidine phenocrysts from Laacher See Tephra (12,900 yr BP): Chronostratigraphic and petrologic significance. Earth and Planetary Science Letters 133: 163-174.

Walker, G. P. L. (1988). Three Hawaiian Calderas: An Origin Through Loading by Shallow Intrusions? J. of Geophysical Research 93: 14,773-14,784.

Zreda-Gostynska, G., Kyle, P. R., and Finnegan, D. L. (1993). Chlorine, Fluorine, and Sulfur Emissions from Mt. Erebus, Antarctica and Estimated Contributions to the Antarctic Atmosphere. Geophysical Research Letters 20: 1959-1962.

APPENDIX C-1. EXPLANATION

The following table contains all of the $^{40}Ar/^{39}Ar$ analytical data from this study. Information for specific samples includes sample number, sample name, weight of material dated, estimate of glass quantity (if applicable) and J-value. Samples are listed according to their intra-laboratory run identification number (Lab#). The isotopic ratios in columns 3, 4 and 5 are corrected for system blank, nuclear interference reactions and radioactive decay ($^{37}Ar_{Ca}$). Nuclear interference correction factors for potassium and calcium, in addition to mass spectrometer discrimination values, are given in the table below. The elemental ratios K/Ca and Cl/K are calculated using the constants $[0.510 \times (^{39}Ar_K/^{37}Ar_{Ca})]$ and $[0.277 \times (^{39}Ar_K/^{38}Ar_{Cl})]$, respectively. Percent radiogenic ^{40}Ar ($^{40}Ar^*$) assumes a trapped $^{40}Ar/^{36}Ar$ ratio of 295.5. All ages are quoted at the 1σ confidence level and propagate uncertainties in J-value (±0.25%), system blank, isotopic peak heights and mass discrimination. Plateau ages are calculated from those heating steps listed by weighting the inverse of the variance. Total gas ages are weighted according to % ^{39}Ar released. All ages are calculated using the decay constants recommended by Steiger and Jagar (1977).

Nuclear interference correction factors and mass spectrometer discrimination values listed by laboratory run identification number.

Lab I.D. #	$(^{40}Ar/^{39}Ar)_K$ $(\times 10^{-2})$	$(^{36}Ar/^{37}Ar)_{Ca}$ $(\times 10^{-4})$	$(^{39}Ar/^{37}Ar)_{Ca}$ $(\times 10^{-4})$	Disc. (1 amu)	Disc. $^{40}Ar/^{36}Ar$
49-84	2.5	2.6	6.7	1.0062	288.3
425-432	2.25	2.6	7.0	1.0081	286.1
830-843	2.2	2.6	7.0	1.0107	283.2
1313-1332	2.2	2.6	7.0	1.0064	288.1
1422	2.2	2.6	7.0	1.0079	286.3
1528-1537	2.2	2.6	7.0	1.0068	287.6
1865	2.2	2.6	7.0	1.0078	286.5
2485-2658	2.2	2.6	7.0	1.0080	286.2

Lab#	Temp (°C)	$^{40}Ar/^{39}Ar$	$^{37}Ar/^{39}Ar$	$^{36}Ar/^{39}Ar$	$^{39}Ar_K$ (moles)	K/Ca	Cl/K	$^{40}Ar^*$ (%)	^{39}Ar (%)	Age (ka)	Err (1σ)
E87026: Caldera Rim, 75.3 mg anorthoclase (? % glass)					**J=0.000175±0.0000008**						
49-01A	600	1.68e+00	1.52e+00	7.40e-03	3.9e-13	0.3	1.6e-04	-24.8	13.58	-132 ±	16
49-01B	750	1.65e+00	1.53e+00	6.26e-03	6.9e-13	0.3	1.2e-04	-6.8	37.81	-35 ±	9
49-01C	900	2.76e+00	1.49e+00	1.00e-02	4.5e-13	0.3	8.5e-05	-4.0	53.53	-35 ±	16
49-01D	1050	1.97e+00	1.58e+00	7.67e-03	3.7e-13	0.3	1.9e-04	-10.2	66.66	-64 ±	15
49-01E	1150	2.74e+00	1.62e+00	1.13e-02	1.6e-13	0.3	9.3e-04	-18.6	72.42	-161 ±	27
49-01F	1250	3.02e+00	1.57e+00	1.05e-02	1.3e-13	0.3	1.2e-03	0.6	76.94	6 ±	33
49-01G	*1350*	*9.19e+01*	*9.44e-01*	*6.06e-01*	*4.8e-16*	*0.5*	*3.8e-02*	*-94.8*	*76.96*	*-27742 ±*	*5542*
49-01H	1450	1.65e+00	2.22e+00	5.45e-03	4.6e-13	0.2	5.9e-03	11.2	93.23	58 ±	10
49-01I	1550	3.22e+00	2.42e+00	1.07e-02	1.3e-13	0.2	6.8e-03	6.8	97.76	69 ±	54
49-01J	1750	8.44e+00	8.34e-01	2.21e-02	6.2e-14	0.6	1.7e-03	23.0	99.95	613 ±	225
49-01K	*1450*	*1.66e+02*	*8.21e-01*	*6.83e-01*	*1.4e-15*	*0.6*	*1.0e-02*	*-21.6*	*100.00*	*-11348 ±*	*3177*
total gas age					2.8e-12				n=9	-30 ±	2
plateau age							B-D		53.08	-42 ±	11
isochron age				$^{40}Ar/^{36}Ar$ = 250.3 ± 7.2			MSWD = 21.9			83 ±	6
EL: Summit Phenocrysts, 52.5 mg anorthoclase (? % glass)					**J=0.000187±0.0000008**						
51-01A	475	4.40e+00	4.60e-01	2.52e-02	2.2e-14	1.1	-1.6e-03	-69.3	1.40	-1029 ±	194
51-01B	525	7.14e+00	4.74e-01	4.80e-02	1.0e-14	1.1	-2.4e-03	-98.4	2.04	-2374 ±	381
51-01C	725	2.29e+00	4.73e-01	1.00e-02	4.0e-13	1.1	3.6e-04	-29.0	27.48	-224 ±	18
51-01D	1050	3.13e+00	4.54e-01	1.05e-02	7.5e-13	1.1	5.2e-05	1.3	75.17	14 ±	9
51-01E	1350	3.43e+00	4.87e-01	1.09e-02	2.5e-13	1.0	1.7e-04	6.8	91.39	79 ±	33
51-01F	1450	1.52e+01	4.96e-01	4.74e-02	3.4e-14	1.0	3.6e-04	7.7	93.57	394 ±	145
51-01G	1550	1.01e+01	5.70e-01	3.32e-02	4.9e-14	0.9	-5.5e-04	3.0	96.72	102 ±	110
51-01H	1750	7.94e+00	5.08e-01	2.18e-02	5.1e-14	1.0	7.1e-05	18.9	99.94	507 ±	158
51-01I	1750	1.51e+02	1.07e+00	3.98e-01	9.0e-16	0.5	-3.1e-02	21.9	100.00	11134 ±	4549
total gas age					1.6e-12				n=9	-30 ±	30
plateau age										N.A.	
isochron age				$^{40}Ar/^{36}Ar$ = 363.8 ± 10.6			MSWD = 25.1			-270 ±	20
E83400: Cape Evans, 25.0 mg anorthoclase (? % glass)					**J=0.000179±0.0000008**						
54-01A	800	3.96e+00	4.51e-01	1.24e-02	4.1e-14	1.1	-2.6e-05	7.9	3.59	101 ±	67
54-01B	900	2.58e+00	4.47e-01	8.26e-03	2.6e-13	1.1	4.0e-05	5.9	26.07	49 ±	16
54-01C	1050	3.92e+00	4.71e-01	1.27e-02	5.4e-13	1.1	-1.3e-05	4.1	72.64	52 ±	13

Lab#	Temp (°C)	$^{40}Ar/^{39}Ar$	$^{37}Ar/^{39}Ar$	$^{36}Ar/^{39}Ar$	$^{39}Ar_K$ (moles)	K/Ca	Cl/K	$^{40}Ar^*$ (%)	^{39}Ar (%)	Age (ka)	Err (1σ)
54-01D	1150	7.25e+00	5.28e-01	2.38e-02	1.2e-13	1.0	1.8e-04	3.1	83.32	73	± 42
54-01E	1250	3.29e+00	5.97e-01	9.86e-03	1.1e-13	0.9	9.6e-04	12.1	92.78	129	± 36
54-01F	1350	7.01e+00	8.96e-01	2.24e-02	5.4e-14	0.6	3.1e-03	6.1	97.49	139	± 67
54-01G	1450	9.42e+00	2.59e+00	3.31e-02	1.1e-14	0.2	1.7e-02	-1.9	98.44	-57	± 231
54-01H	1550	6.60e+00	5.01e-01	2.03e-02	1.8e-14	1.0	6.2e-04	9.3	100.00	197	± 134
total gas age					1.2e-12			n=8		70	± 30
plateau age							A-D		83.32	53	± 11
isochron age				$^{40}Ar/^{36}Ar$ = 302.0 ± 7.5			MSWD = 1.2			36	± 12
E83448: Cape Royds, 2.1 mg anorthoclase (? % glass)				**J=0.000192±0.0000008**							
70-01A	800	2.46e+02	3.30e-01	8.68e-01	5.1e-18	1.5	-1.1e-02	-4.3	0.11	-3667	± 13704
70-01B	900	2.22e+01	5.89e-01	7.45e-02	2.3e-16	0.9	1.1e-05	1.1	5.34	83	± 180
70-01C	1050	2.25e+01	6.02e-01	7.46e-02	4.1e-16	0.8	2.5e-04	2.3	14.54	180	± 103
70-01D	1250	1.61e+01	4.60e-01	4.63e-02	4.6e-16	1.1	7.1e-04	14.8	24.82	825	± 98
70-01E	1750	5.98e+00	2.59e-02	4.65e-03	3.2e-15	19.7	4.3e-05	76.6	95.60	1585	± 11
70-01F	1750	1.76e+01	2.31e-02	4.64e-02	2.0e-16	22.1	-1.8e-03	21.7	100.00	1323	± 178
total gas age					4.5e-15			n=6		1290	± 60
plateau age										N.A.	
isochron age				$^{40}Ar/^{36}Ar$ = 241.0 ± 2.6			MSWD = 4.2			1673	± 12
E83400: Cape Evans, 2.2 mg anorthoclase (? % glass)				**J=0.000191±0.0000008**							
71-01A	800	2.35e+01	3.57e-01	9.19e-02	1.1e-17	1.4	3.1e-04	-15.5	0.54	-1254	± 1811
71-01B	900	8.60e+00	4.46e-01	3.07e-02	2.0e-16	1.1	-4.7e-04	-5.3	10.07	-157	± 130
71-01C	1050	1.15e+01	4.94e-01	3.87e-02	5.5e-16	1.0	9.2e-04	0.3	36.46	12	± 73
71-01D	1250	1.31e+01	5.35e-01	4.14e-02	4.9e-16	1.0	2.7e-04	7.0	60.24	316	± 99
71-01E	1350	2.56e+01	2.84e-01	7.80e-02	1.9e-16	1.8	8.6e-04	9.8	69.28	866	± 212
71-01F	1550	1.27e+01	2.38e-01	3.23e-02	1.5e-16	2.1	1.1e-03	24.5	76.49	1068	± 278
71-01G	1750	1.67e+01	6.35e-02	3.54e-02	1.8e-16	8.0	5.7e-04	37.3	85.18	2143	± 257
71-01H	1750	1.99e+01	3.24e-02	5.22e-02	1.5e-16	15.7	9.1e-04	22.3	92.54	1528	± 192
71-01I	1750	1.79e+01	8.09e-03	4.55e-02	1.5e-16	63.1	8.2e-04	24.9	100.00	1536	± 296
total gas age					2.1e-15			n=9		650	± 170
plateau age										N.A.	
isochron age				$^{40}Ar/^{36}Ar$ = 431.6 ± 21.8			MSWD = 10.2			-1577	± 196

Lab#	Temp (°C)	$^{40}Ar/^{39}Ar$	$^{37}Ar/^{39}Ar$	$^{36}Ar/^{39}Ar$	$^{39}Ar_K$ (moles)	K/Ca	Cl/K	$^{40}Ar^*$ (%)	^{39}Ar (%)	Age (ka)	Err (1σ)
E87026: Caldera Rim, 27.9 mg anorthoclase (? % glass)					**J=0.000183±0.0000008**						
83-01A	800	3.78e+01	1.55e+00	9.68e-02	4.5e-17	0.3	-6.4e-03	24.6	1.05	3077	± 869
83-01B	900	6.87e+00	1.59e+00	2.46e-02	6.8e-16	0.3	-7.0e-04	-4.5	16.82	-102	± 82
83-01C	1050	9.25e+00	1.66e+00	3.06e-02	1.2e-15	0.3	-2.3e-04	3.4	44.22	105	± 28
83-01D	1150	9.72e+00	1.71e+00	3.01e-02	4.4e-16	0.3	-7.1e-05	9.5	54.34	304	± 66
83-01E	1250	6.02e+00	1.76e+00	2.00e-02	7.2e-16	0.3	2.4e-03	3.7	70.88	73	± 199
83-01F	1350	2.50e+00	2.98e+00	9.52e-03	7.8e-16	0.2	1.3e-02	-4.5	88.81	-37	± 27
83-01G	1550	7.45e+00	3.79e+00	2.30e-02	4.5e-16	0.1	2.1e-02	12.5	99.20	307	± 60
83-01H	1750	8.62e+01	1.71e+00	2.41e-01	2.9e-17	0.3	-3.3e-03	17.3	99.86	4929	± 954
83-01I	1750	2.76e+02	1.04e+00	7.77e-01	6.3e-18	0.5	-1.2e-02	16.8	100.00	15194	± 8755
total gas age					4.3e-15				n=9	170	± 100
plateau age										N.A.	
isochron age				$^{40}Ar/^{36}Ar$ = 330.6 ± 4.9			MSWD = 5.7			-161	± 22
EL: Summit Phenocrysts, 21.3 mg anorthoclase (? % glass)					**J=0.000193±0.0000008**						
84-01A	*800*	*1.46e+02*	*0.00e+00*	*2.74e-01*	*5.0e-19*	*- -*	*1.6e-01*	*44.5*	*0.00*	*22450*	*± 40177*
84-01B	*900*	*7.30e+02*	*0.00e+00*	*-2.22e+00*	*5.2e-20*	*- -*	*1.3e+00*	*189.6*	*0.00*	*427418*	*± 1164918*
84-01C	*1050*	*3.62e+00*	*2.84e+00*	*1.53e+00*	*-2.5e-18*	*0.2*	*-1.3e-01*	*-12386.7*	*-0.02*	*-163493*	*± 174191*
84-01D	*1150*	*-3.97e+01*	*2.87e+00*	*-3.25e-01*	*-5.6e-19*	*0.2*	*5.9e-02*	*-142.6*	*-0.02*	*19615*	*± 25110*
84-01E	*1250*	*-6.47e+01*	*3.29e+00*	*1.38e-01*	*-5.9e-19*	*0.2*	*1.5e-01*	*162.6*	*-0.02*	*-37093*	*± 26167*
84-01F	*1350*	*5.98e+01*	*2.99e-01*	*1.99e-01*	*1.5e-17*	*1.7*	*-7.2e-03*	*1.6*	*0.09*	*343*	*± 1347*
84-01G	1550	1.12e+00	4.70e-01	3.74e-03	6.2e-15	1.1	-5.4e-05	2.4	48.45	9	± 5
84-01H	1750	2.68e+00	4.75e-01	8.26e-03	6.6e-15	1.1	3.4e-04	9.4	99.90	87	± 8
84-01I	1750	8.03e+01	7.91e-01	2.34e-01	1.3e-17	0.6	3.7e-03	13.8	100.00	3862	± 1615
total gas age					1.3e-14				n=3	56	± 10
plateau age										N.A.	
isochron age				$^{40}Ar/^{36}Ar$ = 342.1 ± 6.4			MSWD = 0.9			-48	± 10
E81001, Hooper's Shoulder: Anorthoclase, J=0.00024±0.0000003											
425-01		0.73	3.47e-01	2.04e-03	4.0e-15	1.5	3.4e-04	18.2	- -	58	± 16
425-02		0.70	3.58e-01	1.86e-03	4.4e-15	1.4	1.4e-04	22.4	- -	68	± 8

Lab#	Temp (°C)	$^{40}Ar/^{39}Ar$	$^{37}Ar/^{39}Ar$	$^{36}Ar/^{39}Ar$	$^{39}Ar_K$ (moles)	K/Ca	Cl/K	$^{40}Ar^*$ (%)	^{39}Ar (%)	Age (ka)	Err (1σ)
425-03		0.66	3.59e-01	1.93e-03	4.0e-15	1.4	3.6e-04	13.7	- -	39	± 7
425-04		0.65	3.57e-01	1.92e-03	4.9e-15	1.4	2.9e-04	13.6	- -	38	± 5
					Weighted mean		n=4			45	± 4
E83448, Cape Royds: Anorthoclase, J=0.00024±0.0000003											
426-01		1.31	6.15e-01	3.83e-03	3.8e-15	0.8	3.2e-04	15.7	- -	89	± 9
426-02		6.46	5.99e-01	2.15e-02	9.0e-15	0.9	3.9e-04	2.0	- -	57	± 33
426-03		1.69	5.76e-01	4.82e-03	4.1e-15	0.9	4.2e-04	16.9	- -	124	± 10
426-04		1.54	5.84e-01	4.67e-03	3.2e-15	0.9	4.8e-04	11.8	- -	79	± 9
					Weighted mean		n=4			95	± 5
E83400, Cape Evans: Anorthoclase, J=0.000235±0.0000003											
427-01		2.02	4.35e-01	6.57e-03	5.0e-15	1.2	6.5e-04	4.7	- -	40	± 13
427-02		1.90	4.27e-01	6.20e-03	3.8e-15	1.2	6.5e-04	4.2	- -	34	± 11
427-03A		2.95	4.27e-01	9.85e-03	1.1e-15	1.2	2.2e-04	1.8	- -	22	± 29
427-03B		1.22	4.30e-01	3.95e-03	4.7e-15	1.2	6.6e-04	5.5	- -	29	± 10
427-04A		2.49	4.07e-01	8.01e-03	1.4e-15	1.3	6.1e-04	5.4	- -	57	± 33
427-04B		0.91	4.04e-01	2.75e-03	3.5e-15	1.3	8.5e-04	11.6	- -	45	± 10
					Weighted mean		n=6			37	± 5
E87034, Lower Hut Flow: Anorthoclase, J=0.000232±0.0000003											
428-01		2.95	4.89e-01	9.24e-03	3.6e-15	1.0	6.4e-04	7.9	- -	98	± 26
428-02		2.80	4.78e-01	8.81e-03	3.4e-15	1.1	6.5e-04	7.5	- -	88	± 20
428-04A		2.35	4.97e-01	7.32e-03	9.8e-16	1.0	5.8e-04	8.6	- -	84	± 41
428-04B		1.05	4.87e-01	3.36e-03	3.4e-15	1.0	1.1e-03	7.1	- -	31	± 8
					Weighted mean		n=4			45	± 7
E87026, Caldera Rim: Anorthoclase, J=0.0002312±0.0000003											
429-01		4.28	1.12e+00	1.45e-02	2.6e-15	0.5	1.7e-03	1.0	- -	18	± 43
429-02A		6.59	1.25e+00	2.18e-02	6.5e-16	0.4	7.5e-04	3.5	- -	96	± 153
429-02B		4.20	1.28e+00	1.48e-02	1.8e-15	0.4	1.3e-03	-2.0	- -	*-35*	± *18*

Lab#	Temp (°C)	$^{40}Ar/^{39}Ar$	$^{37}Ar/^{39}Ar$	$^{36}Ar/^{39}Ar$	$^{39}Ar_K$ (moles)	K/Ca	Cl/K	$^{40}Ar^*$ (%)	^{39}Ar (%)	Age (ka)	Err (1σ)
429-03A		35.23	1.06e+00	1.25e-01	8.5e-16	0.5	1.6e-03	-5.1	- -	*-746*	± *522*
429-03B		10.72	1.25e+00	3.69e-02	2.7e-15	0.4	1.2e-03	-1.0	- -	-46	± 156
429-04A		9.78	1.21e+00	3.29e-02	6.8e-16	0.4	6.6e-04	1.3	- -	52	± 59
429-04B		8.04	1.35e+00	2.67e-02	3.6e-16	0.4	1.7e-03	3.0	- -	99	± 90
					Weighted mean		n=5			38	± 31
E83433, Cape Barne: Anorthoclase, J=0.0002308±0.0000003											
430-01		1.66	5.23e-01	4.57e-03	3.0e-15	1.0	2.8e-04	19.5	- -	134	± 14
430-02		3.55	5.29e-01	1.14e-02	3.4e-15	1.0	4.2e-04	5.5	- -	81	± 13
430-02A		1.60	5.31e-01	4.41e-03	5.9e-16	1.0	3.7e-04	19.9	- -	133	± 29
430-03		2.27	5.28e-01	6.85e-03	4.2e-15	1.0	3.5e-04	11.8	- -	112	± 11
430-03A		1.42	5.37e-01	4.06e-03	1.0e-15	0.9	4.9e-04	16.8	- -	99	± 25
430-04		2.96	4.97e-01	9.44e-03	4.1e-15	1.0	3.9e-04	6.4	- -	79	± 15
430-04A		1.95	5.22e-01	5.41e-03	1.5e-15	1.0	3.6e-04	19.0	- -	154	± 30
					Weighted mean		n=7			106	± 6
EL Summit Phenocrysts: Anorthoclase, J=0.0002303±0.0000003											
431-01		1.57	4.49e-01	5.21e-03	3.7e-15	1.1	1.0e-03	2.6	- -	17	± 21
431-02		1.39	4.69e-01	3.84e-03	2.1e-15	1.1	5.2e-04	19.6	- -	114	± 53
431-02A		0.57	4.58e-01	2.52e-03	5.6e-16	1.1	1.1e-03	-28.1	- -	-67	± 26
431-03		2.01	4.71e-01	6.95e-03	2.8e-15	1.1	9.0e-04	-1.6	- -	-14	± 64
431-03A		0.98	4.75e-01	3.33e-03	2.4e-15	1.1	8.7e-04	0.6	- -	2	± 12
431-04		1.87	5.26e-01	5.90e-03	2.9e-15	1.0	1.1e-03	7.7	- -	60	± 17
431-04A		0.87	4.72e-01	2.65e-03	2.1e-15	1.1	5.1e-04	11.7	- -	43	± 11
					Weighted mean		n=7			24	± 7
E83454, Aurora Cliffs trachyte: Anorthoclase, J=0.0002301±0.0000003											
432-01A		9.68	1.19e-01	3.73e-02	7.4e-16	4.3	1.7e-02	-13.9		*-560*	± *220*
432-01B		7.56	1.47e-01	2.36e-02	3.9e-15	3.5	1.5e-02	7.6		239	± 30
432-02A		10.35	1.29e-01	3.43e-02	1.1e-15	4.0	1.6e-02	1.9		83	± 164
432-02B		4.57	1.44e-01	1.32e-02	3.4e-15	3.5	1.4e-02	14.5		275	± 19

Lab#	Temp (°C)	$^{40}Ar/^{39}Ar$	$^{37}Ar/^{39}Ar$	$^{36}Ar/^{39}Ar$	$^{39}Ar_K$ (moles)	K/Ca	Cl/K	$^{40}Ar^*$ (%)	^{39}Ar (%)	Age (ka)	Err (1σ)
					Weighted mean		n=3			263	± 16
EL: Summit Phenocrysts, 201.2 mg anorthoclase (<1% glass)					**J=0.0000784±0.0000002**						
830-01A	700	1.98e+01	4.92e-01	6.63e-02	7.0e-17	1.0	1.1e-03	1.2	9.85	35	± 17
830-01B	750	3.06e+00	4.76e-01	9.84e-03	6.1e-17	1.1	1.7e-04	5.3	18.49	23	± 4
830-01C	800	2.43e+01	4.68e-01	8.16e-02	4.4e-17	1.1	7.9e-03	0.8	24.73	29	± 31
830-01D	850	3.04e+00	4.69e-01	9.32e-03	8.6e-17	1.1	6.6e-05	10.0	36.85	43	± 4
830-01E	900	7.41e-01	4.64e-01	1.83e-03	8.3e-17	1.1	1.1e-05	28.8	48.64	30	± 2
830-01F	950	8.85e-01	4.65e-01	2.18e-03	9.1e-17	1.1	2.4e-05	28.9	61.52	36	± 2
830-01G	1000	1.10e+00	4.55e-01	2.24e-03	7.3e-17	1.1	2.3e-05	40.9	71.87	64	± 2
830-01H	1050	1.31e+00	4.50e-01	2.77e-03	5.0e-17	1.1	7.3e-05	38.3	79.00	71	± 3
830-01I	1100	1.79e+00	4.54e-01	4.27e-03	3.4e-17	1.1	3.1e-04	30.2	83.76	76	± 5
830-01J	1150	2.70e+00	4.40e-01	5.43e-03	2.3e-17	1.2	6.3e-04	41.0	87.05	156	± 7
830-01K	1200	3.92e+00	4.45e-01	7.87e-03	1.6e-17	1.1	1.1e-03	41.0	89.30	227	± 11
830-01L	1300	2.49e+00	4.66e-01	3.71e-03	5.0e-17	1.1	1.6e-03	56.6	96.39	199	± 4
830-01M	1450	6.20e+00	6.05e-01	1.62e-02	7.2e-18	0.8	2.9e-03	23.1	97.41	203	± 13
830-01N	1600	6.72e+00	7.68e-01	1.71e-02	1.1e-17	0.7	4.4e-03	25.3	98.94	240	± 12
830-01O	1625	1.33e+02	5.66e-01	4.36e-01	7.5e-18	0.9	7.6e-03	3.4	100.00	637	± 174
total gas age					7.1e-16				n=15	73	± 8
plateau age							A-I		83.76	45	± 6
isochron age				$^{40}Ar/^{36}Ar = 318.6 \pm 1.3$			MSWD = 210.5			48	± 1
EL: Summit Phenocrysts, 209.1 mg anorthoclase (<1% glass)					**J=0.0000784±0.0000002**						
831-01A	700	4.91e+01	4.86e-01	1.65e-01	7.8e-17	1.0	1.1e-03	0.6	9.41	41	± 37
831-01B	850	3.15e+00	4.70e-01	1.02e-02	1.9e-16	1.1	2.0e-04	4.8	32.76	21	± 3
831-01C	950	1.26e+00	4.62e-01	3.87e-03	1.9e-16	1.1	1.2e-04	10.1	55.20	18	± 1
831-01D	1050	1.12e+00	4.56e-01	3.38e-03	1.4e-16	1.1	1.0e-04	12.2	72.55	19	± 1
831-01E	1200	2.61e+00	4.37e-01	7.33e-03	1.1e-16	1.2	4.4e-04	17.4	86.09	64	± 3
831-01F	1600	4.21e+00	3.99e-01	1.02e-02	8.6e-17	1.3	1.5e-03	28.6	96.52	170	± 3
831-01G	1600	1.28e+02	4.43e-01	4.32e-01	2.9e-17	1.2	4.2e-03	0.1	100.00	19	± 113
total gas age					8.3e-16				n=7	44	± 9
plateau age							A-D		72.55	19	± 1
isochron age				$^{40}Ar/^{36}Ar = 321.0 \pm 1.2$			MSWD = 390.7			15	± 1

Lab#	Temp (°C)	$^{40}Ar/^{39}Ar$	$^{37}Ar/^{39}Ar$	$^{36}Ar/^{39}Ar$	$^{39}Ar_K$ (moles)	K/Ca	Cl/K	$^{40}Ar^*$ (%)	^{39}Ar (%)	Age (ka)	Err (1σ)
EL: Summit Phenocrysts, 164.2 mg anorthoclase (1-2% glass)					**J=0.0000784±0.0000002**						
832-01A	700	3.75e+01	4.48e-01	1.11e-01	5.6e-17	1.1	3.3e-03	12.7	8.37	675	± 31
832-01B	850	1.10e+01	4.47e-01	3.14e-02	1.3e-16	1.1	1.4e-03	15.9	28.31	248	± 9
832-01C	950	7.20e+00	4.46e-01	2.22e-02	1.4e-16	1.1	4.9e-04	9.0	49.84	92	± 6
832-01D	1050	7.00e+00	4.42e-01	2.25e-02	1.2e-16	1.2	5.0e-04	5.4	68.15	53	± 6
832-01E	1200	1.11e+01	4.35e-01	3.61e-02	1.1e-16	1.2	8.6e-04	4.2	83.99	65	± 10
832-01F	1450	8.85e+00	4.55e-01	2.68e-02	5.6e-17	1.1	1.2e-03	10.7	92.42	133	± 11
832-01G	1600	1.40e+01	4.65e-01	4.52e-02	5.1e-17	1.1	1.5e-03	4.8	100.00	95	± 15
total gas age					6.7e-16				n=7	165	± 10
plateau age										N.A.	
isochron age				$^{40}Ar/^{36}Ar$ = 339.0 ± 2.4			MSWD = 56.4			-60	± 4
EL: Summit Phenocrysts, 134.2 mg anorthoclase (1-2% glass)					**J=0.0000785±0.0000002**						
833-01A	700	3.41e+01	4.52e-01	9.97e-02	5.4e-17	1.1	3.1e-03	13.7	9.99	661	± 28
833-01B	700	1.10e+01	4.49e-01	3.15e-02	3.2e-17	1.1	1.1e-03	15.4	15.86	239	± 12
833-01C	800	9.65e+00	4.46e-01	2.60e-02	5.4e-17	1.1	8.2e-04	20.7	25.68	283	± 8
833-01D	800	5.85e+00	4.47e-01	1.75e-02	5.8e-17	1.1	2.3e-04	11.8	36.41	98	± 6
833-01E	900	7.28e+00	4.38e-01	2.15e-02	6.9e-17	1.2	4.8e-04	13.0	49.10	134	± 8
833-01F	950	6.72e+00	4.40e-01	2.13e-02	6.6e-17	1.2	3.7e-04	6.4	61.28	61	± 8
833-01G	1050	8.44e+00	4.35e-01	2.72e-02	7.2e-17	1.2	3.1e-04	5.1	74.52	60	± 10
833-01H	1200	1.42e+01	4.34e-01	4.55e-02	7.0e-17	1.2	1.1e-03	5.5	87.45	111	± 13
833-01I	1450	1.14e+01	4.45e-01	3.56e-02	2.3e-17	1.1	1.2e-03	7.6	91.65	122	± 16
833-01J	1600	8.43e+00	4.47e-01	2.60e-02	3.1e-17	1.1	1.1e-03	9.0	97.32	107	± 12
833-01K	1600	4.04e+01	4.43e-01	1.34e-01	1.5e-17	1.2	2.6e-03	2.4	100.00	137	± 42
total gas age					5.4e-16				n=11	181	± 12
plateau age										N.A.	
isochron age				$^{40}Ar/^{36}Ar$ = 325.9 ± 1.8			MSWD = 74.3			30	± 1
EL: Summit Phenocrysts, 204.9 mg anorthoclase (~5% glass)					**J=0.0000785±0.0000002**						
834-01A	600	7.91e+01	4.24e-01	2.65e-01	2.3e-17	1.2	1.3e-02	1.2	2.77	133	± 66
834-01B	700	2.28e+01	4.14e-01	7.32e-02	6.7e-17	1.2	1.1e-02	5.1	10.75	166	± 17

Lab#	Temp (°C)	$^{40}Ar/^{39}Ar$	$^{37}Ar/^{39}Ar$	$^{36}Ar/^{39}Ar$	$^{39}Ar_K$ (moles)	K/Ca	Cl/K	$^{40}Ar^*$ (%)	^{39}Ar (%)	Age (ka)	Err (1σ)
834-01C	700	1.02e+01	4.17e-01	3.11e-02	6.3e-17	1.2	9.5e-03	10.5	18.26	152	± 8
834-01D	800	9.57e+00	4.18e-01	2.67e-02	7.5e-17	1.2	8.5e-03	17.5	27.17	238	± 7
834-01E	800	7.71e+00	4.23e-01	1.82e-02	9.6e-17	1.2	7.5e-03	30.2	38.51	330	± 5
834-01F	900	1.63e+01	4.00e-01	3.55e-02	1.1e-16	1.3	1.1e-02	35.6	51.77	819	± 9
834-01G	950	9.75e+00	4.28e-01	2.59e-02	9.7e-17	1.2	5.9e-03	21.5	63.28	296	± 7
834-01H	1050	1.24e+01	4.43e-01	3.75e-02	1.0e-16	1.2	4.0e-03	10.8	75.36	190	± 9
834-01I	1200	1.74e+01	4.86e-01	5.62e-02	1.1e-16	1.1	2.8e-03	4.8	88.01	118	± 13
834-01J	1450	9.31e+00	8.01e-01	2.87e-02	8.3e-17	0.6	3.2e-03	9.2	97.85	121	± 7
834-01K	1600	1.02e+01	1.16e+00	3.39e-02	1.1e-17	0.4	6.7e-03	2.1	99.11	30	± 17
834-01L	1600	5.66e+01	6.47e-01	1.88e-01	7.5e-18	0.8	3.9e-03	2.0	100.00	161	± 60
total gas age					8.4e-16				n=12	281	± 11
plateau age										N.A.	
isochron age				$^{40}Ar/^{36}Ar$ = 312.5 ± 1.3			MSWD = 546.9			214	± 2
EL: Summit Phenocrysts, 203.2 mg anorthoclase (~5% glass)					**J=0.0000786±0.0000002**						
835-01A	600	8.87e+01	4.24e-01	2.98e-01	2.8e-17	1.2	1.3e-02	0.7	3.53	94	± 70
835-01B	700	2.29e+01	4.18e-01	7.37e-02	7.7e-17	1.2	1.1e-02	5.0	13.20	162	± 17
835-01C	700	1.01e+01	4.24e-01	3.08e-02	6.1e-17	1.2	8.9e-03	10.2	20.87	146	± 9
835-01D	800	1.03e+01	4.18e-01	2.52e-02	8.9e-17	1.2	8.7e-03	27.6	31.99	402	± 7
835-01E	800	7.94e+00	4.30e-01	1.83e-02	9.2e-17	1.2	7.3e-03	32.1	43.44	362	± 5
835-01F	900	1.28e+01	4.12e-01	2.77e-02	1.0e-16	1.2	9.6e-03	36.0	56.09	653	± 8
835-01G	950	1.02e+01	4.31e-01	2.85e-02	8.2e-17	1.2	5.6e-03	17.5	66.29	253	± 7
835-01H	1050	1.39e+01	4.44e-01	4.25e-02	8.4e-17	1.1	4.0e-03	9.8	76.76	194	± 10
835-01I	1200	1.76e+01	4.86e-01	5.67e-02	9.0e-17	1.0	2.7e-03	5.1	88.06	126	± 13
835-01J	1450	9.96e+00	7.32e-01	3.09e-02	7.8e-17	0.7	3.4e-03	8.7	97.82	123	± 8
835-01K	1600	1.12e+01	1.16e+00	3.64e-02	1.1e-17	0.4	6.7e-03	5.0	99.18	80	± 17
835-01L	1600	6.94e+01	5.77e-01	2.28e-01	6.6e-18	0.9	5.0e-03	2.8	100.00	280	± 67
total gas age					8.0e-16				n=12	275	± 12
plateau age										N.A.	
isochron age				$^{40}Ar/^{36}Ar$ = 287.2 ± 1.1			MSWD = 417.9			354	± 4
E83433: Cape Barne, 141.4 mg anorthoclase (<1% glass)					**J=0.0000787±0.0000002**						
836-01A	600	1.29e+01	5.42e-01	4.22e-02	3.5e-17	0.9	3.5e-04	3.1	7.90	57	± 13
836-01B	700	7.00e+00	5.32e-01	2.19e-02	6.6e-17	1.0	1.8e-04	7.9	22.94	78	± 6

Lab#	Temp (°C)	$^{40}Ar/^{39}Ar$	$^{37}Ar/^{39}Ar$	$^{36}Ar/^{39}Ar$	$^{39}Ar_K$ (moles)	K/Ca	Cl/K	$^{40}Ar^*$ (%)	^{39}Ar (%)	Age (ka)	Err (1σ)
836-01C	750	1.95e+00	5.31e-01	4.67e-03	4.0e-17	1.0	1.5e-04	30.0	32.07	83	± 3
836-01D	800	1.58e+00	5.30e-01	3.28e-03	4.1e-17	1.0	7.9e-05	39.7	41.34	89	± 3
836-01E	900	1.73e+00	5.29e-01	3.65e-03	5.9e-17	1.0	6.4e-05	38.9	54.69	96	± 2
836-01F	975	1.30e+00	5.26e-01	2.32e-03	5.2e-17	1.0	7.7e-05	48.8	66.45	90	± 3
836-01G	1025	1.16e+00	5.22e-01	1.85e-03	4.9e-17	1.0	7.1e-05	54.3	77.56	89	± 2
836-01H	1075	1.35e+00	5.23e-01	2.50e-03	3.7e-17	1.0	1.2e-04	46.7	86.05	90	± 4
836-01I	1200	5.60e+00	5.19e-01	1.39e-02	1.8e-17	1.0	1.7e-03	26.7	90.13	212	± 9
836-01K	1600	2.39e+00	5.23e-01	5.78e-03	2.2e-17	1.0	6.0e-04	29.4	95.09	100	± 6
836-01L	1600	1.72e+02	5.22e-01	5.84e-01	2.2e-17	1.0	4.4e-03	-0.1	100.00	-24	± 140
total gas age					4.4E-16				n=11	85	± 11
plateau age							A-H		86.05	89	± 2
isochron age				$^{40}Ar/^{36}Ar$ = 299.6 ± 1.6			MSWD = 29.2			90	± 1
E87034: Lower Hut Flow, 108.6 mg anorthoclase (<1% glass)					**J=0.0000808±0.0000002**						
837-01A	700	1.59e+01	5.04e-01	5.35e-02	6.6e-17	1.0	6.0e-04	0.9	17.22	22	± 14
837-01B	750	1.42e+01	4.92e-01	4.73e-02	3.5e-17	1.0	2.8e-04	1.8	26.26	36	± 15
837-01C	800	7.38e+00	4.94e-01	2.44e-02	3.1e-17	1.0	2.4e-04	2.6	34.31	28	± 9
837-01D	850	5.29e+00	4.97e-01	1.71e-02	3.7e-17	1.0	3.9e-05	4.7	44.03	37	± 7
837-01E	900	3.52e+00	4.95e-01	1.16e-02	2.9e-17	1.0	3.2e-04	2.9	51.68	15	± 6
837-01F	950	2.99e+00	4.97e-01	9.32e-03	2.4e-17	1.0	1.7e-04	8.5	57.81	37	± 6
837-01G	1000	2.35e+00	4.90e-01	7.51e-03	2.3e-17	1.0	2.0e-04	6.3	63.88	22	± 6
837-01H	1050	2.50e+00	4.92e-01	8.07e-03	2.4e-17	1.0	3.0e-04	5.4	70.20	20	± 5
837-01I	1100	4.52e+00	4.99e-01	1.49e-02	1.8e-17	1.0	5.6e-04	2.9	74.94	19	± 7
837-01J	1150	5.32e+00	5.05e-01	1.66e-02	1.1e-17	1.0	9.0e-04	8.4	77.82	65	± 12
837-01K	1200	1.17e+01	5.08e-01	3.64e-02	7.1e-18	1.0	2.4e-03	7.9	79.67	134	± 24
837-01L	1300	2.17e+00	5.12e-01	6.08e-03	4.5e-17	1.0	8.1e-04	17.9	91.32	57	± 4
837-01M	1450	2.15e+00	5.40e-01	5.93e-03	1.3e-17	0.9	7.3e-04	19.4	94.68	61	± 8
837-01N	1600	1.42e+01	5.30e-01	4.78e-02	3.4e-18	1.0	1.1e-03	0.7	95.57	14	± 37
837-01O	1600	3.10e+01	5.31e-01	1.04e-01	1.7e-17	1.0	1.8e-03	0.6	100.00	29	± 28
total gas age					3.9e-16				n=15	34	± 10
plateau age							A-I		74.94	24	± 4
isochron age				$^{40}Ar/^{36}Ar$ = 294.7 ± 1.8			MSWD = 10.7			38	± 2

E83433: Cape Barne, 222.1 mg anorthoclase (~5% glass) **J=0.00008±0.0000002**

Lab#	Temp (°C)	$^{40}Ar/^{39}Ar$	$^{37}Ar/^{39}Ar$	$^{36}Ar/^{39}Ar$	$^{39}Ar_K$ (moles)	K/Ca	Cl/K	$^{40}Ar^*$ (%)	^{39}Ar (%)	Age (ka)	Err (1σ)
838-01A	700	2.05e+01	4.04e-01	6.76e-02	9.4e-17	1.3	2.1e-02	2.6	11.28	77	± 17
838-01B	750	1.47e+01	4.32e-01	4.74e-02	5.9e-17	1.2	2.3e-02	4.8	18.36	102	± 12
838-01C	800	9.82e+00	4.48e-01	3.09e-02	5.6e-17	1.1	2.1e-02	7.3	25.06	103	± 9
838-01D	850	8.25e+00	4.67e-01	2.57e-02	6.3e-17	1.1	1.7e-02	8.0	32.62	95	± 7
838-01E	900	2.03e+02	4.49e-01	6.85e-01	3.5e-17	1.1	1.9e-02	0.0	36.84	13	± 163
838-01F	950	9.85e+00	4.52e-01	3.18e-02	5.0e-17	1.1	1.3e-02	4.9	42.82	69	± 9
838-01G	1000	1.01e+01	4.57e-01	3.27e-02	6.1e-17	1.1	1.1e-02	4.8	50.17	71	± 10
838-01H	1050	1.38e+01	4.56e-01	4.46e-02	7.2e-17	1.1	1.1e-02	4.5	58.81	90	± 11
838-01I	1100	2.62e+01	4.79e-01	8.65e-02	7.3e-17	1.1	1.4e-02	2.6	67.58	99	± 21
838-01J	1150	1.90e+01	5.10e-01	6.15e-02	5.4e-17	1.0	1.1e-02	4.3	74.12	117	± 16
838-01K	1200	1.47e+01	5.48e-01	4.60e-02	4.2e-17	0.9	7.5e-03	7.5	79.18	159	± 13
838-01L	1300	9.67e+00	6.36e-01	3.01e-02	9.6e-17	0.8	4.0e-03	8.5	90.71	118	± 8
838-01M	1450	7.66e+00	7.27e-01	2.38e-02	5.0e-17	0.7	2.9e-03	8.9	96.75	98	± 7
838-01N	1600	7.80e+00	6.73e-01	2.40e-02	2.3e-17	0.8	1.9e-03	9.4	99.47	106	± 10
838-01O	1600	1.04e+02	5.83e-01	3.48e-01	4.4e-18	0.9	3.6e-03	0.8	100.00	123	± 113
total gas age					8.3e-16				n=15	99	± 12
plateau age							A-J		74.12	90	± 6
isochron age				$^{40}Ar/^{36}Ar$ = 296.5 ± 1.2			MSWD = 4.6			94	± 6
E83433: Cape Barne, 197.4 mg anorthoclase (<1% glass)					**J=0.0000788±0.0000002**						
839-01A	700	1.24e+01	5.35e-01	4.02e-02	1.4e-16	1.0	6.0e-04	4.5	21.20	80	± 11
839-01B	750	4.77e+00	5.29e-01	1.43e-02	5.9e-17	1.0	1.4e-04	11.6	30.16	79	± 8
839-01C	800	2.43e+00	5.27e-01	5.98e-03	5.6e-17	1.0	5.0e-05	28.1	38.74	97	± 5
839-01D	850	1.83e+00	5.24e-01	4.21e-03	5.2e-17	1.0	3.9e-05	33.0	46.62	86	± 4
839-01E	900	1.67e+00	5.17e-01	3.38e-03	3.8e-17	1.0	1.3e-04	41.4	52.48	98	± 4
839-01F	950	1.69e+00	5.23e-01	3.56e-03	4.4e-17	1.0	3.3e-05	38.8	59.22	93	± 4
839-01G	1000	1.49e+00	5.26e-01	3.08e-03	4.9e-17	1.0	1.1e-04	40.2	66.67	85	± 3
839-01H	1050	1.47e+00	5.19e-01	2.98e-03	4.9e-17	1.0	1.4e-04	41.4	74.20	87	± 3
839-01I	1100	2.12e+00	5.19e-01	5.16e-03	3.4e-17	1.0	5.0e-06	28.8	79.44	87	± 4
839-01J	1150	3.11e+00	5.20e-01	6.94e-03	1.9e-17	1.0	1.0e-03	34.6	82.28	153	± 11
839-01K	1200	5.02e+00	5.18e-01	1.11e-02	9.8e-18	1.0	1.7e-03	34.7	83.77	248	± 13
839-01L	1300	1.82e+00	5.25e-01	3.20e-03	7.1e-17	1.0	7.3e-04	48.9	94.59	126	± 3
839-01M	1450	6.29e+00	5.28e-01	1.77e-02	7.7e-18	1.0	1.2e-03	17.0	95.76	152	± 20
839-01N	1650	3.28e+00	5.77e-01	7.74e-03	1.8e-17	0.9	1.1e-03	31.0	98.55	145	± 8
839-01O	1650	5.82e+01	5.19e-01	1.89e-01	9.5e-18	1.0	3.2e-03	3.9	100.00	320	± 65

Lab#	Temp (°C)	$^{40}Ar/^{39}Ar$	$^{37}Ar/^{39}Ar$	$^{36}Ar/^{39}Ar$	$^{39}Ar_K$ (moles)	K/Ca	Cl/K	$^{40}Ar^*$ (%)	^{39}Ar (%)	Age (ka)	Err (1σ)
total gas age					6.5e-16				n=15	101 ±	7
plateau age							A-I		79.44	89 ±	2
isochron age				$^{40}Ar/^{36}Ar$ = 297.4 ± 1.9			MSWD = 32.0			97 ±	2
E83433: Cape Barne, 222.9 mg anorthoclase (~5% glass)					**J=0.0000806±0.0000002**						
840-01A	700	1.52e+01	4.03e-01	4.92e-02	8.1e-17	1.3	1.9e-02	4.3	9.50	94 ±	12
840-01B	750	9.56e+00	4.27e-01	2.99e-02	5.3e-17	1.2	2.3e-02	7.6	15.77	105 ±	10
840-01C	800	7.16e+00	4.45e-01	2.21e-02	5.8e-17	1.1	2.1e-02	8.8	22.53	92 ±	6
840-01D	850	6.71e+00	4.69e-01	2.07e-02	6.2e-17	1.1	1.7e-02	9.0	29.82	88 ±	6
840-01E	900	7.39e+00	4.63e-01	2.33e-02	4.8e-17	1.1	1.5e-02	6.9	35.41	75 ±	9
840-01F	950	8.74e+00	4.50e-01	2.78e-02	4.8e-17	1.1	1.2e-02	6.1	41.08	77 ±	9
840-01G	1000	8.97e+00	4.60e-01	2.85e-02	5.9e-17	1.1	8.5e-03	6.2	48.03	81 ±	9
840-01H	1050	1.16e+01	4.61e-01	3.73e-02	7.0e-17	1.1	9.1e-03	4.7	56.22	80 ±	10
840-01I	1100	1.50e+01	4.72e-01	4.88e-02	7.2e-17	1.1	1.2e-02	4.0	64.69	87 ±	12
840-01J	1150	1.53e+01	5.02e-01	4.91e-02	6.6e-17	1.0	1.3e-02	5.2	72.38	115 ±	13
840-01K	1200	1.62e+01	5.26e-01	5.18e-02	4.3e-17	1.0	9.3e-03	5.8	77.39	136 ±	15
840-01L	1300	1.05e+01	6.09e-01	3.30e-02	1.0e-16	0.8	5.4e-03	7.3	89.45	111 ±	8
840-01M	1450	7.67e+00	6.87e-01	2.33e-02	6.0e-17	0.7	3.5e-03	10.4	96.46	117 ±	7
840-01N	1600	7.68e+00	7.45e-01	2.38e-02	2.0e-17	0.7	2.9e-03	8.9	98.80	99 ±	9
840-01O	1600	4.83e+01	5.70e-01	1.60e-01	1.0e-17	0.9	2.3e-03	1.9	100.00	137 ±	50
total gas age					8.5e-16				n=15	97 ±	10
plateau age							A-I		64.69	87 ±	4
isochron age				$^{40}Ar/^{36}Ar$ = 298.7 ± 1.7			MSWD = 3.2			82 ±	7
E81001: Hooper's Shoulder, 97.4 mg anorthoclase (<1% glass)					**J=0.0000811±0.0000002**						
841-01A	700	3.47e+01	3.72e-01	1.17e-01	2.1e-17	1.4	4.4e-04	0.1	5.41	5 ±	36
841-01B	750	1.02e+01	3.60e-01	3.32e-02	2.0e-17	1.4	4.3e-04	3.6	10.67	53 ±	12
841-01C	850	4.68e+00	3.62e-01	1.51e-02	2.8e-17	1.4	3.1e-04	5.0	17.94	34 ±	8
841-01D	900	3.29e+00	3.57e-01	1.03e-02	2.5e-17	1.4	1.6e-04	7.8	24.58	38 ±	8
841-01E	950	2.69e+00	3.56e-01	8.29e-03	1.8e-17	1.4	1.2e-04	9.1	29.24	36 ±	9
841-01F	1050	2.96e+00	3.56e-01	9.24e-03	2.9e-17	1.4	3.9e-05	7.8	36.87	34 ±	6
841-01G	1150	2.63e+00	3.58e-01	8.07e-03	3.5e-17	1.4	-1.6e-04	9.4	46.15	36 ±	6
841-01H	1300	3.60e+00	3.48e-01	1.07e-02	1.1e-16	1.5	2.8e-04	11.9	75.11	63 ±	4
841-01I	1450	2.13e+00	3.67e-01	5.68e-03	3.2e-17	1.4	5.8e-04	21.3	83.56	66 ±	5

Lab#	Temp (°C)	$^{40}Ar/^{39}Ar$	$^{37}Ar/^{39}Ar$	$^{36}Ar/^{39}Ar$	$^{39}Ar_K$ (moles)	K/Ca	Cl/K	$^{40}Ar^*$ (%)	^{39}Ar (%)	Age (ka)	Err (1σ)
841-01J	1650	1.50e+02	4.14e-01	5.06e-01	4.6e-17	1.2	1.7e-04	0.3	95.66	65	± 154
841-01K	1650	1.32e+01	4.03e-01	4.37e-02	1.7e-17	1.3	6.3e-04	2.5	100.00	48	± 19
total gas age					3.8e-16				n=11	47	± 26
plateau age							A-G		46.15	36	± 4
isochron age				$^{40}Ar/^{36}Ar$ = 295.2 ± 1.7			MSWD = 6.3			51	± 3
E87034: Lower Hut Flow, 118.5 mg anorthoclase (<1% glass)					**J=0.0000809±0.0000002**						
842-01A	700	1.31e+01	5.10e-01	4.41e-02	4.2e-17	1.0	2.1e-04	0.6	10.71	12	± 12
842-01B	750	5.64e+00	5.07e-01	1.86e-02	2.9e-17	1.0	2.3e-04	2.8	18.16	23	± 9
842-01C	850	3.28e+00	4.97e-01	1.06e-02	3.0e-17	1.0	2.2e-04	4.6	25.99	22	± 7
842-01D	900	2.00e+00	4.99e-01	6.60e-03	2.3e-17	1.0	1.2e-04	3.1	31.99	9	± 5
842-01E	950	2.07e+00	5.01e-01	7.01e-03	1.5e-17	1.0	7.5e-05	0.8	35.78	2	± 7
842-01F	1050	1.80e+00	5.03e-01	5.90e-03	2.4e-17	1.0	8.5e-06	3.8	41.87	10	± 5
842-01G	1200	1.72e+00	5.03e-01	5.15e-03	2.5e-17	1.0	1.5e-04	12.4	48.28	31	± 4
842-01H	1300	2.51e+00	5.01e-01	7.70e-03	3.5e-17	1.0	3.8e-04	10.2	57.15	37	± 5
842-01I	1450	3.43e+00	5.20e-01	1.01e-02	4.9e-17	1.0	1.3e-03	13.3	69.80	66	± 4
842-01J	1600	7.31e-01	5.16e-01	1.96e-03	9.0e-17	1.0	3.4e-04	23.3	92.98	25	± 1
842-01K	1600	7.30e+00	5.00e-01	2.41e-02	2.7e-17	1.0	5.2e-04	2.6	100.00	28	± 9
total gas age					3.9e-16				n=11	27	± 6
plateau age							A-F		41.87	11	± 4
isochron age				$^{40}Ar/^{36}Ar$ = 299.0 ± 1.5			MSWD = 16.5			24	± 1
E81001: Hooper's Shoulder, 93.3 mg anorthoclase (<1% glass)					**J=0.000081±0.0000002**						
843-01A	700	9.53e+02	2.67e-01	3.18e+00	1.5e-19	1.9	2.7e-03	1.5	0.05	2026	± 4704
843-01B	850	4.38e+01	3.67e-01	1.45e-01	1.9e-18	1.4	1.6e-03	2.5	0.68	160	± 89
843-01C	950	1.36e+01	3.66e-01	4.48e-02	6.6e-18	1.4	3.0e-04	3.0	2.83	60	± 25
843-01D	1100	9.09e+00	3.62e-01	2.98e-02	3.5e-17	1.4	2.8e-04	3.0	14.19	40	± 11
843-01E	1250	3.77e+00	3.59e-01	1.24e-02	3.9e-17	1.4	1.2e-04	3.1	27.03	17	± 6
843-01F	1350	3.24e+00	3.55e-01	1.03e-02	6.7e-17	1.4	9.6e-05	6.5	48.82	31	± 4
843-01G	1450	4.82e+00	3.59e-01	1.45e-02	1.1e-16	1.4	4.7e-04	11.1	85.04	78	± 4
843-01H	1600	2.41e+00	3.94e-01	7.20e-03	3.2e-17	1.3	5.0e-04	12.0	95.53	42	± 5
843-01I	1625	1.12e+01	4.06e-01	3.74e-02	1.4e-17	1.3	7.4e-04	1.1	100.00	18	± 17
total gas age					3.1e-16				n=9	50	± 9
plateau age							C-F		48.14	28	± 5

Lab#	Temp (°C)	$^{40}Ar/^{39}Ar$	$^{37}Ar/^{39}Ar$	$^{36}Ar/^{39}Ar$	$^{39}Ar_K$ (moles)	K/Ca	Cl/K	$^{40}Ar^*$ (%)	^{39}Ar (%)	Age (ka)	Err (1σ)
isochron age				$^{40}Ar/^{36}Ar = 304.0 \pm 2.4$			MSWD = 17.2			28	± 3
E83400: Cape Evans, 157.4 mg anorthoclase (~1% glass)					**J=0.0000686±0.0000002**						
1313-01A	*250*	*4.03e+03*	*5.71e-01*	*1.35e+01*	*2.7e-18*	*0.9*	*-4.0e-02*	*1.2*	*0.26*	*5788*	± *59606*
1313-01B	*400*	*2.88e+03*	*6.50e-01*	*9.66e+00*	*4.7e-17*	*0.8*	*9.5e-03*	*0.8*	*0.43*	*2736*	± *7297*
1313-01C	550	1.62e+02	4.79e-01	5.43e-01	8.1e-16	1.1	1.8e-03	1.2	3.22	235	± 78
1313-01D	700	5.17e+00	4.22e-01	1.64e-02	3.8e-15	1.2	6.9e-04	6.6	16.53	42	± 4
1313-01E	800	2.37e+00	4.24e-01	7.05e-03	3.6e-15	1.2	4.4e-04	12.7	29.05	37	± 3
1313-01F	900	1.96e+00	4.30e-01	5.19e-03	3.7e-15	1.2	2.8e-04	22.3	41.89	54	± 3
1313-01G	1000	3.68e+00	4.18e-01	1.14e-02	1.9e-15	1.2	7.6e-04	9.2	48.35	42	± 6
1313-01H	1100	3.33e+00	4.52e-01	1.05e-02	2.1e-15	1.1	1.0e-03	7.4	55.77	30	± 5
1313-01I	1200	2.97e+00	4.53e-01	8.53e-03	4.0e-15	1.1	6.7e-04	15.7	69.47	58	± 3
1313-01J	1300	5.67e+00	4.65e-01	1.51e-02	2.3e-15	1.1	1.4e-03	21.4	77.44	151	± 5
1313-01K	1400	3.63e+00	4.93e-01	1.04e-02	3.0e-15	1.0	6.2e-04	15.4	87.75	69	± 6
1313-01L	1650	8.90e+00	5.00e-01	2.87e-02	2.9e-15	1.0	5.5e-04	4.7	97.75	52	± 7
1313-01M	1650	1.57e+02	4.86e-01	5.27e-01	4.6e-16	1.0	5.3e-04	0.7	99.35	131	± 105
1313-01N	1650	9.08e+02	4.94e-01	3.05e+00	1.9e-16	1.0	5.0e-03	0.8	100.00	940	± 931
total gas age					2.9e-14				n=12	80	± 40
plateau age							D-H		52.55	42	± 4
isochron age				$^{40}Ar/^{36}Ar = 313.6 \pm 2.1$			MSWD = 65.4			33	± 1
E83448: Cape Royds, 110.9 mg anorthoclase (~2% glass)					**J=0.0000709±0.0000002**						
1314-01A	550	2.26e+02	5.53e-01	7.60e-01	5.9e-16	0.9	1.9e-03	0.8	3.17	234	± 132
1314-01B	700	8.85e+00	5.27e-01	2.78e-02	1.6e-15	1.0	1.1e-03	7.5	12.08	85	± 15
1314-01C	800	-2.94e+00	5.25e-01	-1.16e-02	1.3e-15	1.0	8.3e-04	-17.0	19.38	64	± 7
1314-01D	900	4.09e-01	5.29e-01	-4.74e-04	1.4e-15	1.0	7.3e-04	138.8	27.21	73	± 6
1314-01E	1000	-1.21e-01	5.26e-01	-2.45e-03	1.1e-15	1.0	9.3e-04	-513.1	33.39	79	± 9
1314-01F	1100	5.44e+00	5.12e-01	1.65e-02	1.5e-15	1.0	1.2e-03	10.5	41.62	73	± 7
1314-01G	1200	6.75e+00	5.01e-01	2.02e-02	1.4e-15	1.0	2.2e-03	11.9	48.96	103	± 8
1314-01H	1300	8.49e+00	5.07e-01	1.92e-02	1.1e-15	1.0	3.1e-03	33.3	54.79	362	± 10
1314-01I	1400	3.62e+00	5.65e-01	7.20e-03	3.2e-15	0.9	9.8e-04	41.8	71.85	194	± 3
1314-01J	1600	8.18e+00	5.24e-01	2.44e-02	4.4e-15	1.0	5.2e-04	12.0	95.51	125	± 5
1314-01K	1600	3.35e+01	5.45e-01	1.11e-01	8.3e-16	0.9	6.0e-04	2.4	100.00	104	± 25

Lab#	Temp (°C)	$^{40}Ar/^{39}Ar$	$^{37}Ar/^{39}Ar$	$^{36}Ar/^{39}Ar$	$^{39}Ar_K$ (moles)	K/Ca	Cl/K	$^{40}Ar^*$ (%)	^{39}Ar (%)	Age (ka)	Err (1σ)
total gas age					1.8e-14				n=11	133	± 11
plateau age							B-F		38.45	73	± 5
isochron age				$^{40}Ar/^{36}Ar$ = 297.3 ± 0.9			MSWD = 122.0			158	± 2
AW82015: Turk's Head tephriphonolite, 117.3 mg anorthoclase (~2% glass)							**J=0.0000702±0.0000002**				
1315-01A	550	1.19e+02	1.11e+00	3.96e-01	8.9e-16	0.5	1.3e-03	1.9	7.16	284	± 67
1315-01B	700	8.96e+00	1.11e+00	2.45e-02	2.1e-15	0.5	3.5e-04	19.9	23.70	226	± 8
1315-01C	800	5.32e+00	1.10e+00	1.18e-02	1.6e-15	0.5	3.2e-04	35.5	36.29	239	± 6
1315-01D	900	3.79e+00	1.11e+00	6.58e-03	1.4e-15	0.5	3.9e-04	50.4	47.25	242	± 6
1315-01E	1000	3.74e+00	1.11e+00	6.13e-03	1.2e-15	0.5	5.8e-04	53.3	56.84	253	± 5
1315-01F	1100	6.16e+00	1.12e+00	1.45e-02	1.3e-15	0.5	1.1e-03	31.3	66.87	244	± 7
1315-01G	1200	2.05e+01	1.08e+00	6.19e-02	9.7e-16	0.5	2.3e-03	11.0	74.67	286	± 14
1315-01H	1300	2.31e+01	1.05e+00	6.47e-02	5.4e-16	0.5	3.9e-03	17.5	79.03	511	± 26
1315-01I	1400	8.43e+00	1.12e+00	2.02e-02	1.9e-15	0.5	1.4e-03	30.0	94.61	321	± 5
1315-01J	1500	4.15e+01	1.05e+00	1.33e-01	3.6e-16	0.5	3.0e-03	5.3	97.50	280	± 46
1315-01K	1600	8.28e+01	1.66e+00	2.69e-01	2.2e-16	0.3	8.8e-03	4.0	99.30	424	± 84
1315-01L	1600	2.88e+02	1.15e+00	9.57e-01	8.7e-17	0.4	2.9e-03	1.9	100.00	685	± 369
total gas age					1.2e-14				n=12	278	± 17
plateau age							B-F		59.72	243	± 5
isochron age				$^{40}Ar/^{36}Ar$ = 311.0 ± 4.0			MSWD = 31.9			235	± 4
EL: Summit Phenocrysts, 197.3 mg anorthoclase (~1% glass)							**J=0.0000698±0.0000002**				
1316-01A	600	3.04e+02	5.53e-01	1.02e+00	5.8e-16	0.9	2.3e-03	0.7	1.78	273	± 151
1316-01B	600	8.10e+00	5.22e-01	2.49e-02	3.2e-16	1.0	1.1e-03	9.5	2.77	97	± 22
1316-01C	700	3.42e+00	5.17e-01	1.06e-02	9.4e-16	1.0	5.1e-04	8.7	5.63	38	± 8
1316-01D	700	2.15e+00	5.10e-01	6.58e-03	9.1e-16	1.0	3.7e-04	10.4	8.41	28	± 7
1316-01E	800	1.23e+00	5.04e-01	3.53e-03	2.2e-15	1.0	4.1e-04	16.2	14.97	25	± 3
1316-01F	800	1.45e+00	5.01e-01	4.20e-03	2.1e-15	1.0	4.7e-04	15.5	21.27	28	± 3
1316-01G	900	7.49e-01	5.00e-01	2.07e-03	3.3e-15	1.0	2.5e-04	20.4	31.23	19	± 2
1316-01H	900	7.81e-01	4.98e-01	2.43e-03	3.1e-15	1.0	1.2e-04	10.2	40.60	10	± 2
1316-01I	1000	8.13e-01	5.04e-01	2.47e-03	3.2e-15	1.0	2.2e-04	12.1	50.29	12	± 2
1316-01J	1000	8.86e-01	5.03e-01	2.63e-03	2.9e-15	1.0	1.5e-04	14.3	59.04	16	± 3

Lab#	Temp (°C)	$^{40}Ar/^{39}Ar$	$^{37}Ar/^{39}Ar$	$^{36}Ar/^{39}Ar$	$^{39}Ar_K$ (moles)	K/Ca	Cl/K	$^{40}Ar^*$ (%)	^{39}Ar (%)	Age (ka)	Err (1σ)
1316-01K	1100	1.14e+00	4.94e-01	3.02e-03	2.5e-15	1.0	5.5e-04	23.0	66.62	33	± 3
1316-01L	1100	1.77e+00	4.92e-01	5.02e-03	1.5e-15	1.0	4.5e-04	17.2	71.14	38	± 5
1316-01M	1200	2.38e+00	4.85e-01	5.15e-03	1.4e-15	1.1	1.9e-03	36.9	75.54	111	± 5
1316-01N	1200	4.86e+00	4.92e-01	1.44e-02	9.3e-16	1.0	1.3e-03	12.7	78.38	77	± 8
1316-01O	1300	3.16e+00	4.74e-01	7.01e-03	1.9e-15	1.1	2.5e-03	34.9	84.16	139	± 3
1316-01P	1300	6.56e+00	4.86e-01	2.06e-02	1.3e-15	1.1	1.5e-03	7.3	88.16	61	± 7
1316-01Q	1400	5.19e+00	5.52e-01	1.39e-02	9.5e-16	0.9	2.2e-03	21.2	91.05	139	± 11
1316-01R	1550	5.60e+01	5.36e-01	1.88e-01	2.9e-15	1.0	1.4e-03	0.9	100.00	66	± 24
total gas age					3.3e-14				n=18	48	± 8
plateau age							C-L		68.37	20	± 3
isochron age				$^{40}Ar/^{36}Ar$ = 306.1 ± 0.8			MSWD = 100.5			27	± 1
EL: Summit Phenocrysts, 229.8 mg anorthoclase (~10% glass)					**J=0.0000701±0.0000002**						
1317-01A	600	2.26e+02	4.20e-01	7.53e-01	1.3e-15	1.2	1.1e-01	1.3	2.78	374	± 96
1317-01B	600	1.79e+01	4.02e-01	5.47e-02	7.4e-16	1.3	2.1e-02	10.0	4.40	227	± 18
1317-01C	700	1.20e+01	3.78e-01	3.31e-02	2.1e-15	1.4	1.8e-02	18.2	8.93	275	± 7
1317-01D	700	8.10e+00	3.65e-01	1.99e-02	2.0e-15	1.4	1.8e-02	27.4	13.30	281	± 8
1317-01E	800	6.46e+00	3.72e-01	1.53e-02	4.1e-15	1.4	1.7e-02	30.1	22.27	246	± 4
1317-01F	800	5.28e+00	3.68e-01	1.15e-02	3.6e-15	1.4	1.8e-02	36.0	30.16	240	± 4
1317-01G	900	5.83e+00	3.75e-01	1.27e-02	5.3e-15	1.4	1.7e-02	35.7	41.74	263	± 3
1317-01H	900	4.10e+00	3.79e-01	7.89e-03	4.3e-15	1.3	1.6e-02	43.3	51.20	225	± 3
1317-01I	1000	5.77e+00	3.90e-01	1.40e-02	4.5e-15	1.3	1.4e-02	28.7	60.99	209	± 3
1317-01J	1000	5.01e+00	4.23e-01	1.49e-02	3.0e-15	1.2	8.4e-03	12.2	67.63	78	± 5
1317-01K	1100	7.93e+00	4.17e-01	2.43e-02	2.6e-15	1.2	1.0e-02	9.6	73.34	96	± 6
1317-01L	1100	8.68e+00	4.68e-01	2.97e-02	1.1e-15	1.1	1.8e-03	-1.0	75.70	-11	± 11
1317-01M	1200	1.20e+01	4.76e-01	3.95e-02	2.1e-15	1.1	4.0e-03	2.7	80.20	41	± 8
1317-01N	1200	1.26e+01	5.17e-01	4.22e-02	1.4e-15	1.0	7.4e-04	1.0	83.21	15	± 13
1317-01O	1300	1.09e+01	6.52e-01	3.48e-02	3.0e-15	0.8	2.4e-03	5.7	89.80	78	± 6
1317-01P	1300	7.23e+00	5.97e-01	2.33e-02	1.1e-15	0.9	1.6e-03	5.2	92.16	48	± 13
1317-01Q	1400	5.38e+00	6.64e-01	1.68e-02	1.4e-15	0.8	1.7e-03	8.4	95.21	57	± 8
1317-01R	1550	1.33e+02	7.03e-01	4.46e-01	2.2e-15	0.7	3.3e-03	0.8	99.96	128	± 75
1317-01S	1550	1.95e+03	4.86e-01	6.62e+00	1.8e-17	1.0	6.5e-03	-0.4	100.00	-894	± 12960
total gas age					4.6e-14				n=19	179	± 16

Lab#	Temp (°C)	$^{40}Ar/^{39}Ar$	$^{37}Ar/^{39}Ar$	$^{36}Ar/^{39}Ar$	$^{39}Ar_K$ (moles)	K/Ca	Cl/K	$^{40}Ar^*$ (%)	^{39}Ar (%)	Age (ka)	Err (1σ)
plateau age										N.A.	
isochron age				$^{40}Ar/^{36}Ar = 288.3 \pm 0.7$			MSWD = 220.6			217	± 2
E81001: Hooper's Shoulder Cone, 102.8 mg anorthoclase (~1% glass)						**J=0.0000707±0.0000002**					
1318-01A	550	7.21e+02	4.28e-01	2.39e+00	4.7e-17	1.2	7.1e-03	2.0	0.57	1814	± 1252
1318-01B	700	1.01e+01	3.47e-01	3.49e-02	5.0e-16	1.5	4.0e-04	-2.6	6.66	-33	± 22
1318-01C	800	1.69e+00	3.35e-01	5.18e-03	1.0e-15	1.5	3.4e-04	9.6	19.16	21	± 8
1318-01D	900	1.83e+00	3.34e-01	5.52e-03	1.3e-15	1.5	5.2e-05	11.1	35.37	26	± 7
1318-01E	1000	3.19e+00	3.30e-01	1.00e-02	1.6e-15	1.5	1.1e-04	7.4	54.75	30	± 6
1318-01F	1100	2.57e+00	3.21e-01	7.53e-03	1.4e-15	1.6	2.3e-04	13.4	72.05	44	± 6
1318-01G	1200	5.03e+00	3.30e-01	1.62e-02	1.1e-15	1.5	3.4e-04	4.7	85.16	30	± 9
1318-01H	1300	1.05e+01	3.29e-01	3.13e-02	8.0e-16	1.5	9.6e-04	12.0	94.96	162	± 13
1318-01I	1400	4.79e+01	3.66e-01	1.59e-01	1.4e-16	1.4	1.2e-03	2.0	96.71	123	± 92
1318-01J	1500	5.79e+01	3.92e-01	1.89e-01	8.5e-17	1.3	2.0e-03	3.4	97.75	250	± 124
1318-01K	1550	2.49e+02	3.64e-01	8.37e-01	1.0e-16	1.4	8.9e-04	0.8	99.02	250	± 343
1318-01L	1550	3.72e+02	4.29e-01	1.25e+00	7.9e-17	1.2	8.5e-03	0.7	100.00	341	± 412
total gas age					8.1e-15				n=12	60	± 30
plateau age							C-G		78.50	32	± 5
isochron age				$^{40}Ar/^{36}Ar = 318.6 \pm 3.2$			MSWD = 9.0			10	± 1
E81001: Hooper's Shoulder Cone, 100.1 mg anorthoclase (~5% glass)						**J=0.0000708±0.0000002**					
1319-01A	550	2.65e+03	1.20e+00	8.96e+00	6.7e-18	0.4	3.4e-02	0.3	0.04	933	± 20180
1319-01B	700	1.95e+01	3.42e-01	6.46e-02	3.2e-16	1.5	9.9e-04	2.4	1.77	59	± 44
1319-01C	800	-1.63e+00	3.28e-01	-5.93e-03	1.6e-15	1.6	5.9e-04	-7.9	10.46	16	± 7
1319-01D	900	4.46e+00	3.27e-01	1.39e-02	2.1e-15	1.6	4.9e-04	8.3	21.47	48	± 8
1319-01E	1000	2.23e-01	3.29e-01	-9.33e-04	2.8e-15	1.5	4.4e-04	225.0	36.50	64	± 5
1319-01F	1100	2.47e+00	3.28e-01	5.88e-03	3.4e-15	1.6	5.8e-04	29.8	54.46	94	± 3
1319-01G	1200	2.63e+00	3.29e-01	6.14e-03	2.2e-15	1.6	5.3e-04	31.2	66.31	105	± 4
1319-01H	1300	4.51e+00	3.27e-01	9.28e-03	2.4e-15	1.6	1.3e-03	39.2	79.38	226	± 4
1319-01I	1400	3.30e+00	3.44e-01	8.45e-03	1.5e-15	1.5	8.0e-04	24.5	87.25	103	± 7
1319-01J	1500	5.99e+00	3.46e-01	1.81e-02	1.4e-15	1.5	8.3e-04	10.7	94.96	82	± 8
1319-01K	1550	3.93e+01	3.44e-01	1.30e-01	4.9e-16	1.5	1.5e-03	2.1	97.59	108	± 33

Lab#	Temp (°C)	$^{40}Ar/^{39}Ar$	$^{37}Ar/^{39}Ar$	$^{36}Ar/^{39}Ar$	$^{39}Ar_K$ (moles)	K/Ca	Cl/K	$^{40}Ar^*$ (%)	^{39}Ar (%)	Age (ka)	Err (1σ)
1319-01L	1560	4.94e+01	3.49e-01	1.67e-01	4.5e-16	1.5	8.4e-04	0.0	100.00	1	± 41
total gas age					1.9e-14				n=12	94	± 15
plateau age							C-G		64.54	84	± 12
isochron age				$^{40}Ar/^{36}Ar$ = 293.6 ± 1.3			MSWD = 8.3			93	± 2
E83400: Cape Evans, 96.4 mg anorthoclase (~5% glass)					**J=0.0000695±0.0000002**						
1320-01A	550	1.13e+04	1.25e+00	3.83e+01	3.7e-17	0.4	2.4e-02	-0.1	0.21	-1407	± 48445
1320-01B	700	6.45e+01	4.38e-01	2.16e-01	6.5e-16	1.2	3.4e-03	1.2	3.79	94	± 47
1320-01C	800	4.81e+00	3.37e-01	1.58e-02	2.4e-15	1.5	2.0e-03	3.2	16.79	19	± 5
1320-01D	900	1.53e+00	3.91e-01	4.33e-03	2.3e-15	1.3	1.5e-03	17.1	29.26	33	± 4
1320-01E	1000	1.62e+00	4.10e-01	4.64e-03	1.4e-15	1.2	3.4e-03	15.8	37.07	32	± 5
1320-01F	1100	3.53e+00	4.40e-01	1.07e-02	2.0e-15	1.2	4.0e-03	10.3	48.06	45	± 5
1320-01G	1200	2.46e+01	4.46e-01	8.04e-02	2.2e-15	1.1	4.2e-03	3.6	60.01	112	± 16
1320-01H	1300	6.25e+00	4.44e-01	1.88e-02	2.7e-15	1.1	1.7e-03	11.4	74.83	89	± 6
1320-01I	1400	4.83e+00	4.76e-01	1.49e-02	1.8e-15	1.1	5.5e-04	9.2	84.48	55	± 6
1320-01J	1500	7.91e+00	4.69e-01	2.53e-02	1.1e-15	1.1	6.8e-04	5.5	90.71	55	± 10
1320-01K	1550	1.41e+01	4.58e-01	4.64e-02	1.4e-15	1.1	5.7e-04	2.6	98.62	46	± 11
1320-01L	1550	6.86e+01	4.62e-01	2.28e-01	2.5e-16	1.1	-4.3e-04	1.7	100.00	148	± 68
total gas age					1.8e-14				n=12	60	± 110
plateau age							C-F		44.27	32	± 6
isochron age				$^{40}Ar/^{36}Ar$ = 301.6 ± 1.1			MSWD = 12.1			33	± 2
E83454: Aurora Cliffs trachyte, 106.2 mg anorthoclase (~3% glass)					**J=0.0000699±0.0000002**						
1321-01A	550	3.22e+03	2.78e-01	1.07e+01	2.0e-17	1.8	5.7e-02	1.7	0.08	7047	± 9528
1321-01B	700	8.34e+01	1.58e-01	2.66e-01	1.5e-16	3.2	1.1e-02	5.7	0.61	603	± 113
1321-01C	800	1.95e+01	1.54e-01	6.07e-02	6.1e-16	3.3	4.3e-03	7.9	2.88	194	± 19
1321-01D	900	1.02e+01	1.55e-01	2.99e-02	1.4e-15	3.3	1.6e-03	13.5	8.09	174	± 10
1321-01E	1000	8.81e+00	1.52e-01	2.56e-02	2.4e-15	3.3	1.0e-03	13.9	16.89	155	± 7
1321-01F	1100	7.78e+00	1.58e-01	2.04e-02	5.0e-15	3.2	6.5e-04	22.4	35.26	220	± 4
1321-01G	1200	8.95e+00	1.61e-01	2.57e-02	6.6e-15	3.2	2.4e-04	14.9	59.63	168	± 4
1321-01H	1300	7.62e+00	1.60e-01	2.06e-02	5.7e-15	3.2	1.6e-04	19.9	80.60	192	± 4
1321-01I	1400	6.30e+00	1.63e-01	1.54e-02	2.0e-15	3.1	1.0e-04	27.7	88.09	220	± 5

Lab#	Temp (°C)	$^{40}Ar/^{39}Ar$	$^{37}Ar/^{39}Ar$	$^{36}Ar/^{39}Ar$	$^{39}Ar_K$ (moles)	K/Ca	Cl/K	$^{40}Ar^*$ (%)	^{39}Ar (%)	Age (ka)	Err (1σ)
1321-01J	1500	7.28e+00	1.78e-01	1.96e-02	2.1e-15	2.9	3.2e-04	20.2	95.90	185	± 6
1321-01K	1575	1.98e+01	1.90e-01	6.15e-02	7.7e-16	2.7	-2.4e-05	8.4	98.76	209	± 17
1321-01L	1550	5.27e+01	1.82e-01	1.72e-01	3.4e-16	2.8	4.7e-04	3.5	100.00	231	± 50
total gas age					2.7e-14				n=12	192	± 16
plateau age							D-G		56.76	166	± 5
isochron age				$^{40}Ar/^{36}Ar$ = 294.2 ± 1.5			MSWD = 20.2			197	± 4
E83448: Cape Royds, 117.0 mg anorthoclase (~20% glass)					**J=0.0000709±0.0000002**						
1322-01A	*600*	*-1.80e+02*	*2.18e-01*	*3.61e+00*	*-3.5e-20*	*2.3*	*-6.2e-01*	*692.1*	*0.00*	*-166976*	*± 424171*
1322-01C	700	-1.49e+01	1.79e-01	-5.36e-02	1.5e-16	2.9	4.3e-02	-6.3	0.74	120	± 123
1322-01D	700	7.39e+00	1.90e-01	2.30e-02	1.5e-15	2.7	5.3e-02	8.0	8.27	75	± 12
1322-01E	800	6.27e+01	2.31e-01	2.05e-01	1.2e-15	2.2	7.2e-02	3.5	14.13	278	± 47
1322-01F	800	1.19e+02	2.73e-01	4.01e-01	8.8e-16	1.9	6.5e-02	0.7	18.52	103	± 86
1322-01G	900	6.44e+01	3.11e-01	2.11e-01	9.2e-16	1.6	4.7e-02	3.0	23.08	245	± 64
1322-01H	900	3.73e+01	3.48e-01	1.14e-01	4.5e-16	1.5	4.4e-02	9.4	25.28	448	± 52
1322-01I	1000	6.08e+01	2.78e-01	2.03e-01	7.6e-16	1.8	3.2e-02	1.5	29.03	116	± 45
1322-01J	1000	1.19e+01	3.69e-01	3.93e-02	4.7e-16	1.4	2.2e-02	2.7	31.37	41	± 25
1322-01K	1100	3.76e+01	2.53e-01	1.25e-01	2.4e-15	2.0	3.1e-02	1.3	43.10	63	± 23
1322-01L	1100	1.96e+01	3.02e-01	6.42e-02	9.9e-16	1.7	2.2e-02	3.2	48.01	81	± 24
1322-01M	1200	5.79e+01	4.48e-01	1.91e-01	4.3e-15	1.1	1.9e-02	2.4	69.08	178	± 40
1322-01N	1200	1.95e+01	5.76e-01	6.01e-02	4.7e-16	0.9	4.6e-03	9.1	71.39	229	± 33
1322-01O	1300	3.96e+01	6.95e-01	1.26e-01	9.3e-16	0.7	3.6e-03	6.4	76.02	324	± 38
1322-01P	1300	1.09e+01	6.67e-01	3.31e-02	9.6e-16	0.8	1.4e-03	10.2	80.79	142	± 13
1322-01Q	1400	7.67e+00	6.75e-01	2.27e-02	9.2e-16	0.8	1.4e-03	13.0	85.33	128	± 15
1322-01R	1550	8.56e+00	5.78e-01	2.58e-02	2.1e-15	0.9	1.4e-03	11.3	95.65	124	± 9
1322-01S	1550	1.68e+01	5.14e-01	5.42e-02	8.8e-16	1.0	1.1e-03	4.8	100.00	103	± 22
total gas age					2.0e-14				n=17	150	± 30
plateau age										N.A.	
isochron age				$^{40}Ar/^{36}Ar$ = 298.9 ± 0.8			MSWD = 7.5			102	± 6
E81002: Abbott Peak tephriphonolite, 107.6 mg plagioclase (<1% glass)					**J=0.0000702±0.0000002**						
1326-01A	550	3.67e+03	3.16e+00	1.23e+01	1.6e-17	0.2	3.4e-02	0.6	0.36	2826	± 31565

Lab#	Temp (°C)	$^{40}Ar/^{39}Ar$	$^{37}Ar/^{39}Ar$	$^{36}Ar/^{39}Ar$	$^{39}Ar_K$ (moles)	K/Ca	Cl/K	$^{40}Ar^*$ (%)	^{39}Ar (%)	Age (ka)	Err (1σ)
1326-01B	700	2.03e+02	4.65e+00	6.77e-01	2.5e-16	0.1	1.4e-03	1.6	6.22	420 ±	143
1326-01C	800	8.91e+00	5.04e+00	1.68e-02	1.2e-15	0.1	3.9e-04	48.3	34.77	546 ±	8
1326-01D	900	5.84e+00	5.26e+00	6.23e-03	8.7e-16	0.1	3.7e-04	75.0	55.13	556 ±	10
1326-01E	1000	6.52e+00	4.42e+00	1.08e-02	6.7e-16	0.1	9.7e-04	55.9	70.85	463 ±	13
1326-01F	1100	6.52e+00	4.77e+00	1.03e-02	3.6e-16	0.1	9.0e-04	58.7	79.12	486 ±	30
1326-01G	1200	5.98e+00	4.00e+00	5.80e-03	2.5e-16	0.1	2.4e-03	76.1	84.86	578 ±	38
1326-01H	1300	2.93e+00	3.52e+00	-2.47e-04	1.1e-16	0.1	4.6e-03	111.0	87.52	412 ±	93
1326-01I	1400	2.35e+01	4.54e+00	6.01e-02	1.7e-16	0.1	3.4e-03	25.7	91.50	767 ±	67
1326-01J	1500	1.93e+01	3.96e+00	5.47e-02	2.3e-16	0.1	2.6e-03	17.8	96.88	437 ±	34
1326-01K	1550	1.25e+02	5.39e+00	3.98e-01	7.1e-17	0.1	7.2e-04	6.6	98.53	1044 ±	251
1326-01L	1550	1.46e+02	3.90e+00	4.79e-01	6.3e-17	0.1	2.6e-03	3.5	100.00	647 ±	232
total gas age					4.3e-15				n=12	540 ±	150
plateau age							B-F		78.76	531 ±	19
isochron age				$^{40}Ar/^{36}Ar$ = 295.0 ± 4.1			MSWD = 15.3			536 ±	7
E82405: Bomb Peak trachyte, 115.6 mg anorthoclase (<1% glass)						**J=0.0000701±0.0000002**					
1327-01A	550	8.45e+02	9.88e-01	2.86e+00	4.0e-17	0.5	-1.2e-03	0.1	0.10	59 ±	1762
1327-01B	700	5.86e+02	2.09e-01	1.96e+00	5.8e-17	2.4	3.0e-03	1.1	0.24	838 ±	891
1327-01C	800	8.01e+00	1.06e-01	2.26e-02	5.5e-16	4.8	4.8e-04	16.4	1.59	166 ±	17
1327-01D	900	3.26e+00	6.34e-02	6.98e-03	2.1e-15	8.0	1.1e-04	36.2	6.83	149 ±	4
1327-01E	1000	2.72e+00	5.64e-02	5.02e-03	4.4e-15	9.0	1.3e-04	44.9	17.73	154 ±	2
1327-01F	1100	2.47e+00	5.00e-02	4.22e-03	6.7e-15	10.2	8.5e-06	48.8	34.36	152 ±	1
1327-01G	1200	2.39e+00	5.35e-02	3.69e-03	9.5e-15	9.5	-8.1e-07	53.6	57.96	162 ±	1
1327-01H	1300	2.41e+00	4.97e-02	3.85e-03	1.0e-14	10.3	3.4e-05	52.1	83.86	159 ±	1
1327-01I	1400	2.94e+00	5.07e-02	5.42e-03	4.3e-15	10.1	-7.4e-05	44.9	94.44	167 ±	2
1327-01J	1500	1.24e+01	7.19e-02	3.66e-02	5.3e-16	7.1	3.9e-06	12.3	95.74	192 ±	19
1327-01K	1550	9.29e+00	1.59e-01	2.65e-02	1.1e-15	3.2	-3.3e-05	15.8	98.41	185 ±	10
1327-01L	1550	1.46e+01	1.38e-01	4.40e-02	6.4e-16	3.7	-1.6e-04	11.0	100.00	203 ±	18
total gas age					4.0e-14				n=12	161 ±	6
plateau age							D-G		56.37	157 ±	3
isochron age				$^{40}Ar/^{36}Ar$ = 303.4 ± 2.1			MSWD = 6.6			154 ±	1

Lab#	Temp (°C)	$^{40}Ar/^{39}Ar$	$^{37}Ar/^{39}Ar$	$^{36}Ar/^{39}Ar$	$^{39}Ar_K$ (moles)	K/Ca	Cl/K	$^{40}Ar^*$ (%)	^{39}Ar (%)	Age (ka)	Err (1σ)
E80020: Three Sister's Cones, 104.1 mg anorthoclase (~1% glass)					**J=0.0000694±0.0000002**						
1328-01A	550	3.15e+03	8.08e-01	1.06e+01	3.7e-17	0.6	1.6e-02	0.2	0.17	915	± 8345
1328-01B	700	2.00e+02	5.46e-01	6.60e-01	2.8e-16	0.9	1.9e-03	2.6	1.49	665	± 152
1328-01C	800	3.28e+00	4.19e-01	7.92e-03	2.6e-15	1.2	2.2e-04	28.9	13.92	118	± 3
1328-01D	900	1.36e+00	4.00e-01	1.89e-03	3.5e-15	1.3	1.4e-04	59.6	30.51	102	± 2
1328-01E	1000	1.52e+00	3.92e-01	2.36e-03	4.9e-15	1.3	1.2e-04	54.6	53.50	104	± 2
1328-01F	1100	1.97e+00	3.79e-01	3.06e-03	4.3e-15	1.3	1.4e-04	54.5	73.54	135	± 2
1328-01G	1200	4.64e+00	3.69e-01	4.70e-03	2.2e-15	1.4	1.9e-04	70.2	83.75	407	± 3
1328-01H	1300	2.62e+01	4.04e-01	1.29e-02	1.6e-15	1.3	1.1e-03	85.5	91.24	2800	± 9
1328-01I	1400	4.61e+01	5.86e-01	6.02e-02	3.3e-16	0.9	2.3e-03	61.5	92.77	3545	± 44
1328-01J	1500	4.42e+01	6.58e-01	7.72e-02	3.4e-16	0.8	2.4e-03	48.4	94.37	2677	± 36
1328-01K	1650	3.79e+01	5.11e-01	1.16e-01	9.6e-16	1.0	1.2e-03	9.5	98.88	453	± 24
1328-01L	1650	2.18e+02	1.90e-01	7.18e-01	2.4e-16	2.7	1.8e-03	2.9	100.00	781	± 207
total gas age					2.1e-14				n=12	470	± 20
plateau age							C-F		72.05	111	± 8
isochron age				$^{40}Ar/^{36}Ar$ = 814.8 ± 3.6			MSWD = 4679.4			-34	± 1
E80020: Three Sister's Cones, 110.5 mg anorthoclase (~4% glass)					**J=0.0000699±0.0000002**						
1329-01A	550	2.46e+03	7.29e-01	8.29e+00	7.8e-17	0.7	1.4e-02	0.4	0.36	1101	± 3972
1329-01B	700	5.75e+01	5.21e-01	1.91e-01	2.3e-16	1.0	8.8e-04	1.8	1.44	131	± 68
1329-01C	800	1.86e+00	4.05e-01	5.83e-03	1.9e-15	1.3	4.7e-04	8.0	10.04	19	± 5
1329-01D	900	9.25e-01	3.81e-01	2.54e-03	3.2e-15	1.3	3.4e-04	19.8	24.77	23	± 3
1329-01E	1000	7.23e-01	3.78e-01	1.75e-03	4.5e-15	1.3	3.1e-04	29.3	45.57	27	± 2
1329-01F	1100	1.23e+00	3.66e-01	3.44e-03	4.3e-15	1.4	3.6e-04	17.6	65.36	27	± 2
1329-01G	1200	1.64e+00	3.61e-01	4.50e-03	2.9e-15	1.4	4.3e-04	19.1	78.86	40	± 3
1329-01H	1300	2.96e+00	3.67e-01	8.29e-03	2.4e-15	1.4	1.0e-03	17.6	89.83	66	± 4
1329-01I	1400	1.19e+01	3.62e-01	3.68e-02	5.5e-16	1.4	1.0e-03	8.4	92.39	125	± 20
1329-01J	1500	1.16e+01	4.08e-01	3.63e-02	6.8e-16	1.2	6.8e-04	7.7	95.54	112	± 19
1329-01K	1650	2.88e+01	4.00e-01	9.42e-02	8.5e-16	1.3	7.3e-04	3.4	99.48	123	± 25
1329-01L	1650	2.70e+02	4.25e-01	9.38e-01	1.1e-16	1.2	-1.7e-03	-2.8	100.00	-945	± 870
total gas age					2.2e-14				n=12	40	± 20
plateau age							C-F		63.93	26	± 2
isochron age				$^{40}Ar/^{36}Ar$ = 311.8 ± 1.8			MSWD = 10.4			24	± 1

Lab#	Temp (°C)	$^{40}Ar/^{39}Ar$	$^{37}Ar/^{39}Ar$	$^{36}Ar/^{39}Ar$	$^{39}Ar_K$ (moles)	K/Ca	Cl/K	$^{40}Ar^*$ (%)	^{39}Ar (%)	Age (ka)	Err (1σ)
EL: Summit Phenocrysts, 206.6 mg anorthoclase (~1% glass)					**J=0.00007±0.0000002**						
1330-01A	550	4.51e+03	1.03e+00	1.52e+01	2.2e-17	0.5	3.0e-02	0.8	0.06	4371	± 16125
1330-01B	600	3.47e+03	6.17e-01	1.17e+01	6.0e-17	0.8	1.2e-02	0.1	0.21	507	± 6650
1330-01C	600	6.05e+02	4.24e-01	2.04e+00	9.8e-17	1.2	-8.7e-04	0.1	0.45	86	± 745
1330-01D	700	8.11e+01	4.39e-01	2.70e-01	5.1e-16	1.2	9.6e-04	1.6	1.72	166	± 54
1330-01E	700	9.25e+00	4.27e-01	3.03e-02	9.5e-16	1.2	2.6e-04	3.5	4.10	41	± 12
1330-01F	800	1.43e+00	4.19e-01	3.99e-03	1.9e-15	1.2	3.4e-04	18.1	8.74	33	± 5
1330-01G	800	1.86e+00	4.28e-01	5.76e-03	2.5e-15	1.2	1.6e-04	9.0	14.88	21	± 3
1330-01H	900	7.54e-01	4.30e-01	2.17e-03	3.6e-15	1.2	2.2e-04	16.6	23.87	16	± 2
1330-01I	900	7.94e-01	4.23e-01	2.48e-03	4.3e-15	1.2	9.5e-05	9.0	34.75	9	± 2
1330-01J	1000	1.02e+00	4.27e-01	3.21e-03	4.5e-15	1.2	1.2e-04	8.1	45.99	10	± 2
1330-01K	1000	1.22e+00	4.23e-01	4.04e-03	4.8e-15	1.2	1.5e-04	3.0	57.95	5	± 2
1330-01L	1100	1.20e+00	4.17e-01	3.37e-03	3.6e-15	1.2	4.8e-04	18.1	67.02	28	± 2
1330-01M	1100	2.20e+00	4.13e-01	7.06e-03	2.2e-15	1.2	1.7e-04	5.6	72.63	15	± 4
1330-01N	1200	3.54e+00	4.07e-01	8.23e-03	1.9e-15	1.3	1.5e-03	31.6	77.35	142	± 4
1330-01O	1200	5.72e+00	4.04e-01	1.71e-02	1.1e-15	1.3	9.5e-04	12.0	80.05	86	± 9
1330-01P	1300	2.53e+00	4.05e-01	4.59e-03	2.9e-15	1.3	1.8e-03	46.6	87.38	149	± 2
1330-01Q	1300	4.48e+00	4.17e-01	1.30e-02	2.0e-15	1.2	1.0e-03	14.5	92.43	82	± 5
1330-01R	1400	7.78e+00	4.28e-01	2.44e-02	5.1e-16	1.2	1.3e-03	7.4	93.72	72	± 13
1330-01S	1400	3.40e+01	4.29e-01	1.13e-01	3.0e-16	1.2	1.4e-03	2.0	94.46	88	± 44
1330-01T	1500	6.03e+00	4.32e-01	1.81e-02	1.4e-15	1.2	8.5e-04	11.5	97.95	88	± 8
1330-01U	1650	3.86e+01	4.51e-01	1.27e-01	7.6e-16	1.1	1.0e-03	2.7	99.84	129	± 25
1330-01V	1650	5.78e+02	5.02e-01	1.94e+00	6.3e-17	1.0	3.9e-03	0.9	100.00	671	± 834
total gas age					4.0e-14				n=22	50	± 30
plateau age							I-K		34.08	8	± 2
isochron age				$^{40}Ar/^{36}Ar$ = 316.6 ± 0.9			MSWD = 185.2			24	± 1
EL: Summit Phenocrysts #2, 202.4 mg anorthoclase (30-40% glass)					**J=0.000069±0.0000002**						
1331-01A	550	4.21e+03	6.44e-01	1.41e+01	4.5e-17	0.8	3.5e-01	1.1	0.12	5867	± 11980
1331-01B	600	1.45e+03	3.93e-01	4.79e+00	7.7e-17	1.3	6.9e-02	2.6	0.31	4716	± 2044
1331-01C	600	3.33e+02	3.44e-01	1.08e+00	9.2e-17	1.5	2.7e-02	4.3	0.55	1801	± 479

Lab#	Temp (°C)	$^{40}Ar/^{39}Ar$	$^{37}Ar/^{39}Ar$	$^{36}Ar/^{39}Ar$	$^{39}Ar_K$ (moles)	K/Ca	Cl/K	$^{40}Ar^*$ (%)	^{39}Ar (%)	Age (ka)	Err (1σ)
1331-01D	700	4.29e+01	3.68e-01	1.15e-01	4.9e-16	1.4	1.7e-02	20.9	1.82	1120	± 39
1331-01E	700	2.06e+01	3.66e-01	4.29e-02	1.0e-15	1.4	1.3e-02	38.4	4.49	984	± 17
1331-01F	800	1.64e+01	3.62e-01	2.82e-02	2.2e-15	1.4	1.2e-02	49.3	10.22	1010	± 9
1331-01G	800	1.34e+01	3.71e-01	1.96e-02	2.3e-15	1.4	1.1e-02	56.9	16.20	950	± 7
1331-01H	900	1.22e+01	3.84e-01	1.86e-02	3.6e-15	1.3	9.3e-03	54.9	25.38	834	± 5
1331-01I	900	1.05e+01	3.85e-01	1.33e-02	3.7e-15	1.3	8.9e-03	62.9	34.91	824	± 5
1331-01J	1000	1.46e+01	3.59e-01	1.46e-02	4.8e-15	1.4	1.3e-02	70.4	47.33	1278	± 5
1331-01K	1000	8.91e+00	3.92e-01	1.31e-02	3.5e-15	1.3	6.3e-03	56.6	56.48	628	± 5
1331-01L	1100	1.12e+01	3.89e-01	1.82e-02	3.2e-15	1.3	7.5e-03	52.3	64.84	732	± 6
1331-01M	1100	5.94e+00	4.40e-01	2.01e-02	1.3e-15	1.2	2.2e-04	0.1	68.20	1	± 9
1331-01N	1200	7.97e+00	4.69e-01	2.41e-02	1.8e-15	1.1	1.6e-03	10.9	72.94	109	± 7
1331-01O	1200	9.57e+00	5.18e-01	3.31e-02	1.0e-15	1.0	2.4e-04	-2.0	75.61	-24	± 12
1331-01P	1300	6.15e+00	7.33e-01	1.67e-02	3.7e-15	0.7	3.4e-03	20.1	85.22	154	± 5
1331-01Q	1300	6.07e+00	6.18e-01	1.84e-02	1.9e-15	0.8	1.7e-03	11.1	90.04	84	± 6
1331-01R	1400	5.40e+00	6.23e-01	1.59e-02	1.5e-15	0.8	1.8e-03	13.3	93.89	90	± 7
1331-01T	1500	1.08e+01	5.20e-01	3.52e-02	8.1e-16	1.0	1.3e-03	4.2	95.97	56	± 11
1331-01U	1650	2.48e+01	5.93e-01	8.19e-02	1.2e-15	0.9	2.4e-03	2.3	99.04	71	± 16
1331-01V	1650	1.12e+02	5.11e-01	3.71e-01	3.7e-16	1.0	1.7e-03	1.8	100.00	248	± 93
total gas age					3.9e-14				n=21	640	± 30
plateau age										N.A.	
isochron age				$^{40}Ar/^{36}Ar$ = 594.2 ± 3.2			MSWD = 2648.8			-23	± 1
EL: 151.0 mg Summit (bomb) glass (100% glass)					**J=0.0000694±0.0000002**						
1332-01A	550	1.37e+03	4.88e-01	4.76e+00	3.6e-17	1.0	6.6e-02	-2.3	0.08	-4029	± 3499
1332-01B	600	4.75e+02	1.91e-01	1.65e+00	1.8e-16	2.7	5.5e-02	-2.4	0.49	-1446	± 367
1332-01C	600	1.44e+02	1.67e-01	4.91e-01	1.1e-16	3.1	5.4e-02	-0.5	0.73	-86	± 194
1332-01D	700	1.32e+01	1.49e-01	4.34e-02	8.9e-16	3.4	5.0e-02	2.6	2.78	43	± 14
1332-01E	700	2.21e+00	1.53e-01	6.80e-03	1.6e-15	3.3	4.8e-02	8.5	6.40	23	± 6
1332-01F	800	1.80e+01	1.52e-01	6.01e-02	3.4e-15	3.3	4.8e-02	1.5	14.25	33	± 10
1332-01G	800	3.01e-01	1.57e-01	3.09e-05	4.1e-15	3.3	4.9e-02	93.7	23.58	35	± 2
1332-01H	900	8.10e+01	1.53e-01	2.67e-01	7.7e-15	3.3	4.8e-02	2.4	41.26	246	± 27
1332-01I	900	1.61e+00	1.53e-01	3.69e-03	6.9e-15	3.3	4.9e-02	31.7	57.18	64	± 1
1332-01J	1000	1.64e+00	1.53e-01	3.29e-03	6.0e-15	3.3	4.8e-02	40.0	70.85	82	± 1

Lab#	Temp (°C)	$^{40}Ar/^{39}Ar$	$^{37}Ar/^{39}Ar$	$^{36}Ar/^{39}Ar$	$^{39}Ar_K$ (moles)	K/Ca	Cl/K	$^{40}Ar^*$ (%)	^{39}Ar (%)	Age (ka)	Err (1σ)
1332-01K	1000	1.77e+00	1.52e-01	3.12e-03	3.6e-15	3.4	4.8e-02	47.2	79.16	104	± 2
1332-01L	1100	2.05e+00	1.52e-01	3.48e-03	5.1e-15	3.4	4.8e-02	49.3	90.89	126	± 2
1332-01M	1100	2.97e+00	1.44e-01	6.61e-03	1.8e-15	3.5	4.9e-02	33.8	95.11	126	± 5
1332-01N	1200	4.46e+00	1.70e-01	1.09e-02	1.6e-15	3.0	4.8e-02	27.4	98.71	153	± 6
1332-01O	1200	1.34e+01	4.25e-01	4.09e-02	2.4e-16	1.2	4.9e-02	10.0	99.26	168	± 42
1332-01P	1300	1.78e+01	2.45e+00	5.61e-02	1.8e-16	0.2	6.0e-02	7.7	99.67	172	± 36
1332-01Q	1300	1.62e+02	6.41e+00	5.44e-01	3.2e-17	0.1	8.1e-02	1.3	99.74	263	± 449
1332-01R	1400	1.67e+02	1.03e+01	5.76e-01	2.0e-17	0.0	9.3e-02	-1.6	99.79	-337	± 609
1332-01S	1400	1.88e+03	2.88e+01	6.12e+00	3.8e-18	0.0	2.6e-01	3.9	99.80	9419	± 22142
1332-01T	1650	4.64e+02	2.96e+00	1.55e+00	8.9e-17	0.2	4.0e-02	1.1	100.00	650	± 491
total gas age					4.4e-14			n=20		101	± 16
plateau age										N.A	
isochron age				$^{40}Ar/^{36}Ar$ = 307.5 ± 0.6			MSWD = 192.5			54	± 1
AW82038: Turks Head tephrite, 148.6 mg plagioclase (~5% glass)						**J=0.0000704±0.0000002**					
1422-01A	700	9.29e+01	6.40e+00	3.06e-01	1.6e-15	0.1	1.2e-02	3.2	27.18	377	± 52
1422-01B	850	8.47e+00	7.51e+00	1.96e-02	1.2e-15	0.1	6.8e-03	38.0	46.90	412	± 11
1422-01C	1000	6.13e+00	7.47e+00	1.29e-02	9.5e-16	0.1	5.0e-03	47.0	62.88	368	± 9
1422-01D	1100	7.52e+00	7.79e+00	1.79e-02	5.9e-16	0.1	4.1e-03	37.3	72.81	359	± 11
1422-01E	1200	1.25e+01	7.84e+00	3.33e-02	4.3e-16	0.1	7.4e-03	25.8	80.15	411	± 17
1422-01F	1300	2.30e+01	8.47e+00	7.16e-02	1.6e-16	0.1	4.9e-03	10.8	82.79	317	± 57
1422-01G	1450	4.00e+01	8.59e+00	1.25e-01	3.0e-16	0.1	4.7e-03	9.3	87.91	478	± 47
1422-01H	1700	4.05e+01	8.69e+00	1.28e-01	7.2e-16	0.1	1.8e-03	8.0	100.00	412	± 32
total gas age					5.9e-15			n=8		390	± 30
plateau age							A-D		72.81	378	± 14
isochron age				$^{40}Ar/^{36}Ar$ = 297.4 ± 1.1			MSWD = 5.4			376	± 5
E83432: Cape Barne tephrite, 91.7 mg whole rock						**J=0.0000692±0.0000002**					
1528-01A	500	1.91e+02	1.03e+00	5.97e-01	9.7e-16	0.5	1.1e-01	7.5	5.56	1785	± 118
1528-01B	600	1.77e+01	9.61e-01	2.49e-02	2.0e-15	0.5	8.6e-02	58.8	17.27	1301	± 10
1528-01C	675	1.42e+01	8.90e-01	1.30e-02	3.0e-15	0.6	9.2e-02	73.2	34.29	1297	± 7
1528-01D	825	1.18e+01	3.52e-01	1.31e-03	6.0e-17	1.5	1.0e-01	96.8	34.63	1424	± 160

Lab#	Temp (°C)	$^{40}Ar/^{39}Ar$	$^{37}Ar/^{39}Ar$	$^{36}Ar/^{39}Ar$	$^{39}Ar_K$ (moles)	K/Ca	Cl/K	$^{40}Ar^*$ (%)	^{39}Ar (%)	Age (ka)	Err (1σ)
1528-01E	900	1.58e+01	6.02e-01	1.78e-02	6.5e-15	0.8	9.2e-02	66.9	71.76	1318	± 6
1528-01F	1050	1.82e+01	7.83e-01	2.60e-02	2.0e-15	0.7	8.2e-02	58.1	83.36	1323	± 10
1528-01G	1250	3.81e+01	2.27e+00	9.60e-02	1.3e-15	0.2	6.1e-02	25.9	90.60	1230	± 27
1528-01H	1650	5.44e+01	1.20e+01	1.56e-01	1.5e-15	0.0	1.4e-01	16.9	99.42	1156	± 35
1528-01I	1650	1.43e+02	1.67e+01	4.62e-01	1.0e-16	0.0	8.5e-02	5.3	100.00	958	± 271
total gas age					1.7e-14			n=9		1316	± 19
plateau age							B-E		66.19	1310	± 8
isochron age				$^{40}Ar/^{36}Ar$ = 290.6 ± 2.4			MSWD =	4.0		1321	± 8
E77012: Tryggve Pt. dike phonotephrite, 109.5 mg plagioclase (~1% glass)						**J=0.0000704±0.0000002**					
1536-01A	500	2.15e+02	3.23e+00	7.18e-01	3.0e-16	0.2	2.7e-02	1.4	2.80	375	± 244
1536-01B	600	2.41e+01	3.21e+00	7.23e-02	6.2e-16	0.2	1.3e-02	12.3	8.48	377	± 27
1536-01C	*675*	*6.16e+01*	*3.02e-01*	*7.65e-02*	*1.9e-18*	*1.7*	*5.0e-02*	*63.3*	*8.50*	*4949*	*± 3993*
1536-01D	750	9.10e+00	3.29e+00	2.09e-02	1.2e-15	0.2	1.5e-02	34.8	19.67	402	± 12
1536-01E	783	7.90e+00	3.47e+00	1.77e-02	2.3e-16	0.1	2.3e-02	36.8	21.78	370	± 33
1536-01F	900	7.06e+00	3.05e+00	1.29e-02	8.7e-16	0.2	2.1e-02	49.0	29.75	441	± 14
1536-01G	1050	3.89e+00	3.31e+00	4.47e-03	1.1e-15	0.2	7.1e-03	72.1	40.23	357	± 11
1536-01H	1250	6.99e+00	2.56e+00	6.87e-03	1.1e-15	0.2	5.3e-02	73.4	50.77	653	± 10
1536-01I	1650	4.87e+00	4.14e+00	7.84e-03	5.4e-15	0.1	4.6e-03	58.5	100.00	363	± 3
total gas age					1.1e-14			n=8		375	± 16
plateau age							B-I		97.20	368	± 9
isochron age				$^{40}Ar/^{36}Ar$ = 302.1 ± 3.0			MSWD = 11.6			374	± 7
E83407: Inaccessible Island phonolite, 99.0 mg whole rock						**J=0.0000705±0.0000002**					
1537-01A	500	3.14e+01	1.09e-01	8.34e-02	1.7e-15	4.7	1.3e-02	21.5	4.11	859	± 25
1537-01B	600	6.92e+00	6.44e-02	1.00e-02	3.9e-15	7.9	6.9e-03	56.9	13.50	500	± 6
1537-01C	675	8.01e+00	5.99e-02	1.29e-02	6.2e-15	8.5	1.1e-02	52.1	28.36	530	± 6
1537-01D	750	-1.10e+01	0.00e+00	-5.22e-02	7.1e-17	- -	1.7e-02	-39.9	28.53	559	± 131
1537-01E	825	8.20e+00	8.49e-02	1.34e-02	6.5e-15	6.0	2.2e-02	51.5	44.06	537	± 4
1537-01F	900	7.58e+00	1.01e-01	1.09e-02	3.7e-15	5.1	3.4e-02	57.4	52.81	553	± 5
1537-01G	1050	7.10e+00	1.36e-01	9.44e-03	7.9e-15	3.7	3.5e-02	60.5	71.62	546	± 3
1537-01H	1250	8.16e+00	6.16e-01	1.33e-02	9.6e-15	0.8	3.0e-02	52.2	94.39	541	± 4

Lab#	Temp (°C)	$^{40}Ar/^{39}Ar$	$^{37}Ar/^{39}Ar$	$^{36}Ar/^{39}Ar$	$^{39}Ar_K$ (moles)	K/Ca	Cl/K	$^{40}Ar^*$ (%)	^{39}Ar (%)	Age (ka)	Err (1σ)
1537-01I	1650	1.10e+01	5.58e-01	2.23e-02	2.4e-15	0.9	8.0e-03	40.0	100.00	558	± 10
total gas age					4.2e-14			n=9		551	± 6
plateau age							B-I		95.89	539	± 6
isochron age				$^{40}Ar/^{36}Ar$ = 304.0 ± 5.0			MSWD = 10.9			527	± 8
E83453: SW of Abbott Peak phonotephrite, 100.5 mg whole rock					**J=0.0000696±0.0000002**						
1865-01A	500	4.33e+03	1.36e+00	1.45e+01	3.8e-16	0.4	6.3e-02	1.4	1.05	7573	± 5463
1865-01B	600	3.10e+02	3.00e-01	1.02e+00	2.8e-15	1.7	1.8e-02	2.6	8.97	1027	± 176
1865-01C	700	3.03e+01	3.32e-01	9.08e-02	7.1e-15	1.5	1.0e-02	11.4	28.70	434	± 16
1865-01D	800	2.64e+01	3.86e-01	7.66e-02	4.2e-15	1.3	6.7e-03	14.1	40.52	468	± 15
1865-01E	900	2.70e+01	4.78e-01	7.82e-02	3.4e-15	1.1	7.2e-03	14.6	49.91	495	± 20
1865-01F	1000	4.39e+01	6.08e-01	1.34e-01	2.5e-15	0.8	9.3e-03	9.7	56.78	537	± 26
1865-01G	1100	1.07e+02	6.59e-01	3.47e-01	1.9e-15	0.8	1.0e-02	3.8	62.15	507	± 64
1865-01H	1200	1.52e+01	1.54e+00	4.18e-02	1.1e-14	0.3	1.6e-02	19.3	92.27	369	± 9
1865-01I	1300	1.55e+01	7.43e+00	4.19e-02	2.6e-15	0.1	3.6e-02	23.6	99.60	461	± 12
1865-01J	1400	5.08e+01	1.99e+01	1.46e-01	1.6e-16	0.0	4.4e-02	18.1	100.04	1172	± 129
1865-01K	*1650*	*3.20e+02*	*7.54e+01*	*1.20e+00*	*2.7e-17*	*0.0*	*3.5e-02*	*-9.3*	*100.12*	*-3954*	*± 2883*
1865-01L	1650	-2.07e+02	0.00e+00	-8.18e-01	-4.2e-17	- -	1.9e-02	-16.6	100.00	4309	± 1411
total gas age					3.6e-14			n=11		550	± 90
plateau age							C-I		90.63	430	20
isochron age				$^{40}Ar/^{36}Ar$ = 301.2 ± 1.0			MSWD = 10.8			388	± 9
E80020: Three Sisters Cones, 115.2 mg anorthoclase (~1% glass)					**J=0.00006967±0.0000002**						
2485-01A	550	1.62e+03	9.54e+00	5.48e+00	5.5e-16	0.1	7.3e-03	0.1	0.90	249	± 2021
2485-01B	750	1.25e+01	6.59e-01	3.97e-02	6.7e-15	0.8	-7.2e-05	6.1	11.94	95	± 11
2485-01C	800	2.35e+00	6.14e-01	6.36e-03	1.2e-14	0.8	9.8e-05	20.9	31.26	62	± 3
2485-01D	900	1.54e+00	7.58e-01	4.13e-03	1.4e-14	0.7	7.8e-05	22.9	53.85	44	± 2
2485-01E	1000	1.64e+00	1.11e+01	4.29e-03	1.2e-14	0.0	2.8e-04	73.3	74.11	152	± 3
2485-01F	1100	3.65e+00	5.17e+01	8.49e-03	7.9e-15	0.0	1.3e-03	139.4	87.02	664	± 6
2485-01G	1200	9.22e+00	6.69e+01	2.16e-02	2.7e-15	0.0	4.7e-03	86.1	91.38	1047	± 14
2485-01H	1300	5.51e+00	1.31e+01	1.59e-02	4.0e-15	0.0	1.4e-03	32.6	97.92	228	± 9
2485-01I	1400	4.70e+01	0.00e+00	1.73e-01	5.1e-16	- -	2.4e-03	-8.5	98.75	-504	± 80

Lab#	Temp (°C)	$^{40}Ar/^{39}Ar$	$^{37}Ar/^{39}Ar$	$^{36}Ar/^{39}Ar$	$^{39}Ar_K$ (moles)	K/Ca	Cl/K	$^{40}Ar^*$ (%)	^{39}Ar (%)	Age (ka)	Err (1σ)
2485-01J	1500	3.50e+02	0.00e+00	1.19e+00	3.4e-16	- -	1.3e-02	-0.4	99.31	-180	± 549
2485-01K	1650	9.21e+02	0.00e+00	3.14e+00	3.0e-16	- -	1.3e-02	-0.9	99.81	-1019	± 1408
2485-01L	1750	3.76e+03	0.00e+00	1.27e+01	1.2e-16	- -	-1.1e-02	-0.1	100.00	-323	± 9467
total gas age					6.1e-14				n=12	200	± 50
plateau age							B-D		52.95	52	± 8
isochron age				$^{40}Ar/^{36}Ar$ = 2558.3 ± 10.4			MSWD = 12780.6			-212	± 9
E87035: Nausea Knob, 133.8 mg anorthoclase (<1% glass)					**J=0.000075894±0.0000002**						
2642-01A	550	8.15e+01	5.03e-01	2.82e-01	8.6e-16	1.0	4.6e-03	-2.3	1.34	-254	± 149
2642-01B	700	5.48e+00	4.64e-01	1.55e-02	7.9e-15	1.1	-6.3e-05	16.5	13.72	124	± 13
2642-01C	800	2.48e+00	4.69e-01	7.39e-03	1.1e-14	1.1	8.1e-05	12.5	30.16	43	± 4
2642-01D	900	1.95e+00	4.67e-01	5.93e-03	1.2e-14	1.1	-2.7e-05	10.9	48.87	29	± 3
2642-01E	1000	2.38e+00	4.42e-01	6.44e-03	1.2e-14	1.2	1.4e-04	20.6	66.81	67	± 3
2642-01F	1100	2.85e+00	4.38e-01	8.77e-03	8.0e-15	1.2	7.7e-04	9.5	79.29	37	± 4
2642-01G	1200	6.45e+00	4.22e-01	1.86e-02	3.6e-15	1.2	1.3e-02	15.1	84.83	134	± 10
2642-01H	1300	4.05e+00	4.40e-01	1.10e-02	6.8e-15	1.2	2.3e-03	20.1	95.44	111	± 6
2642-01I	1400	5.29e+00	4.47e-01	1.61e-02	9.6e-16	1.1	4.6e-03	10.1	96.94	73	± 20
2642-01J	1550	8.96e+00	5.06e-01	3.22e-02	6.7e-16	1.0	3.1e-03	-6.1	97.98	-75	± 108
2642-01K	1750	2.04e+01	4.53e-01	6.89e-02	1.2e-15	1.1	1.2e-03	0.5	99.80	13	± 32
2642-01L	1750	9.95e+01	3.74e-01	3.24e-01	1.3e-16	1.4	-3.2e-03	3.7	100.00	501	± 373
total gas age					6.4e-14				n=12	62	± 10
plateau age							C-F		65.57	46	± 9
isochron age				$^{40}Ar/^{36}Ar$ = 309.7 ± 2.4			MSWD = 25.3			39	± 2
E86026: Northeast Flow, 132.3 mg anorthoclase (<1% glass)					**J=0.000076038±0.0000002**						
2643-01A	550	1.56e+02	4.08e-01	5.46e-01	3.8e-16	1.2	1.1e-02	-3.4	0.65	-734	± 764
2643-01B	700	3.50e+00	4.62e-01	1.09e-02	6.4e-15	1.1	5.2e-04	8.5	11.67	41	± 29
2643-01C	800	2.16e+00	4.86e-01	5.22e-03	1.1e-14	1.1	6.2e-04	29.4	31.09	87	± 10
2643-01D	900	1.79e+00	4.51e-01	4.00e-03	8.6e-15	1.1	-1.0e-04	34.6	45.81	85	± 6
2643-01E	1000	1.86e+00	4.33e-01	3.63e-03	1.1e-14	1.2	-3.7e-05	42.8	64.16	109	± 4
2643-01F	1100	2.74e+00	4.38e-01	6.01e-03	7.9e-15	1.2	5.7e-04	35.7	77.67	134	± 4
2643-01G	1200	3.18e+00	4.36e-01	8.98e-03	4.0e-15	1.2	1.0e-02	17.0	84.55	74	± 8

Lab#	Temp (°C)	$^{40}Ar/^{39}Ar$	$^{37}Ar/^{39}Ar$	$^{36}Ar/^{39}Ar$	$^{39}Ar_K$ (moles)	K/Ca	Cl/K	$^{40}Ar^*$ (%)	^{39}Ar (%)	Age (ka)	Err (1σ)
2643-01H	1300	2.14e+00	4.41e-01	4.40e-03	5.2e-15	1.2	2.7e-03	39.8	93.50	117	± 4
2643-01I	1400	1.46e+00	4.51e-01	2.34e-03	1.8e-15	1.1	5.2e-03	53.6	96.55	107	± 10
2643-01J	1550	6.36e+00	4.55e-01	2.15e-02	7.2e-16	1.1	5.0e-03	0.3	97.79	3	± 26
2643-01K	1750	1.97e+01	4.49e-01	6.52e-02	1.2e-15	1.1	1.3e-03	2.2	99.76	60	± 42
2643-01L	1750	1.06e+02	3.56e-01	3.55e-01	1.4e-16	1.4	-4.5e-04	1.2	100.00	175	± 578
total gas age					5.9e-14				n=12	87	± 16
plateau age							B-F		77.02	110	± 10
isochron age				$^{40}Ar/^{36}Ar$ = 314.9 ± 10.0			MSWD = 14.7			99	± 5
E93011: NW of Hooper's Shoulder Cone, 119.1 mg anorthoclase (~2% glass)							**J=0.000075488±0.0000002**				
2644-01A	550	1.38e+02	3.09e-01	5.44e-01	3.6e-16	1.7	3.3e-02	-16.3	0.72	-3070	± 857
2644-01B	700	1.45e+01	6.21e-01	4.47e-02	3.2e-15	0.8	2.1e-03	9.2	7.00	183	± 76
2644-01C	800	6.40e+00	5.65e-01	1.92e-02	7.9e-15	0.9	7.2e-04	11.7	22.57	102	± 11
2644-01D	900	4.75e+00	5.58e-01	1.29e-02	8.7e-15	0.9	3.5e-04	19.8	39.69	128	± 7
2644-01E	1000	4.05e+00	5.45e-01	1.05e-02	1.0e-14	0.9	1.0e-04	23.8	59.91	131	± 5
2644-01F	1100	4.14e+00	5.41e-01	1.14e-02	8.0e-15	0.9	4.4e-04	19.3	75.76	109	± 5
2644-01G	1200	7.02e+00	5.37e-01	1.89e-02	5.1e-15	1.0	8.5e-03	20.9	85.84	200	± 9
2644-01H	1300	5.69e+00	5.36e-01	1.22e-02	4.3e-15	1.0	1.8e-03	37.1	94.36	288	± 7
2644-01I	1400	4.22e+00	5.52e-01	7.33e-03	1.6e-15	0.9	1.3e-03	49.2	97.53	283	± 22
2644-01J	1550	1.25e+01	5.54e-01	3.47e-02	5.9e-16	0.9	9.8e-04	18.3	98.71	313	± 75
2644-01K	1750	4.34e+01	5.45e-01	1.41e-01	9.3e-16	0.9	8.9e-04	4.0	100.55	238	± 122
2644-01L	1750	-1.09e+02	6.58e-01	-3.62e-01	-2.8e-16	0.8	-4.0e-03	1.4	100.00	-212	± 401
total gas age					5.1e-14				n=12	135	± 19
plateau age							C-F		68.76	121	± 7
isochron age				$^{40}Ar/^{36}Ar$ = 380.0 ± 8.6			MSWD = 66.9			11	± 0
E93021: SE of Hooper's Shoulder Cone, 115.5 mg anorthoclase (~2% glass)							**J=0.000075547±0.0000002**				
2645-01A	550	2.00e+02	2.84e-01	6.64e-01	3.9e-16	1.8	1.8e-02	1.8	0.87	502	± 1294
2645-01B	700	1.23e+01	5.96e-01	3.89e-02	2.7e-15	0.9	5.6e-04	6.6	6.81	111	± 18
2645-01C	800	4.85e+00	5.72e-01	1.40e-02	9.6e-15	0.9	1.2e-04	15.1	28.15	100	± 6
2645-01D	900	4.52e+00	5.67e-01	1.22e-02	7.2e-15	0.9	1.0e-04	20.6	44.28	127	± 7
2645-01E	1000	4.31e+00	5.66e-01	1.19e-02	7.1e-15	0.9	5.7e-05	18.9	60.06	111	± 6

Lab#	Temp (°C)	$^{40}Ar/^{39}Ar$	$^{37}Ar/^{39}Ar$	$^{36}Ar/^{39}Ar$	$^{39}Ar_K$ (moles)	K/Ca	Cl/K	$^{40}Ar^*$ (%)	^{39}Ar (%)	Age (ka)	Err (1σ)
2645-01F	1100	5.07e+00	5.59e-01	1.47e-02	6.2e-15	0.9	6.2e-04	14.7	73.91	102	± 7
2645-01G	1200	1.15e+01	5.52e-01	3.41e-02	3.1e-15	0.9	1.5e-02	12.4	80.78	194	± 16
2645-01H	1300	5.44e+00	5.24e-01	1.28e-02	8.6e-16	1.0	2.0e-03	30.8	82.71	228	± 22
2645-01I	1400	2.48e+00	5.68e-01	4.15e-03	2.8e-15	0.9	9.0e-04	51.5	88.91	174	± 7
2645-01J	1550	4.62e+00	5.77e-01	1.14e-02	2.2e-15	0.9	1.1e-03	27.5	93.79	173	± 11
2645-01K	1750	2.44e+01	5.62e-01	7.69e-02	2.4e-15	0.9	2.5e-04	6.9	99.21	230	± 29
2645-01L	1750	1.28e+02	5.53e-01	4.18e-01	3.5e-16	0.9	2.2e-03	3.2	100.00	559	± 202
total gas age					4.5e-14				n=12	140	± 20
plateau age							B-F		73.04	110	± 6
isochron age				$^{40}Ar/^{36}Ar$ = 298.4 ± 2.3			MSWD = 20.6			124	± 4
E93013: Caldera Rim, 110.9 mg anorthoclase (~1% glass)					**J=0.00007546±0.0000002**						
2646-01A	550	2.04e+02	4.68e-01	7.20e-01	1.9e-16	1.1	2.0e-02	-4.2	0.41	-1158	± 526
2646-01B	700	7.67e+00	5.21e-01	2.37e-02	4.9e-15	1.0	3.0e-04	9.1	11.01	95	± 10
2646-01C	800	6.45e+00	5.09e-01	1.93e-02	5.0e-15	1.0	3.2e-04	12.0	21.82	105	± 8
2646-01D	900	4.88e+00	5.13e-01	1.45e-02	5.5e-15	1.0	-2.3e-04	12.3	33.58	82	± 7
2646-01E	1000	3.58e+00	5.19e-01	9.86e-03	5.0e-15	1.0	1.6e-04	19.2	44.30	94	± 6
2646-01F	1100	4.36e+00	5.23e-01	1.31e-02	5.2e-15	1.0	5.6e-04	11.3	55.47	67	± 7
2646-01G	1200	9.50e+00	5.21e-01	2.91e-02	3.1e-15	1.0	1.2e-02	9.6	62.18	124	± 13
2646-01H	1300	3.58e+00	5.09e-01	8.27e-03	7.1e-15	1.0	9.0e-04	32.3	77.33	157	± 5
2646-01I	1400	1.79e+00	5.23e-01	3.60e-03	4.0e-15	1.0	3.5e-04	41.4	85.83	101	± 4
2646-01J	1550	3.50e+00	5.32e-01	9.29e-03	2.7e-15	1.0	5.3e-04	22.1	91.55	105	± 8
2646-01K	1750	2.73e+01	5.33e-01	8.77e-02	3.2e-15	1.0	6.8e-04	5.0	98.42	184	± 32
2646-01L	1750	7.91e+01	5.21e-01	2.57e-01	7.3e-16	1.0	6.8e-04	3.9	100.00	420	± 102
total gas age					4.7e-14				n=12	110	± 13
plateau age							B-F		55.06	87	± 7
isochron age				$^{40}Ar/^{36}Ar$ = 293.3 ± 2.4			MSWD = 28.5			112	± 3
E93019: between William's Cliff and Turk's Head, 115.4 mg anorthoclase (~2% glass)							**J=0.000075951±0.0000002**				
2647-01A	550	1.25e+02	9.47e-01	4.89e-01	2.8e-16	0.5	2.5e-02	-15.5	0.96	-2663	± 1410
2647-01B	700	7.99e+00	1.32e+00	2.17e-02	4.9e-15	0.4	2.6e-04	20.9	17.85	229	± 10
2647-01C	800	7.69e+00	1.30e+00	2.02e-02	5.6e-15	0.4	6.3e-04	23.6	36.87	248	± 10

Lab#	Temp (°C)	$^{40}Ar/^{39}Ar$	$^{37}Ar/^{39}Ar$	$^{36}Ar/^{39}Ar$	$^{39}Ar_K$ (moles)	K/Ca	Cl/K	$^{40}Ar^*$ (%)	^{39}Ar (%)	Age (ka)	Err (1σ)
2647-01D	900	6.37e+00	1.30e+00	1.58e-02	5.3e-15	0.4	-1.7e-04	28.0	55.06	245	± 9
2647-01E	1000	7.30e+00	1.34e+00	1.83e-02	3.3e-15	0.4	1.5e-04	27.0	66.23	270	± 10
2647-01F	1100	6.21e+00	1.36e+00	1.57e-02	2.9e-15	0.4	1.2e-03	26.5	76.18	226	± 11
2647-01G	1200	1.35e+01	1.36e+00	3.91e-02	1.7e-15	0.4	3.6e-02	15.0	81.97	278	± 20
2647-01H	1300	3.00e+01	1.45e+00	9.48e-02	1.3e-15	0.4	3.0e-03	7.0	86.44	287	± 42
2647-01I	1400	8.91e+00	1.49e+00	2.45e-02	3.1e-15	0.3	1.4e-03	19.6	97.00	240	± 12
2647-01J	1550	3.15e+01	1.43e+00	9.85e-02	3.1e-16	0.4	2.5e-03	7.8	98.04	338	± 77
2647-01K	1750	1.94e+02	1.08e+00	6.42e-01	3.9e-16	0.5	1.9e-03	2.5	99.38	663	± 274
2647-01L	1750	3.24e+02	8.62e-01	1.08e+00	1.8e-16	0.6	6.5e-03	1.8	100.00	810	± 542
total gas age					2.9e-14				n=12	230	± 30
plateau age							B-F		75.22	243	± 9
isochron age				$^{40}Ar/^{36}Ar$ = 301.3 ± 3.4			MSWD = 2.4			229	± 10
E93020: William's Cliff, 109.0 mg anorthoclase (~2% glass)					**J=0.000075854±0.0000002**						
2648-01A	550	1.88e+02	6.96e-01	6.52e-01	2.3e-16	0.7	3.3e-02	-2.7	0.67	-703	± 926
2648-01B	700	1.48e+01	8.19e-01	4.86e-02	2.8e-15	0.6	4.5e-04	3.1	8.71	63	± 19
2648-01C	800	7.86e+00	8.07e-01	2.53e-02	6.1e-15	0.6	8.2e-04	5.5	26.18	60	± 10
2648-01D	900	6.25e+00	8.30e-01	1.99e-02	4.6e-15	0.6	2.3e-04	6.6	39.27	56	± 10
2648-01E	1000	6.15e+00	8.37e-01	1.92e-02	3.5e-15	0.6	4.6e-04	8.3	49.32	70	± 11
2648-01F	1100	4.87e+00	8.30e-01	1.51e-02	3.8e-15	0.6	1.4e-03	9.0	60.19	60	± 9
2648-01G	1200	1.22e+01	8.11e-01	4.01e-02	2.4e-15	0.6	2.0e-02	2.8	67.14	46	± 19
2648-01H	1300	1.57e+01	7.87e-01	5.24e-02	3.5e-15	0.6	1.9e-03	1.7	77.28	36	± 21
2648-01I	1400	5.90e+00	8.36e-01	1.88e-02	4.2e-15	0.6	1.0e-03	6.4	89.25	52	± 9
2648-01J	1550	9.18e+00	8.30e-01	3.03e-02	1.0e-15	0.6	1.3e-03	3.0	92.25	38	± 25
2648-01K	1750	2.74e+01	8.29e-01	9.00e-02	2.2e-15	0.6	6.8e-04	3.1	98.67	118	± 32
2648-01L	1750	6.53e+01	8.17e-01	2.17e-01	4.6e-16	0.6	-7.0e-04	2.0	100.00	178	± 111
total gas age					3.5e-14				n=12	60	± 20
plateau age							B-J		91.58	57	± 5
isochron age				$^{40}Ar/^{36}Ar$ = 293.1 ± 2.9			MSWD = 0.5			65	± 9
E93014: Caldera Rim, 116.6 mg anorthoclase (~1% glass)					**J=0.000075825±0.0000002**						
2649-01A	550	1.71e+02	3.69e-01	6.07e-01	1.5e-16	1.4	-5.9e-03	-4.7	0.34	-1091	± 1900

Lab#	Temp (°C)	$^{40}Ar/^{39}Ar$	$^{37}Ar/^{39}Ar$	$^{36}Ar/^{39}Ar$	$^{39}Ar_K$ (moles)	K/Ca	Cl/K	$^{40}Ar^*$ (%)	^{39}Ar (%)	Age (ka)	Err (1σ)
2649-01B	700	1.00e+01	5.06e-01	3.04e-02	3.9e-15	1.0	7.2e-04	10.5	8.84	144	± 13
2649-01C	800	6.12e+00	4.84e-01	1.73e-02	5.5e-15	1.1	4.5e-04	16.7	20.76	140	± 8
2649-01D	900	5.65e+00	4.92e-01	1.59e-02	5.5e-15	1.0	1.2e-04	17.3	32.81	134	± 8
2649-01E	1000	6.11e+00	4.91e-01	1.59e-02	3.1e-15	1.0	3.4e-04	23.1	39.62	194	± 10
2649-01F	1100	4.09e+00	5.11e-01	1.08e-02	5.4e-15	1.0	4.8e-04	22.4	51.48	125	± 6
2649-01G	1200	5.59e+00	4.77e-01	1.15e-02	5.4e-15	1.1	8.1e-03	39.3	63.29	301	± 6
2649-01H	1300	4.81e+00	4.50e-01	4.65e-03	9.6e-15	1.1	6.3e-04	71.7	84.32	472	± 3
2649-01I	1400	1.45e+00	5.02e-01	1.60e-03	5.3e-15	1.0	4.9e-04	68.6	95.88	136	± 4
2649-01J	1550	2.84e+00	5.07e-01	8.00e-03	1.9e-15	1.0	5.1e-04	17.4	100.00	68	± 10
total gas age					4.6e-14				n=10	222	± 14
plateau age							B-F		51.15	141	± 12
isochron age				$^{40}Ar/^{36}Ar$ = 379.7 ± 3.4			MSWD = 985.7			218	± 2
E86026: Northeast Flow, 127.5 mg anorthoclase (<1% glass)					**J=0.000075988±0.0000002**						
2650-01A	550	6.23e+01	4.84e-01	2.04e-01	9.9e-16	1.1	4.0e-03	3.3	1.81	279	± 80
2650-01B	700	4.18e+00	4.84e-01	1.15e-02	1.0e-14	1.1	6.9e-05	19.1	20.33	110	± 5
2650-01C	800	2.78e+00	4.50e-01	7.62e-03	9.9e-15	1.1	-1.2e-04	19.5	38.54	74	± 4
2650-01D	900	3.24e+00	4.53e-01	9.32e-03	9.1e-15	1.1	5.5e-06	15.3	55.25	68	± 5
2650-01E	1000	3.35e+00	4.50e-01	9.34e-03	8.5e-15	1.1	7.0e-05	18.0	70.95	83	± 5
2650-01F	1200	7.68e+00	4.48e-01	2.15e-02	7.0e-15	1.1	6.8e-03	17.3	83.77	182	± 9
2650-01G	1350	3.06e+00	5.18e-01	7.73e-03	5.4e-15	1.0	1.1e-03	26.0	93.67	109	± 6
2650-01H	1500	3.37e+00	5.75e-01	2.83e-03	1.3e-15	0.9	1.5e-03	75.9	96.08	351	± 11
2650-01I	1750	4.27e+00	9.34e-01	8.32e-03	1.8e-15	0.5	7.6e-04	43.6	99.35	255	± 10
2650-01J	1750	9.80e+00	2.26e+00	2.50e-02	3.6e-16	0.2	2.4e-04	26.1	100.00	351	± 39
total gas age					5.4e-14				n=10	116	± 7
plateau age							C-E		50.62	75	± 5
isochron age				$^{40}Ar/^{36}Ar$ = 351.1 ± 5.4			MSWD = 10.5			18	± 3
E93005: Fang Ridge tephriphonolite, 111.5 mg plagioclase (<1% glass)						**J=0.00007544±0.0000002**					
2651-01A	550	4.63e+02	1.35e+00	1.64e+00	9.7e-17	0.4	7.7e-02	-4.5	2.67	-2865	± 5006
2651-01B	700	7.09e+01	8.77e+00	2.23e-01	3.2e-16	0.1	6.2e-03	8.1	11.48	784	± 130
2651-01C	800	1.96e+01	9.42e+00	4.98e-02	9.9e-16	0.1	2.2e-03	28.5	38.69	765	± 33

Lab#	Temp (°C)	$^{40}Ar/^{39}Ar$	$^{37}Ar/^{39}Ar$	$^{36}Ar/^{39}Ar$	$^{39}Ar_K$ (moles)	K/Ca	Cl/K	$^{40}Ar^*$ (%)	^{39}Ar (%)	Age (ka)	Err (1σ)
2651-01D	900	2.25e+01	9.46e+00	5.42e-02	5.2e-16	0.1	2.1e-03	32.0	52.85	988	± 51
2651-01E	1000	2.32e+01	9.26e+00	4.85e-02	2.9e-16	0.1	3.2e-03	41.2	60.94	1306	± 71
2651-01F	1150	2.06e+01	9.24e+00	4.91e-02	6.3e-16	0.1	4.6e-03	32.8	78.31	923	± 37
2651-01G	*1300*	*5.30e+01*	*8.32e+00*	*1.40e-01*	*1.9e-16*	*0.1*	*1.8e-01*	*23.2*	*83.52*	*1686*	*± 133*
2651-01H	1450	2.03e+01	8.54e+00	5.41e-02	6.0e-16	0.1	1.3e-02	24.2	100.00	672	± 40
total gas age					3.6e-15				n=6	700	± 200
plateau age										N.A.	
isochron age				$^{40}Ar/^{36}Ar$ = 315.8 ± 5.2			MSWD = 25.0			718	± 33
E93007: Fang Ridge tephriphonolite, 124.6 mg plagioclase (<1% glass)						**J=0.00007593±0.0000002**					
2652-01A	550	1.78e+02	3.97e+00	6.00e-01	8.1e-17	0.1	5.3e-02	0.7	1.38	181	± 2018
2652-01B	700	2.63e+01	9.36e+00	6.79e-02	4.1e-16	0.1	3.2e-03	26.3	8.41	951	± 59
2652-01C	800	1.95e+01	9.60e+00	4.63e-02	6.5e-16	0.1	2.3e-03	33.6	19.55	906	± 36
2652-01D	900	2.78e+01	9.21e+00	7.17e-02	2.7e-16	0.1	2.9e-03	26.3	24.12	1008	± 82
2652-01E	1000	2.82e+01	8.78e+00	6.70e-02	1.6e-16	0.1	5.8e-03	32.0	26.85	1241	± 111
2652-01F	1150	5.17e+01	8.30e+00	1.62e-01	1.9e-16	0.1	1.5e-02	8.7	30.07	621	± 115
2652-01G	*1300*	*1.25e+02*	*7.51e+00*	*3.90e-01*	*1.8e-16*	*0.1*	*1.7e-01*	*8.0*	*33.17*	*1372*	*± 221*
2652-01H	1450	1.67e+01	8.74e+00	3.95e-02	6.8e-16	0.1	7.1e-03	34.0	44.71	781	± 30
2652-01I	1750	9.39e+00	9.45e+00	1.51e-02	3.1e-15	0.1	8.7e-04	60.0	96.97	777	± 10
2652-01J	1750	2.24e+01	8.67e+00	6.12e-02	1.8e-16	0.1	-6.5e-04	22.0	100.00	679	± 103
total gas age					5.9e-15				n=8	810	± 60
plateau age							F-J		73.15	776	± 14
isochron age				$^{40}Ar/^{36}Ar$ = 308.2 ± 2.7			MSWD = 5.7			758	± 10
E93023: NE of Abbott Peak, 105.2 mg whole rock						**J=0.000075377±0.0000002**					
2653-01A	550	4.21e+01	3.38e-01	1.29e-01	2.3e-15	1.5	4.0e-02	9.6	4.03	549	± 56
2653-01B	650	7.10e+00	3.24e-01	1.45e-02	7.9e-15	1.6	1.7e-02	39.7	18.02	383	± 7
2653-01C	775	8.39e+00	3.41e-01	1.79e-02	7.6e-15	1.5	2.3e-02	37.1	31.39	423	± 8
2653-01D	900	8.51e+00	2.45e-01	1.80e-02	5.5e-15	2.1	2.1e-02	37.3	41.07	431	± 8
2653-01E	1000	8.17e+00	2.39e-01	1.72e-02	5.3e-15	2.1	1.8e-02	37.6	50.35	418	± 8
2653-01F	1100	7.18e+00	2.45e-01	1.45e-02	8.2e-15	2.1	2.3e-02	40.4	64.82	394	± 6
2653-01G	1250	6.85e+00	8.19e-01	1.33e-02	2.0e-14	0.6	2.5e-02	43.1	99.27	401	± 5

Lab#	Temp (°C)	$^{40}Ar/^{39}Ar$	$^{37}Ar/^{39}Ar$	$^{36}Ar/^{39}Ar$	$^{39}Ar_K$ (moles)	K/Ca	Cl/K	$^{40}Ar^*$ (%)	^{39}Ar (%)	Age (ka)	Err (1σ)
2653-01H	1400	3.60e+01	1.01e+01	1.12e-01	4.1e-16	0.1	2.3e-02	10.3	99.99	507	± 80
2653-01I	1750	1.13e+02	1.62e+01	3.76e-01	1.4e-16	0.0	-9.6e-02	2.4	100.25	369	± 377
2653-01J	1750	-1.32e+01	0.00e+00	-6.06e-02	-1.4e-16	--	1.1e-01	-35.8	100.00	642	± 120
total gas age					5.7e-14				n=10	410	± 10
plateau age							B-G		95.24	406	± 8
isochron age				$^{40}Ar/^{36}Ar$ = 315.4 ± 5.4			MSWD = 4.2			364	± 12
E93012: Fang Ridge tephrite, 114.7 mg whole rock					**J=0.00007617±0.0000002**						
2654-01A	550	6.28e+02	2.17e+00	2.04e+00	1.4e-15	0.2	2.9e-02	3.9	19.18	3329	± 760
2654-01B	650	2.69e+02	3.32e+00	8.93e-01	1.2e-15	0.2	9.0e-03	1.8	36.42	680	± 1010
2654-01C	775	4.30e+01	2.89e+00	1.09e-01	1.2e-15	0.2	1.0e-02	25.5	54.03	1511	± 231
2654-01D	900	4.01e+01	2.56e+00	9.67e-02	5.5e-16	0.2	9.3e-03	29.2	61.84	1608	± 148
2654-01E	1000	3.61e+01	4.92e+00	9.68e-02	2.3e-16	0.1	1.9e-02	21.7	65.08	1079	± 112
2654-01F	1100	5.40e+01	7.02e+00	1.31e-01	1.6e-16	0.1	2.3e-02	29.4	67.30	2189	± 573
2654-01G	1250	4.75e+01	3.02e+01	1.46e-01	1.3e-15	0.0	6.4e-02	14.0	85.61	931	± 61
2654-01H	1400	6.19e+01	5.31e+01	1.93e-01	5.8e-16	0.0	3.1e-02	14.2	93.81	1255	± 95
2654-01I	1750	3.89e+01	1.37e+01	1.15e-01	3.2e-16	0.0	5.8e-03	15.6	98.36	843	± 91
2654-01J	1750	2.85e+01	5.94e+00	6.54e-02	1.2e-16	0.1	1.6e-03	33.8	100.00	1330	± 224
total gas age					7.1e-15				n=10	1500	± 400
plateau age							B-J		80.82	1070	± 90
isochron age				$^{40}Ar/^{36}Ar$ = 307.1 ± 8.9			MSWD = 8.5			849	± 97
E93024: between Abbott Peak and E93011, 115.9 mg whole rock					**J=0.000075726±0.0000002**						
2655-01A	550	9.03e+02	5.93e-01	2.98e+00	9.3e-16	0.9	4.1e-02	2.4	1.74	2918	± 2381
2655-01B	650	1.28e+02	3.97e-01	4.13e-01	3.5e-15	1.3	2.7e-02	4.8	8.18	842	± 137
2655-01C	775	3.12e+01	4.01e-01	9.25e-02	8.7e-15	1.3	2.9e-02	12.4	24.48	529	± 83
2655-01D	900	2.88e+01	3.58e-01	8.11e-02	6.0e-15	1.4	1.8e-02	16.7	35.64	656	± 100
2655-01E	1000	2.53e+01	4.09e-01	7.51e-02	5.2e-15	1.2	2.2e-02	12.5	45.28	432	± 46
2655-01F	1100	1.12e+01	3.98e-01	2.85e-02	1.0e-14	1.3	2.9e-02	25.1	64.78	385	± 13
2655-01G	1250	7.65e+00	1.49e+00	1.72e-02	1.9e-14	0.3	2.7e-02	34.9	99.57	365	± 7
2655-01H	1400	6.60e+01	1.14e+01	2.09e-01	3.9e-16	0.0	5.5e-02	7.8	100.29	705	± 233
2655-01I	1750	-9.10e+02	0.00e+00	-2.88e+00	-2.1e-17	--	4.8e-01	6.4	100.25	-8021	± 32702

Lab#	Temp (°C)	$^{40}Ar/^{39}Ar$	$^{37}Ar/^{39}Ar$	$^{36}Ar/^{39}Ar$	$^{39}Ar_K$ (moles)	K/Ca	Cl/K	$^{40}Ar^*$ (%)	^{39}Ar (%)	Age (ka)	Err (1σ)
2655-01J	1750	-1.28e+01	0.00e+00	-3.74e-02	-1.4e-16	--	5.6e-02	13.9	100.00	-243	± 222
total gas age					5.4e-14				n=10	520	± 70
plateau age							E-G		63.92	370	± 10
isochron age				$^{40}Ar/^{36}Ar$ = 306.0 ± 2.1			MSWD = 1.0			342	± 9
E93010: west of Abbott Peak, 108.6 mg whole rock				**J=0.000075951±0.0000002**							
2656-01A	550	5.61e+01	2.43e-01	1.63e-01	2.6e-15	2.1	3.4e-02	14.3	4.16	1099	± 91
2656-01B	650	8.32e+00	1.66e-01	1.53e-02	1.2e-14	3.1	1.8e-02	45.6	23.91	520	± 8
2656-01C	775	8.94e+00	1.67e-01	1.72e-02	1.4e-14	3.1	3.4e-02	43.0	45.86	527	± 12
2656-01D	900	9.29e+00	1.99e-01	1.80e-02	9.8e-15	2.6	4.6e-02	42.8	61.76	545	± 12
2656-01E	1000	9.17e+00	2.36e-01	1.70e-02	6.5e-15	2.2	3.7e-02	45.3	72.26	569	± 10
2656-01F	1100	7.72e+00	4.31e-01	1.32e-02	4.6e-15	1.2	4.2e-03	49.6	79.66	525	± 9
2656-01G	1250	9.07e+00	8.94e-01	1.79e-02	1.2e-14	0.6	2.4e-02	42.1	98.37	524	± 8
2656-01H	1400	2.95e+01	2.49e+00	8.53e-02	1.6e-15	0.2	-5.1e-03	15.2	100.00	617	± 39
2656-01I	1750	-1.18e+02	0.00e+00	-4.08e-01	-6.9e-17	--	5.5e-01	-2.0	100.00	319	± 1452
2656-01J	1750	5.35e+00	0.00e+00	3.99e-03	-5.0e-16	--	9.6e-02	77.5	100.00	568	± 60
total gas age					6.2e-14				n=10	559	± 12
plateau age							B-G		94.21	533	± 9
isochron age				$^{40}Ar/^{36}Ar$ = 306.3 ± 4.1			MSWD = 3.8			508	± 10
E93008: Crash Nunatak, 104.8 mg whole rock				**J=0.000076158±0.0000002**							
2657-01A	550	6.89e+01	1.50e-01	2.18e-01	4.1e-15	3.4	1.4e-02	6.4	15.35	604	± 100
2657-01B	650	6.50e+01	8.24e-01	2.10e-01	3.1e-15	0.6	5.4e-02	4.4	26.73	397	± 95
2657-01C	775	5.09e+01	9.89e-01	1.60e-01	7.3e-15	0.5	2.8e-02	6.9	53.76	483	± 53
2657-01D	900	7.01e+01	9.35e-01	2.23e-01	5.1e-15	0.5	1.8e-02	6.3	72.69	607	± 77
2657-01E	1000	2.30e+02	1.46e+00	7.48e-01	2.0e-15	0.3	5.5e-02	4.1	79.93	1288	± 248
2657-01F	1100	3.37e+02	1.84e+00	1.11e+00	1.9e-15	0.3	7.7e-02	2.9	87.11	1358	± 365
2657-01G	1250	7.31e+02	1.15e+01	2.36e+00	1.7e-15	0.0	1.7e-01	4.7	93.47	4702	± 837
2657-01H	1400	1.06e+03	1.55e+01	3.42e+00	1.4e-15	0.0	2.1e-01	4.4	98.82	6508	± 1380
2657-01I	1750	2.02e+02	7.55e+00	6.72e-01	2.1e-16	0.1	1.9e-02	1.8	99.59	512	± 381
2657-01J	1750	6.62e+01	6.12e+00	2.00e-01	1.1e-16	0.1	-1.6e-03	11.1	100.00	1015	± 303
total gas age					2.7e-14				n=10	1200	± 200

Lab#	Temp (°C)	$^{40}Ar/^{39}Ar$	$^{37}Ar/^{39}Ar$	$^{36}Ar/^{39}Ar$	$^{39}Ar_K$ (moles)	K/Ca	Cl/K	$^{40}Ar^*$ (%)	^{39}Ar (%)	Age (ka)	Err (1σ)
plateau age							A-D		72.69	520 ±	60
isochron age				$^{40}Ar/^{36}Ar$ = 306.6 ± 1.5			MSWD = 1.1			220 ±	48
E93032: Cape Barne tephrite, 103.7 mg whole rock					**J=0.000075978±0.0000002**						
2658-01A	550	2.16e+01	7.91e-01	4.61e-02	2.3e-15	0.6	8.4e-02	37.0	7.02	1096 ±	119
2658-01B	650	1.31e+01	7.11e-01	1.18e-02	5.2e-15	0.7	6.4e-02	73.7	22.64	1322 ±	41
2658-01C	775	1.28e+01	6.43e-01	1.03e-02	1.2e-14	0.8	7.6e-02	76.3	59.24	1338 ±	22
2658-01D	900	1.53e+01	8.19e-01	1.75e-02	7.6e-15	0.6	6.4e-02	66.6	82.04	1401 ±	33
2658-01E	1000	2.20e+01	1.85e+00	4.48e-02	2.0e-15	0.3	5.4e-02	40.4	88.09	1219 ±	79
2658-01F	1100	2.38e+01	3.77e+00	5.13e-02	1.2e-15	0.1	4.0e-02	37.5	91.72	1227 ±	60
2658-01G	1250	4.08e+01	1.28e+01	1.11e-01	2.3e-15	0.0	1.3e-01	22.2	98.61	1253 ±	48
2658-01H	1400	8.20e+01	1.85e+01	2.41e-01	2.1e-16	0.0	1.4e-01	14.8	99.23	1685 ±	363
2658-01I	1750	6.38e+01	8.24e+00	1.81e-01	1.8e-16	0.1	2.6e-02	16.9	99.76	1483 ±	771
2658-01J	1750	5.51e+01	6.64e+00	1.66e-01	7.9e-17	0.1	1.6e-03	11.9	100.00	903 ±	437
total gas age					3.3e-14				n=10	1320 ±	50
plateau age							A-G		98.61	1330 ±	30
isochron age				$^{40}Ar/^{36}Ar$ = 288.9 ± 3.3			MSWD = 2.3			1355 ±	18

APPENDIX C-2. EXPLANATION

Lab ID#	Sample ID#	Sample Name	Rock type	Material Dated	Approx. glass content	Plateau	Isochron	Integrated (total gas) age	Excess Argon (too old)	Poor Analysis	Page No.
49	E87026	Caldera Rim	anorth. tephriphonolite	an.	N.A.					•	C- 41
51	N.A.	Anorthoclase phenocryst	anorth. phonolite bomb	an.	N.A.					•	C- 42
54	E83400	Cape Evans	anorth. tephriphonolite	an.	N.A.	•					C- 43
70	E83448	Cape Royds	anorth. tephriphonolite	an.	N.A.					•	C- 44
71	E83400	Cape Evans	anorth. tephriphonolite	an.	N.A.					•	C- 45
83	E87026	Caldera Rim	anorth. tephriphonolite	an.	N.A.				•		C- 46
84	N.A.	Anorthoclase phenocryst	anorth. phonolite bomb	an.	N.A.					•	C- 47
425	E81001	Hooper's Shoulder	anorth. phonolite	an.	N.A.					•	C- 48
426	E83448	Cape Royds	anorth. tephriphonolite	an.	N.A.					•	C- 49
427	E83400	Cape Evans	anorth. tephriphonolite	an.	N.A.			•			C- 50
428	E87034	Lower Hut Flow	anorth. phonolite	an.	N.A.					•	C- 51
429	E87026	Caldera Rim	anorth. tephriphonolite	an.	N.A.					•	C- 52
430	E83433	Cape Barne	anorth. tephriphonolite	an.	N.A.					•	C- 53
431	N.A.	Anorthoclase phenocryst	anorth. phonolite bomb	an.	N.A.					•	C- 54
432	E83454	Aurora Cliffs	trachyte	an.	N.A.					•	C- 55

Lab ID#	Sample ID#	Sample Name	Rock type	Material Dated	Approx. glass content	Plateau	Isochron	Integrated (total gas) age	Excess Argon (too old)	Poor Analysis	Page No.
830	N.A.	Anorthoclase phenocryst	anorth. phonolite bomb	an.	1%				•		C- 56
831	N.A.	Anorthoclase phenocryst	anorth. phonolite bomb	an.	1%				•		C- 57
832	N.A.	Anorthoclase phenocryst	anorth. phonolite bomb	an.	2%				•		C- 58
833	N.A.	Anorthoclase phenocryst	anorth. phonolite bomb	an.	2%				•		C- 59
834	N.A.	Anorthoclase phenocryst	anorth. phonolite bomb	an.	5%				•		C- 60
835	N.A.	Anorthoclase phenocryst	anorth. phonolite bomb	an.	5%				•		C- 61
836	E83433	Cape Barne	anorth. tephriphonolite	an.	1%	•					C- 62
837	E87034	Lower Hut Flow	anorth. phonolite	an.	1%				•		C- 63
838	E83433	Cape Barne	anorth. tephriphonolite	an.	5%	•					C- 64
839	E83433	Cape Barne	anorth. tephriphonolite	an.	1%	•					C- 65
840	E83433	Cape Barne	anorth. tephriphonolite	an.	5%	•					C- 66
841	E81001	Hooper's Shoulder	anorth. phonolite	an.	1%	•					C- 67
842	E87034	Lower Hut Flow	anorth. phonolite	an.	1%	•					C- 68
843	E81001	Hooper's Shoulder	anorth. phonolite	an.	1%	•					C- 69
1313	E83400	Cape Evans	anorth. tephriphonolite	an.	1%	•					C- 70
1314	E83448	Cape Royds	anorth. tephriphonolite	an.	2%	•					C- 71

Lab ID#	Sample ID#	Sample Name	Rock type	Material Dated	Approx. glass content	Plateau	Isochron	Integrated (total gas) age	Excess Argon (too old)	Poor Analysis	Page No.
1315	AW82015	Turks Head	anorth. tephriphonolite	an.	2%	•					C- 72
1316	N.A.	Anorthoclase phenocryst	anorth. phonolite bomb	an.	1%				•		C- 73
1317	N.A.	Anorthoclase phenocryst	anorth. phonolite bomb	an.	10%				•		C- 74
1318	E81001	Hooper's Shoulder	anorth. phonolite	an.	1%	•					C- 75
1319	E81001	Hooper's Shoulder	anorth. phonolite	an.	5%				•		C- 76
1320	E83400	Cape Evans	anorth. tephriphonolite	an.	5%	•					C- 77
1321	E83454	Aurora Cliffs	trachyte	an.	3%	•					C- 78
1322	E83448	Cape Royds	anorth. tephriphonolite	an.	20%				•		C- 79
1326	E81002	Abbotts Peak	tephriphonolite	pl.	1%	•					C- 80
1327	E82405	Bomb Peak	trachyte	an.	1%	•					C- 81
1328	E80020	Three Sisters Cones	anorth. phonolite	an.	1%				•		C- 82
1329	E80020	Three Sisters Cones	anorth. phonolite	an.	4%	•					C- 83
1330	N.A.	Anorthoclase phenocryst #2	anorth. phonolite bomb	an.	1%				•		C- 84
1331	N.A.	Anorthoclase phenocryst #2	anorth. phonolite bomb	an.	30%				•		C- 85
1332	N.A.	Bomb Matrix Glass	anorth. phonolite bomb	gm.	100%				•		C- 86
1422	AW82038	Turks Head	plag. tephriphonolite	pl.	5%	•					C- 87

Lab ID#	Sample ID#	Sample Name	Rock type	Material Dated	Approx. glass content	Plateau	Isochron	Integrated (total gas) age	Excess Argon (too old)	Poor Analysis	Page No.
1528	E83432	Cape Barne	basanite	gm.	N.A.	•					C- 88
1536	E77012	Tryggve Point Dike	plag. tephriphonolite	pl.	2%	•					C- 89
1537	E83407	Inaccessible Island	phonolite	gm.	N.A.	•					C- 90
1865	E83453	SW of Abbotts Peak	phonotephrite	gm.	N.A.	•					C- 91
2485	E80020	Three Sisters Cones	anorth. phonolite	an.	1%				•		C- 92
2642	E87035	Nausea Knob	anorth. tephriphonolite	an.	1%	•					C- 93
2643	E86026	Northeast Flow	anorth. phonolite	an.	1%			•			C- 94
2644	E93011	NW of Hoopers Shoulder	anorth. tephriphonolite	an.	2%	•					C- 95
2645	E93021	South of Hoopers Shoulder	anorth. tephriphonolite	an.	2%	•					C- 96
2646	E93013	Caldera Rim #1	anorth. tephriphonolite	an.	1%	•					C- 97
2647	E93019	Btwn Williams Cl/Turks Head	anorth. tephriphonolite	an.	2%	•					C- 98
2648	E93020	Williams Cliff	anorth. tephriphonolite	an.	2%	•					C- 99
2649	E93014	Caldera Rim #2	anorth. tephriphonolite	an.	1%				•		C- 100
2650	E86026	Northeast Flow	anorth. phonolite	an.	1%	•					C- 101
2651	E93005	Fang Ridge #1	plag. tephriphonolite	pl.	1%		•				C- 102
2652	E93007	Fang Ridge #2	plag. tephriphonolite	pl.	1%		•				C- 103

Lab ID#	Sample ID#	Sample Name	Rock type	Material Dated	Approx. glass content	Plateau	Isochron	Integrated (total gas) age	Excess Argon (too old)	Poor Analysis	Page No.
2653	E93023	NE of Abbotts Peak	phonotephrite (?)	gm.	N.A.		•				C- 104
2654	E93012	Fang Ridge #3	tephrite	gm.	N.A.	•					C- 105
2655	E93024	South of Abbotts Peak	phonotephrite (?)	gm.	N.A.		•				C- 106
2656	E93010	West of Abbotts Peak	phonotephrite (?)	gm.	N.A.		•				C- 107
2657	E93008	Crash Nunatak	phonotephrite (?)	gm.	N.A.	•					C- 108
2658	E93032	Cape Barne	basanite	gm.	N.A.	•					C- 109

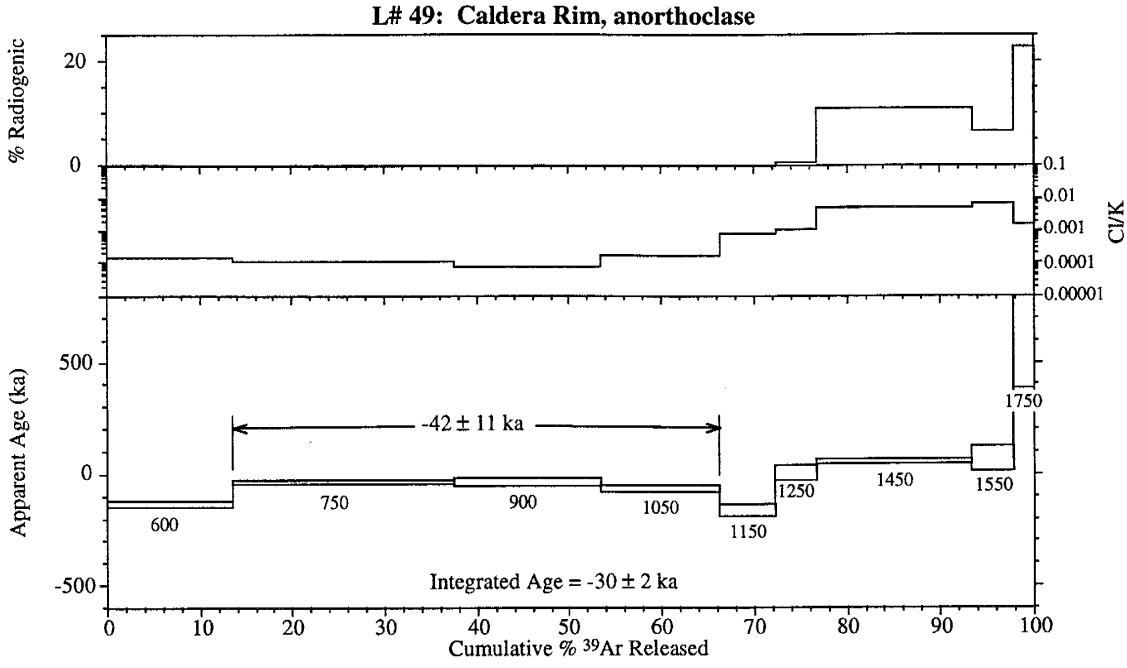
L# 49: Caldera Rim, anorthoclase
% Radiogenic
20
0
0.1
0.01
0.001
0.0001
0.00001
Cl/K
500
0
-500
Apparent Age (ka)
-42 ± 11 ka
600
750
900
1050
1150
1250
1450
1550
1750
Integrated Age = -30 ± 2 ka
0
10
20
30
40
50
60
70
80
90
100
Cumulative % 39Ar Released

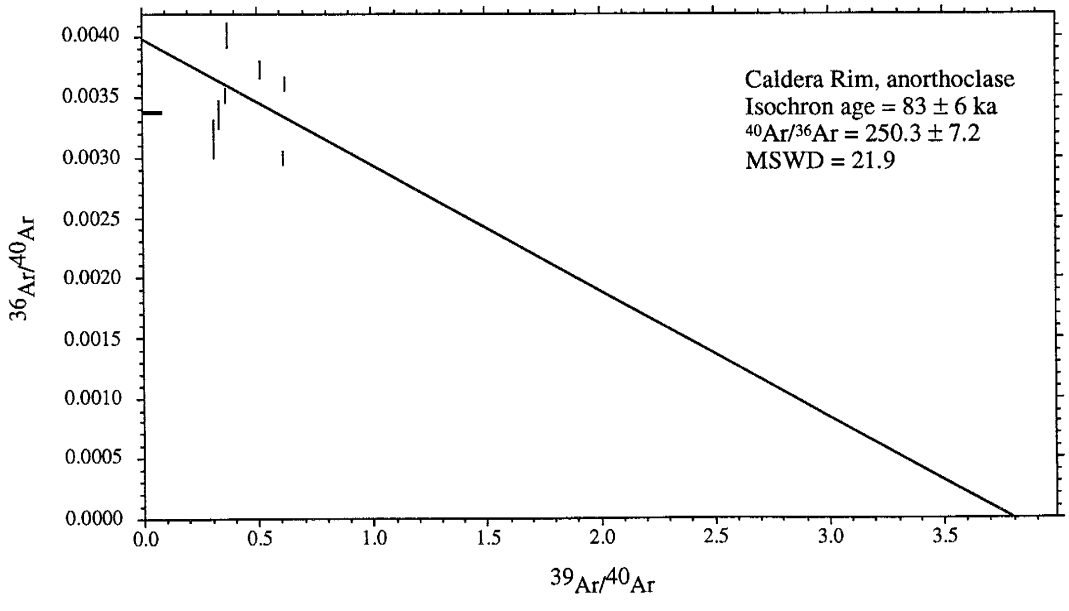
Caldera Rim, anorthoclase
Isochron age = 83 ± 6 ka
40Ar/36Ar = 250.3 ± 7.2
MSWD = 21.9
0.0040
0.0035
0.0030
0.0025
0.0020
0.0015
0.0010
0.0005
0.0000
36Ar/40Ar
0.0
0.5
1.0
1.5
2.0
2.5
3.0
3.5
39Ar/40Ar

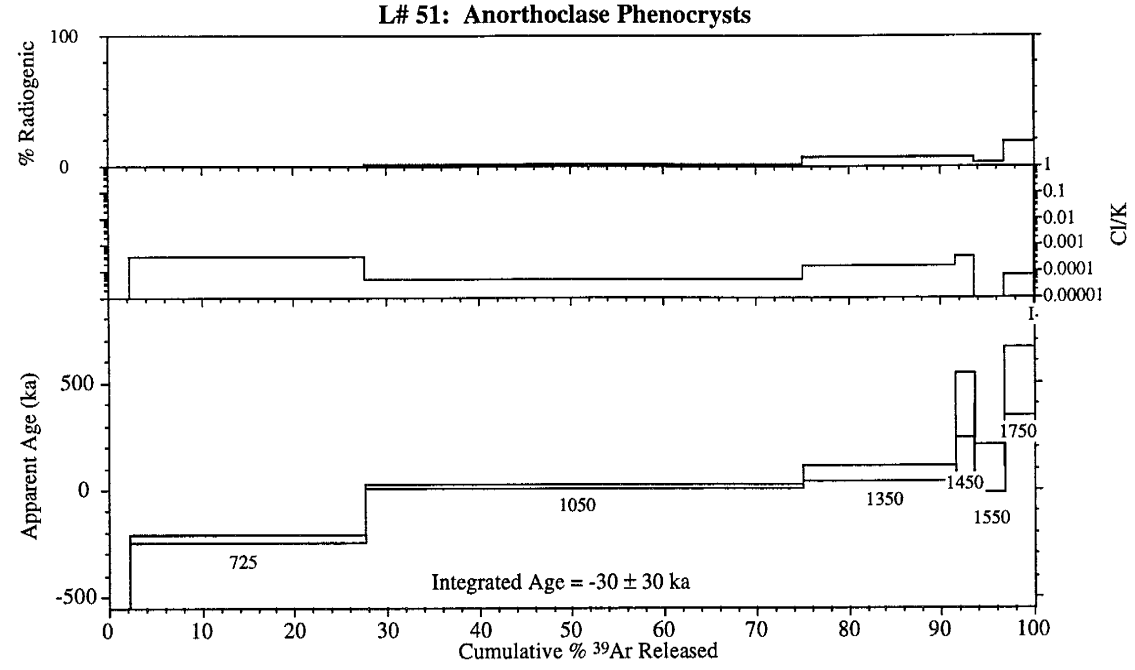
L# 51: Anorthoclase Phenocrysts
% Radiogenic
100
0
Cl/K
1
0.1
0.01
0.001
0.0001
0.00001
Apparent Age (ka)
500
0
-500
725
1050
1350
1450
1550
1750
Integrated Age = -30 ± 30 ka
0
10
20
30
40
50
60
70
80
90
100
Cumulative % 39Ar Released

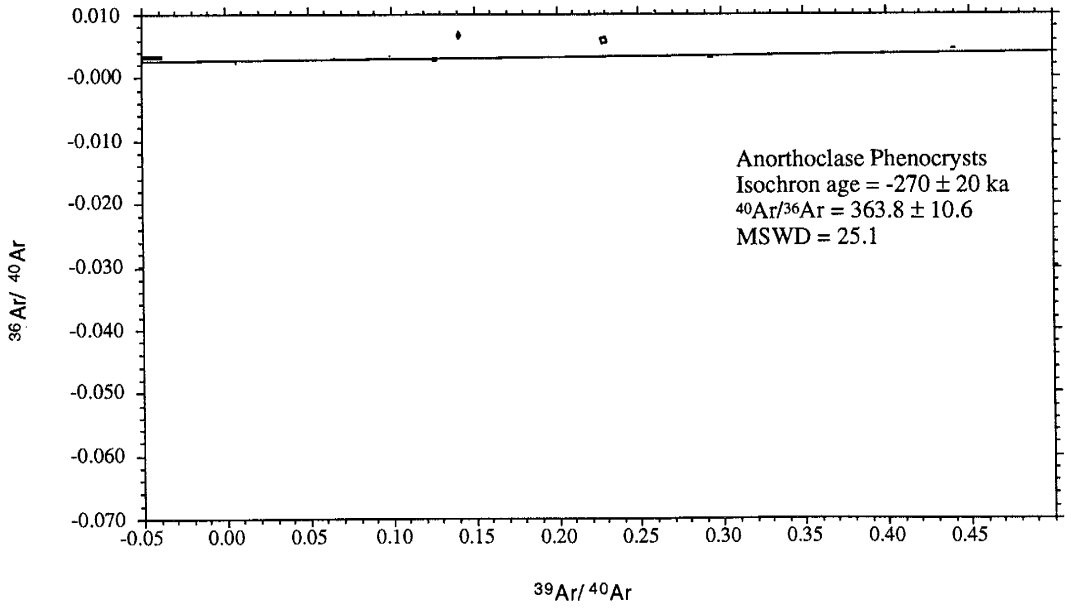
0.010
-0.000
-0.010
-0.020
-0.030
-0.040
-0.050
-0.060
-0.070
36Ar/ 40Ar
-0.05
0.00
0.05
0.10
0.15
0.20
0.25
0.30
0.35
0.40
0.45
39Ar/ 40Ar
Anorthoclase Phenocrysts
Isochron age = -270 ± 20 ka
40Ar/36Ar = 363.8 ± 10.6
MSWD = 25.1

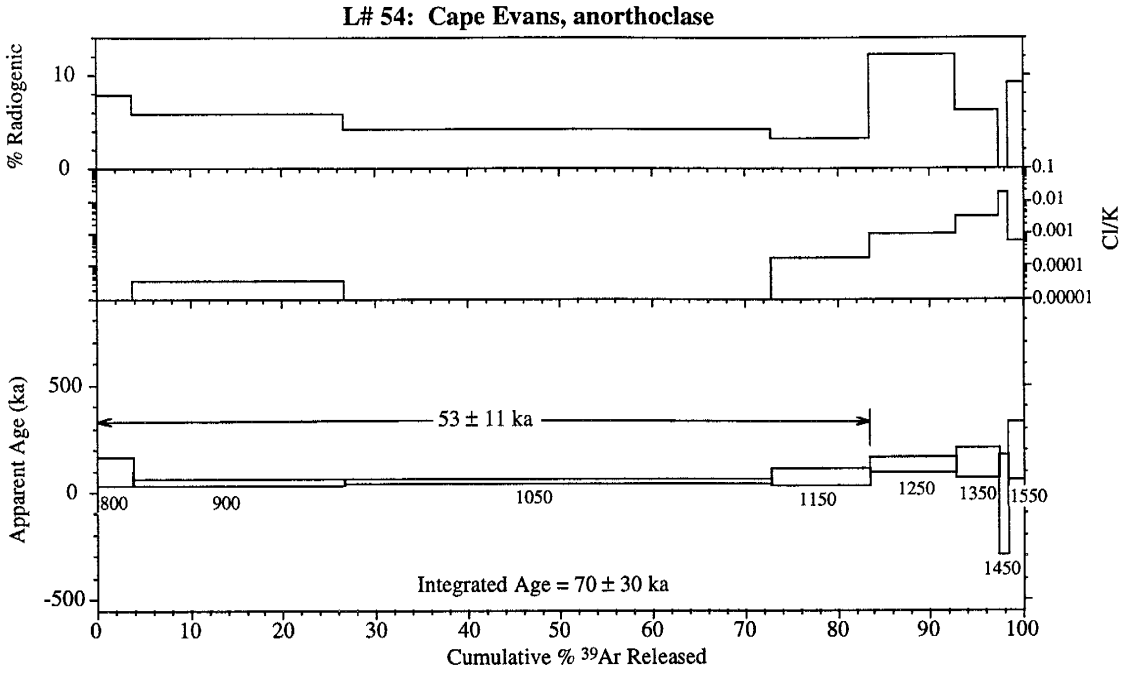
L# 54: Cape Evans, anorthoclase
% Radiogenic
10
0
0.1
0.01
0.001
0.0001
0.00001
Cl/K
Apparent Age (ka)
500
0
-500
53 ± 11 ka
800
900
1050
1150
1250
1350
1550
1450
Integrated Age = 70 ± 30 ka
0
10
20
30
40
50
60
70
80
90
100
Cumulative % 39Ar Released

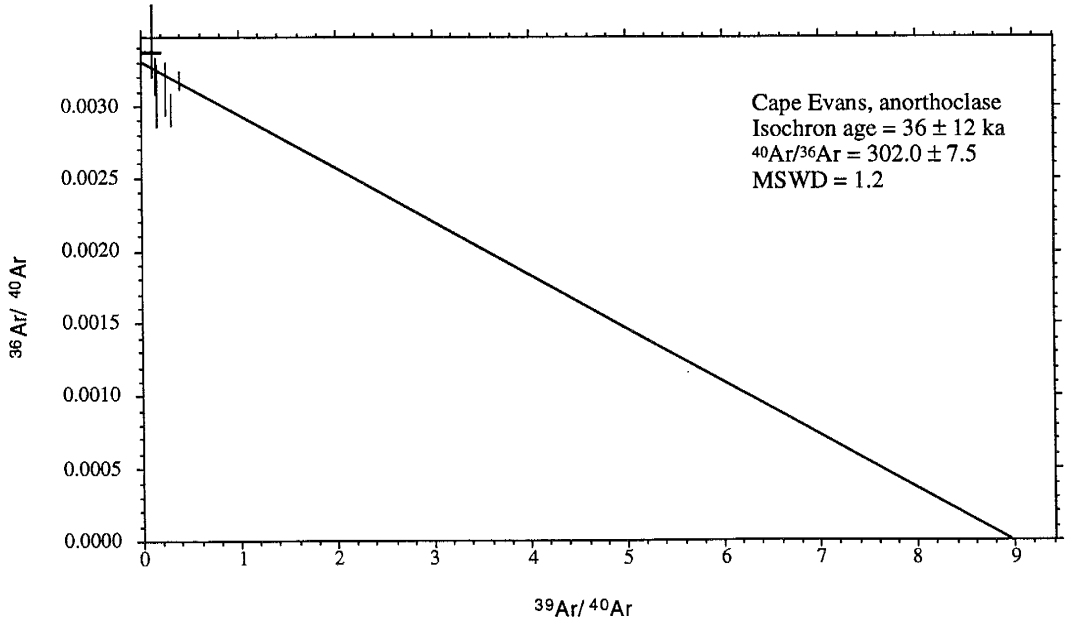
Cape Evans, anorthoclase
Isochron age = 36 ± 12 ka
40Ar/36Ar = 302.0 ± 7.5
MSWD = 1.2
36Ar/ 40Ar
0.0030
0.0025
0.0020
0.0015
0.0010
0.0005
0.0000
0
1
2
3
4
5
6
7
8
9
39Ar/ 40Ar

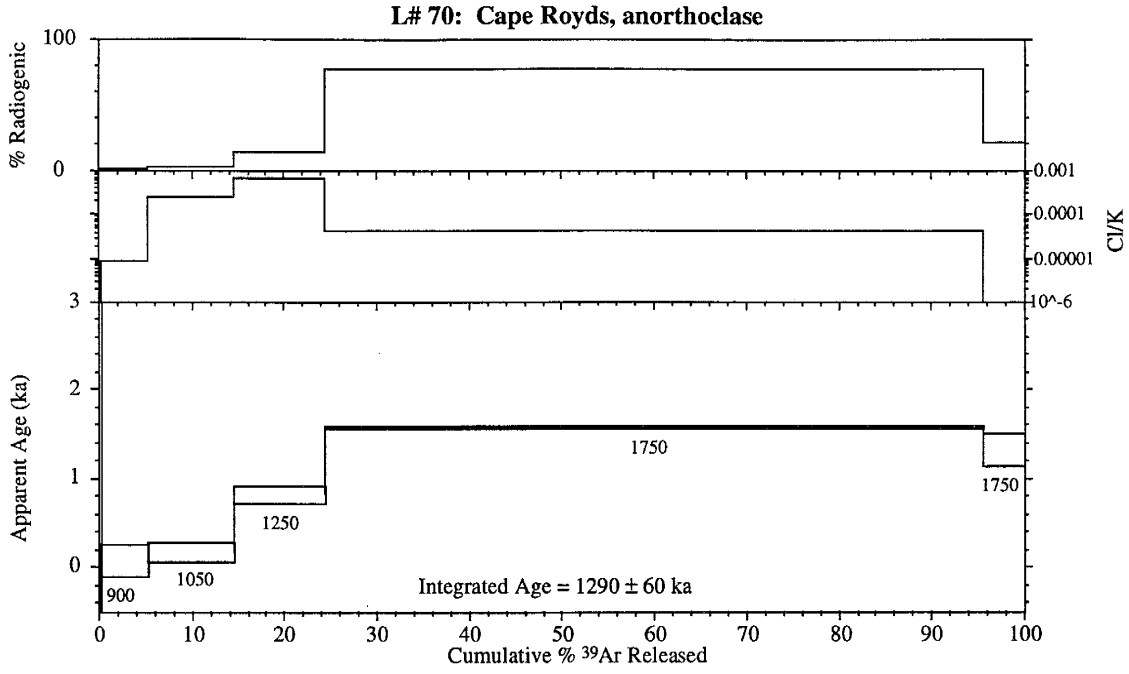
L# 70: Cape Royds, anorthoclase
% Radiogenic
100
0
Cl/K
0.001
0.0001
0.00001
10^-6
Apparent Age (ka)
3
2
1
0
900
1050
1250
1750
1750
Integrated Age = 1290 ± 60 ka
0
10
20
30
40
50
60
70
80
90
100
Cumulative % 39Ar Released

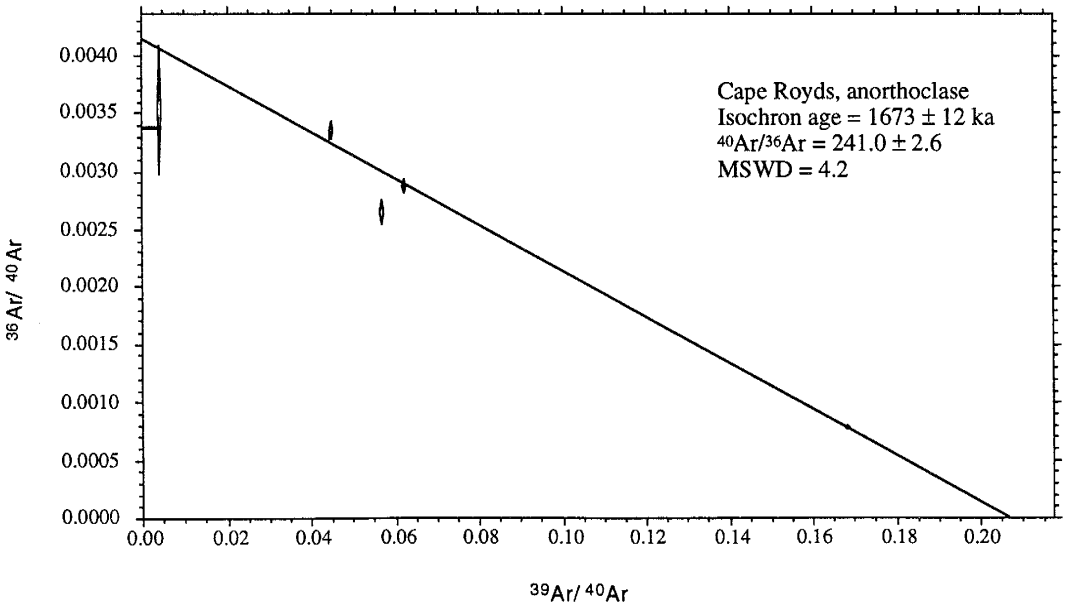
Cape Royds, anorthoclase
Isochron age = 1673 ± 12 ka
40Ar/36Ar = 241.0 ± 2.6
MSWD = 4.2
36Ar/ 40Ar
0.0040
0.0035
0.0030
0.0025
0.0020
0.0015
0.0010
0.0005
0.0000
0.00
0.02
0.04
0.06
0.08
0.10
0.12
0.14
0.16
0.18
0.20
39Ar/ 40Ar

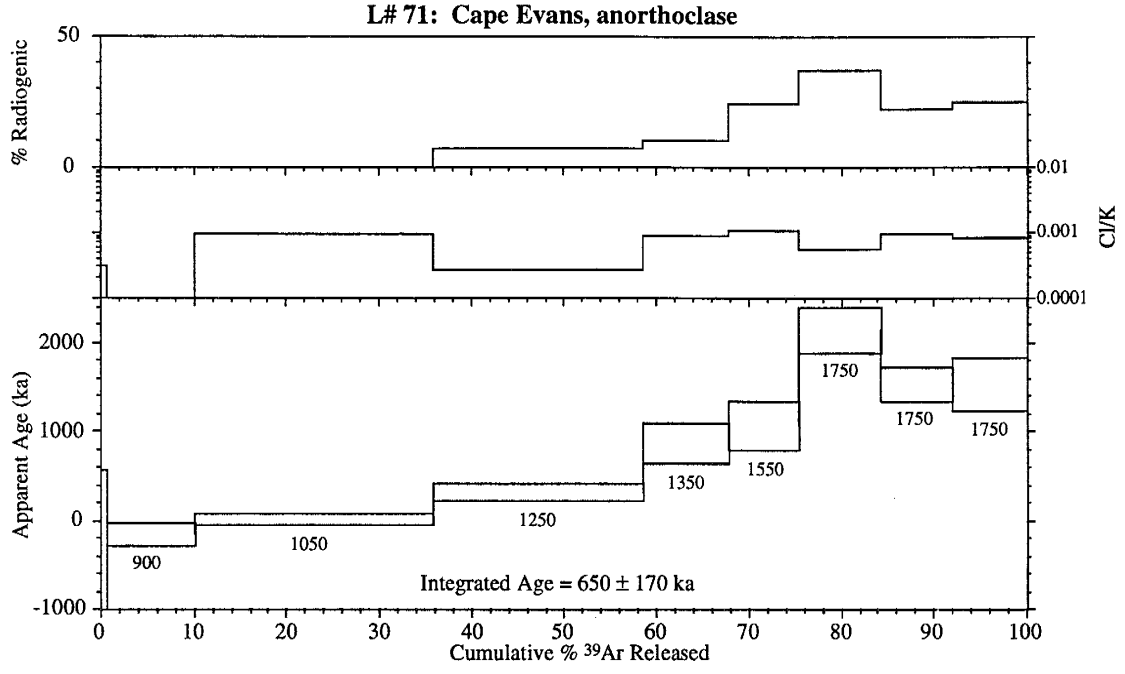
L# 71: Cape Evans, anorthoclase
% Radiogenic
50
0
0.01
0.001
0.0001
Cl/K
Apparent Age (ka)
2000
1000
0
-1000
900
1050
1250
1350
1550
1750
1750
1750
Integrated Age = 650 ± 170 ka
0
10
20
30
40
50
60
70
80
90
100
Cumulative % 39Ar Released

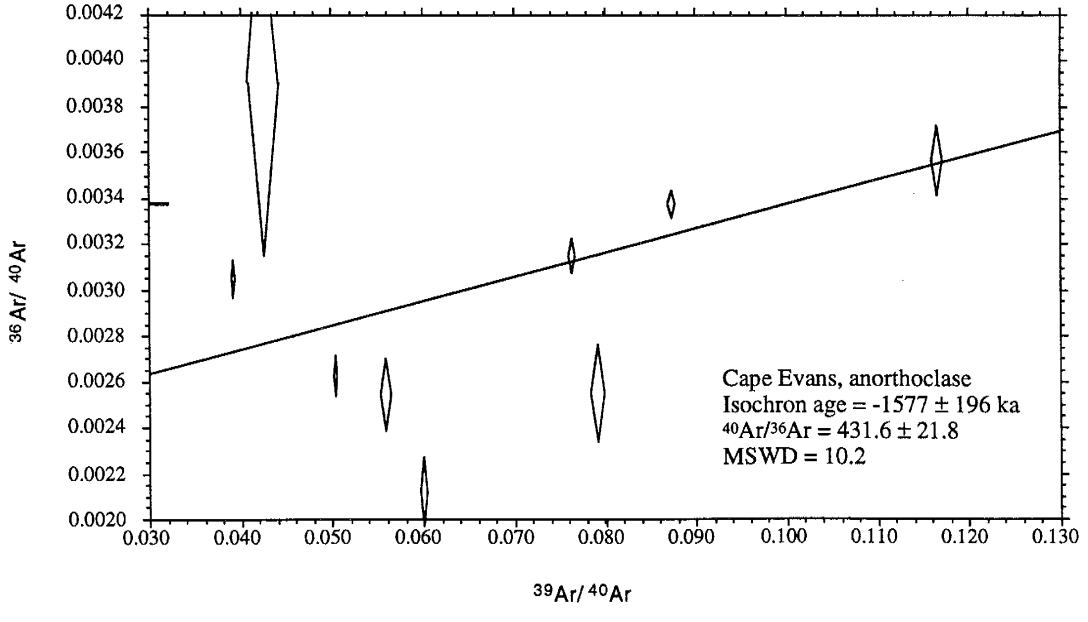
36Ar/ 40Ar
0.0042
0.0040
0.0038
0.0036
0.0034
0.0032
0.0030
0.0028
0.0026
0.0024
0.0022
0.0020
0.030
0.040
0.050
0.060
0.070
0.080
0.090
0.100
0.110
0.120
0.130
39Ar/ 40Ar
Cape Evans, anorthoclase
Isochron age = -1577 ± 196 ka
40Ar/36Ar = 431.6 ± 21.8
MSWD = 10.2

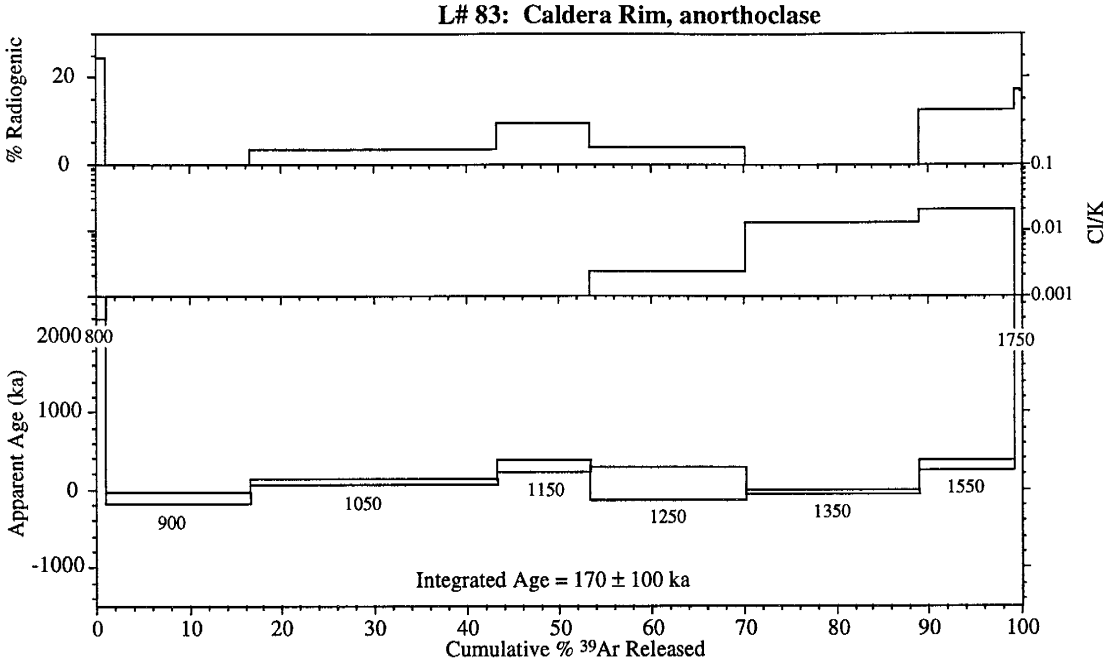
L# 83: Caldera Rim, anorthoclase
% Radiogenic
20
0
0.1
0.01
0.001
Cl/K
2000
1000
0
-1000
Apparent Age (ka)
800
1750
900
1050
1150
1250
1350
1550
Integrated Age = 170 ± 100 ka
0
10
20
30
40
50
60
70
80
90
100
Cumulative % 39Ar Released

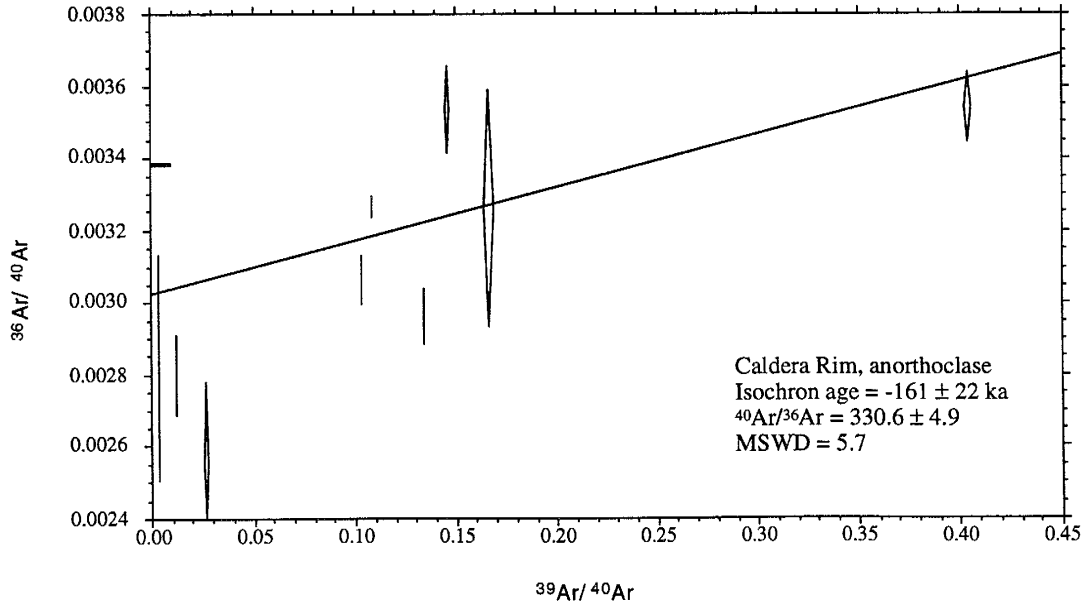
0.0038
0.0036
0.0034
0.0032
0.0030
0.0028
0.0026
0.0024
36Ar/ 40Ar
0.00
0.05
0.10
0.15
0.20
0.25
0.30
0.35
0.40
0.45
39Ar/ 40Ar
Caldera Rim, anorthoclase
Isochron age = -161 ± 22 ka
40Ar/36Ar = 330.6 ± 4.9
MSWD = 5.7

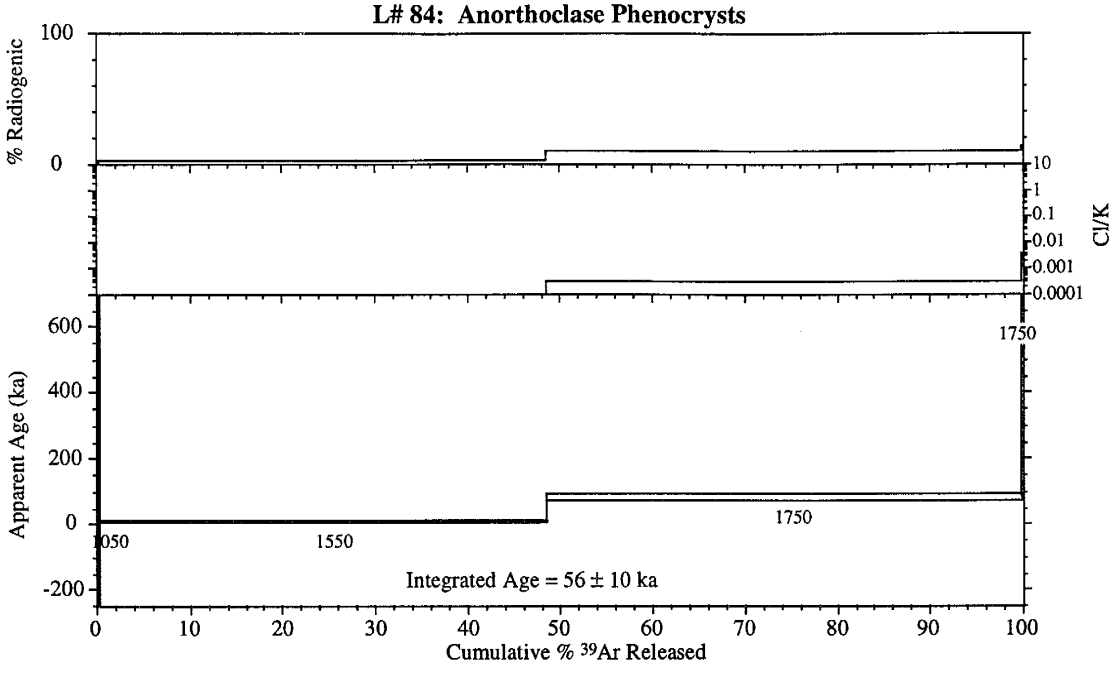
L# 84: Anorthoclase Phenocrysts
% Radiogenic
100
0
10
1
0.1
0.01
0.001
0.0001
Cl/K
1750
600
400
200
0
-200
Apparent Age (ka)
1050
1550
1750
Integrated Age = 56 ± 10 ka
0
10
20
30
40
50
60
70
80
90
100
Cumulative % 39Ar Released

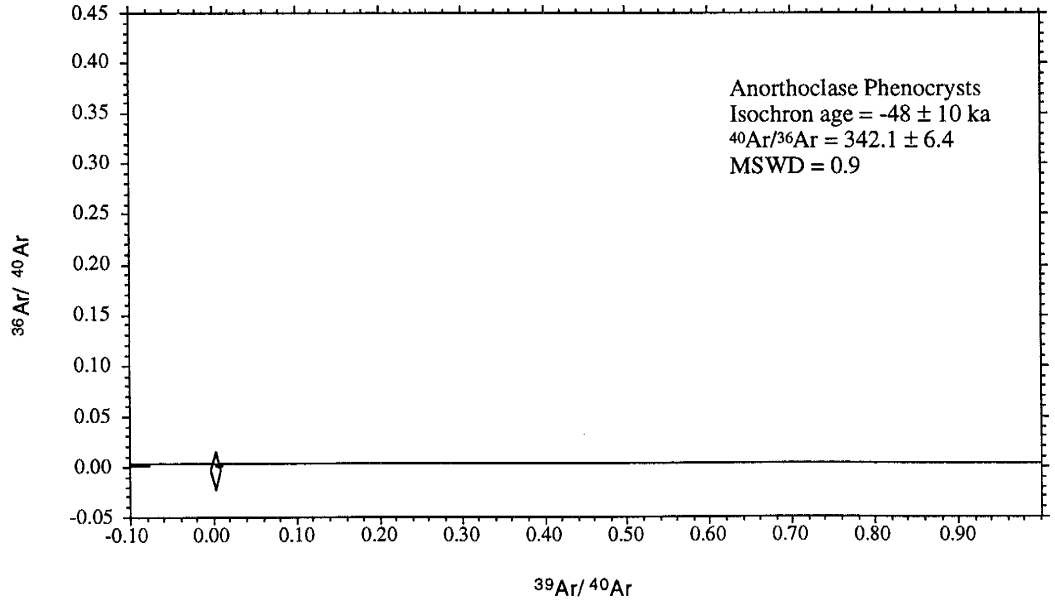
Anorthoclase Phenocrysts
Isochron age = -48 ± 10 ka
40Ar/36Ar = 342.1 ± 6.4
MSWD = 0.9
36Ar/ 40Ar
0.45
0.40
0.35
0.30
0.25
0.20
0.15
0.10
0.05
0.00
-0.05
-0.10
0.00
0.10
0.20
0.30
0.40
0.50
0.60
0.70
0.80
0.90
39Ar/ 40Ar

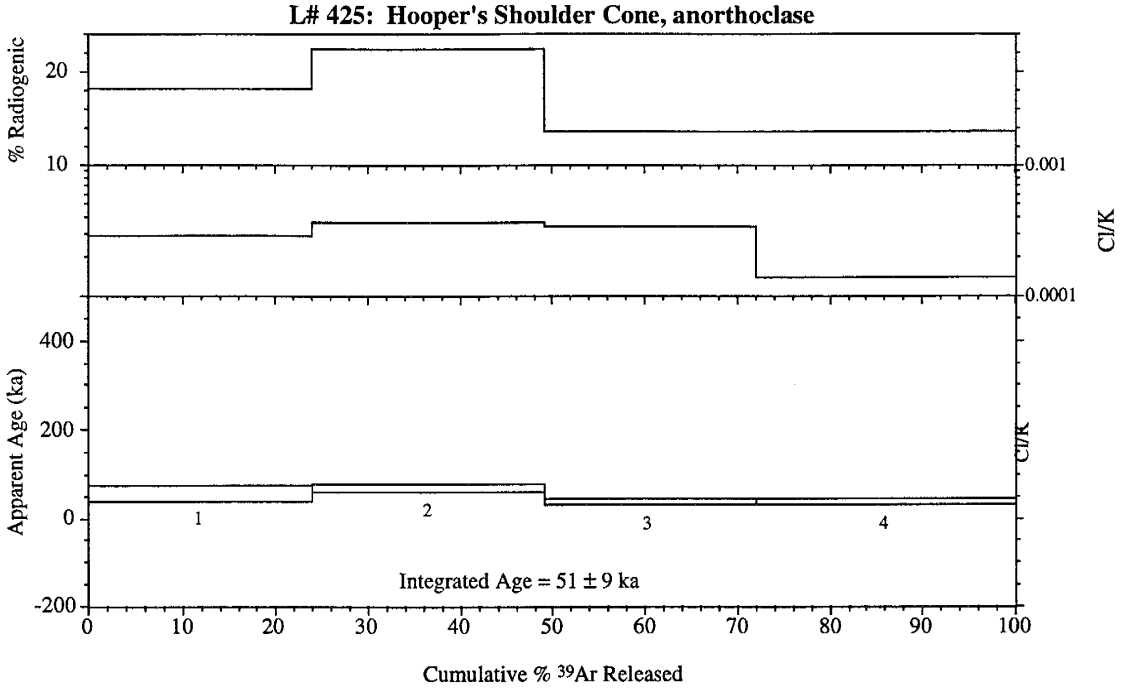
L# 425: Hooper's Shoulder Cone, anorthoclase
% Radiogenic
20
10
0.001
0.0001
Cl/K
400
200
0
-200
Apparent Age (ka)
Cl/K
1
2
3
4
Integrated Age = 51 ± 9 ka
0
10
20
30
40
50
60
70
80
90
100
Cumulative % 39Ar Released

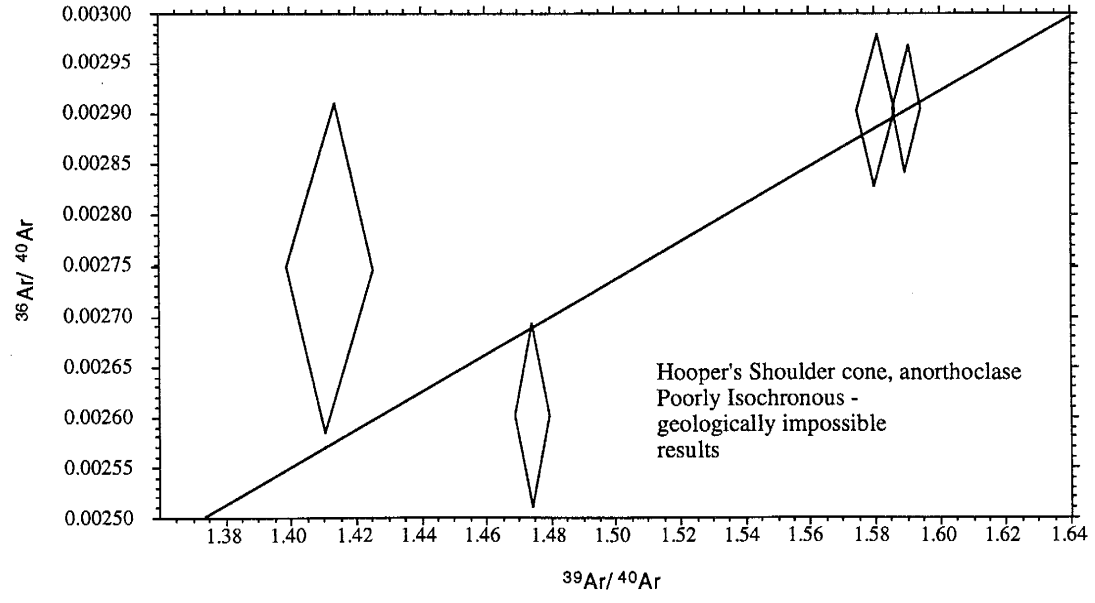
0.00300
0.00295
0.00290
0.00285
0.00280
0.00275
0.00270
0.00265
0.00260
0.00255
0.00250
36Ar/ 40Ar
Hooper's Shoulder cone, anorthoclase
Poorly Isochronous -
geologically impossible
results
1.38
1.40
1.42
1.44
1.46
1.48
1.50
1.52
1.54
1.56
1.58
1.60
1.62
1.64
39Ar/ 40Ar

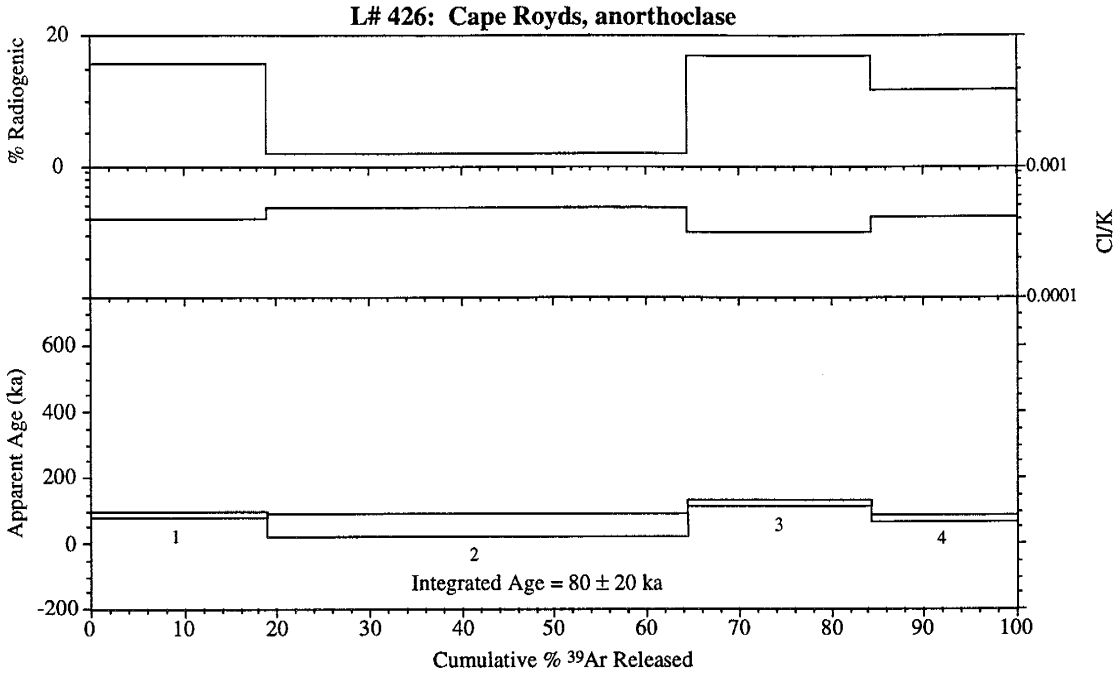
L# 426: Cape Royds, anorthoclase
% Radiogenic
20
0
Cl/K
0.001
0.0001
Apparent Age (ka)
600
400
200
0
-200
1
2
3
4
Integrated Age = 80 ± 20 ka
0
10
20
30
40
50
60
70
80
90
100
Cumulative % 39Ar Released

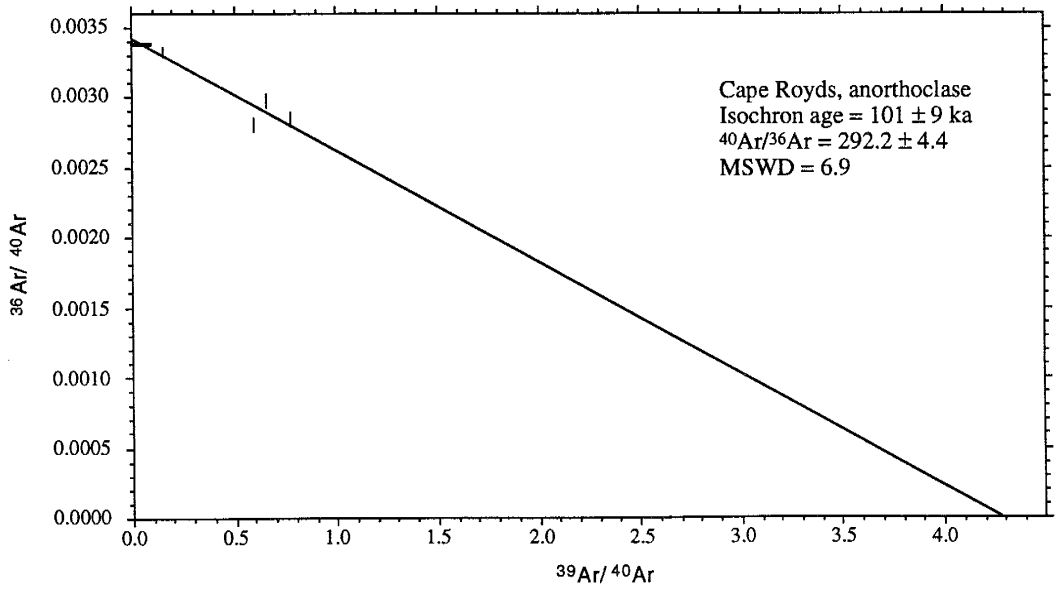
Cape Royds, anorthoclase
Isochron age = 101 ± 9 ka
40Ar/36Ar = 292.2 ± 4.4
MSWD = 6.9
36Ar/ 40Ar
0.0035
0.0030
0.0025
0.0020
0.0015
0.0010
0.0005
0.0000
0.0
0.5
1.0
1.5
2.0
2.5
3.0
3.5
4.0
39Ar/ 40Ar

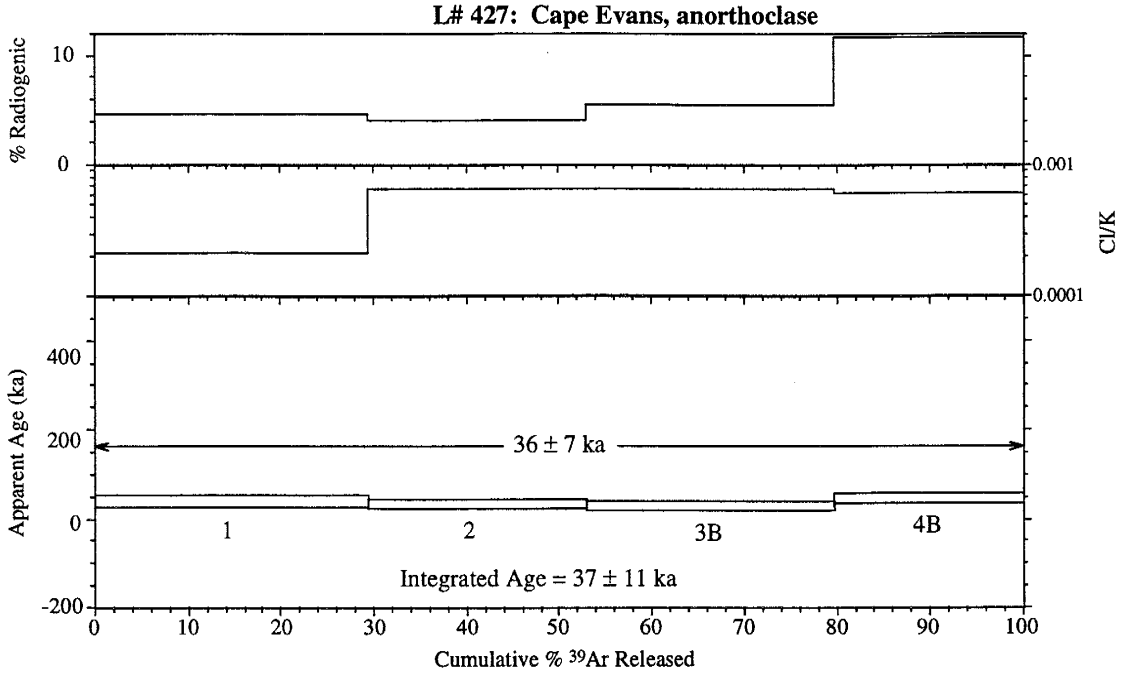
L# 427: Cape Evans, anorthoclase
% Radiogenic
10
0
0.001
0.0001
Cl/K
400
200
0
-200
Apparent Age (ka)
36 ± 7 ka
1
2
3B
4B
Integrated Age = 37 ± 11 ka
0
10
20
30
40
50
60
70
80
90
100
Cumulative % 39Ar Released

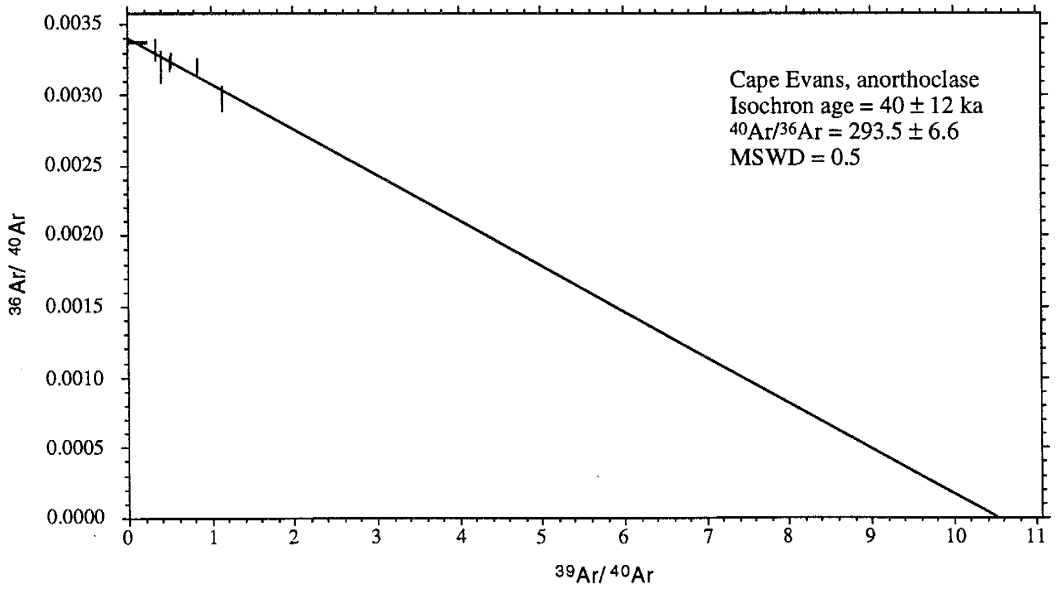
0.0035
0.0030
0.0025
0.0020
0.0015
0.0010
0.0005
0.0000
36Ar/ 40Ar
Cape Evans, anorthoclase
Isochron age = 40 ± 12 ka
40Ar/36Ar = 293.5 ± 6.6
MSWD = 0.5
0
1
2
3
4
5
6
7
8
9
10
11
39Ar/ 40Ar

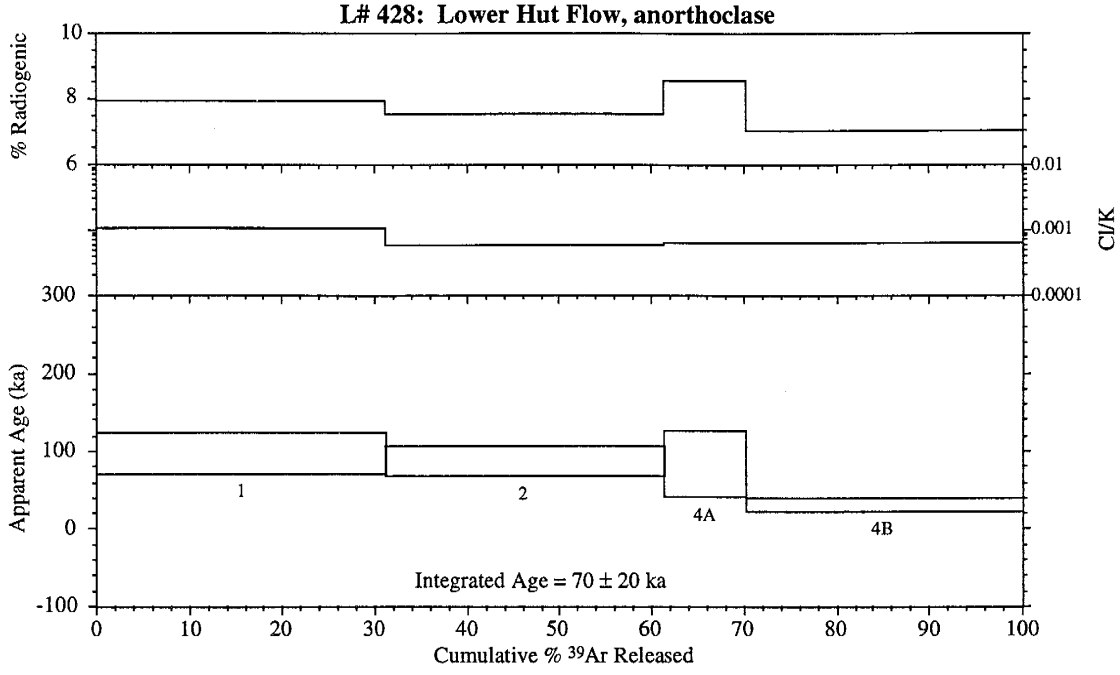
L# 428: Lower Hut Flow, anorthoclase
% Radiogenic
10
8
6
0.01
0.001
0.0001
Cl/K
300
200
100
0
-100
Apparent Age (ka)
1
2
4A
4B
Integrated Age = 70 ± 20 ka
0
10
20
30
40
50
60
70
80
90
100
Cumulative % 39Ar Released

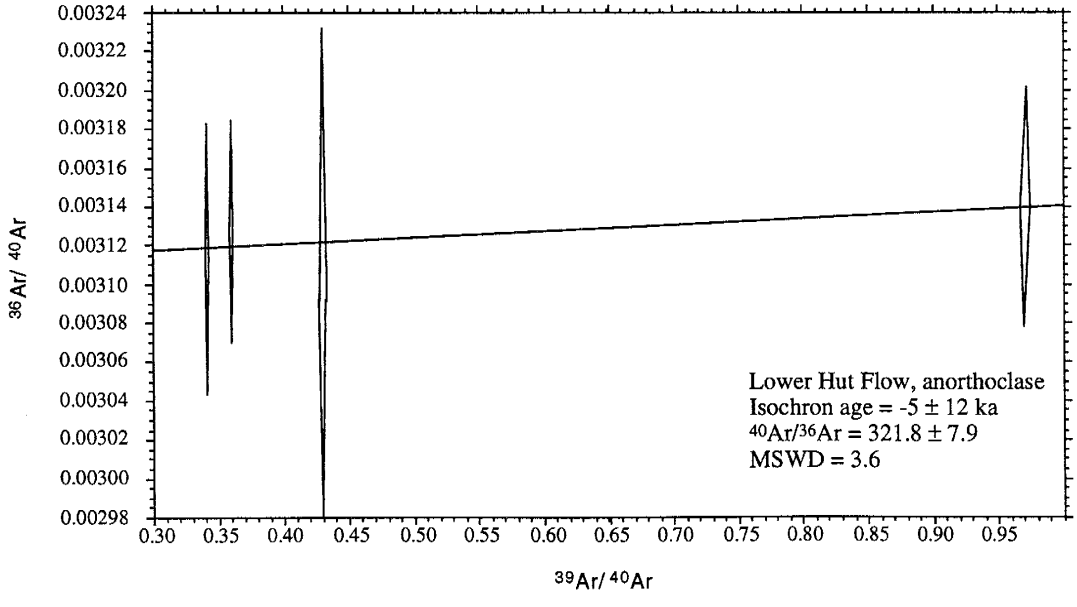
0.00324
0.00322
0.00320
0.00318
0.00316
0.00314
0.00312
0.00310
0.00308
0.00306
0.00304
0.00302
0.00300
0.00298
36Ar/ 40Ar
Lower Hut Flow, anorthoclase
Isochron age = -5 ± 12 ka
40Ar/36Ar = 321.8 ± 7.9
MSWD = 3.6
0.30
0.35
0.40
0.45
0.50
0.55
0.60
0.65
0.70
0.75
0.80
0.85
0.90
0.95
39Ar/ 40Ar

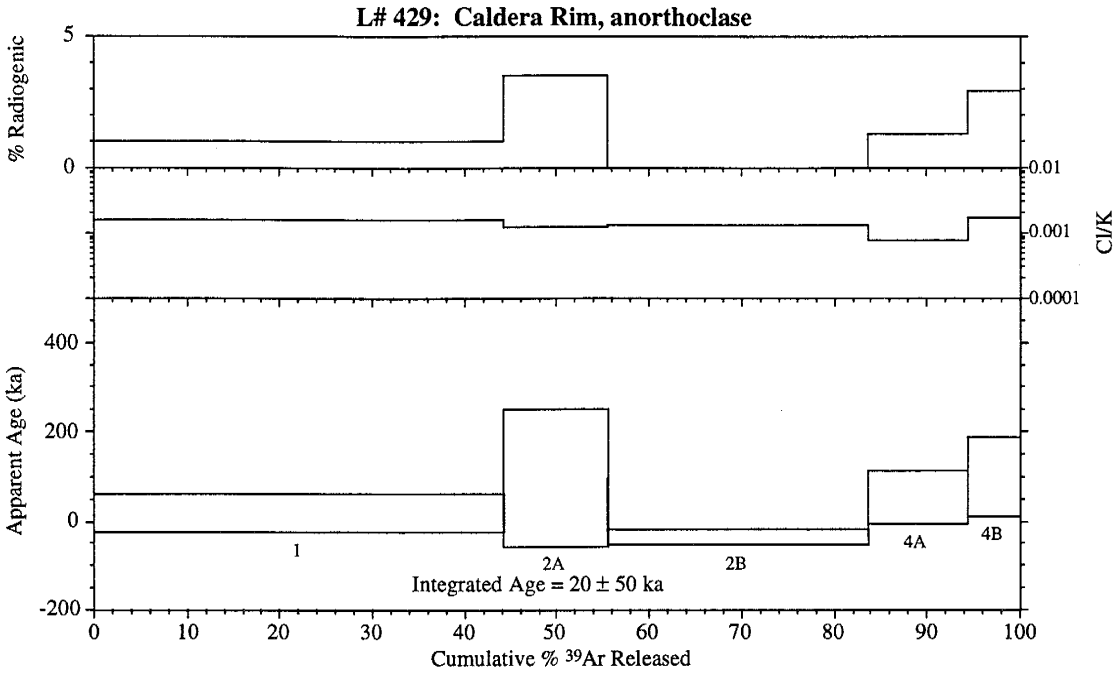
L# 429: Caldera Rim, anorthoclase
% Radiogenic
5
0
0.01
0.001
0.0001
Cl/K
Apparent Age (ka)
400
200
0
-200
1
2A
2B
4A
4B
Integrated Age = 20 ± 50 ka
0
10
20
30
40
50
60
70
80
90
100
Cumulative % 39Ar Released

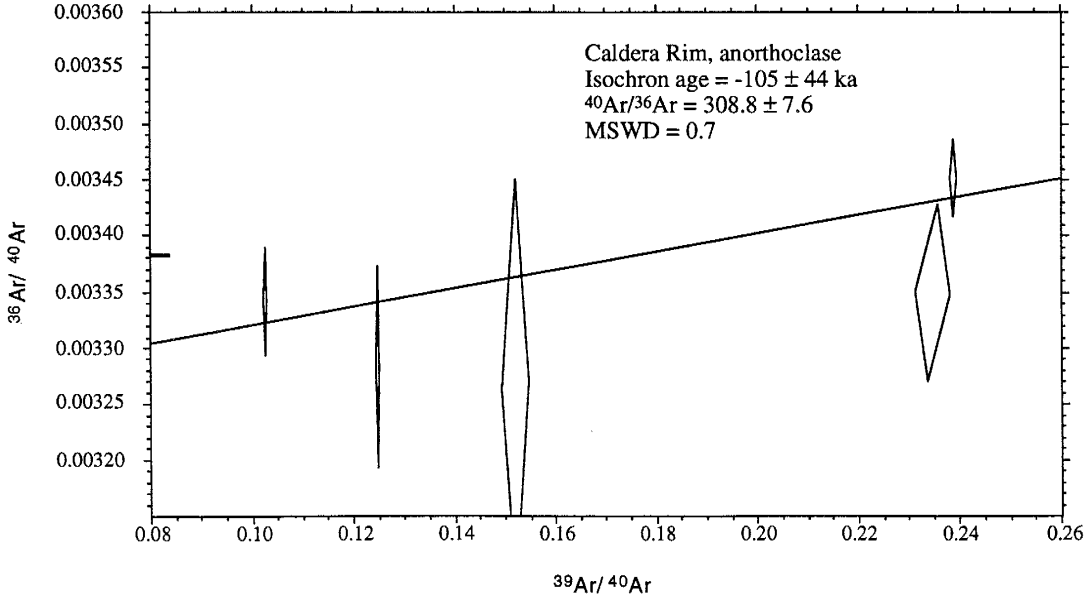
Caldera Rim, anorthoclase
Isochron age = -105 ± 44 ka
40Ar/36Ar = 308.8 ± 7.6
MSWD = 0.7
36Ar/ 40Ar
0.00360
0.00355
0.00350
0.00345
0.00340
0.00335
0.00330
0.00325
0.00320
0.08
0.10
0.12
0.14
0.16
0.18
0.20
0.22
0.24
0.26
39Ar/ 40Ar

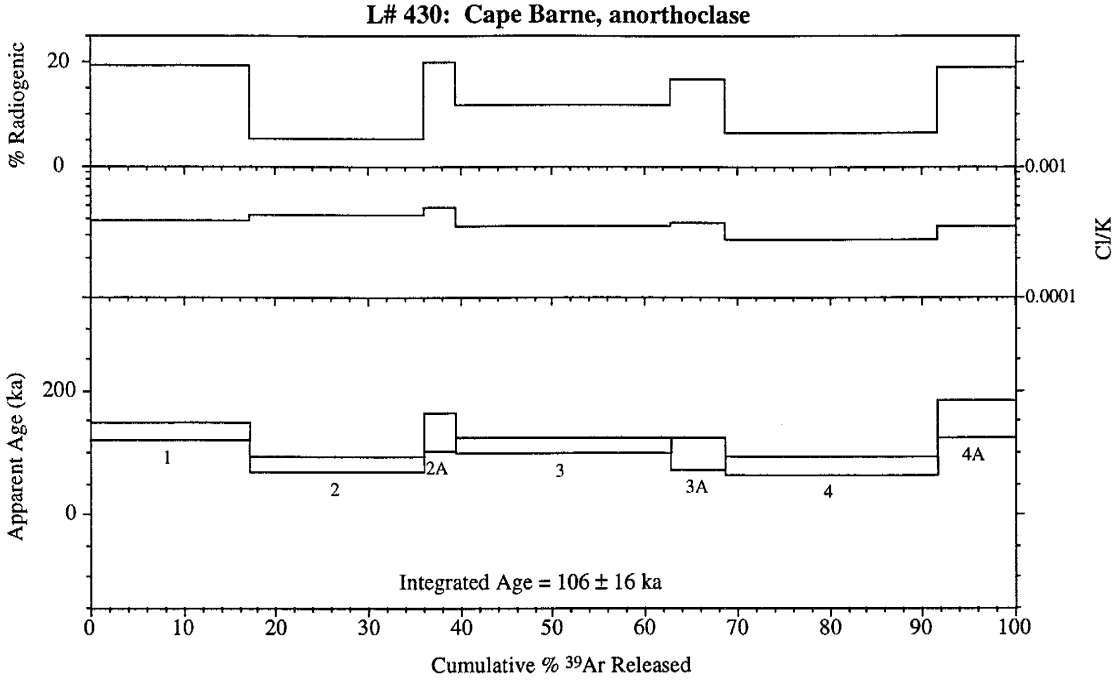
L# 430: Cape Barne, anorthoclase
% Radiogenic
20
0
0.001
0.0001
Cl/K
Apparent Age (ka)
200
0
1
2
2A
3
3A
4
4A
Integrated Age = 106 ± 16 ka
0
10
20
30
40
50
60
70
80
90
100
Cumulative % 39Ar Released

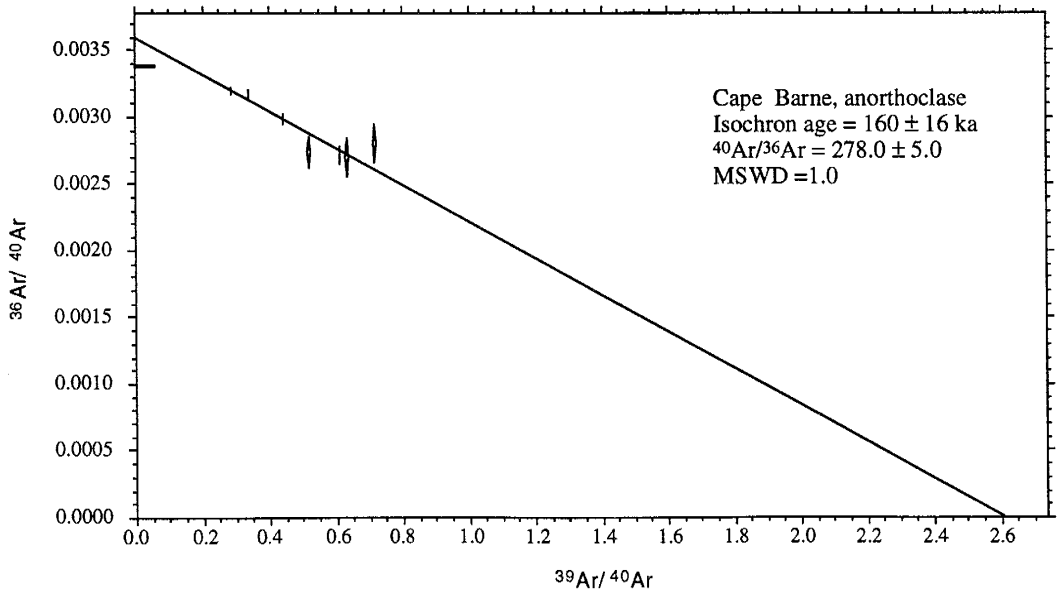
Cape Barne, anorthoclase
Isochron age = 160 ± 16 ka
40Ar/36Ar = 278.0 ± 5.0
MSWD =1.0
36Ar/ 40Ar
0.0035
0.0030
0.0025
0.0020
0.0015
0.0010
0.0005
0.0000
0.0
0.2
0.4
0.6
0.8
1.0
1.2
1.4
1.6
1.8
2.0
2.2
2.4
2.6
39Ar/ 40Ar

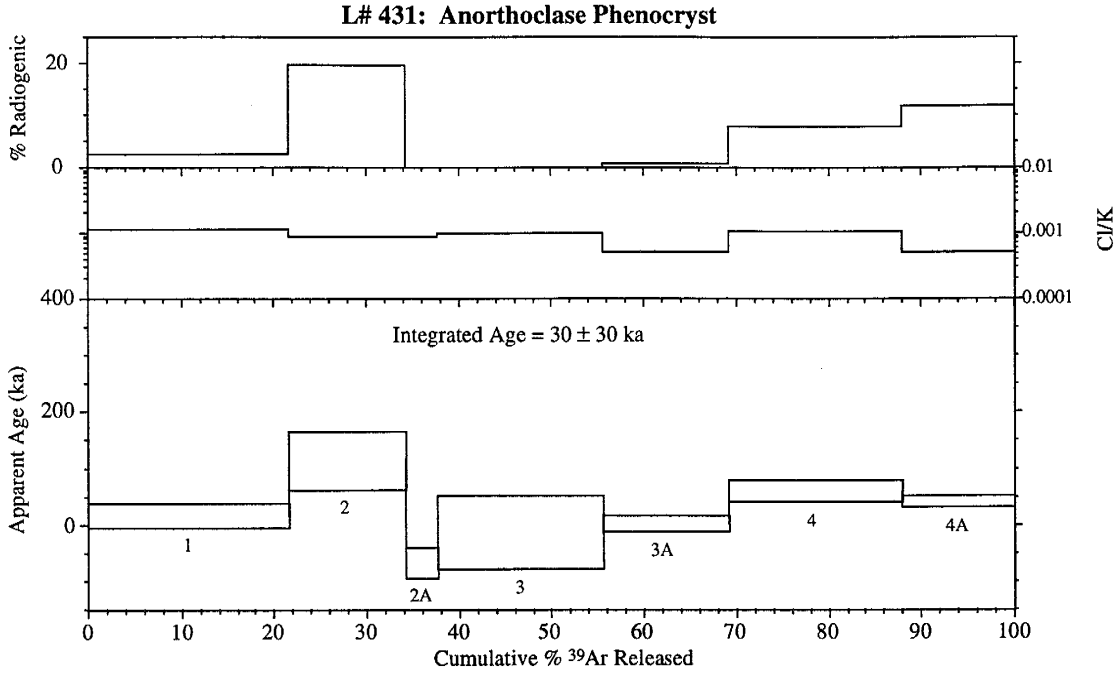
L# 431: Anorthoclase Phenocryst
% Radiogenic
20
0
0.01
0.001
0.0001
Cl/K
400
Integrated Age = 30 ± 30 ka
Apparent Age (ka)
200
0
1
2
2A
3
3A
4
4A
0
10
20
30
40
50
60
70
80
90
100
Cumulative % 39Ar Released

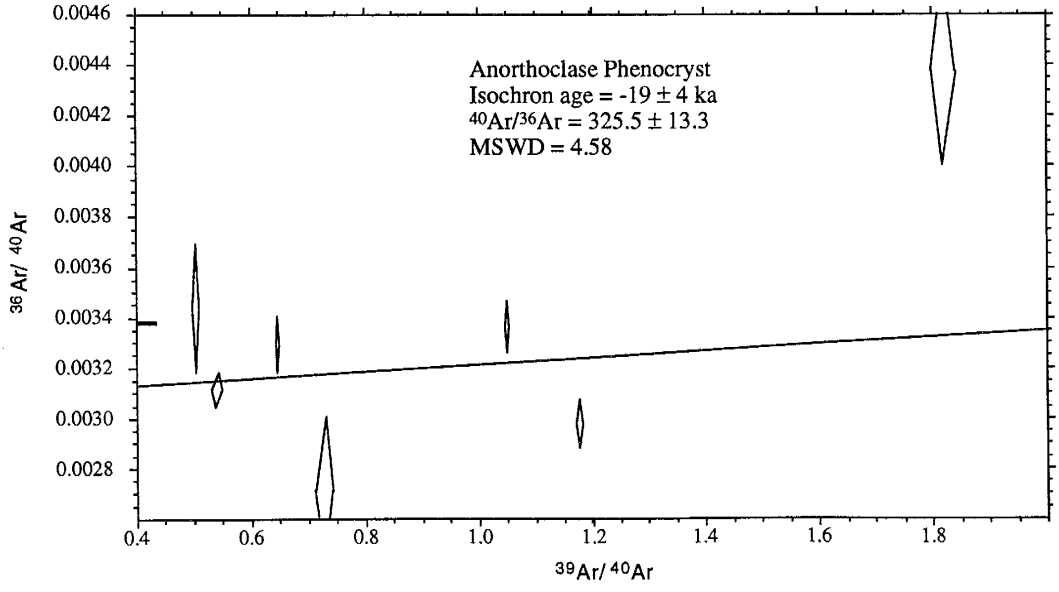
Anorthoclase Phenocryst
Isochron age = -19 ± 4 ka
40Ar/36Ar = 325.5 ± 13.3
MSWD = 4.58
36Ar/ 40Ar
0.0046
0.0044
0.0042
0.0040
0.0038
0.0036
0.0034
0.0032
0.0030
0.0028
0.4
0.6
0.8
1.0
1.2
1.4
1.6
1.8
39Ar/ 40Ar

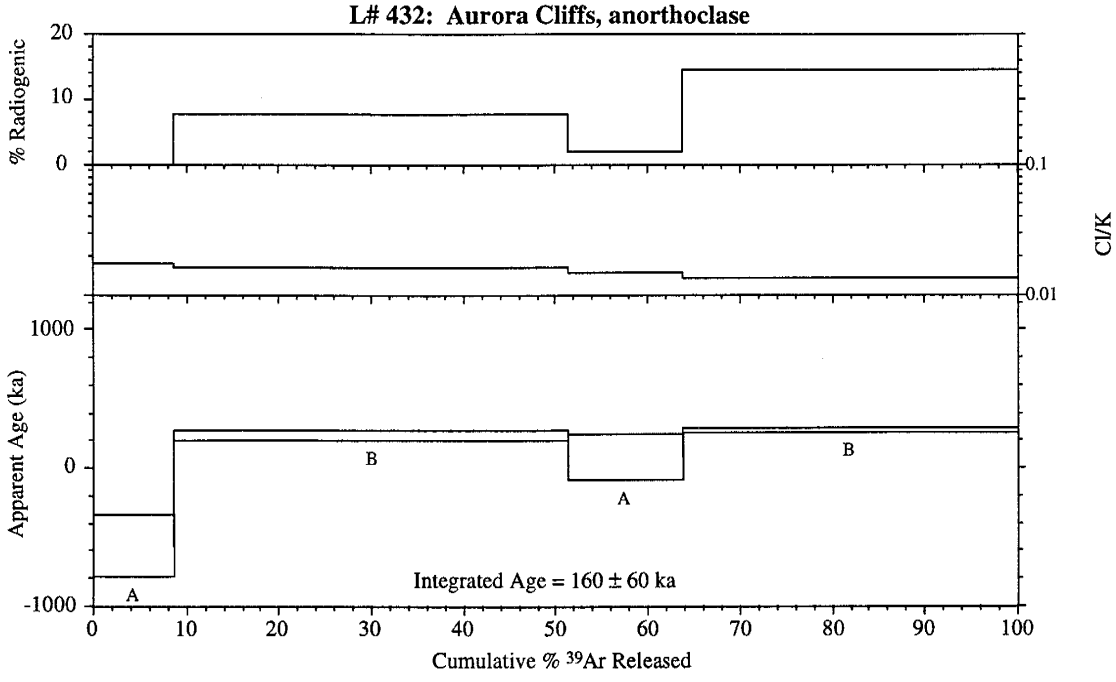
L# 432: Aurora Cliffs, anorthoclase
% Radiogenic
20
10
0
0.1
0.01
Cl/K
1000
0
-1000
Apparent Age (ka)
A
B
A
B
Integrated Age = 160 ± 60 ka
0
10
20
30
40
50
60
70
80
90
100
Cumulative % 39Ar Released

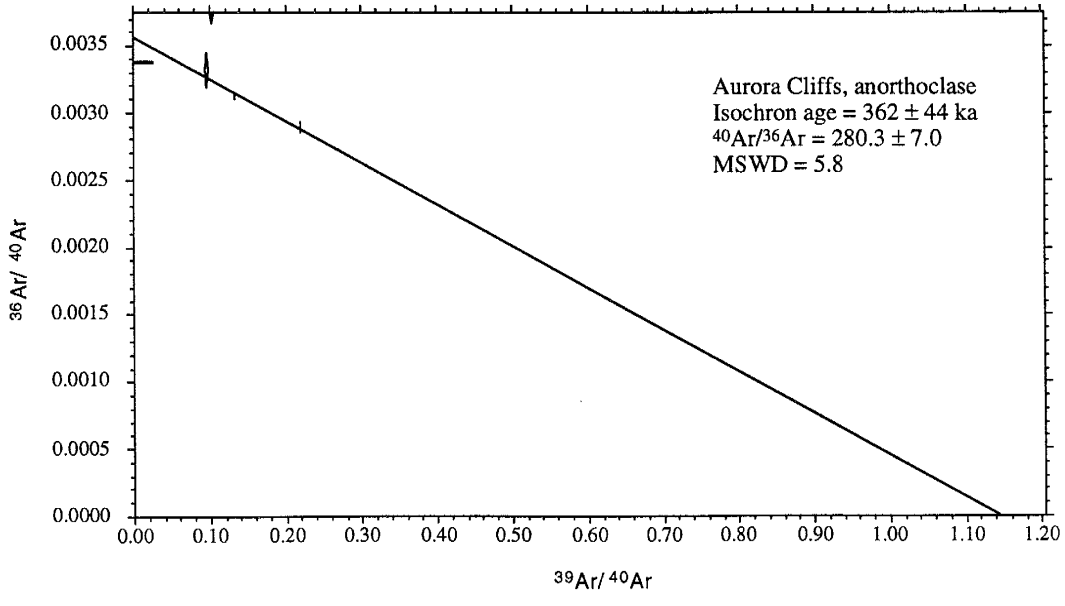
Aurora Cliffs, anorthoclase
Isochron age = 362 ± 44 ka
40Ar/36Ar = 280.3 ± 7.0
MSWD = 5.8
36Ar/ 40Ar
0.0035
0.0030
0.0025
0.0020
0.0015
0.0010
0.0005
0.0000
0.00
0.10
0.20
0.30
0.40
0.50
0.60
0.70
0.80
0.90
1.00
1.10
1.20
39Ar/ 40Ar

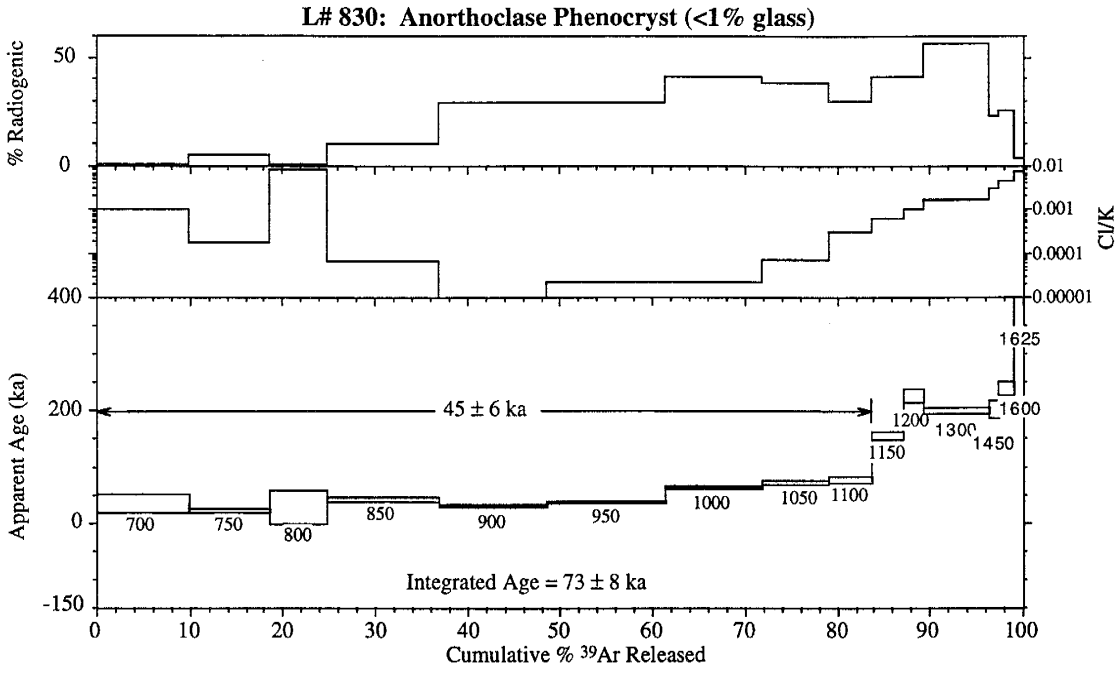
L# 830: Anorthoclase Phenocryst (<1% glass)
% Radiogenic
50
0
Cl/K
0.01
0.001
0.0001
0.00001
400
200
0
-150
Apparent Age (ka)
45 ± 6 ka
700
750
800
850
900
950
1000
1050
1100
1150
1200
1300
1450
1600
1625
Integrated Age = 73 ± 8 ka
0
10
20
30
40
50
60
70
80
90
100
Cumulative % 39Ar Released

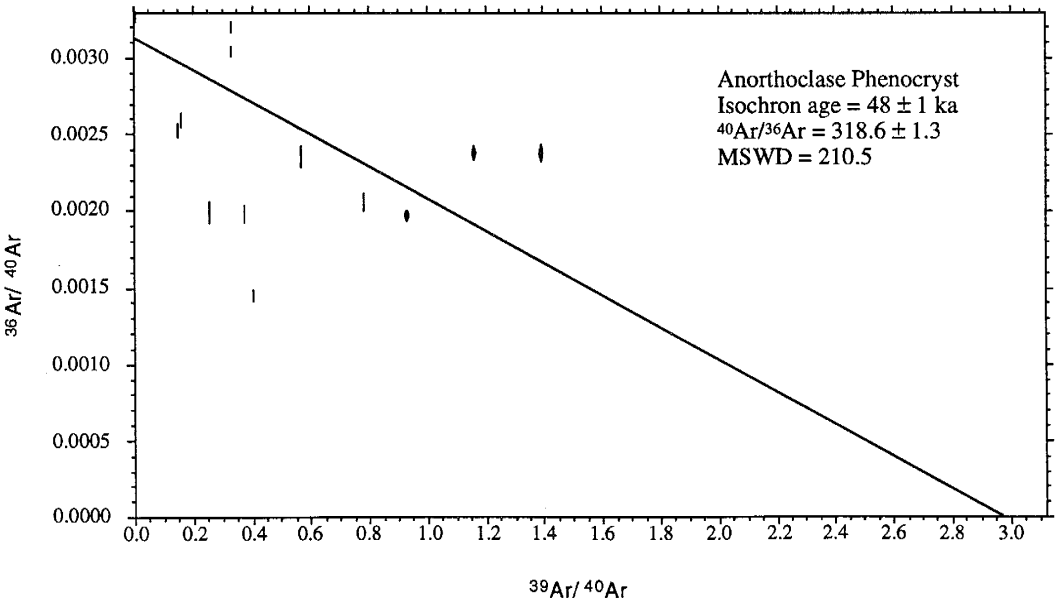
Anorthoclase Phenocryst
Isochron age = 48 ± 1 ka
40Ar/36Ar = 318.6 ± 1.3
MSWD = 210.5
36Ar/ 40Ar
0.0030
0.0025
0.0020
0.0015
0.0010
0.0005
0.0000
0.0
0.2
0.4
0.6
0.8
1.0
1.2
1.4
1.6
1.8
2.0
2.2
2.4
2.6
2.8
3.0
39Ar/ 40Ar

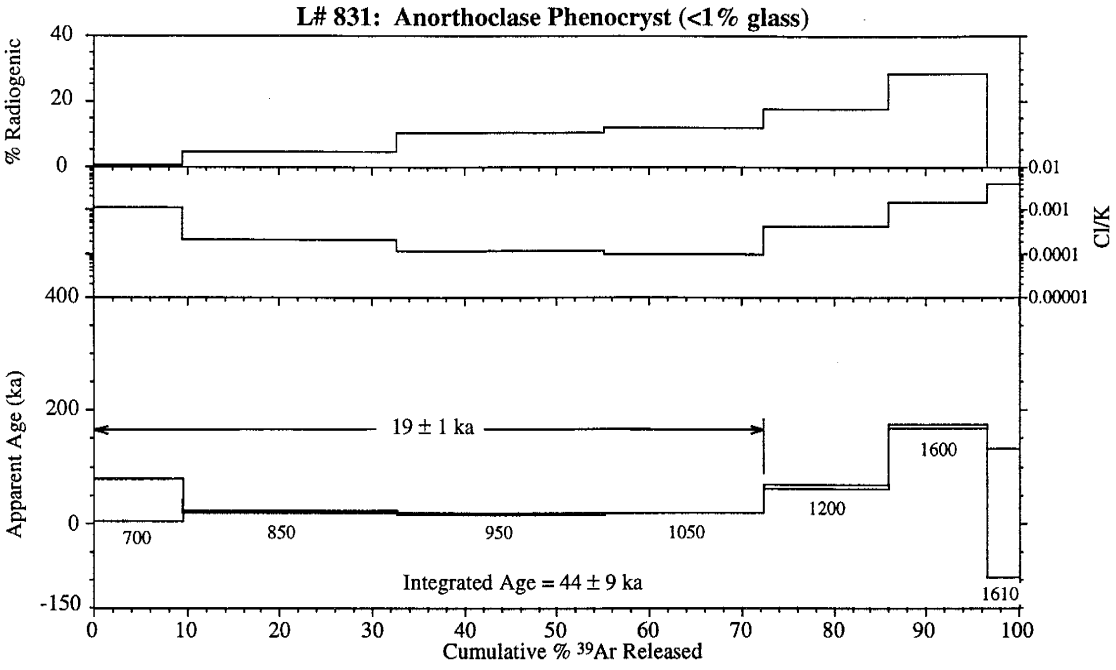
L# 831: Anorthoclase Phenocryst (<1% glass)
% Radiogenic
40
20
0
0.01
0.001
0.0001
0.00001
Cl/K
400
200
0
-150
Apparent Age (ka)
19 ± 1 ka
700
850
950
1050
1200
1600
1610
Integrated Age = 44 ± 9 ka
0
10
20
30
40
50
60
70
80
90
100
Cumulative % 39Ar Released

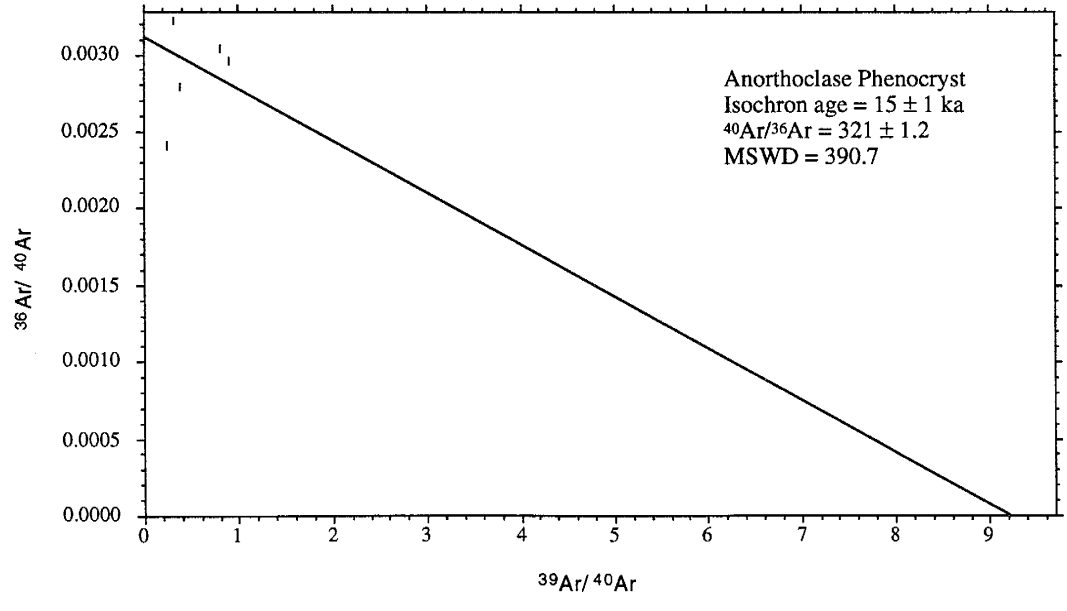
Anorthoclase Phenocryst
Isochron age = 15 ± 1 ka
40Ar/36Ar = 321 ± 1.2
MSWD = 390.7
0.0030
0.0025
0.0020
0.0015
0.0010
0.0005
0.0000
36Ar/ 40Ar
0
1
2
3
4
5
6
7
8
9
39Ar/ 40Ar

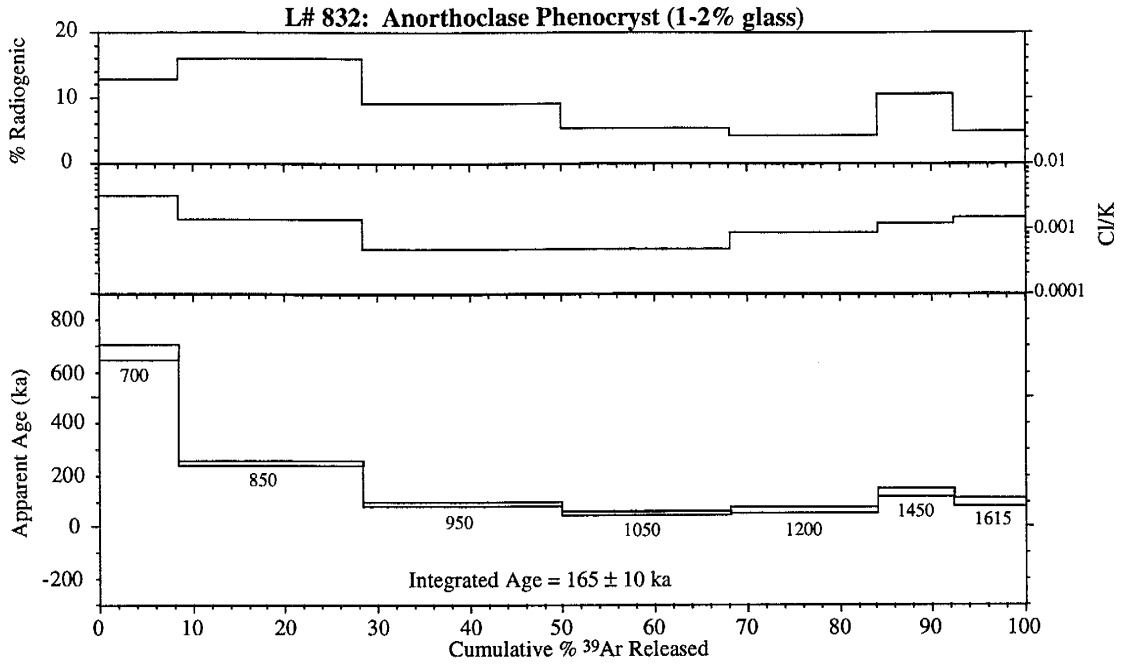
L# 832: Anorthoclase Phenocryst (1-2% glass)
% Radiogenic
20
10
0
0.01
0.001
0.0001
Cl/K
800
600
400
200
0
-200
Apparent Age (ka)
700
850
950
1050
1200
1450
1615
Integrated Age = 165 ± 10 ka
0
10
20
30
40
50
60
70
80
90
100
Cumulative % 39Ar Released

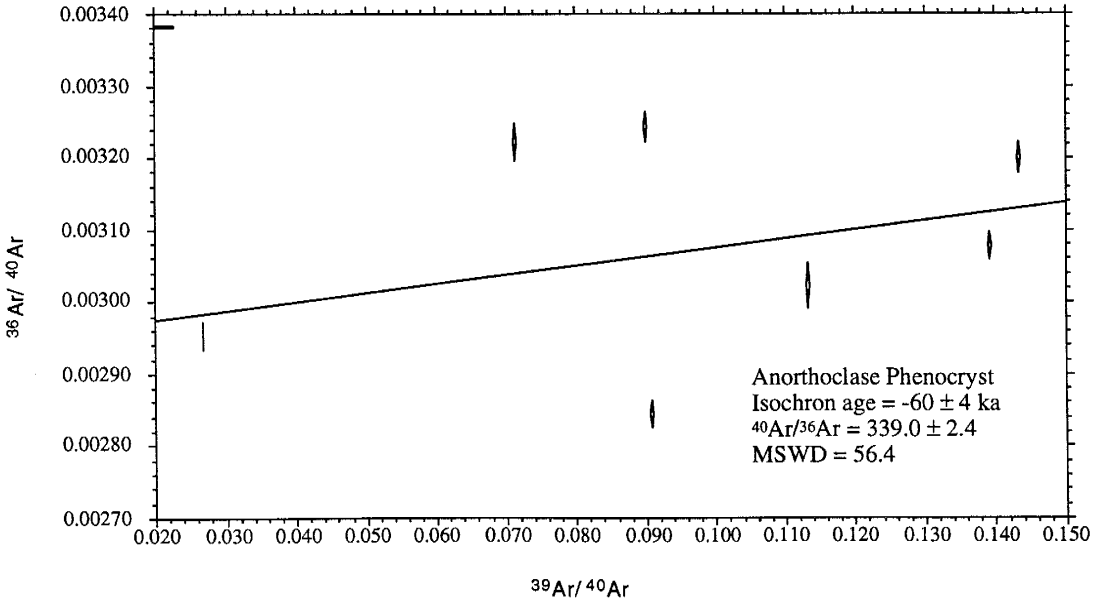
0.00340
0.00330
0.00320
0.00310
0.00300
0.00290
0.00280
0.00270
36Ar/ 40Ar
Anorthoclase Phenocryst
Isochron age = -60 ± 4 ka
40Ar/36Ar = 339.0 ± 2.4
MSWD = 56.4
0.020
0.030
0.040
0.050
0.060
0.070
0.080
0.090
0.100
0.110
0.120
0.130
0.140
0.150
39Ar/ 40Ar

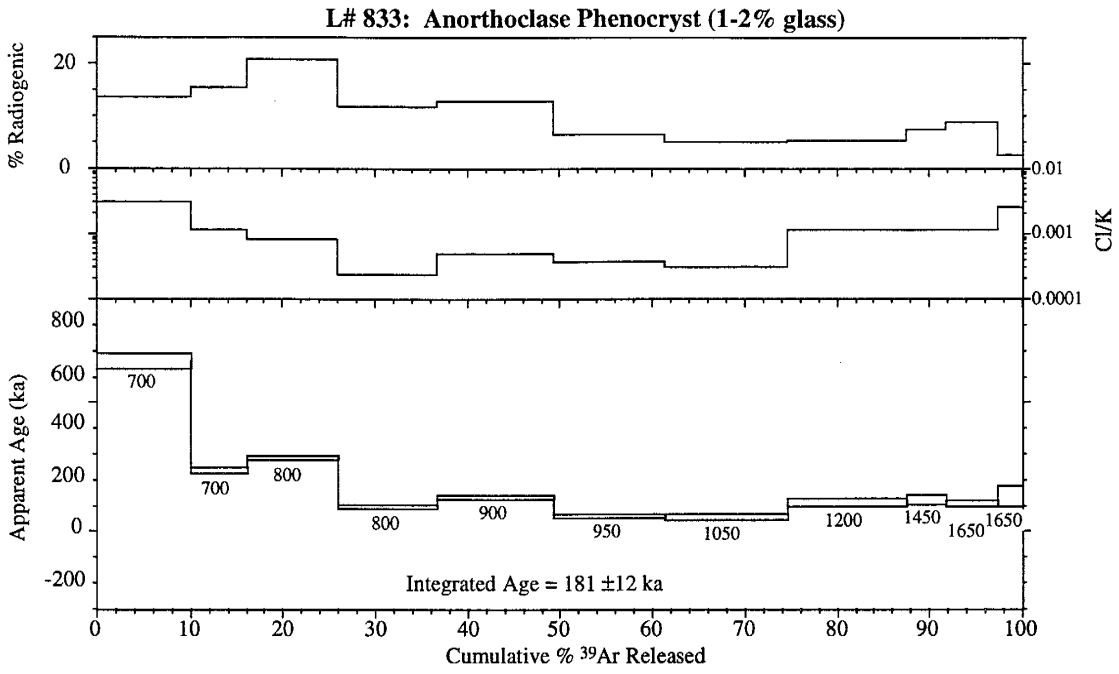
L# 833: Anorthoclase Phenocryst (1-2% glass)
% Radiogenic
20
0
0.01
0.001
0.0001
Cl/K
800
600
400
200
0
-200
Apparent Age (ka)
700
700
800
800
900
950
1050
1200
1450
1650
1650
Integrated Age = 181 ±12 ka
0
10
20
30
40
50
60
70
80
90
100
Cumulative % 39Ar Released

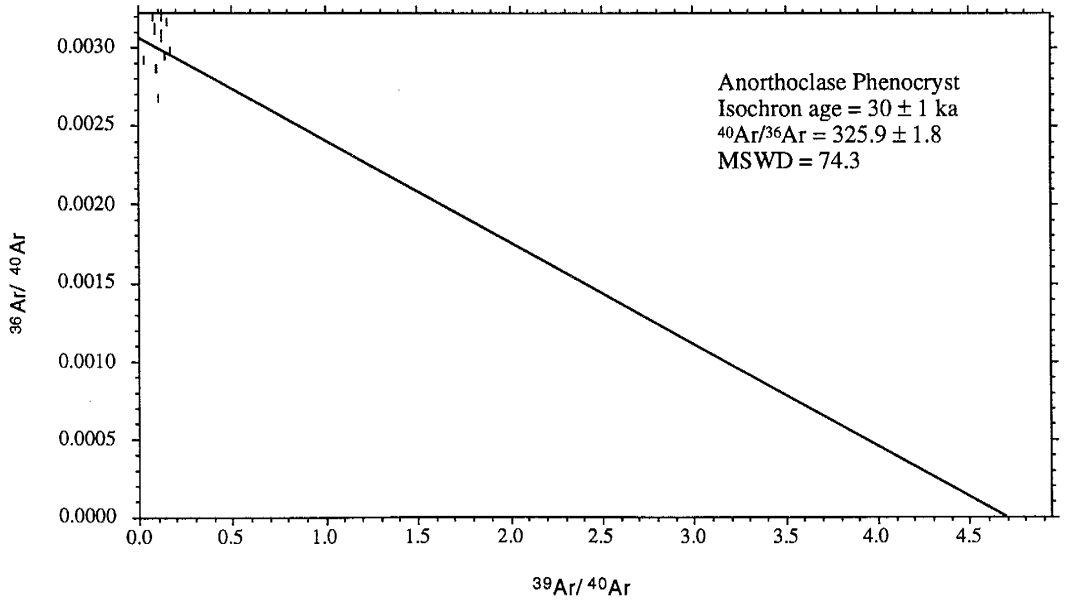
Anorthoclase Phenocryst
Isochron age = 30 ± 1 ka
40Ar/36Ar = 325.9 ± 1.8
MSWD = 74.3
0.0030
0.0025
0.0020
0.0015
0.0010
0.0005
0.0000
36Ar/ 40Ar
0.0
0.5
1.0
1.5
2.0
2.5
3.0
3.5
4.0
4.5
39Ar/ 40Ar

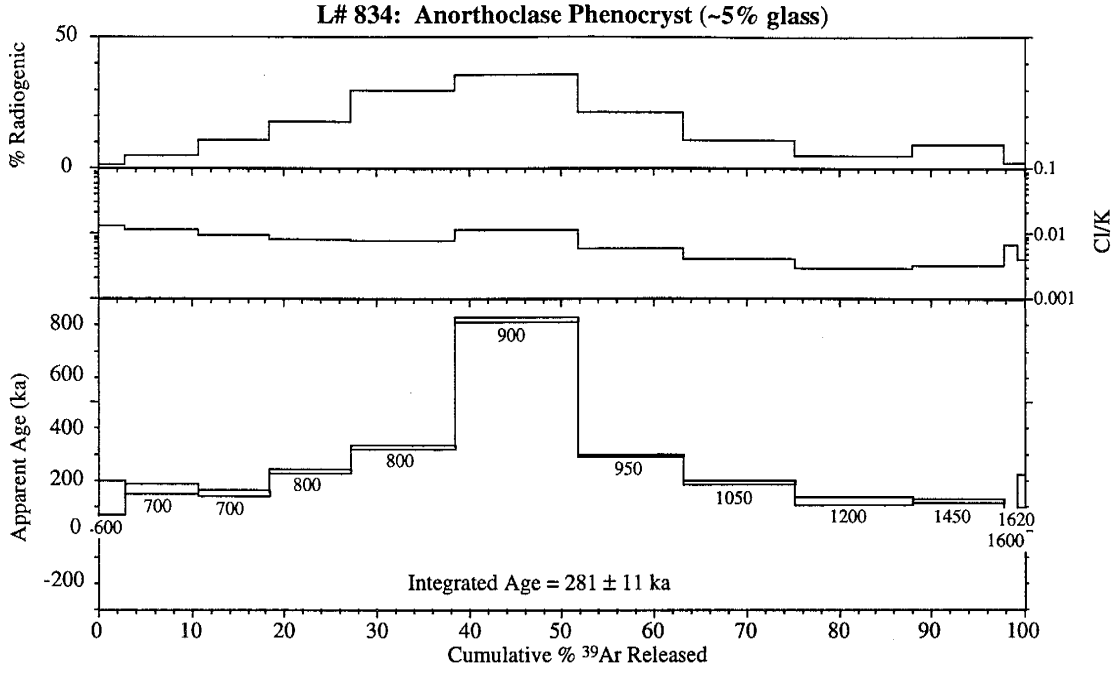
L# 834: Anorthoclase Phenocryst (~5% glass)
% Radiogenic
50
0
0.1
0.01
0.001
Cl/K
Apparent Age (ka)
800
600
400
200
0
-200
600
700
700
800
800
900
950
1050
1200
1450
1620
1600
Integrated Age = 281 ± 11 ka
0
10
20
30
40
50
60
70
80
90
100
Cumulative % 39Ar Released

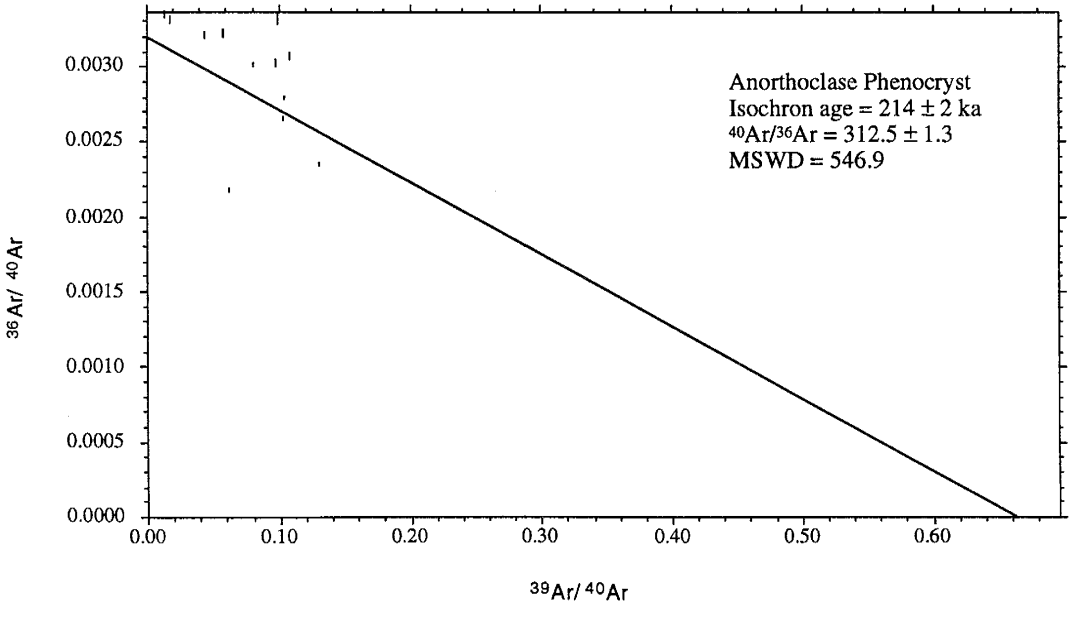
Anorthoclase Phenocryst
Isochron age = 214 ± 2 ka
40Ar/36Ar = 312.5 ± 1.3
MSWD = 546.9
36Ar/ 40Ar
0.0030
0.0025
0.0020
0.0015
0.0010
0.0005
0.0000
0.00
0.10
0.20
0.30
0.40
0.50
0.60
39Ar/ 40Ar

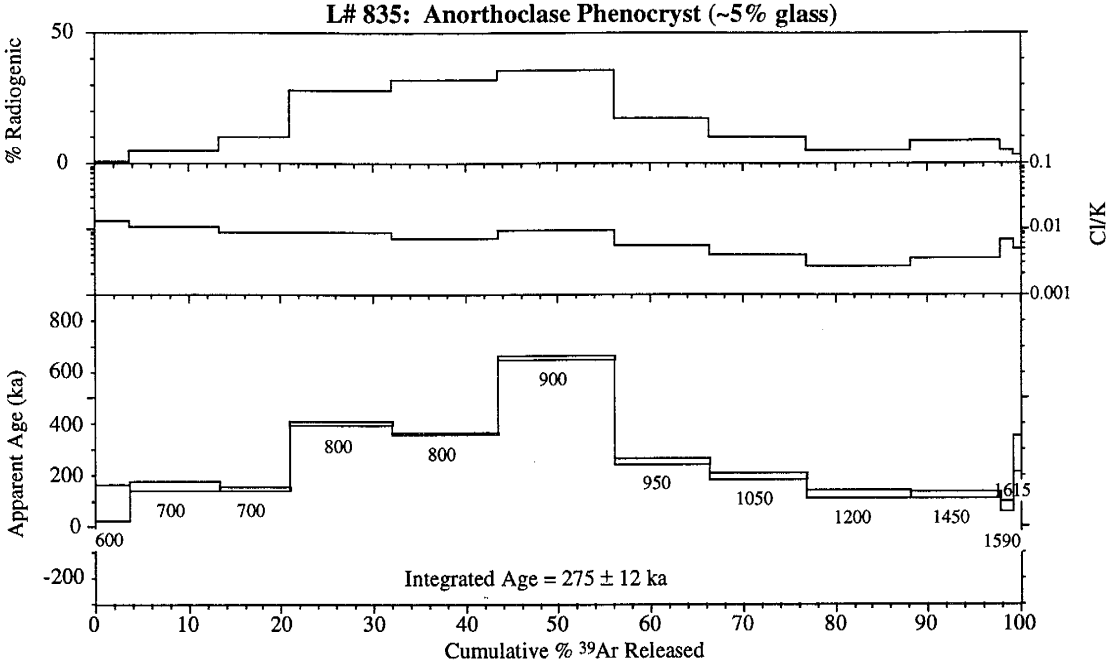
L# 835: Anorthoclase Phenocryst (~5% glass)
% Radiogenic
50
0
0.1
0.01
0.001
Cl/K
Apparent Age (ka)
800
600
400
200
0
-200
600
700
700
800
800
900
950
1050
1200
1450
1590
1615
Integrated Age = 275 ± 12 ka
0
10
20
30
40
50
60
70
80
90
100
Cumulative % 39Ar Released

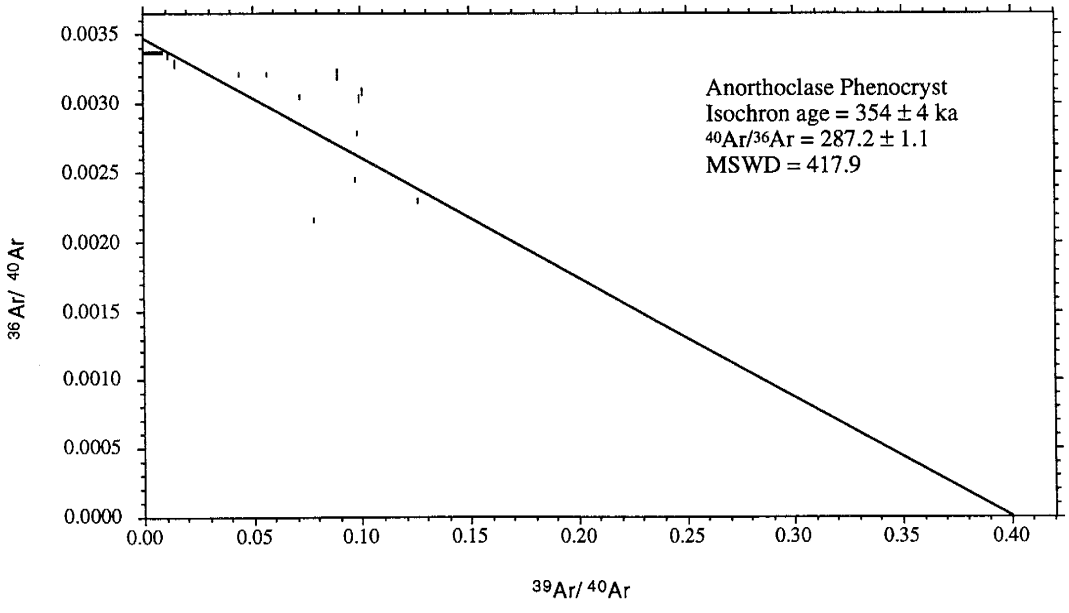
Anorthoclase Phenocryst
Isochron age = 354 ± 4 ka
40Ar/36Ar = 287.2 ± 1.1
MSWD = 417.9
36Ar/ 40Ar
0.0035
0.0030
0.0025
0.0020
0.0015
0.0010
0.0005
0.0000
0.00
0.05
0.10
0.15
0.20
0.25
0.30
0.35
0.40
39Ar/ 40Ar

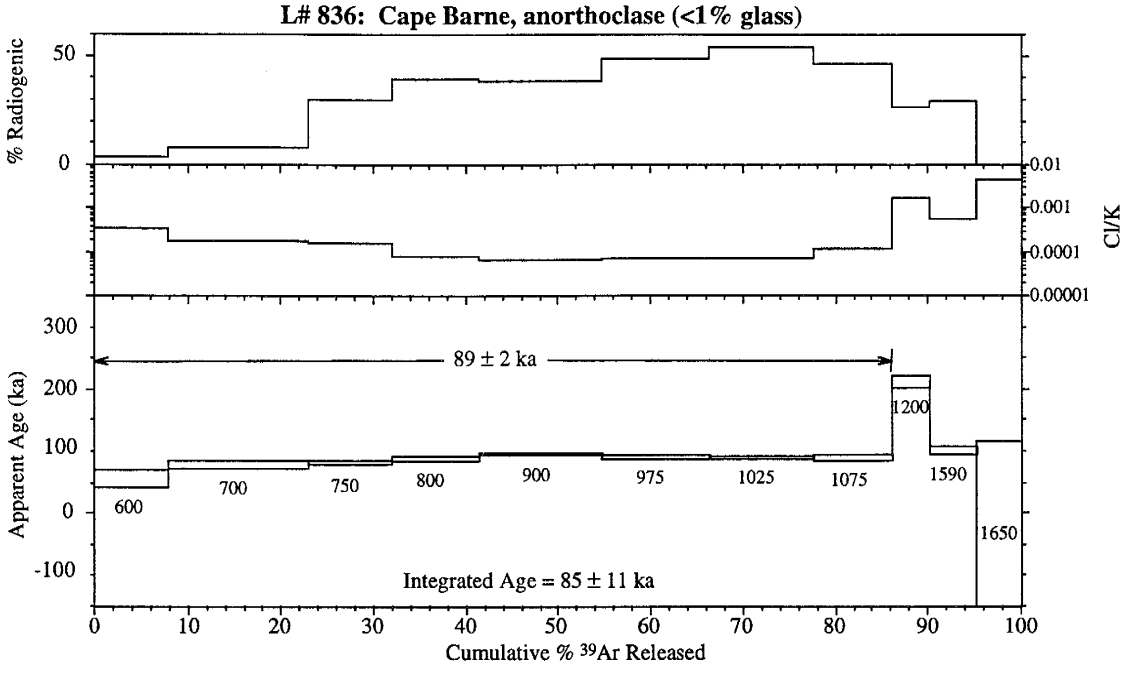
L# 836: Cape Barne, anorthoclase (<1% glass)
% Radiogenic
50
0
0.01
0.001
0.0001
0.00001
Cl/K
300
200
100
0
-100
Apparent Age (ka)
89 ± 2 ka
600
700
750
800
900
975
1025
1075
1200
1590
1650
Integrated Age = 85 ± 11 ka
0
10
20
30
40
50
60
70
80
90
100
Cumulative % 39Ar Released

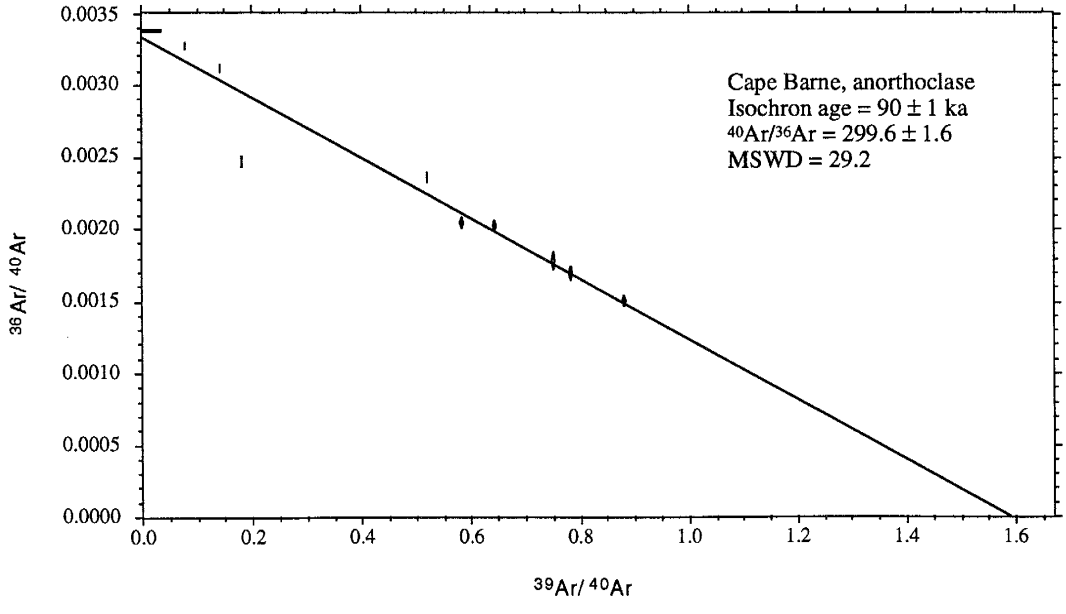
0.0035
0.0030
0.0025
0.0020
0.0015
0.0010
0.0005
0.0000
36Ar/ 40Ar
Cape Barne, anorthoclase
Isochron age = 90 ± 1 ka
40Ar/36Ar = 299.6 ± 1.6
MSWD = 29.2
0.0
0.2
0.4
0.6
0.8
1.0
1.2
1.4
1.6
39Ar/ 40Ar

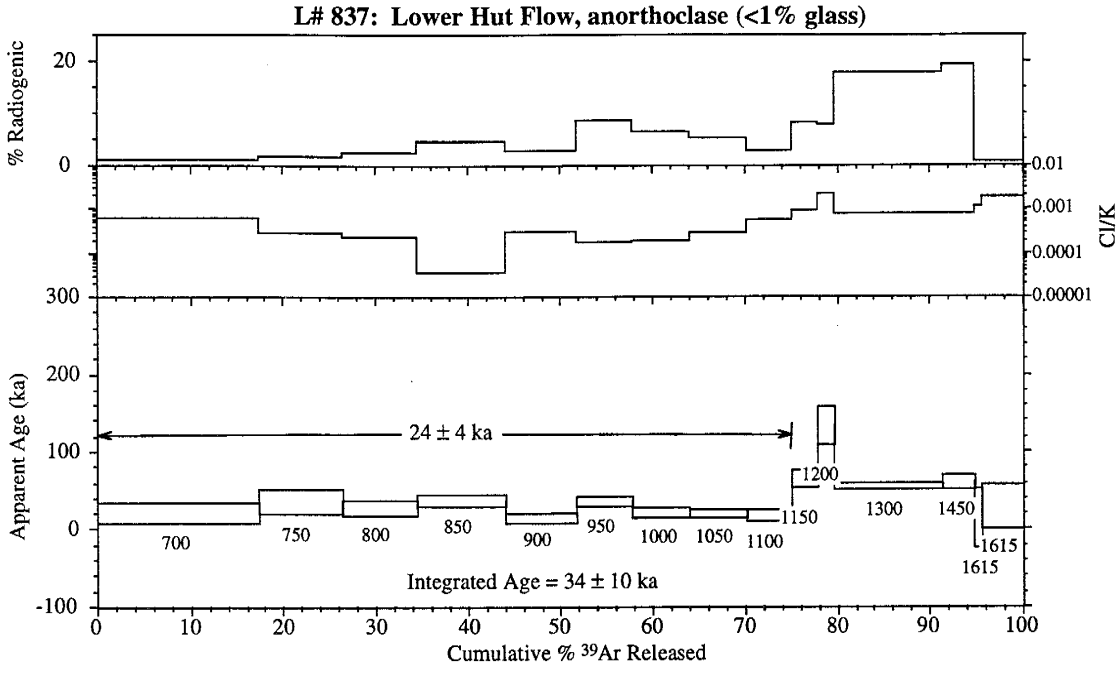
L# 837: Lower Hut Flow, anorthoclase (<1% glass)
% Radiogenic
20
0
0.01
0.001
0.0001
0.00001
Cl/K
300
200
100
0
-100
Apparent Age (ka)
24 ± 4 ka
700
750
800
850
900
950
1000
1050
1100
1150
1200
1300
1450
1615
1615
Integrated Age = 34 ± 10 ka
0
10
20
30
40
50
60
70
80
90
100
Cumulative % 39Ar Released

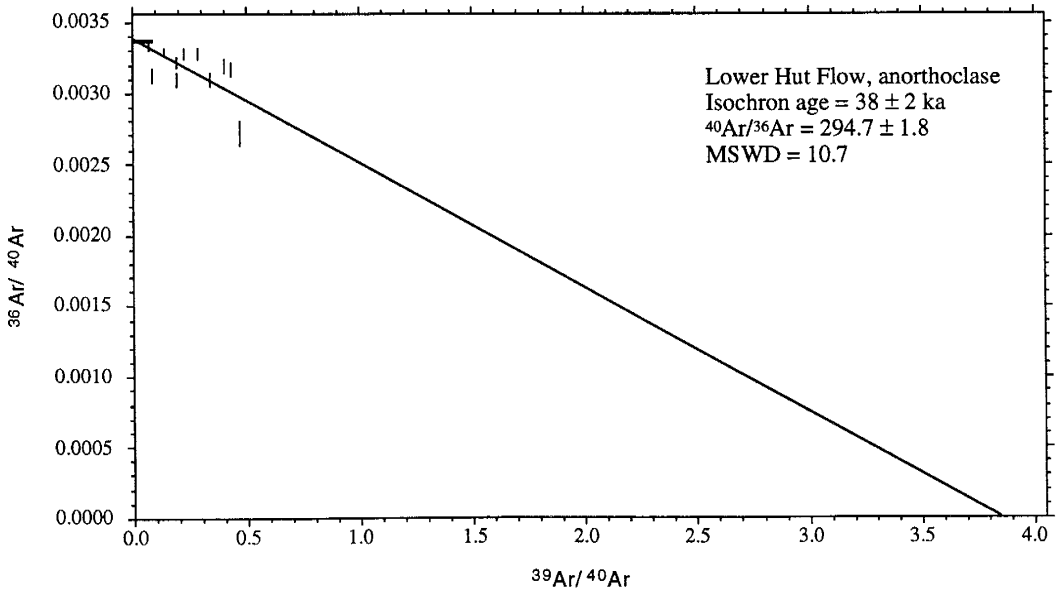
0.0035
0.0030
0.0025
0.0020
0.0015
0.0010
0.0005
0.0000
36Ar/ 40Ar
Lower Hut Flow, anorthoclase
Isochron age = 38 ± 2 ka
40Ar/36Ar = 294.7 ± 1.8
MSWD = 10.7
0.0
0.5
1.0
1.5
2.0
2.5
3.0
3.5
4.0
39Ar/ 40Ar

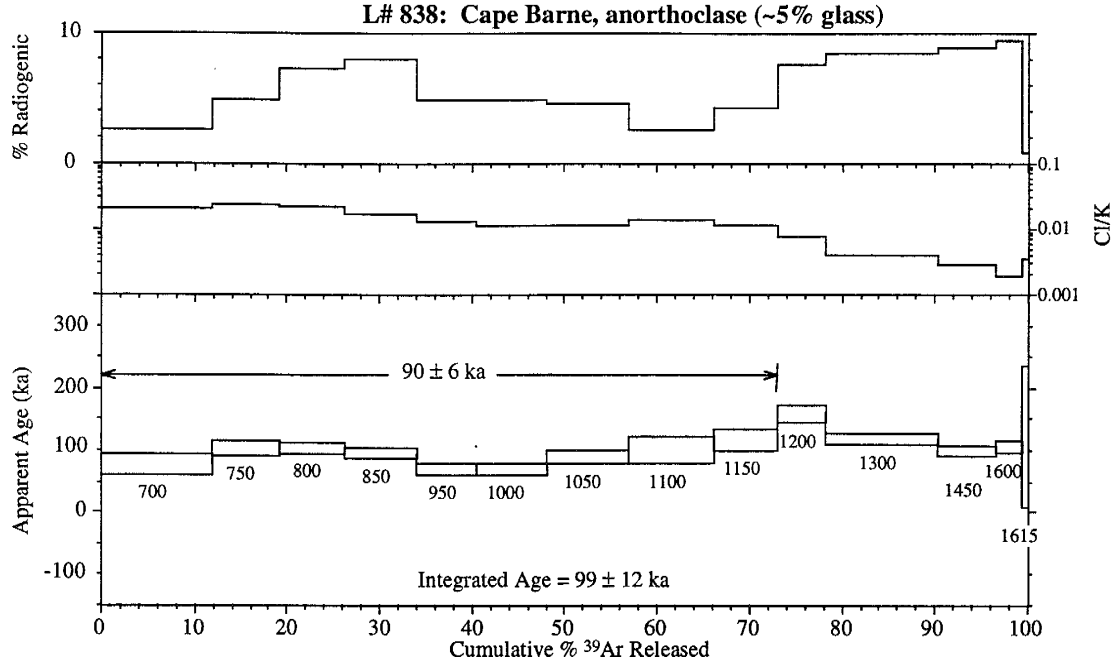
L# 838: Cape Barne, anorthoclase (~5% glass)
% Radiogenic
10
0
0.1
0.01
0.001
Cl/K
300
200
100
0
-100
Apparent Age (ka)
90 ± 6 ka
700
750
800
850
950
1000
1050
1100
1150
1200
1300
1450
1600
1615
Integrated Age = 99 ± 12 ka
0
10
20
30
40
50
60
70
80
90
100
Cumulative % 39Ar Released

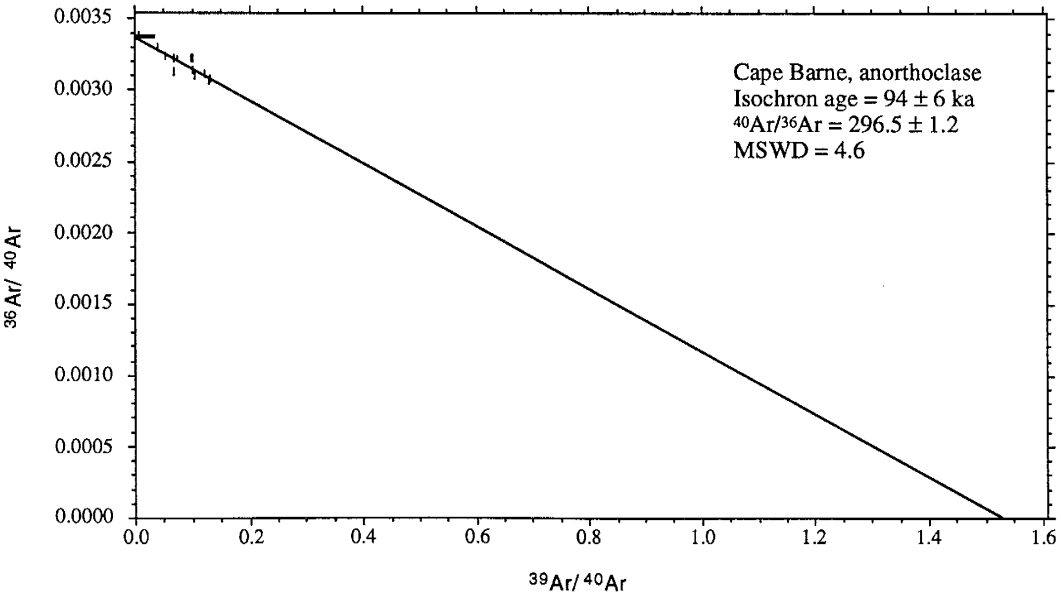
0.0035
0.0030
0.0025
0.0020
0.0015
0.0010
0.0005
0.0000
36Ar/ 40Ar
Cape Barne, anorthoclase
Isochron age = 94 ± 6 ka
40Ar/36Ar = 296.5 ± 1.2
MSWD = 4.6
0.0
0.2
0.4
0.6
0.8
1.0
1.2
1.4
1.6
39Ar/ 40Ar

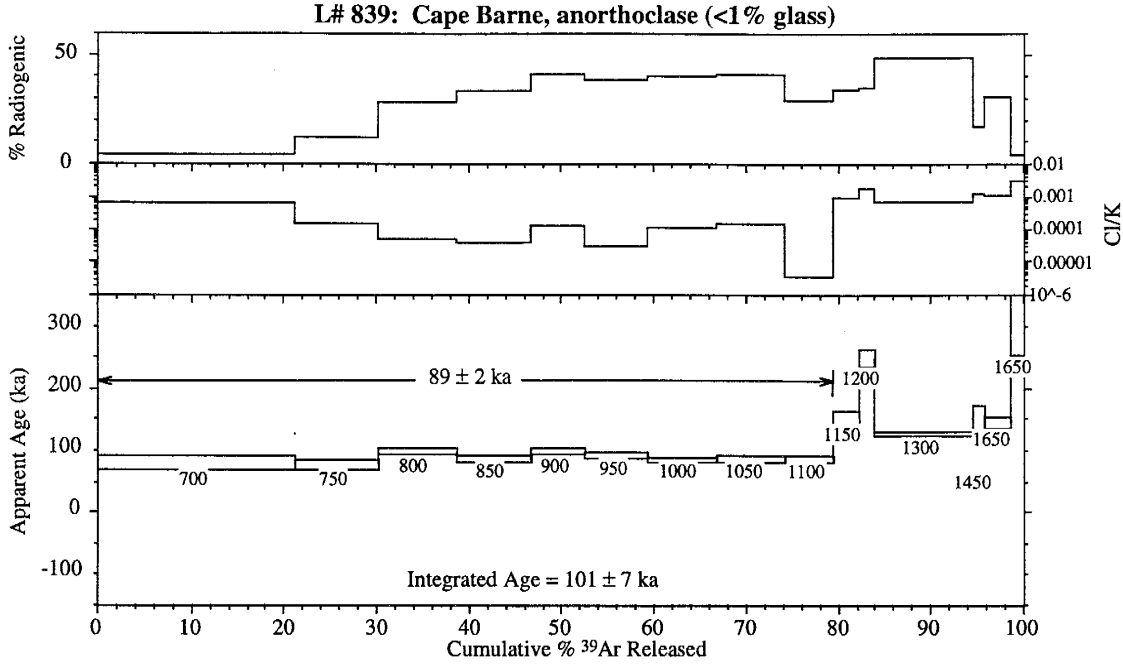
L# 839: Cape Barne, anorthoclase (<1% glass)
% Radiogenic
50
0
0.01
0.001
0.0001
0.00001
10^-6
Cl/K
300
200
100
0
-100
Apparent Age (ka)
89 ± 2 ka
700
750
800
850
900
950
1000
1050
1100
1150
1200
1300
1450
1650
1650
Integrated Age = 101 ± 7 ka
0
10
20
30
40
50
60
70
80
90
100
Cumulative % 39Ar Released

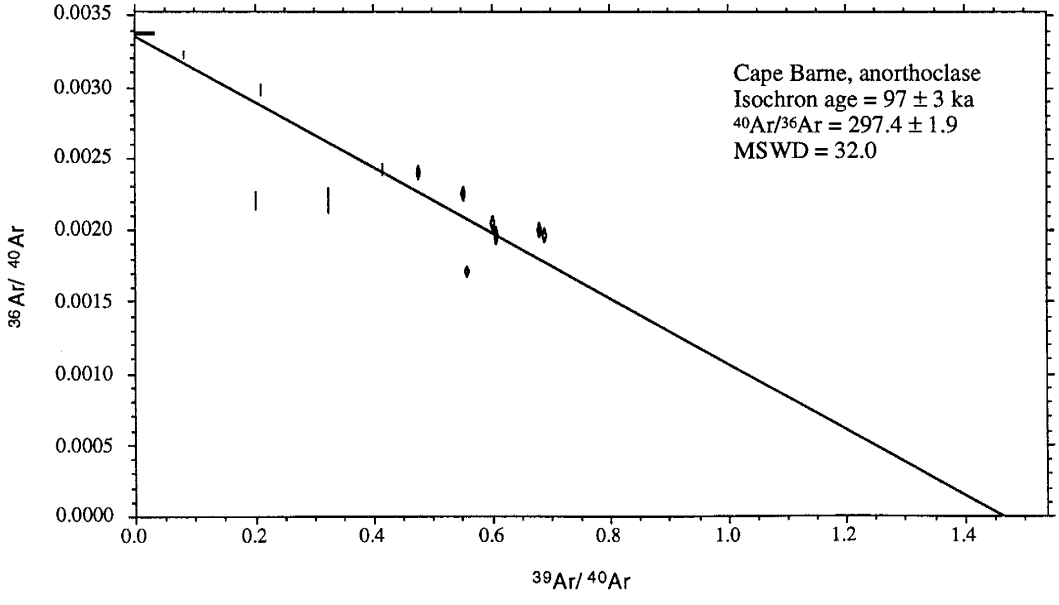
Cape Barne, anorthoclase
Isochron age = 97 ± 3 ka
40Ar/36Ar = 297.4 ± 1.9
MSWD = 32.0
0.0035
0.0030
0.0025
0.0020
0.0015
0.0010
0.0005
0.0000
36Ar/ 40Ar
0.0
0.2
0.4
0.6
0.8
1.0
1.2
1.4
39Ar/ 40Ar

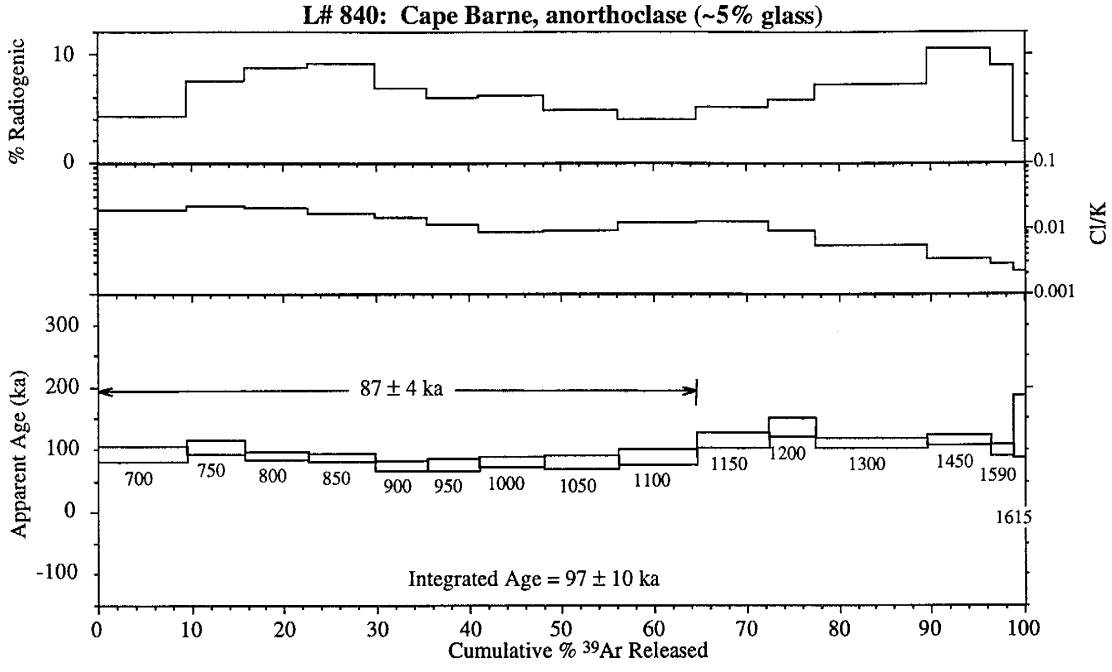
L# 840: Cape Barne, anorthoclase (~5% glass)
% Radiogenic
10
0
0.1
0.01
0.001
Cl/K
300
200
100
0
-100
Apparent Age (ka)
87 ± 4 ka
700
750
800
850
900
950
1000
1050
1100
1150
1200
1300
1450
1590
1615
Integrated Age = 97 ± 10 ka
0
10
20
30
40
50
60
70
80
90
100
Cumulative % 39Ar Released

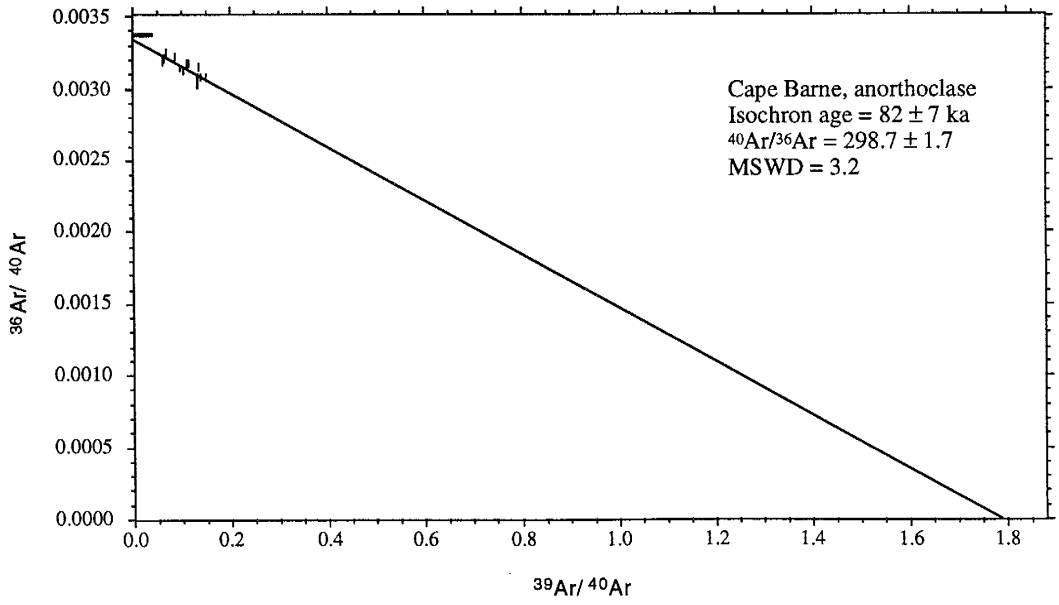
0.0035
0.0030
0.0025
0.0020
0.0015
0.0010
0.0005
0.0000
36Ar/ 40Ar
Cape Barne, anorthoclase
Isochron age = 82 ± 7 ka
40Ar/36Ar = 298.7 ± 1.7
MSWD = 3.2
0.0
0.2
0.4
0.6
0.8
1.0
1.2
1.4
1.6
1.8
39Ar/ 40Ar

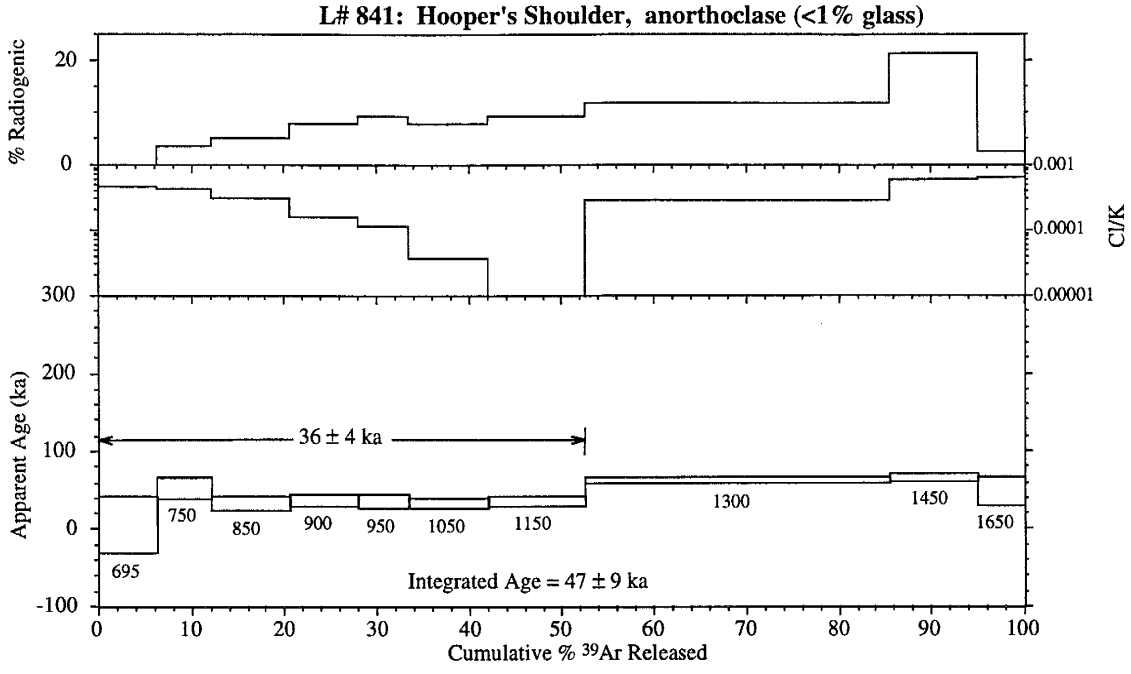
L# 841: Hooper's Shoulder, anorthoclase (<1% glass)
% Radiogenic
20
0
0.001
0.0001
0.00001
Cl/K
300
200
100
0
-100
Apparent Age (ka)
36 ± 4 ka
695
750
850
900
950
1050
1150
1300
1450
1650
Integrated Age = 47 ± 9 ka
0
10
20
30
40
50
60
70
80
90
100
Cumulative % 39Ar Released

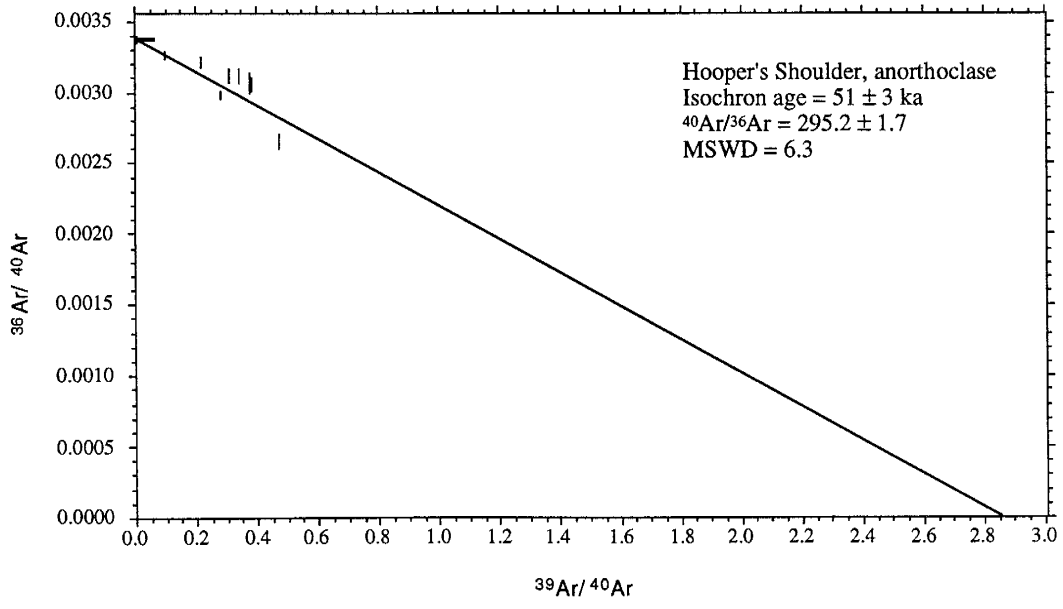
Hooper's Shoulder, anorthoclase
Isochron age = 51 ± 3 ka
40Ar/36Ar = 295.2 ± 1.7
MSWD = 6.3
0.0035
0.0030
0.0025
0.0020
0.0015
0.0010
0.0005
0.0000
36Ar/ 40Ar
0.0
0.2
0.4
0.6
0.8
1.0
1.2
1.4
1.6
1.8
2.0
2.2
2.4
2.6
2.8
3.0
39Ar/ 40Ar

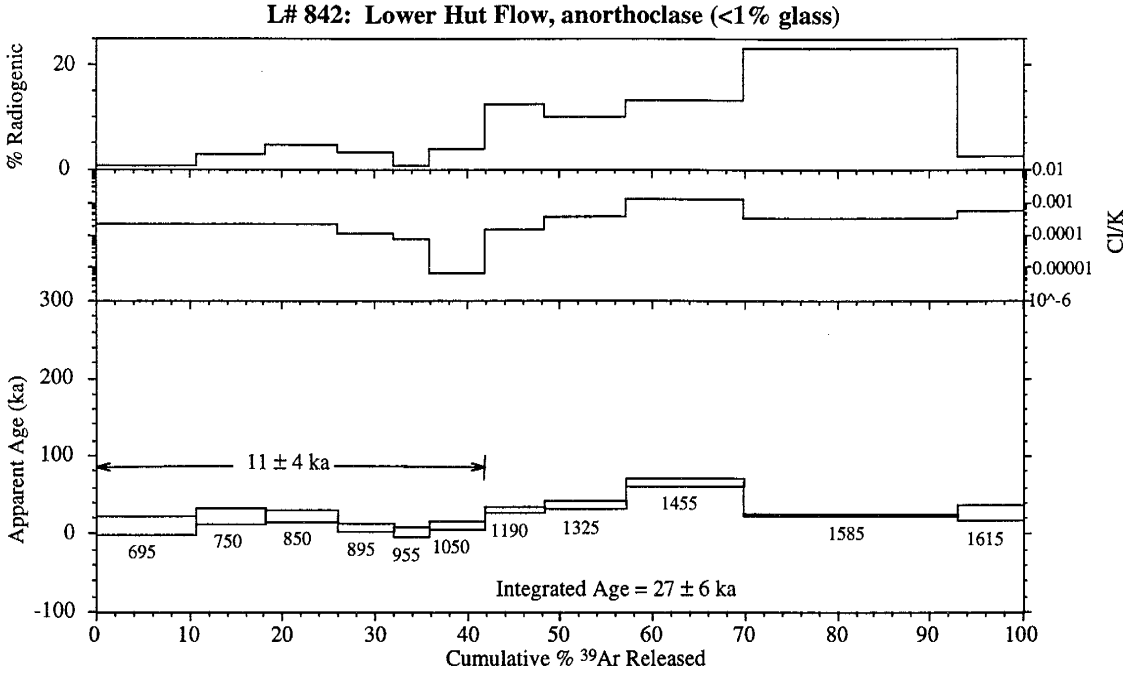
L# 842: Lower Hut Flow, anorthoclase (<1% glass)
% Radiogenic
20
0
0.01
0.001
0.0001
0.00001
10^-6
Cl/K
300
200
100
0
-100
Apparent Age (ka)
11 ± 4 ka
695
750
850
895
955
1050
1190
1325
1455
1585
1615
Integrated Age = 27 ± 6 ka
0
10
20
30
40
50
60
70
80
90
100
Cumulative % 39Ar Released

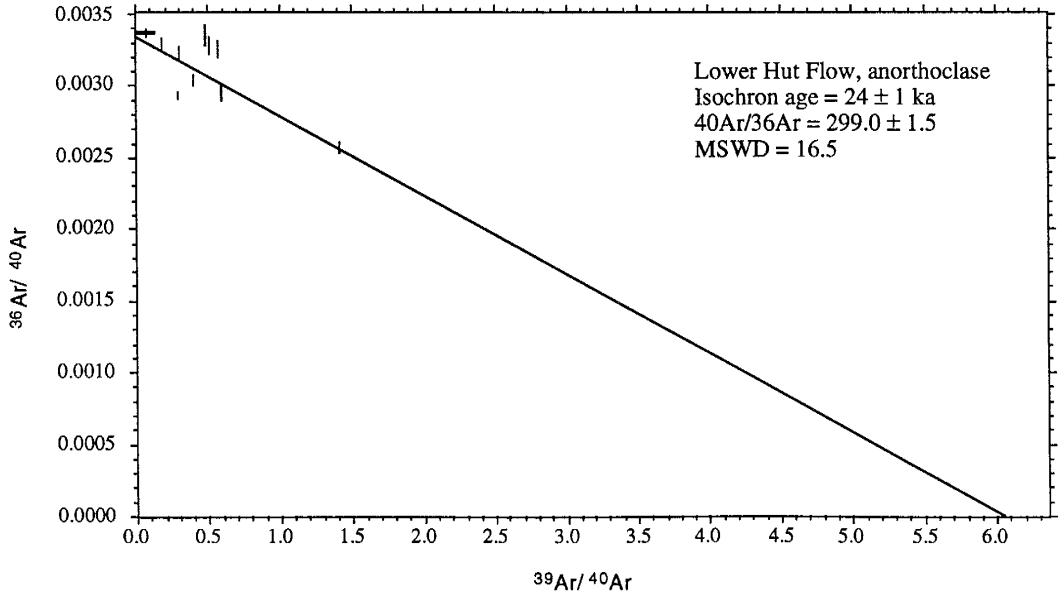
0.0035
0.0030
0.0025
0.0020
0.0015
0.0010
0.0005
0.0000
36Ar/ 40Ar
Lower Hut Flow, anorthoclase
Isochron age = 24 ± 1 ka
40Ar/36Ar = 299.0 ± 1.5
MSWD = 16.5
0.0
0.5
1.0
1.5
2.0
2.5
3.0
3.5
4.0
4.5
5.0
5.5
6.0
39Ar/ 40Ar

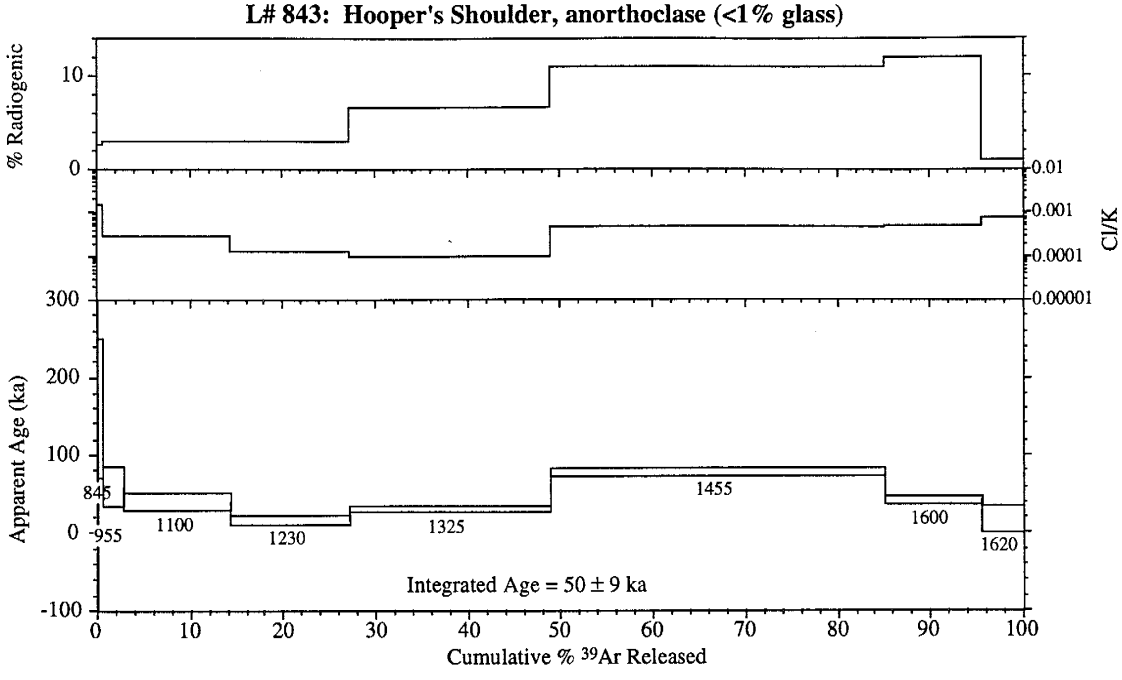
L# 843: Hooper's Shoulder, anorthoclase (<1% glass)
% Radiogenic
10
0
0.01
0.001
0.0001
0.00001
Cl/K
300
200
100
0
-100
Apparent Age (ka)
845
955
1100
1230
1325
1455
1600
1620
Integrated Age = 50 ± 9 ka
0
10
20
30
40
50
60
70
80
90
100
Cumulative % 39Ar Released

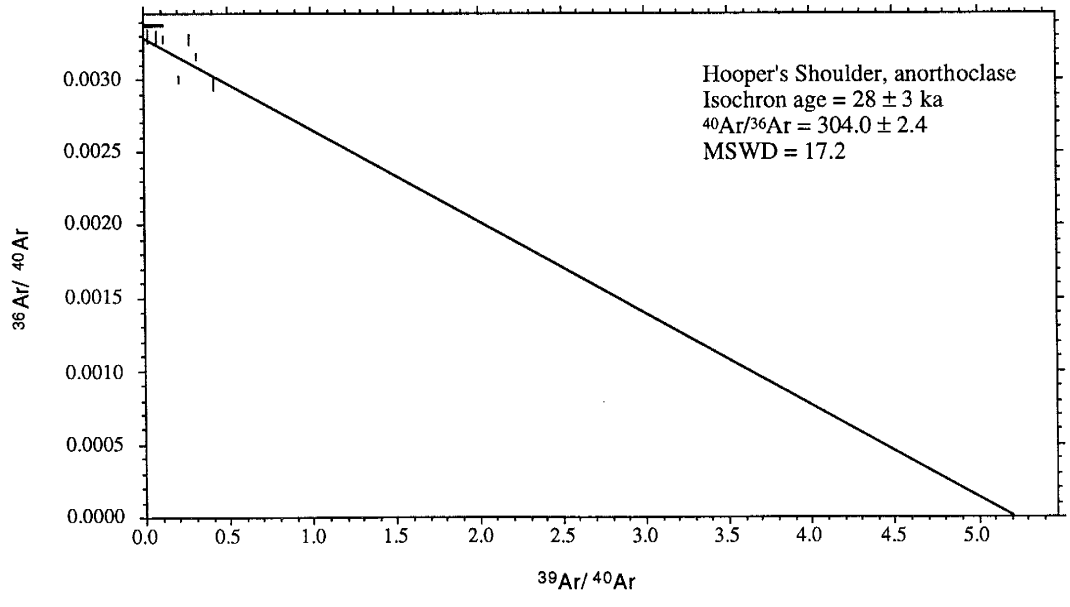
Hooper's Shoulder, anorthoclase
Isochron age = 28 ± 3 ka
40Ar/36Ar = 304.0 ± 2.4
MSWD = 17.2
36Ar/ 40Ar
0.0030
0.0025
0.0020
0.0015
0.0010
0.0005
0.0000
0.0
0.5
1.0
1.5
2.0
2.5
3.0
3.5
4.0
4.5
5.0
39Ar/ 40Ar

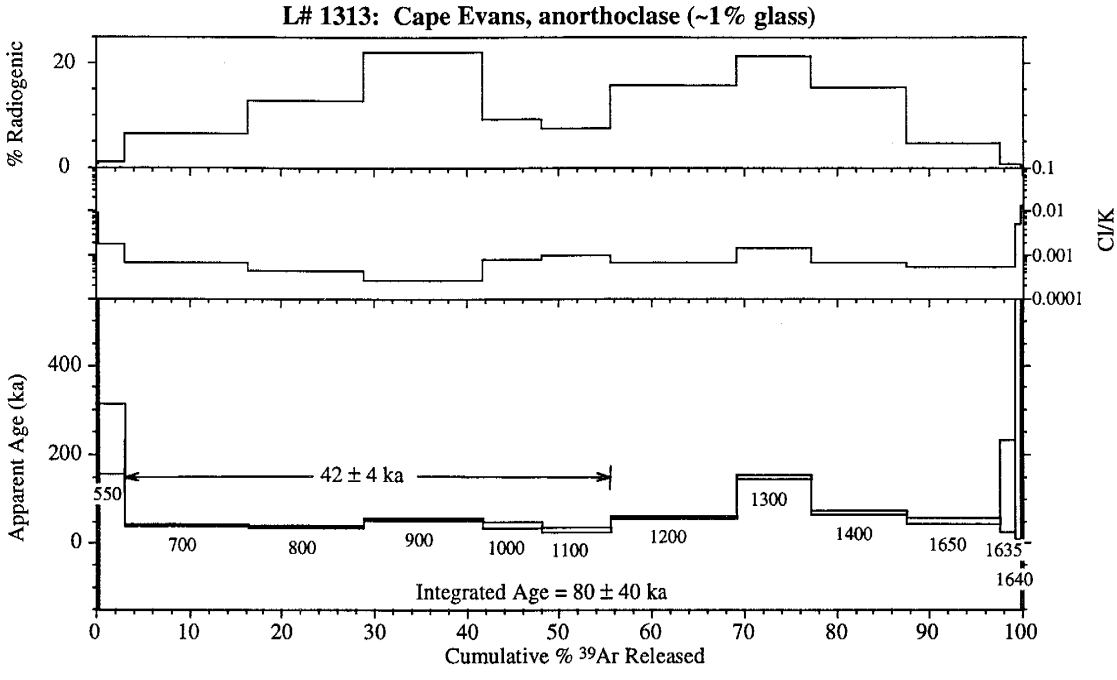
L# 1313: Cape Evans, anorthoclase (~1% glass)
% Radiogenic
20
0
0.1
0.01
0.001
0.0001
Cl/K
400
200
0
Apparent Age (ka)
42 ± 4 ka
550
700
800
900
1000
1100
1200
1300
1400
1650
1635
1640
Integrated Age = 80 ± 40 ka
0
10
20
30
40
50
60
70
80
90
100
Cumulative % 39Ar Released

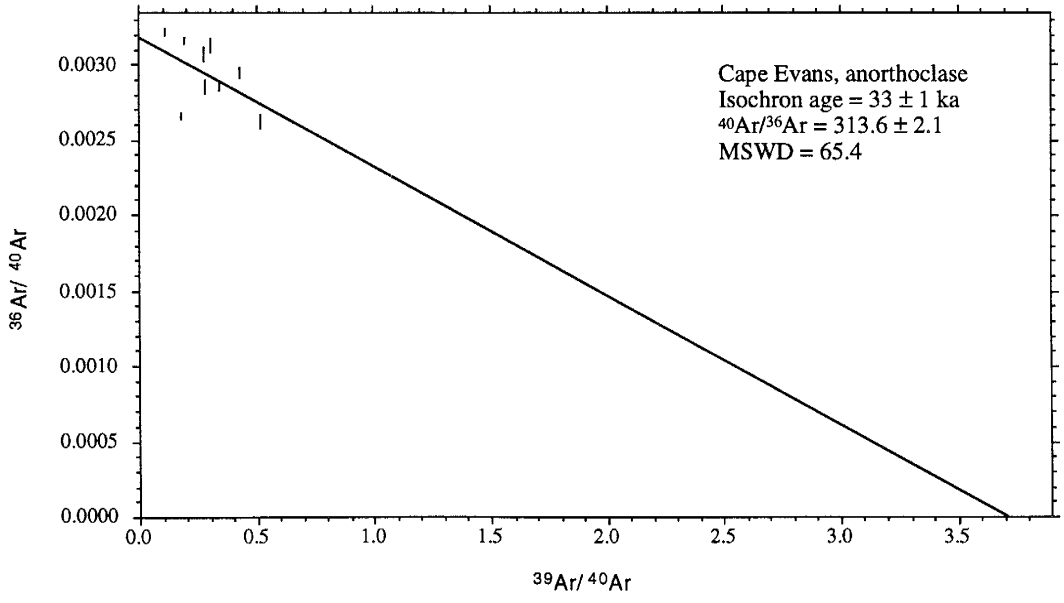
Cape Evans, anorthoclase
Isochron age = 33 ± 1 ka
40Ar/36Ar = 313.6 ± 2.1
MSWD = 65.4
0.0030
0.0025
0.0020
0.0015
0.0010
0.0005
0.0000
36Ar/ 40Ar
0.0
0.5
1.0
1.5
2.0
2.5
3.0
3.5
39Ar/ 40Ar

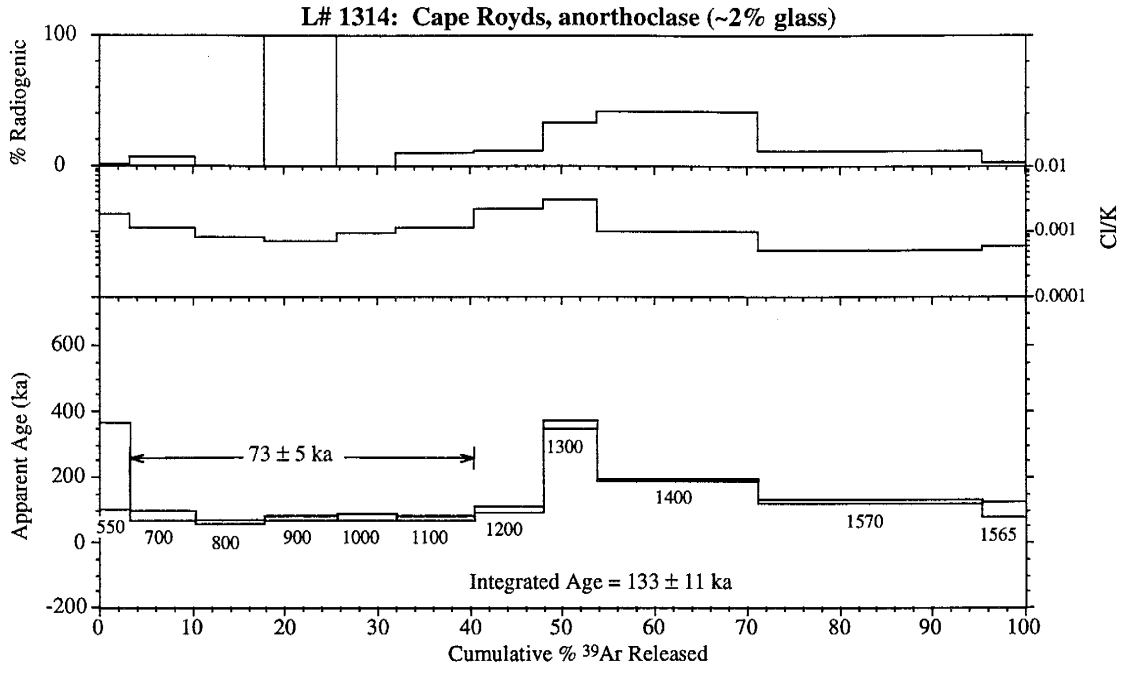
L# 1314: Cape Royds, anorthoclase (~2% glass)
% Radiogenic
100
0
0.01
0.001
0.0001
Cl/K
Apparent Age (ka)
600
400
200
0
-200
73 ± 5 ka
550
700
800
900
1000
1100
1200
1300
1400
1570
1565
Integrated Age = 133 ± 11 ka
0
10
20
30
40
50
60
70
80
90
100
Cumulative % 39Ar Released

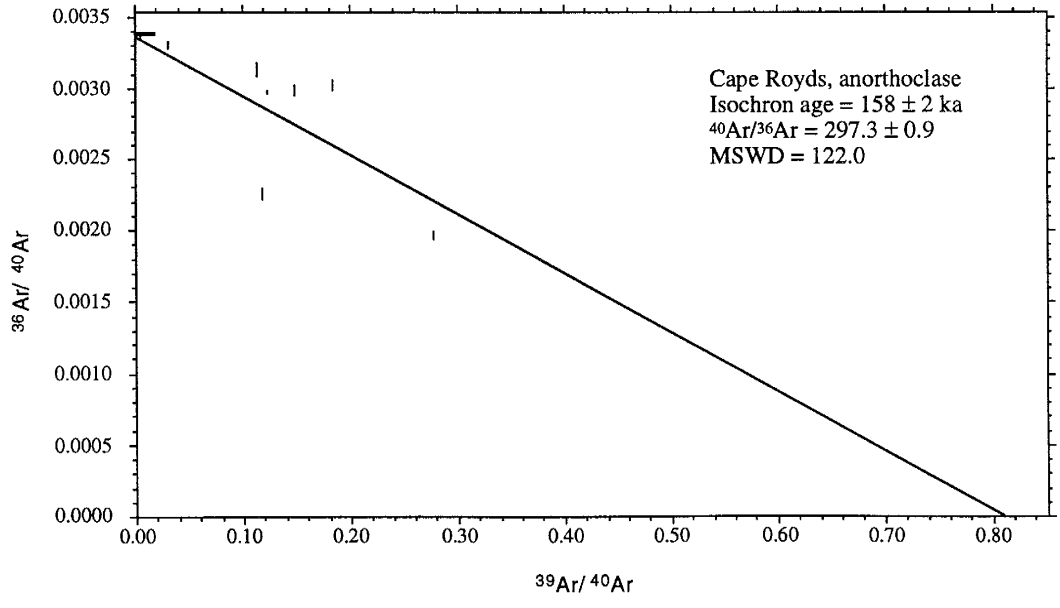
0.0035
0.0030
0.0025
0.0020
0.0015
0.0010
0.0005
0.0000
36Ar/ 40Ar
Cape Royds, anorthoclase
Isochron age = 158 ± 2 ka
40Ar/36Ar = 297.3 ± 0.9
MSWD = 122.0
0.00
0.10
0.20
0.30
0.40
0.50
0.60
0.70
0.80
39Ar/ 40Ar

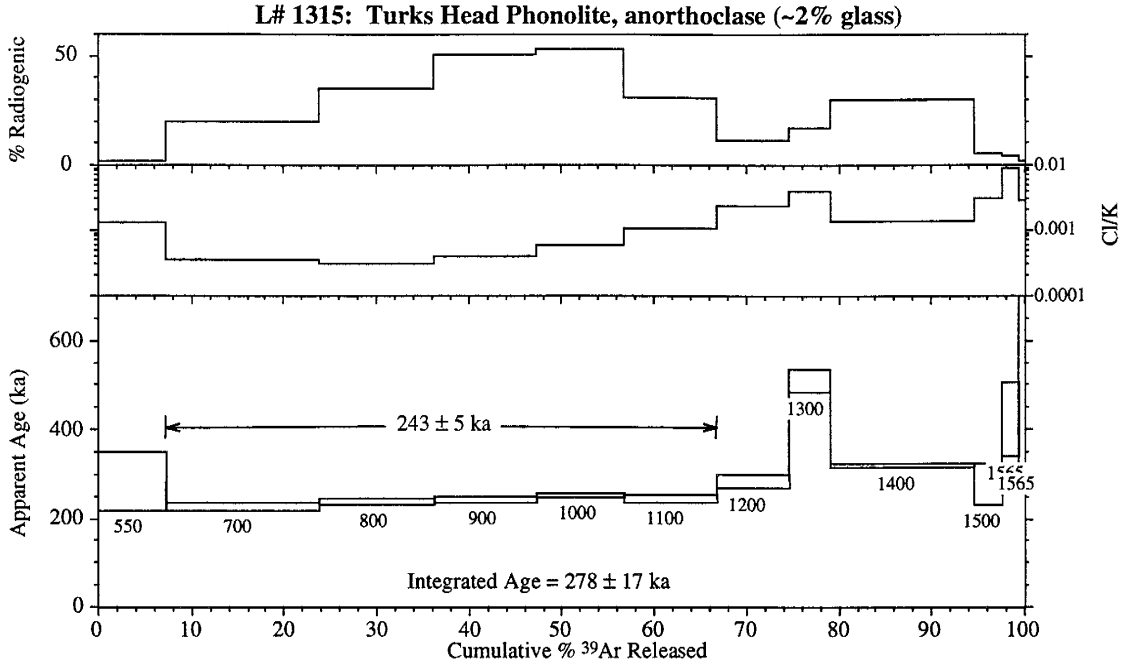
L# 1315: Turks Head Phonolite, anorthoclase (~2% glass)
% Radiogenic
50
0
0.01
0.001
0.0001
Cl/K
600
400
200
0
Apparent Age (ka)
243 ± 5 ka
1300
1400
1565
550
700
800
900
1000
1100
1200
1500
Integrated Age = 278 ± 17 ka
0
10
20
30
40
50
60
70
80
90
100
Cumulative % 39Ar Released

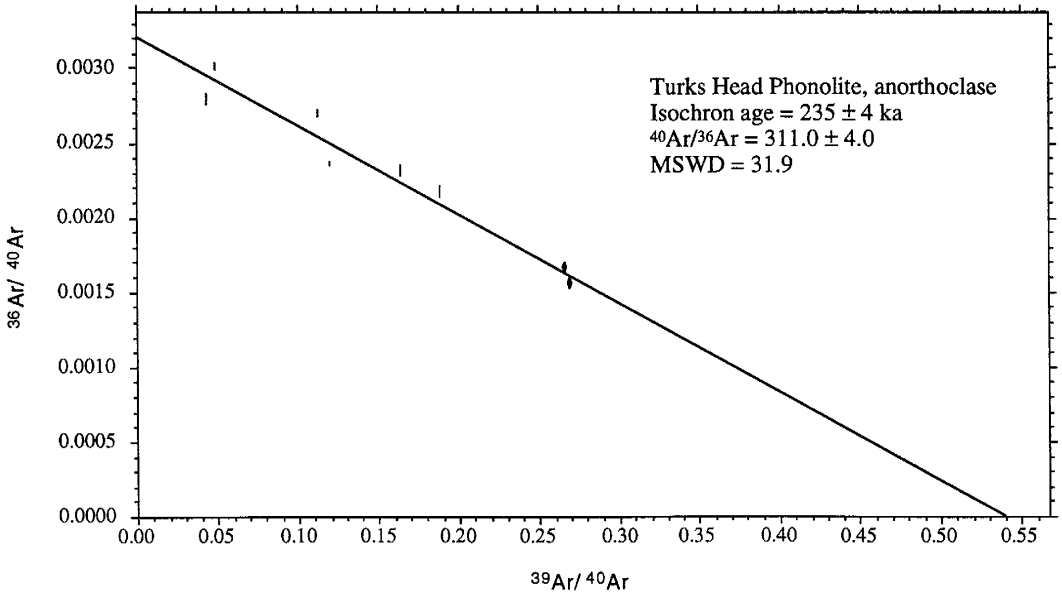
Turks Head Phonolite, anorthoclase
Isochron age = 235 ± 4 ka
40Ar/36Ar = 311.0 ± 4.0
MSWD = 31.9
36Ar/ 40Ar
0.0030
0.0025
0.0020
0.0015
0.0010
0.0005
0.0000
0.00
0.05
0.10
0.15
0.20
0.25
0.30
0.35
0.40
0.45
0.50
0.55
39Ar/ 40Ar

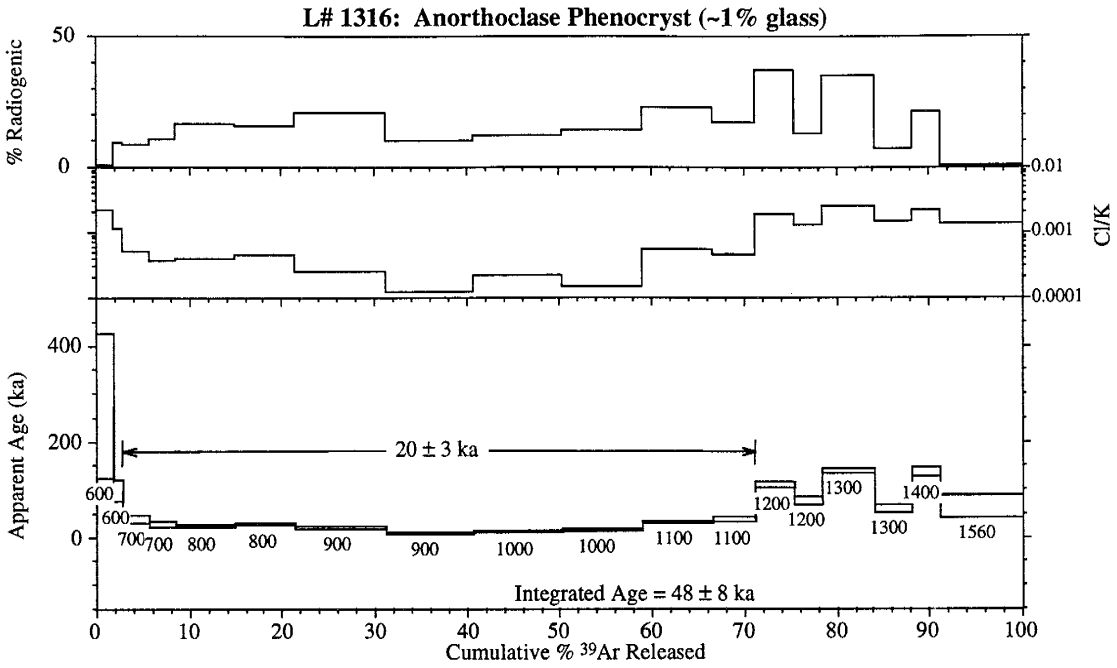
L# 1316: Anorthoclase Phenocryst (~1% glass)
% Radiogenic
50
0
0.01
0.001
0.0001
Cl/K
Apparent Age (ka)
400
200
0
20 ± 3 ka
600
600
700
700
800
800
900
900
1000
1000
1100
1100
1200
1200
1300
1300
1400
1560
Integrated Age = 48 ± 8 ka
0
10
20
30
40
50
60
70
80
90
100
Cumulative % 39Ar Released

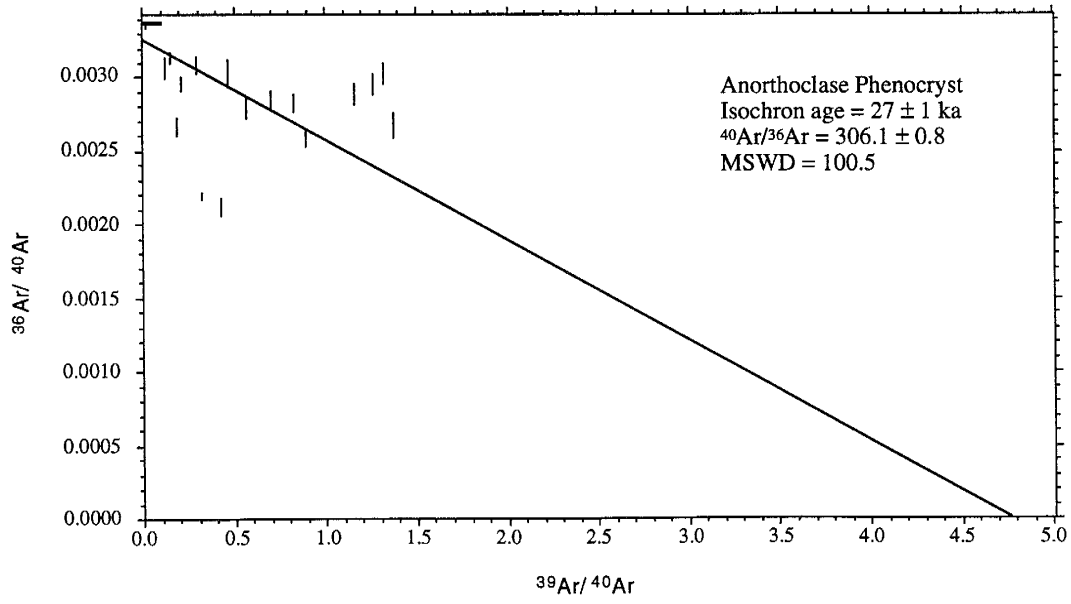
Anorthoclase Phenocryst
Isochron age = 27 ± 1 ka
40Ar/36Ar = 306.1 ± 0.8
MSWD = 100.5
36Ar/ 40Ar
0.0030
0.0025
0.0020
0.0015
0.0010
0.0005
0.0000
0.0
0.5
1.0
1.5
2.0
2.5
3.0
3.5
4.0
4.5
5.0
39Ar/ 40Ar

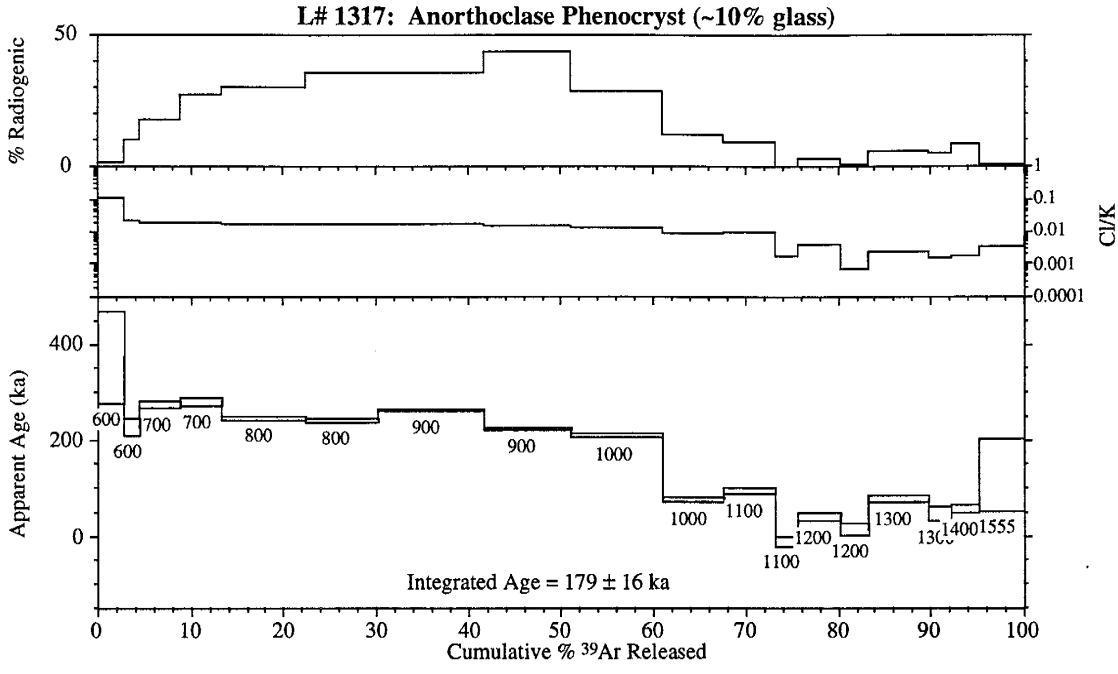
L# 1317: Anorthoclase Phenocryst (~10% glass)
% Radiogenic
50
0
Cl/K
1
0.1
0.01
0.001
0.0001
Apparent Age (ka)
400
200
0
600
600
700
700
800
800
900
900
1000
1000
1100
1100
1200
1200
1300
1400
1555
Integrated Age = 179 ± 16 ka
0
10
20
30
40
50
60
70
80
90
100
Cumulative % 39Ar Released

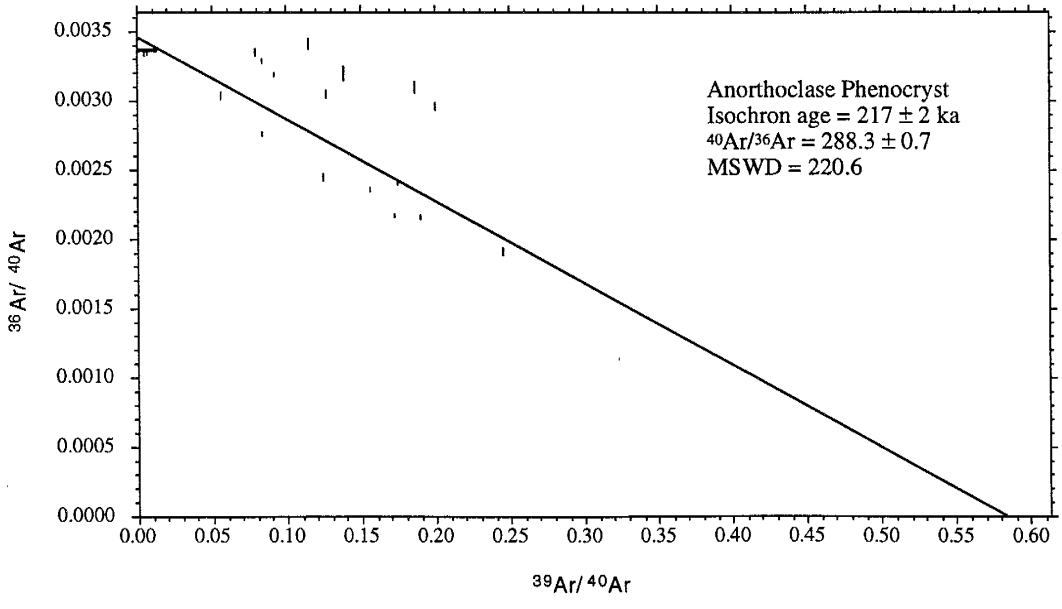
Anorthoclase Phenocryst
Isochron age = 217 ± 2 ka
40Ar/36Ar = 288.3 ± 0.7
MSWD = 220.6
36Ar/ 40Ar
0.0035
0.0030
0.0025
0.0020
0.0015
0.0010
0.0005
0.0000
0.00
0.05
0.10
0.15
0.20
0.25
0.30
0.35
0.40
0.45
0.50
0.55
0.60
39Ar/ 40Ar

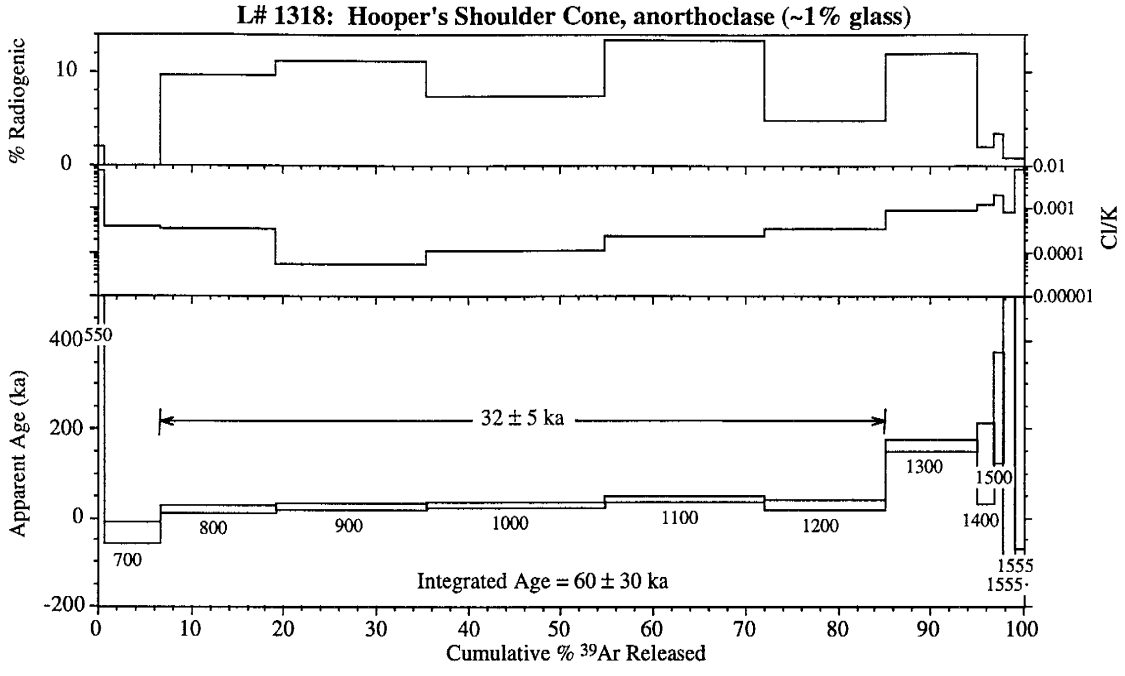
L# 1318: Hooper's Shoulder Cone, anorthoclase (~1% glass)
% Radiogenic
10
0
0.01
0.001
0.0001
0.00001
Cl/K
400
200
0
-200
Apparent Age (ka)
550
32 ± 5 ka
1300
1500
1400
800
900
1000
1100
1200
700
1555
1555
Integrated Age = 60 ± 30 ka
0
10
20
30
40
50
60
70
80
90
100
Cumulative % 39Ar Released

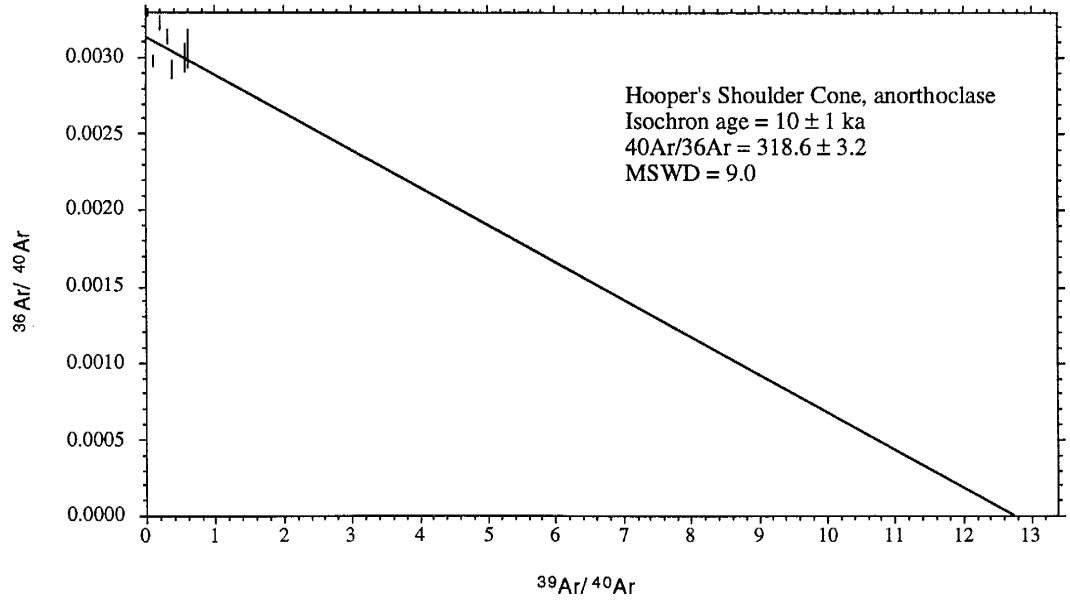
Hooper's Shoulder Cone, anorthoclase
Isochron age = 10 ± 1 ka
40Ar/36Ar = 318.6 ± 3.2
MSWD = 9.0
36Ar/ 40Ar
0.0030
0.0025
0.0020
0.0015
0.0010
0.0005
0.0000
0
1
2
3
4
5
6
7
8
9
10
11
12
13
39Ar/ 40Ar

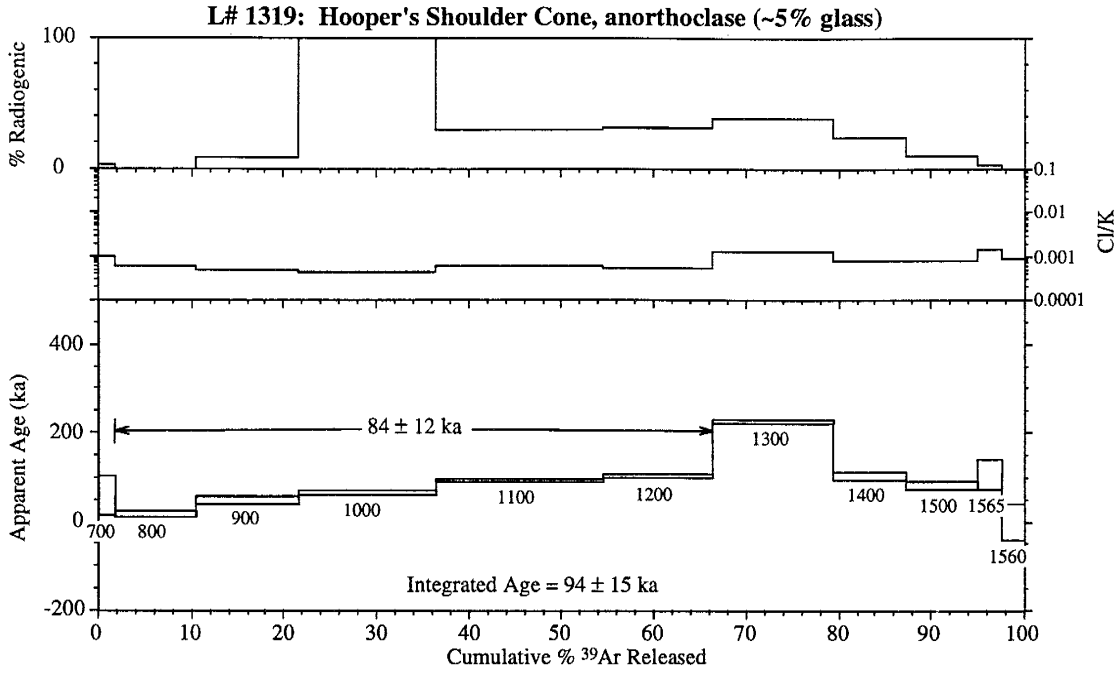
L# 1319: Hooper's Shoulder Cone, anorthoclase (~5% glass)
% Radiogenic
100
0
Cl/K
0.1
0.01
0.001
0.0001
Apparent Age (ka)
400
200
0
-200
84 ± 12 ka
700
800
900
1000
1100
1200
1300
1400
1500
1565
1560
Integrated Age = 94 ± 15 ka
0
10
20
30
40
50
60
70
80
90
100
Cumulative % 39Ar Released

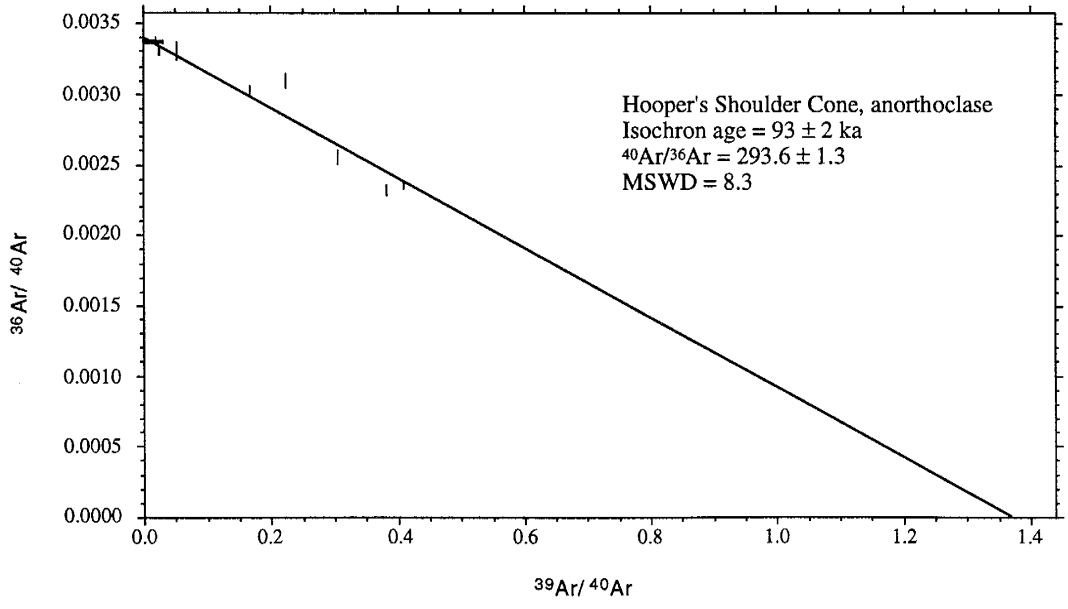
Hooper's Shoulder Cone, anorthoclase
Isochron age = 93 ± 2 ka
40Ar/36Ar = 293.6 ± 1.3
MSWD = 8.3
36Ar/ 40Ar
0.0035
0.0030
0.0025
0.0020
0.0015
0.0010
0.0005
0.0000
0.0
0.2
0.4
0.6
0.8
1.0
1.2
1.4
39Ar/ 40Ar

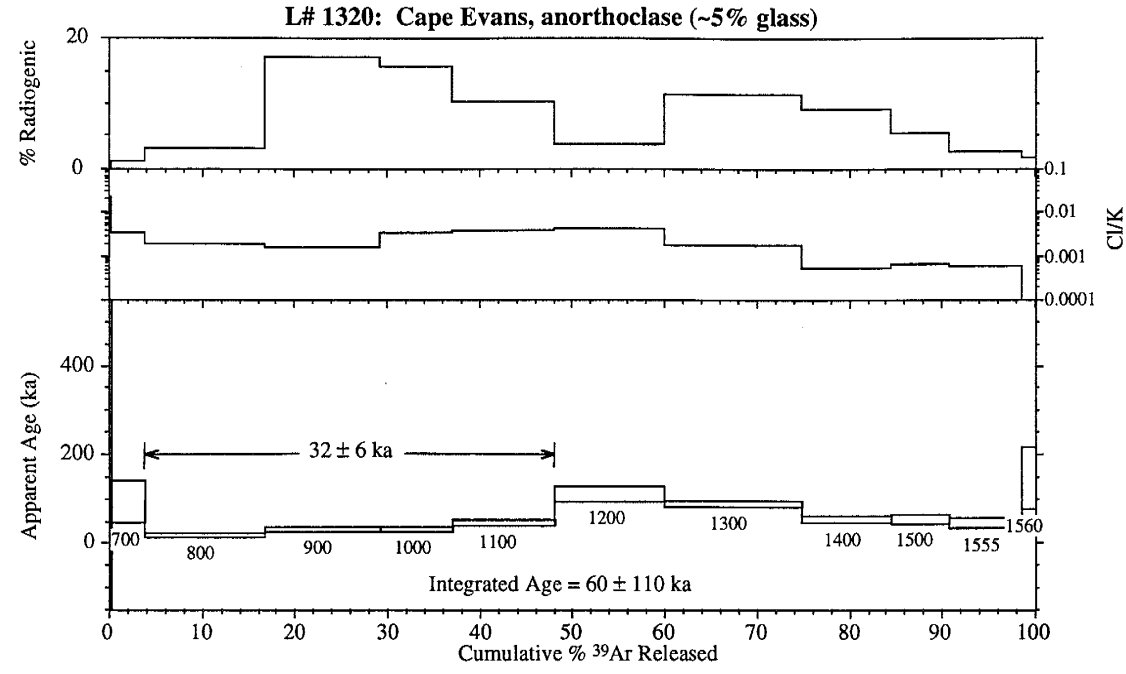
L# 1320: Cape Evans, anorthoclase (~5% glass)
% Radiogenic
20
0
0.1
0.01
0.001
0.0001
Cl/K
Apparent Age (ka)
400
200
0
32 ± 6 ka
700
800
900
1000
1100
1200
1300
1400
1500
1555
1560
Integrated Age = 60 ± 110 ka
0
10
20
30
40
50
60
70
80
90
100
Cumulative % 39Ar Released

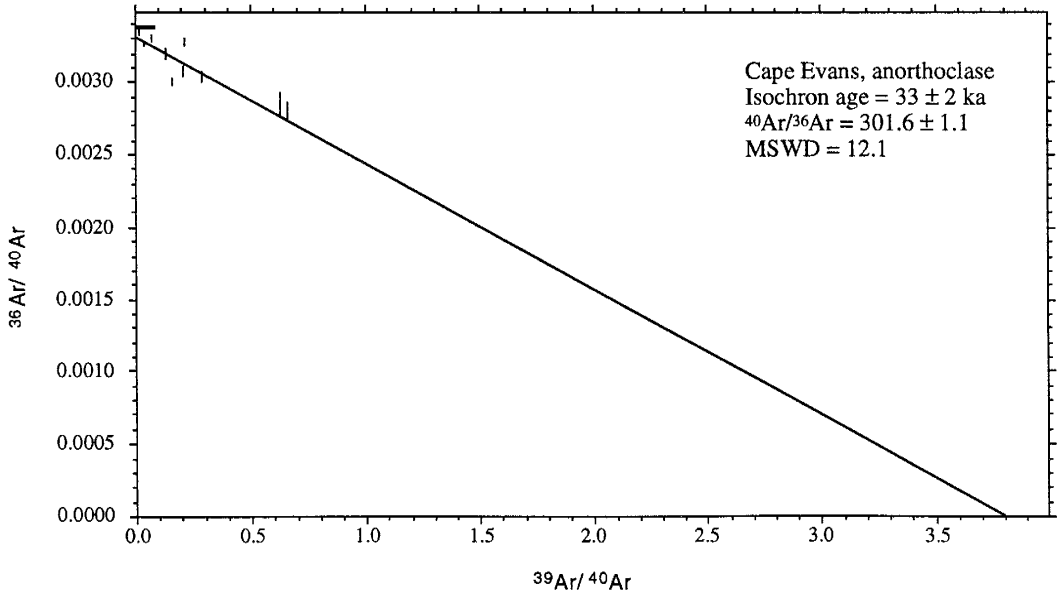
Cape Evans, anorthoclase
Isochron age = 33 ± 2 ka
40Ar/36Ar = 301.6 ± 1.1
MSWD = 12.1
36Ar/ 40Ar
0.0030
0.0025
0.0020
0.0015
0.0010
0.0005
0.0000
0.0
0.5
1.0
1.5
2.0
2.5
3.0
3.5
39Ar/ 40Ar

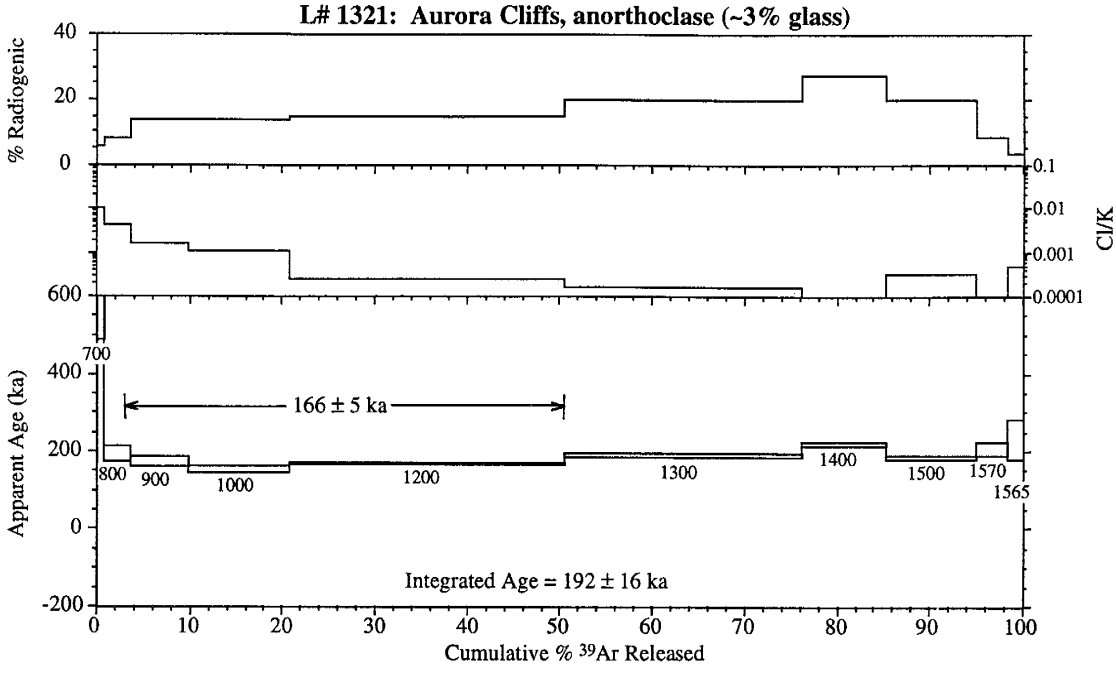
L# 1321: Aurora Cliffs, anorthoclase (~3% glass)
% Radiogenic
40
20
0
0.1
0.01
0.001
0.0001
Cl/K
600
700
400
200
0
-200
Apparent Age (ka)
166 ± 5 ka
800
900
1000
1200
1300
1400
1500
1570
1565
Integrated Age = 192 ± 16 ka
0
10
20
30
40
50
60
70
80
90
100
Cumulative % 39Ar Released

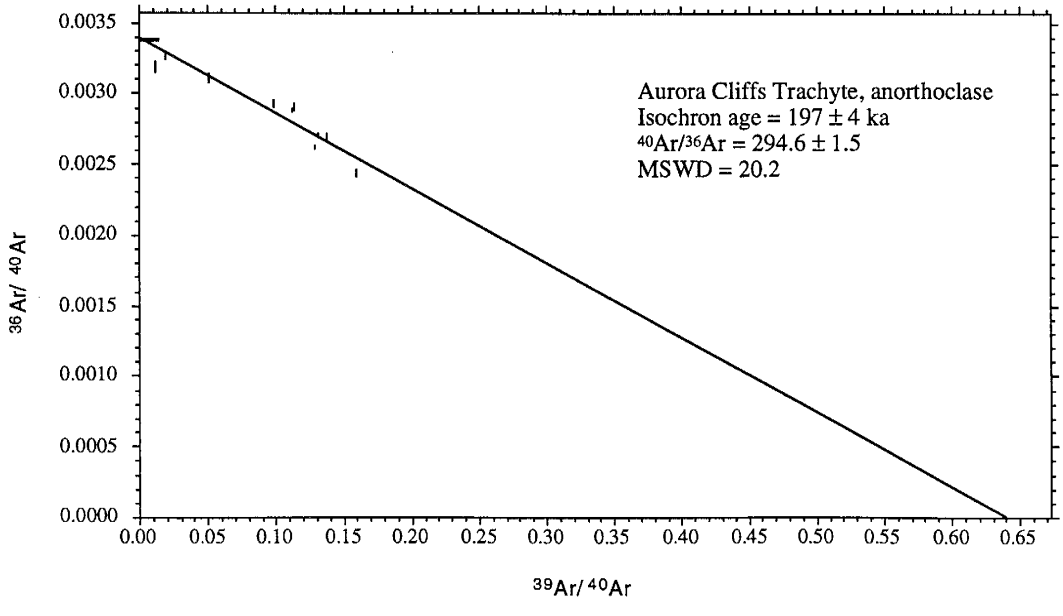
Aurora Cliffs Trachyte, anorthoclase
Isochron age = 197 ± 4 ka
40Ar/36Ar = 294.6 ± 1.5
MSWD = 20.2
0.0035
0.0030
0.0025
0.0020
0.0015
0.0010
0.0005
0.0000
36Ar/ 40Ar
0.00
0.05
0.10
0.15
0.20
0.25
0.30
0.35
0.40
0.45
0.50
0.55
0.60
0.65
39Ar/40Ar

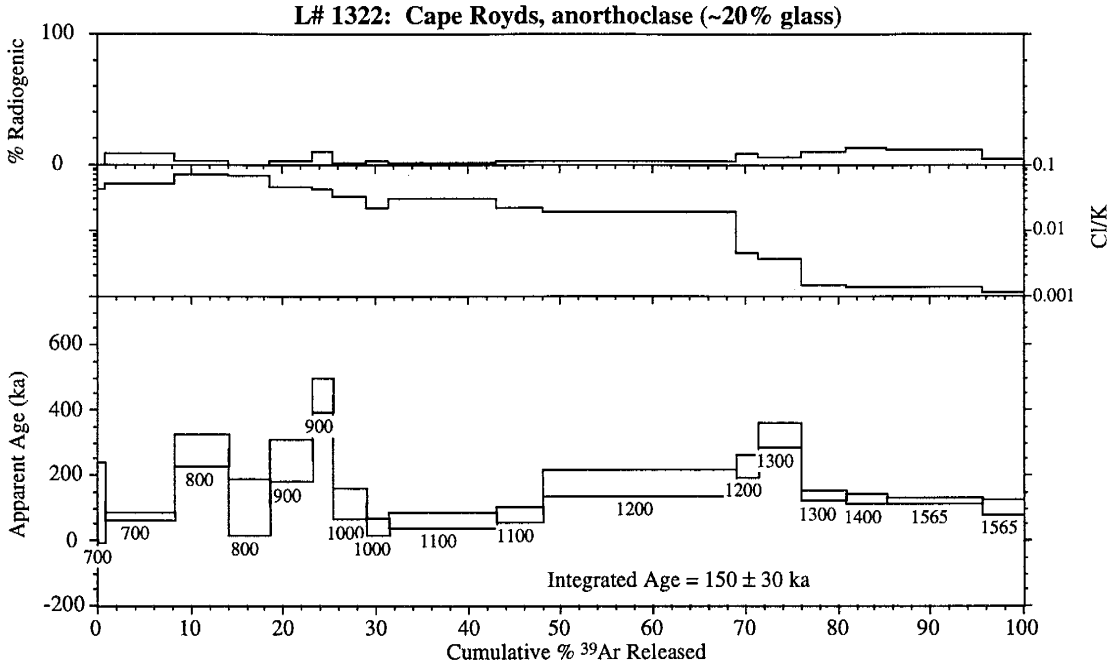
L# 1322: Cape Royds, anorthoclase (~20% glass)
% Radiogenic
100
0
0.1
0.01
0.001
Cl/K
Apparent Age (ka)
600
400
200
0
-200
700
800
900
1000
1100
1200
1300
1400
1565
Integrated Age = 150 ± 30 ka
0
10
20
30
40
50
60
70
80
90
100
Cumulative % 39Ar Released

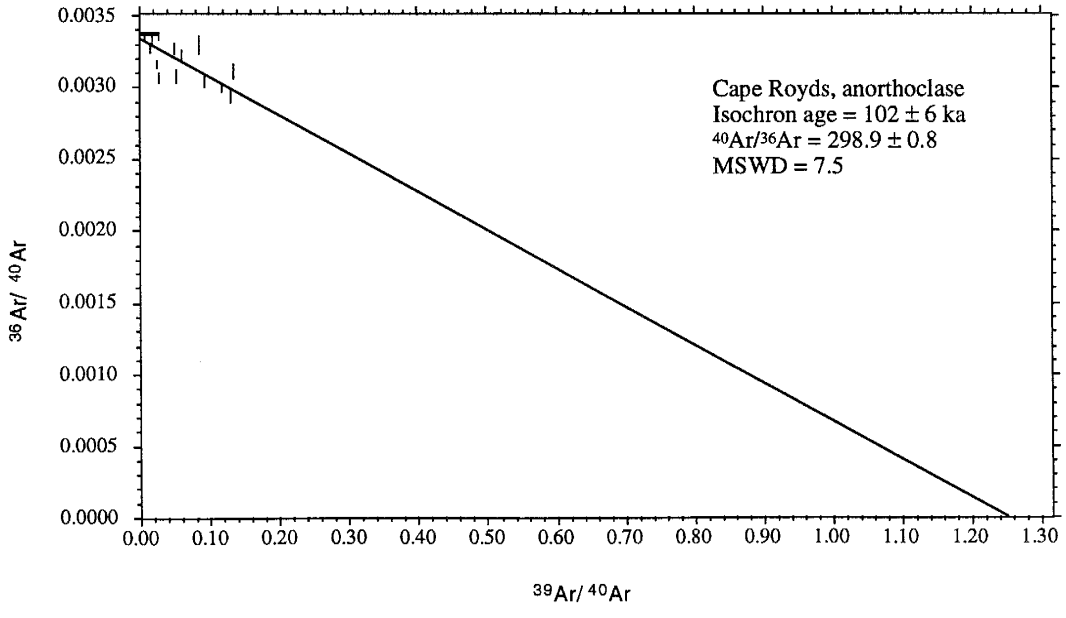
Cape Royds, anorthoclase
Isochron age = 102 ± 6 ka
40Ar/36Ar = 298.9 ± 0.8
MSWD = 7.5
36Ar/ 40Ar
0.0035
0.0030
0.0025
0.0020
0.0015
0.0010
0.0005
0.0000
0.00
0.10
0.20
0.30
0.40
0.50
0.60
0.70
0.80
0.90
1.00
1.10
1.20
1.30
39Ar/ 40Ar

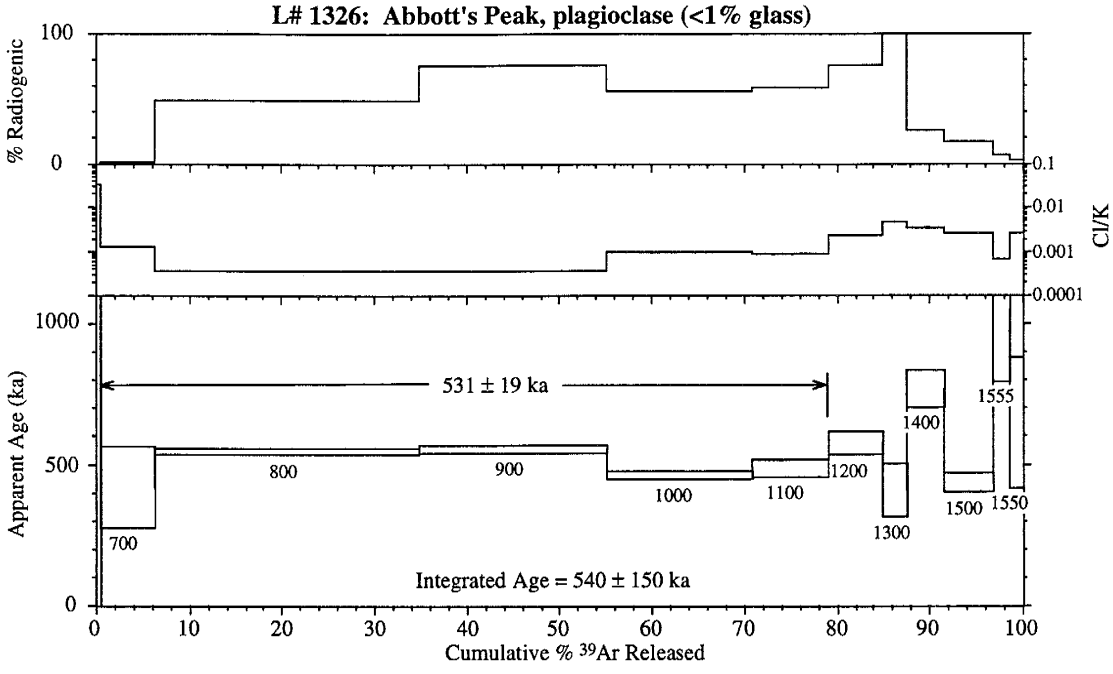
L# 1326: Abbott's Peak, plagioclase (<1% glass)
% Radiogenic
100
0
0.1
0.01
0.001
0.0001
Cl/K
1000
500
0
Apparent Age (ka)
531 ± 19 ka
700
800
900
1000
1100
1200
1300
1400
1500
1555
1550
Integrated Age = 540 ± 150 ka
0
10
20
30
40
50
60
70
80
90
100
Cumulative % 39Ar Released

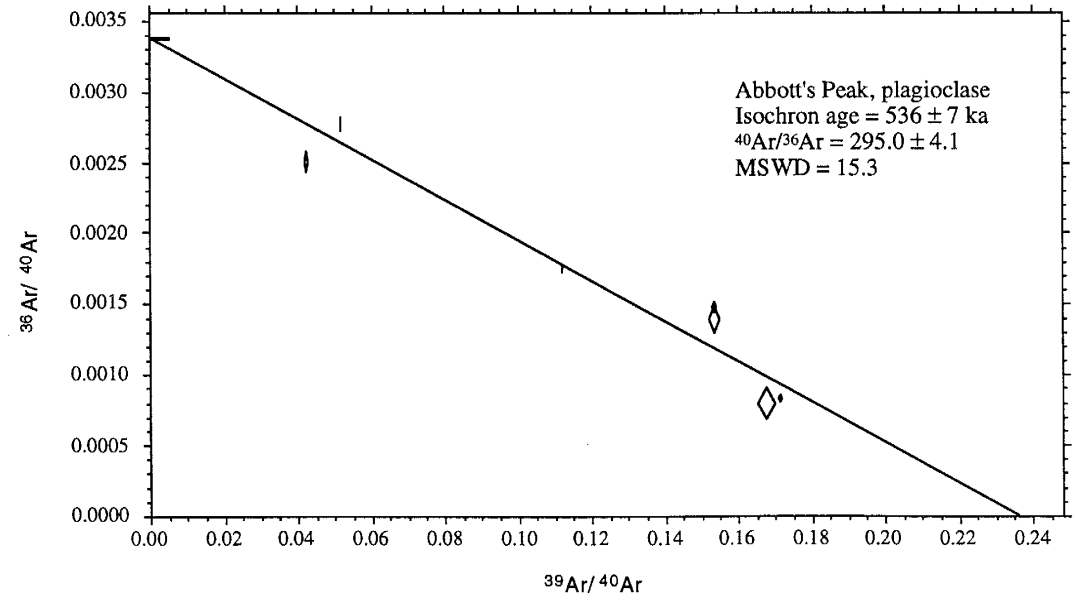
Abbott's Peak, plagioclase
Isochron age = 536 ± 7 ka
40Ar/36Ar = 295.0 ± 4.1
MSWD = 15.3
36Ar/ 40Ar
0.0035
0.0030
0.0025
0.0020
0.0015
0.0010
0.0005
0.0000
0.00
0.02
0.04
0.06
0.08
0.10
0.12
0.14
0.16
0.18
0.20
0.22
0.24
39Ar/ 40Ar

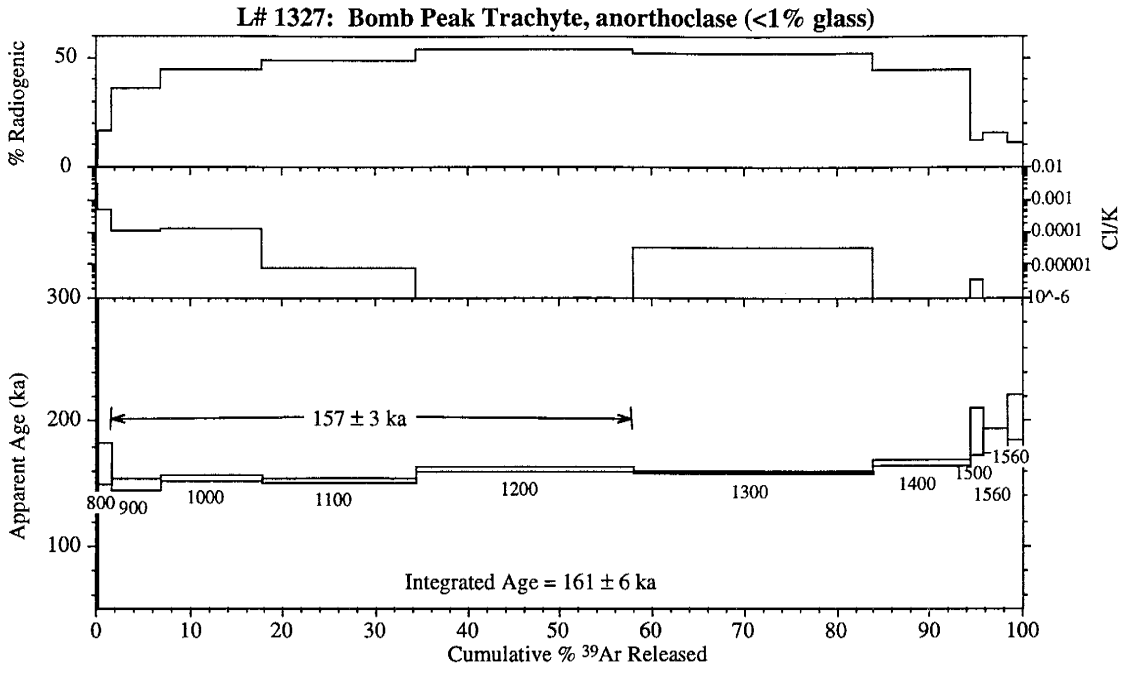
L# 1327: Bomb Peak Trachyte, anorthoclase (<1% glass)
% Radiogenic
50
0
0.01
0.001
0.0001
0.00001
10^-6
Cl/K
300
200
100
Apparent Age (ka)
157 ± 3 ka
800
900
1000
1100
1200
1300
1400
1500
1560
1560
Integrated Age = 161 ± 6 ka
0
10
20
30
40
50
60
70
80
90
100
Cumulative % 39Ar Released

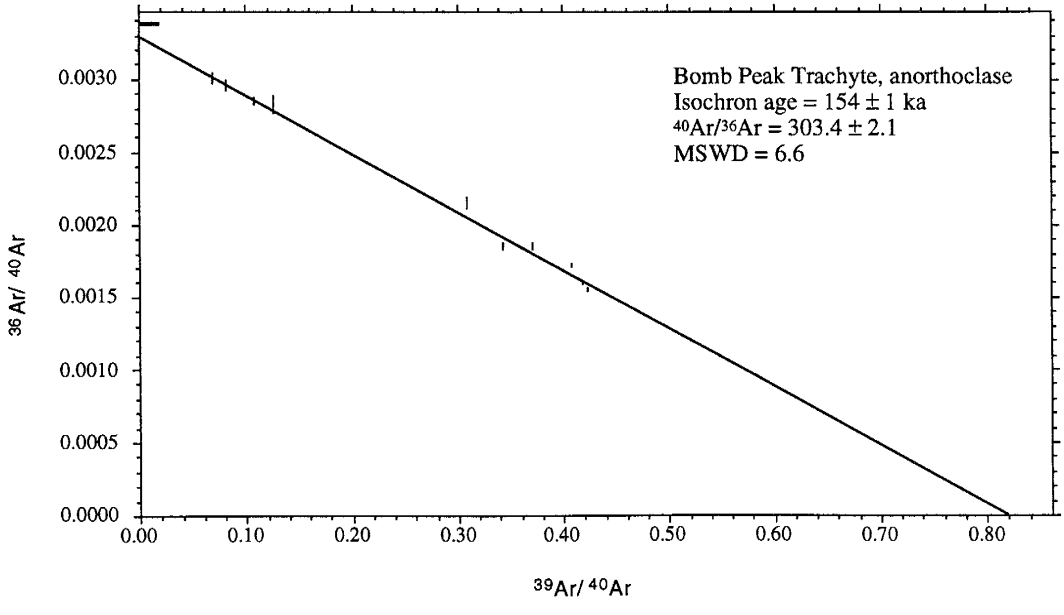
Bomb Peak Trachyte, anorthoclase
Isochron age = 154 ± 1 ka
40Ar/36Ar = 303.4 ± 2.1
MSWD = 6.6
0.0030
0.0025
0.0020
0.0015
0.0010
0.0005
0.0000
36Ar/ 40Ar
0.00
0.10
0.20
0.30
0.40
0.50
0.60
0.70
0.80
39Ar/ 40Ar

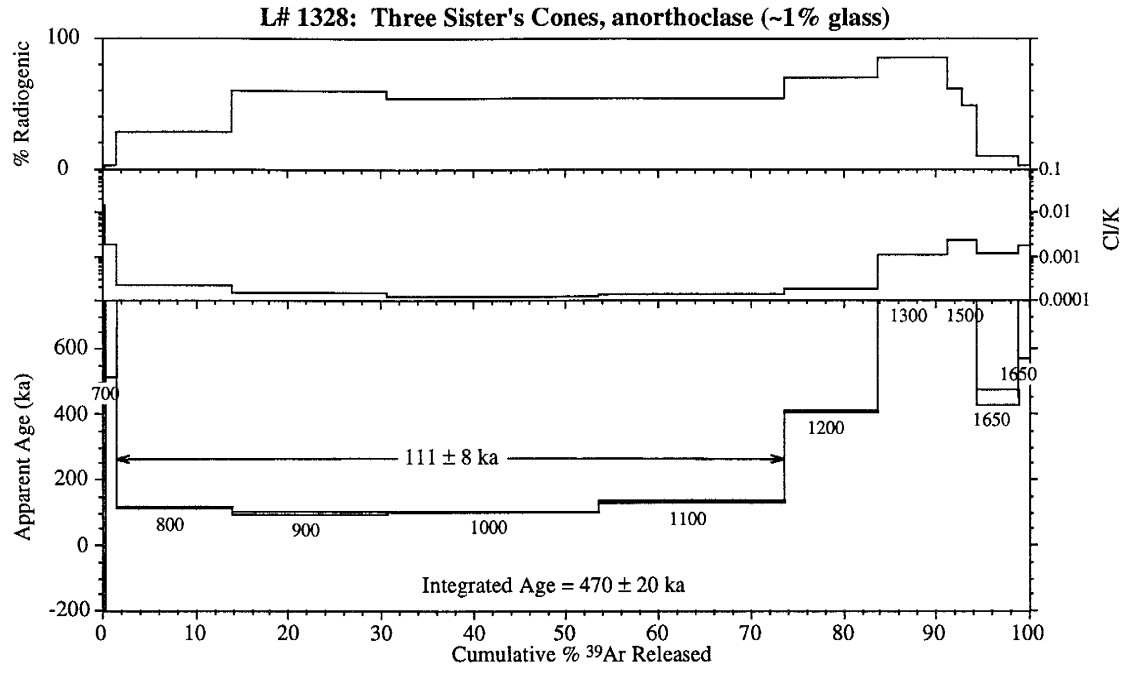
L# 1328: Three Sister's Cones, anorthoclase (~1% glass)
% Radiogenic
100
0
0.1
0.01
0.001
0.0001
Cl/K
600
400
200
0
-200
Apparent Age (ka)
700
800
900
1000
1100
1200
1300
1500
1650
1650
111 ± 8 ka
Integrated Age = 470 ± 20 ka
0
10
20
30
40
50
60
70
80
90
100
Cumulative % 39Ar Released

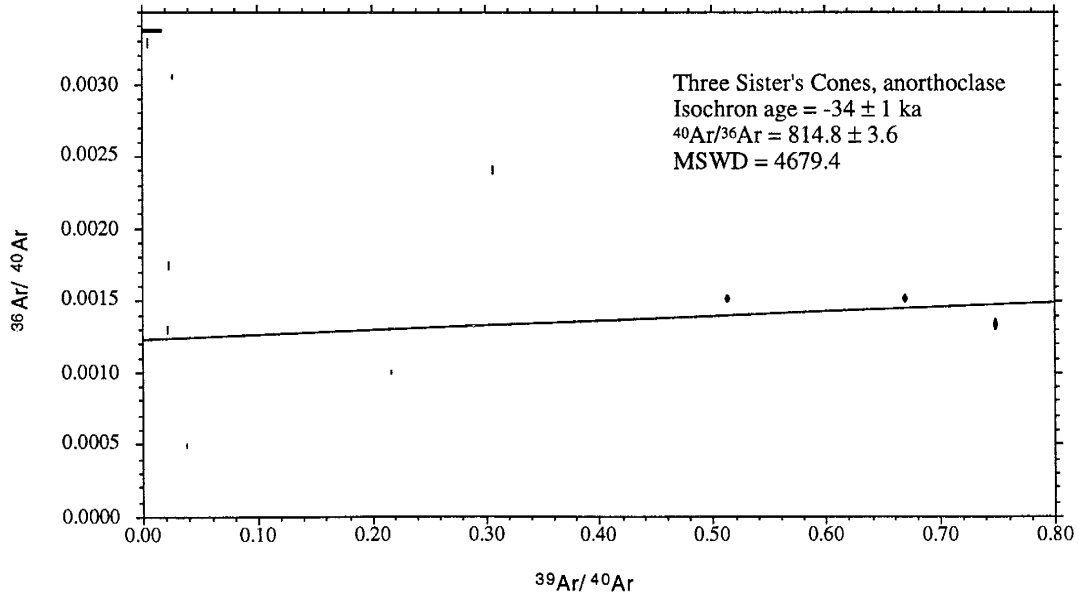
Three Sister's Cones, anorthoclase
Isochron age = -34 ± 1 ka
40Ar/36Ar = 814.8 ± 3.6
MSWD = 4679.4
0.0030
0.0025
0.0020
0.0015
0.0010
0.0005
0.0000
36Ar/ 40Ar
0.00
0.10
0.20
0.30
0.40
0.50
0.60
0.70
0.80
39Ar/ 40Ar

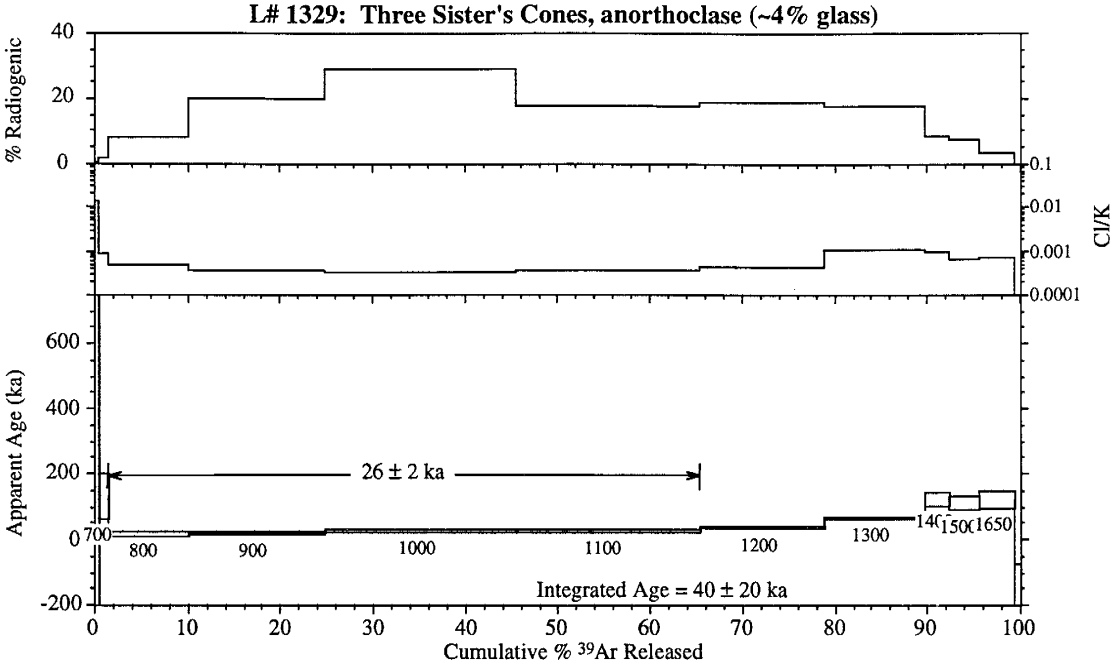
L# 1329: Three Sister's Cones, anorthoclase (~4% glass)
% Radiogenic
Cl/K
Apparent Age (ka)
26 ± 2 ka
Integrated Age = 40 ± 20 ka
Cumulative % 39Ar Released

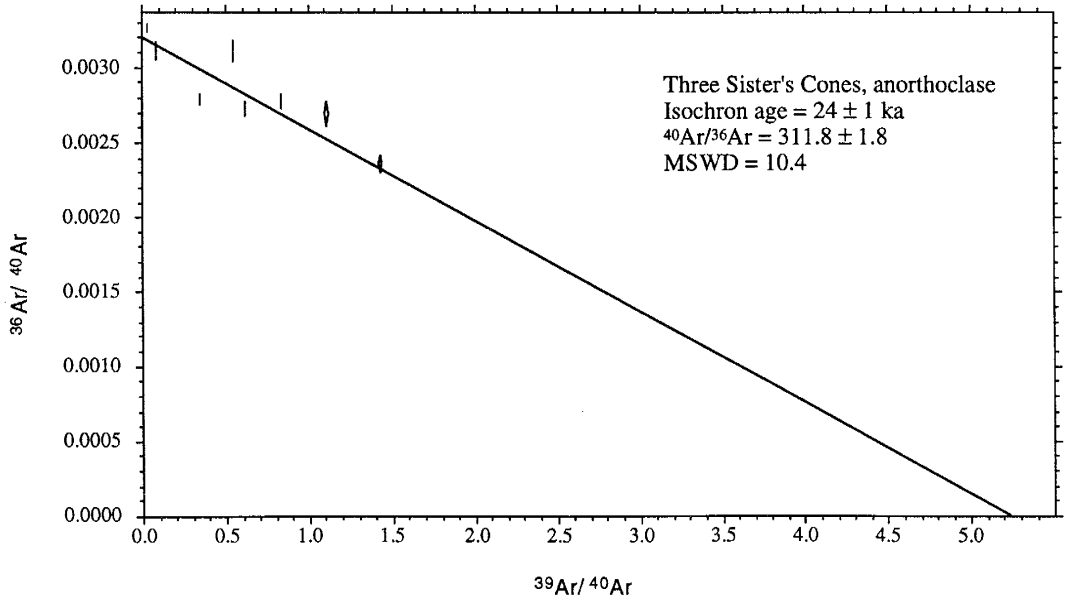
Three Sister's Cones, anorthoclase
Isochron age = 24 ± 1 ka
40Ar/36Ar = 311.8 ± 1.8
MSWD = 10.4
36Ar/ 40Ar
39Ar/ 40Ar

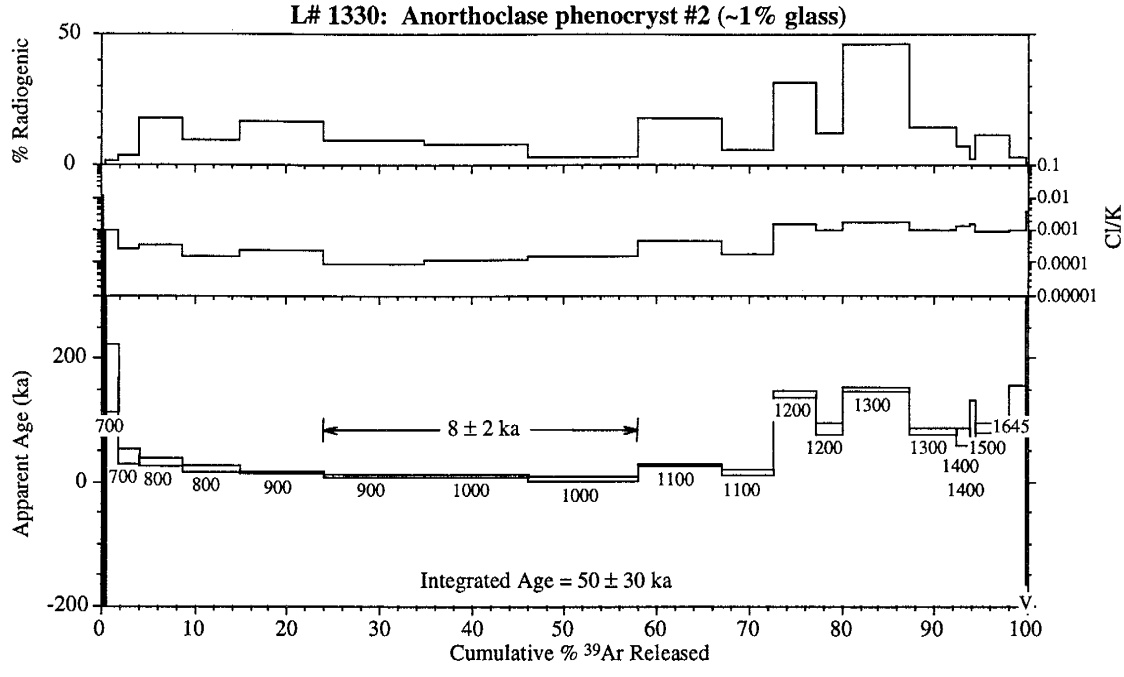
L# 1330: Anorthoclase phenocryst #2 (~1% glass)
% Radiogenic
50
0
0.1
0.01
0.001
0.0001
0.00001
Cl/K
200
0
-200
Apparent Age (ka)
700
700 800
800
900
900
1000
1000
1100
1100
1200
1200
1300
1300
1400
1400
1500
1645
8 ± 2 ka
Integrated Age = 50 ± 30 ka
0
10
20
30
40
50
60
70
80
90
100
Cumulative % 39Ar Released

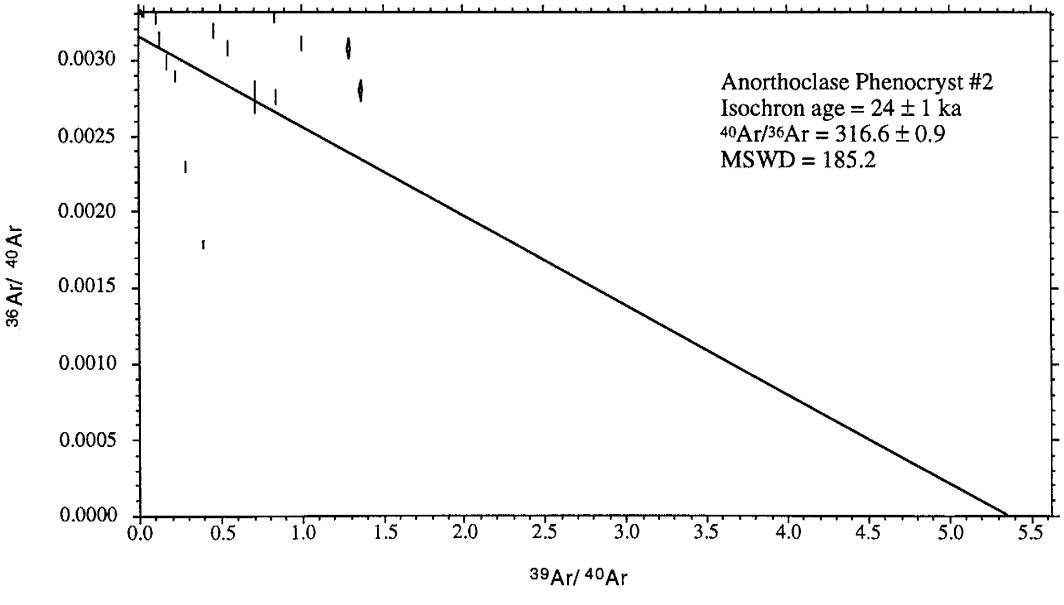
Anorthoclase Phenocryst #2
Isochron age = 24 ± 1 ka
40Ar/36Ar = 316.6 ± 0.9
MSWD = 185.2
36Ar/ 40Ar
0.0030
0.0025
0.0020
0.0015
0.0010
0.0005
0.0000
0.0
0.5
1.0
1.5
2.0
2.5
3.0
3.5
4.0
4.5
5.0
5.5
39Ar/ 40Ar

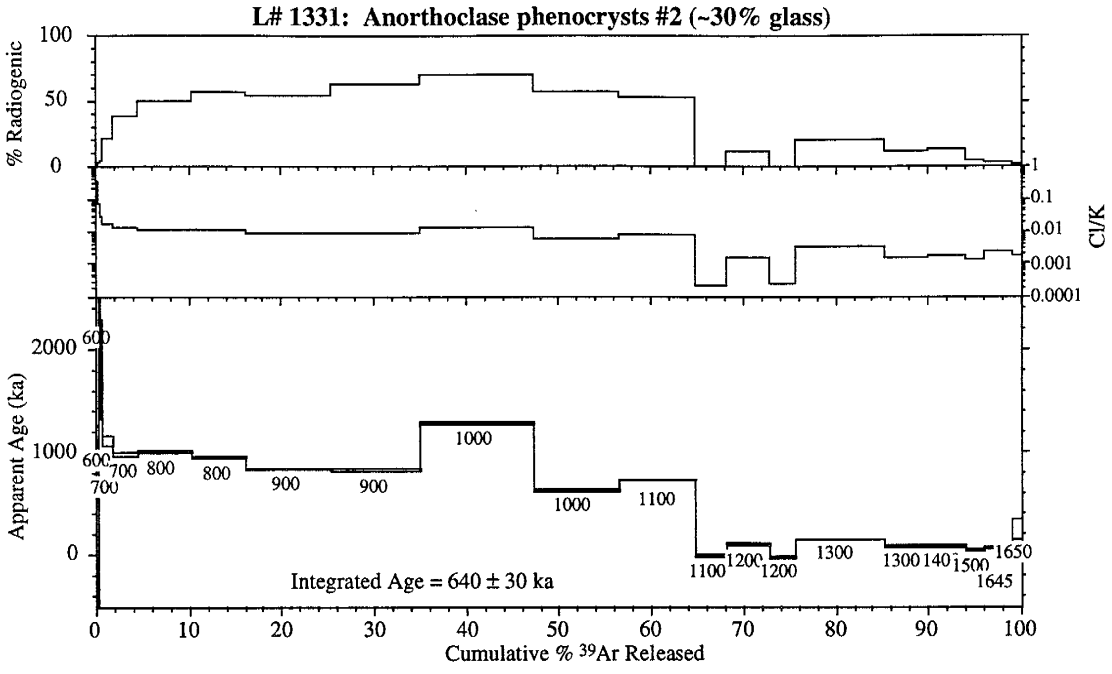
L# 1331: Anorthoclase phenocrysts #2 (~30% glass)
% Radiogenic
100
50
0
Cl/K
1
0.1
0.01
0.001
0.0001
Apparent Age (ka)
2000
1000
0
600
700
800
800
900
900
1000
1000
1100
1100
1200
1200
1300
1300
1400
1500
1650
1645
Integrated Age = 640 ± 30 ka
0
10
20
30
40
50
60
70
80
90
100
Cumulative % 39Ar Released

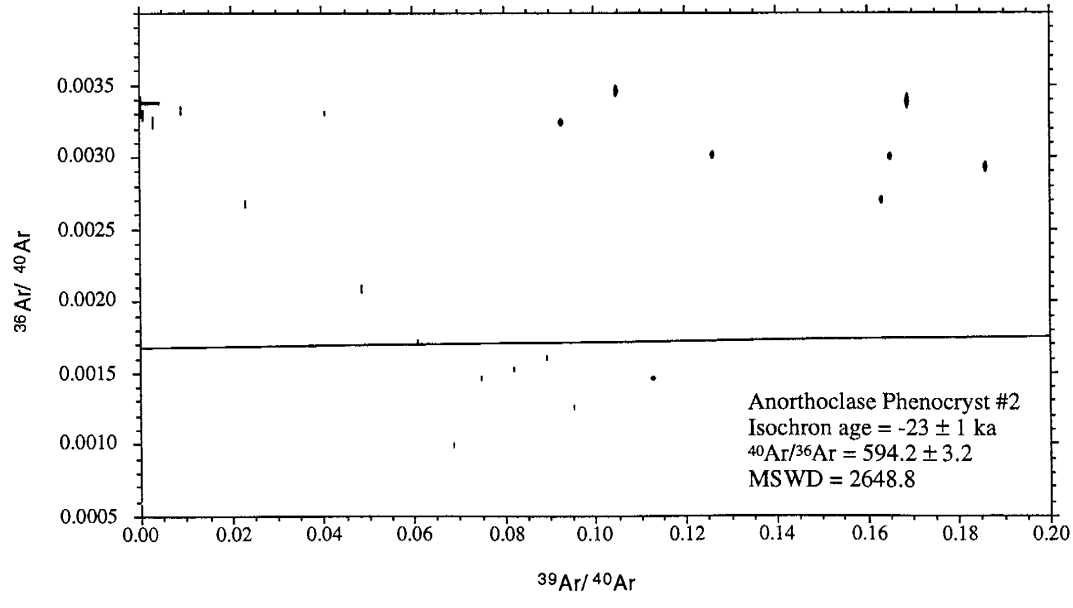
36Ar/ 40Ar
0.0035
0.0030
0.0025
0.0020
0.0015
0.0010
0.0005
Anorthoclase Phenocryst #2
Isochron age = -23 ± 1 ka
40Ar/36Ar = 594.2 ± 3.2
MSWD = 2648.8
0.00
0.02
0.04
0.06
0.08
0.10
0.12
0.14
0.16
0.18
0.20
39Ar/ 40Ar

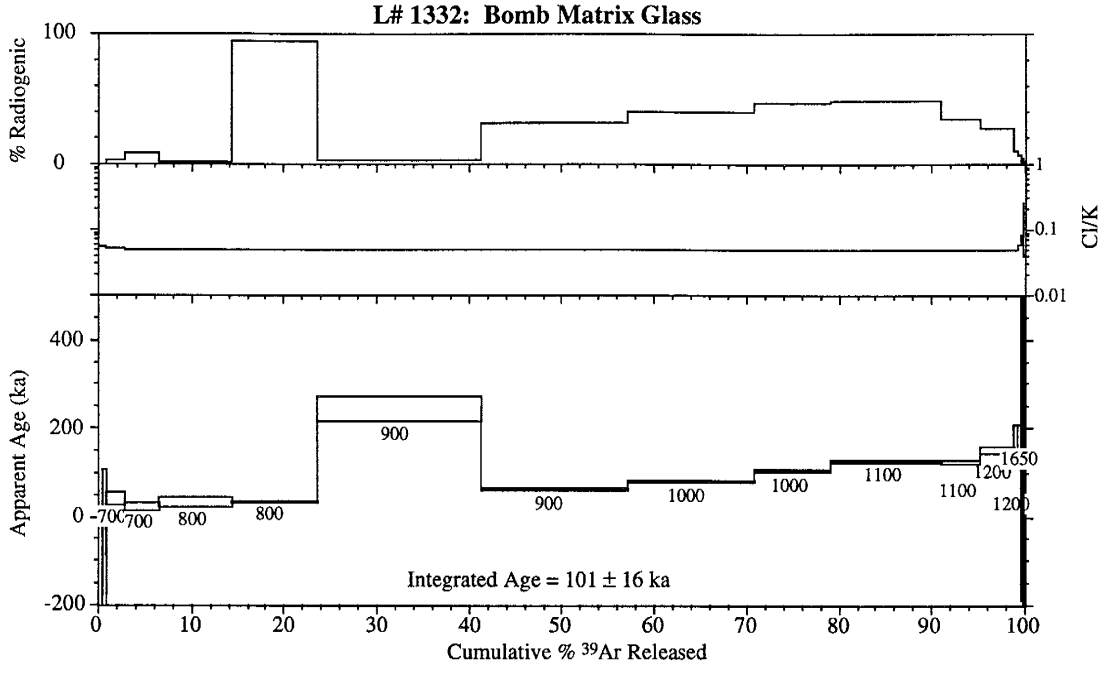
L# 1332: Bomb Matrix Glass
% Radiogenic
100
0
Cl/K
1
0.1
0.01
Apparent Age (ka)
400
200
0
-200
700
700
800
800
900
900
1000
1000
1100
1100
1200
1200
1650
Integrated Age = 101 ± 16 ka
0
10
20
30
40
50
60
70
80
90
100
Cumulative % 39Ar Released

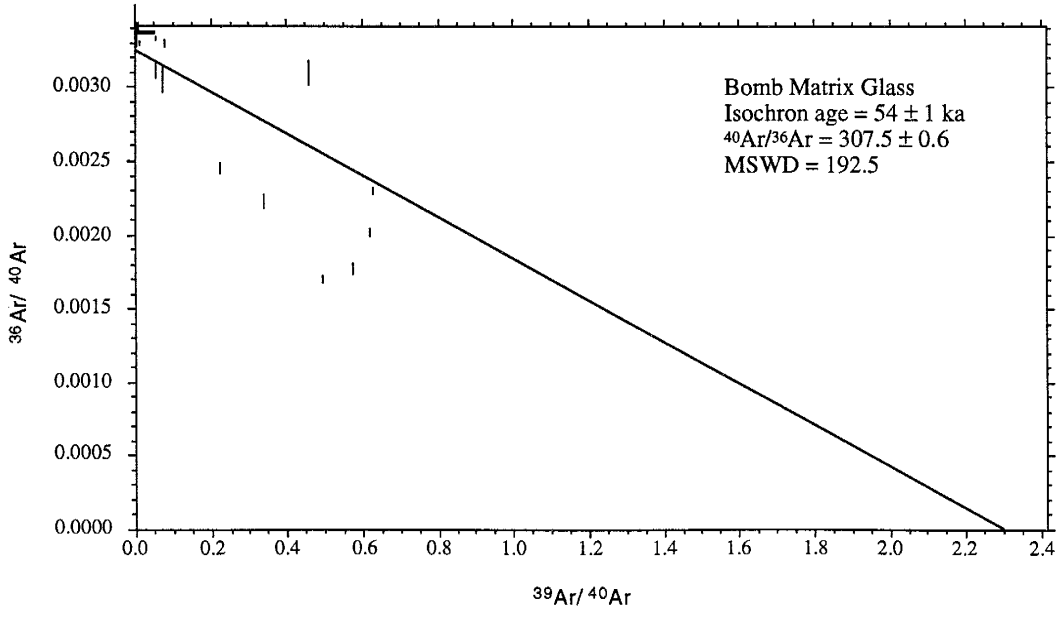
Bomb Matrix Glass
Isochron age = 54 ± 1 ka
40Ar/36Ar = 307.5 ± 0.6
MSWD = 192.5
36Ar/ 40Ar
0.0030
0.0025
0.0020
0.0015
0.0010
0.0005
0.0000
0.0
0.2
0.4
0.6
0.8
1.0
1.2
1.4
1.6
1.8
2.0
2.2
2.4
39Ar/ 40Ar

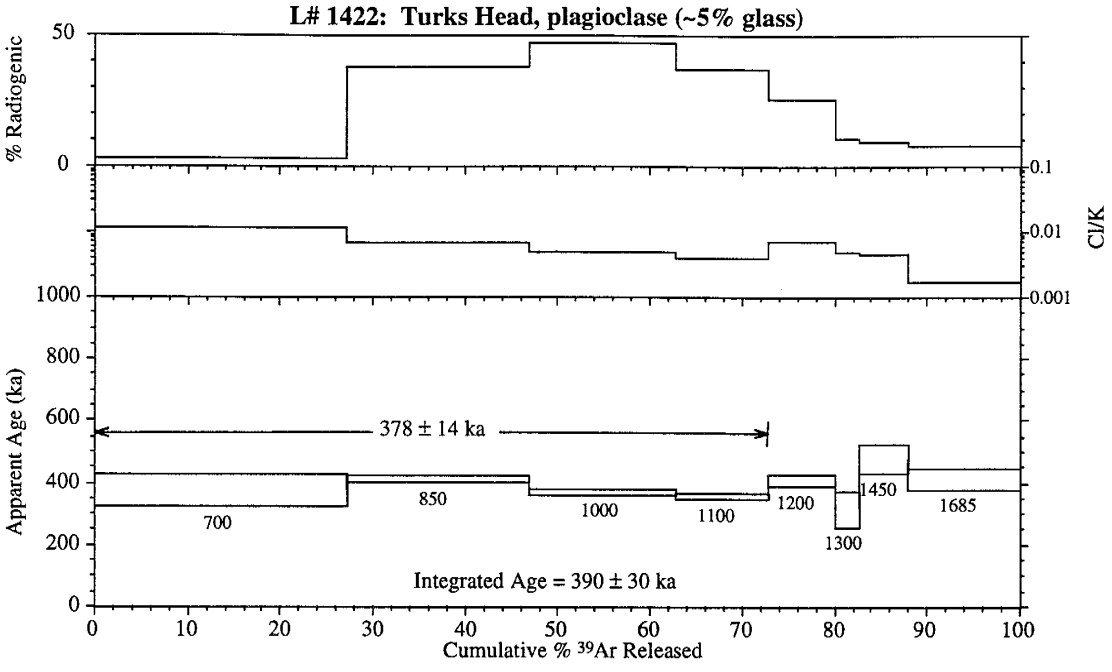
L# 1422: Turks Head, plagioclase (~5% glass)
% Radiogenic
50
0
0.1
0.01
0.001
Cl/K
1000
800
600
400
200
0
Apparent Age (ka)
378 ± 14 ka
700
850
1000
1100
1200
1300
1450
1685
Integrated Age = 390 ± 30 ka
0
10
20
30
40
50
60
70
80
90
100
Cumulative % 39Ar Released

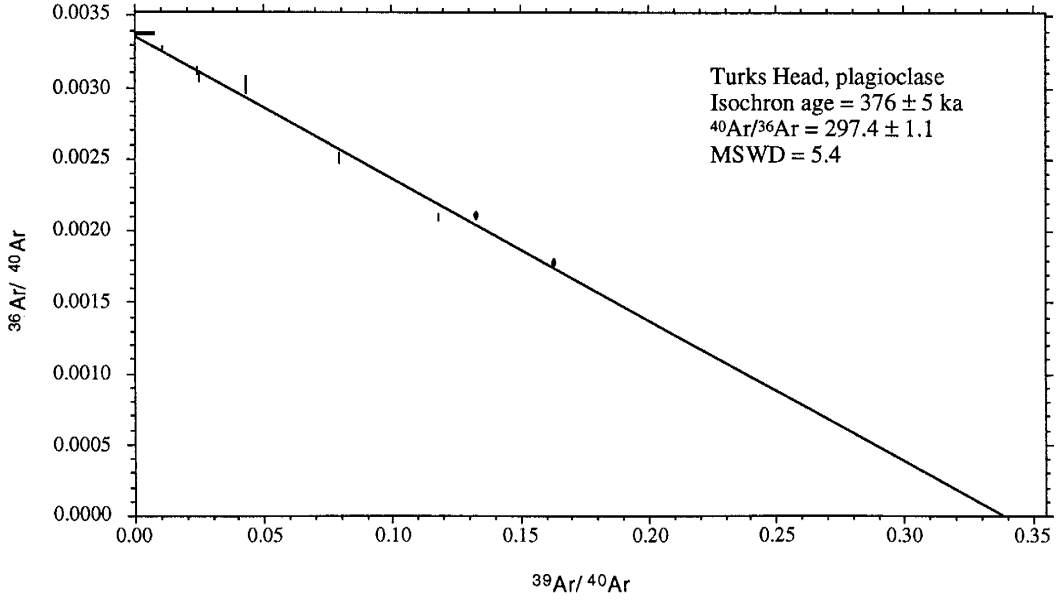
0.0035
0.0030
0.0025
0.0020
0.0015
0.0010
0.0005
0.0000
36Ar/ 40Ar
Turks Head, plagioclase
Isochron age = 376 ± 5 ka
40Ar/36Ar = 297.4 ± 1.1
MSWD = 5.4
0.00
0.05
0.10
0.15
0.20
0.25
0.30
0.35
39Ar/ 40Ar

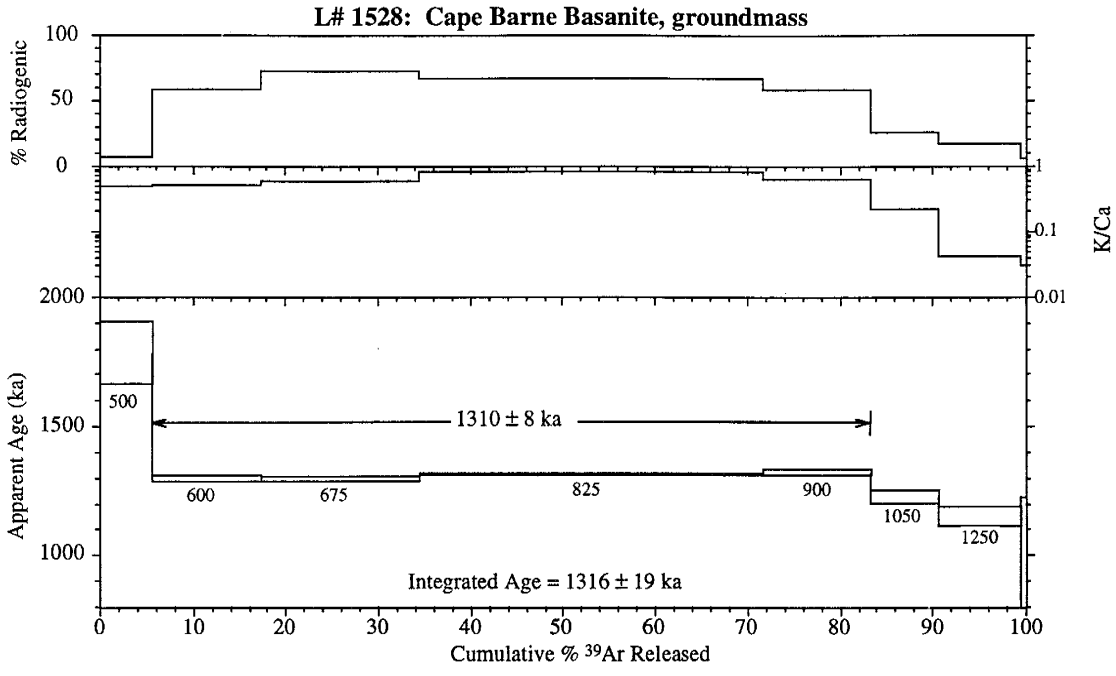
L# 1528: Cape Barne Basanite, groundmass
% Radiogenic
100
50
0
K/Ca
1
0.1
0.01
Apparent Age (ka)
2000
1500
1000
500
1310 ± 8 ka
600
675
825
900
1050
1250
Integrated Age = 1316 ± 19 ka
0
10
20
30
40
50
60
70
80
90
100
Cumulative % 39Ar Released

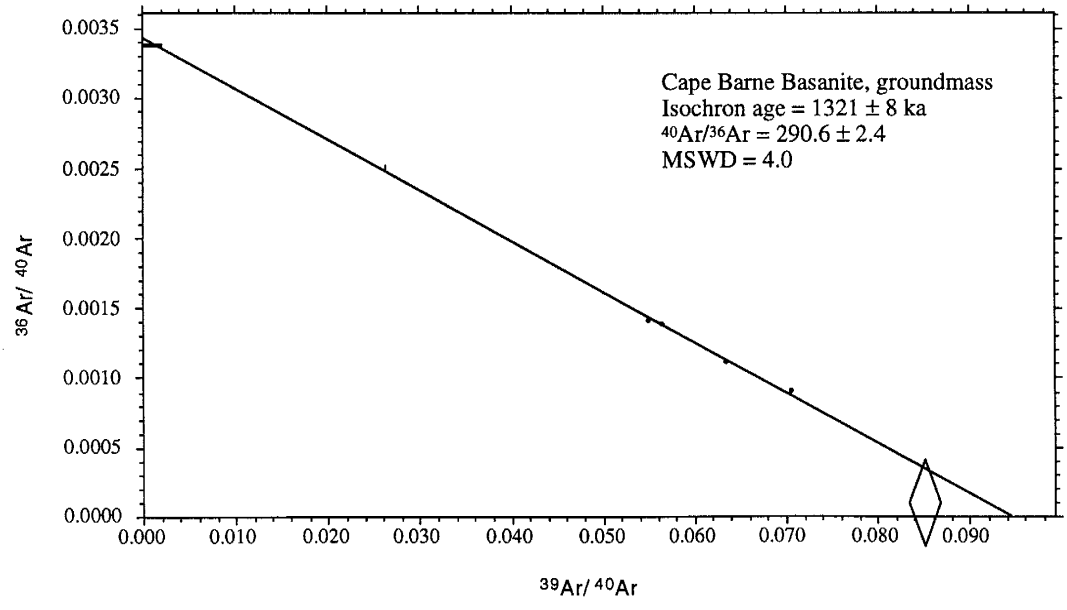
Cape Barne Basanite, groundmass
Isochron age = 1321 ± 8 ka
40Ar/36Ar = 290.6 ± 2.4
MSWD = 4.0
36Ar/ 40Ar
0.0035
0.0030
0.0025
0.0020
0.0015
0.0010
0.0005
0.0000
0.000
0.010
0.020
0.030
0.040
0.050
0.060
0.070
0.080
0.090
39Ar/ 40Ar

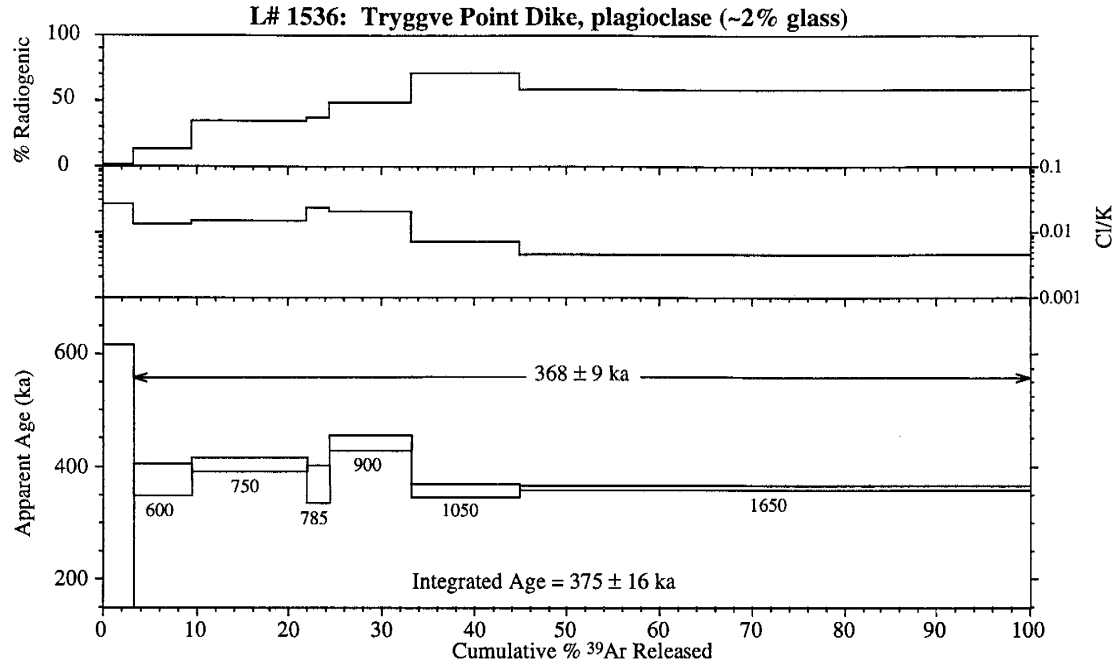
L# 1536: Tryggve Point Dike, plagioclase (~2% glass)
% Radiogenic
100
50
0
0.1
0.01
0.001
Cl/K
Apparent Age (ka)
600
400
200
368 ± 9 ka
600
750
785
900
1050
1650
Integrated Age = 375 ± 16 ka
0
10
20
30
40
50
60
70
80
90
100
Cumulative % 39Ar Released

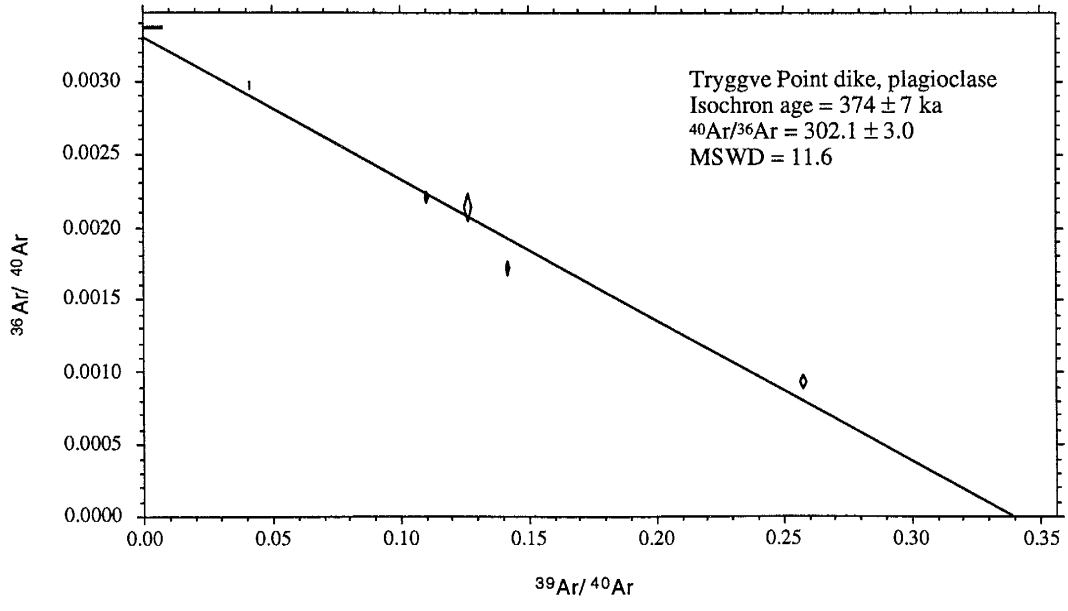
Tryggve Point dike, plagioclase
Isochron age = 374 ± 7 ka
40Ar/36Ar = 302.1 ± 3.0
MSWD = 11.6
36Ar/ 40Ar
0.0030
0.0025
0.0020
0.0015
0.0010
0.0005
0.0000
0.00
0.05
0.10
0.15
0.20
0.25
0.30
0.35
39Ar/ 40Ar

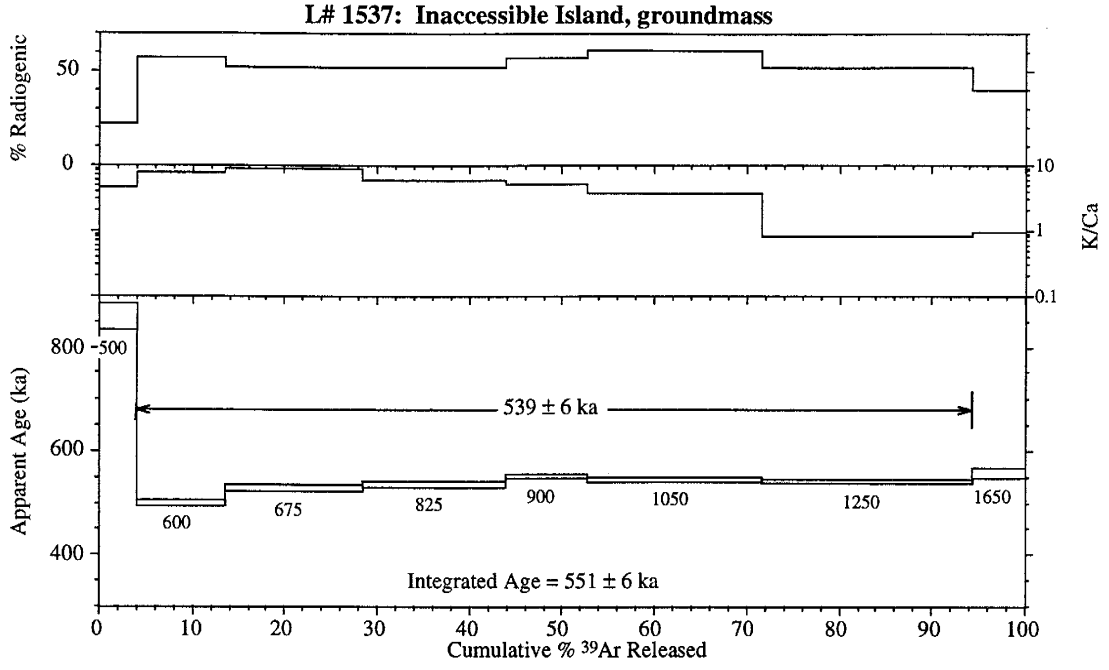
L# 1537: Inaccessible Island, groundmass
% Radiogenic
50
0
10
1
0.1
K/Ca
800
600
400
Apparent Age (ka)
500
539 ± 6 ka
600
675
825
900
1050
1250
1650
Integrated Age = 551 ± 6 ka
0
10
20
30
40
50
60
70
80
90
100
Cumulative % 39Ar Released

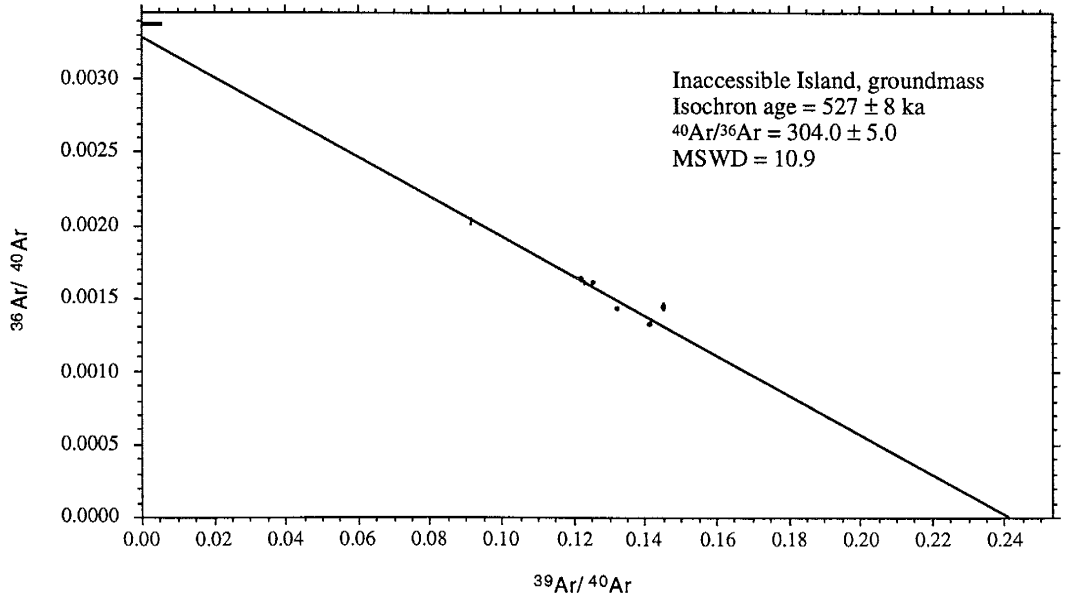
Inaccessible Island, groundmass
Isochron age = 527 ± 8 ka
40Ar/36Ar = 304.0 ± 5.0
MSWD = 10.9
0.0030
0.0025
0.0020
0.0015
0.0010
0.0005
0.0000
36Ar/ 40Ar
0.00
0.02
0.04
0.06
0.08
0.10
0.12
0.14
0.16
0.18
0.20
0.22
0.24
39Ar/ 40Ar

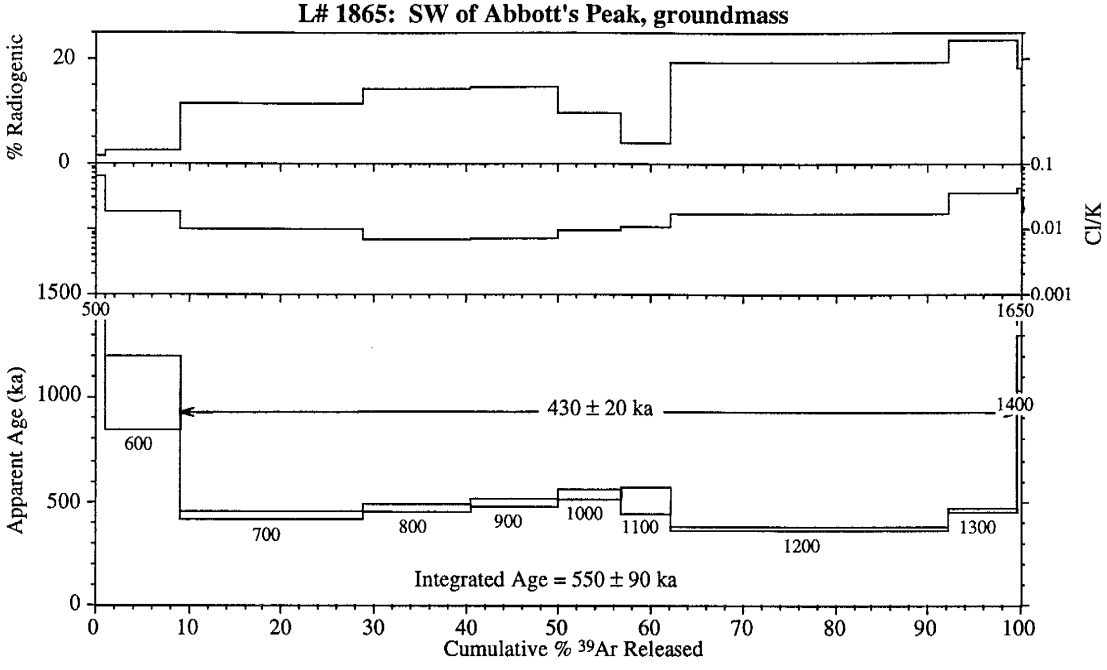
L# 1865: SW of Abbott's Peak, groundmass
% Radiogenic
20
0
0.1
0.01
0.001
Cl/K
1500
500
1650
Apparent Age (ka)
1000
500
0
430 ± 20 ka
1400
600
700
800
900
1000
1100
1200
1300
Integrated Age = 550 ± 90 ka
0
10
20
30
40
50
60
70
80
90
100
Cumulative % 39Ar Released

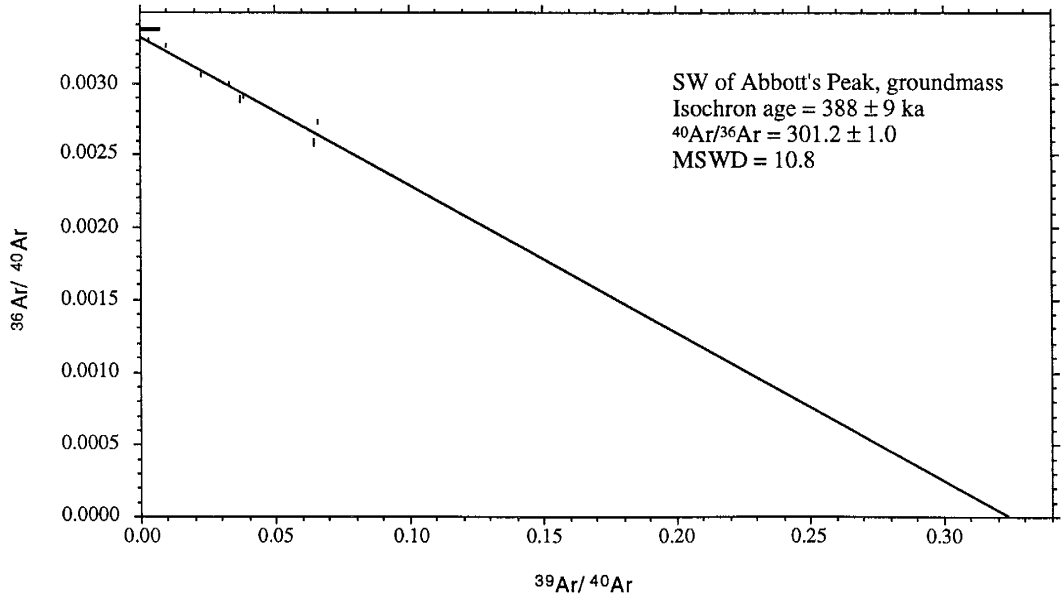
SW of Abbott's Peak, groundmass
Isochron age = 388 ± 9 ka
40Ar/36Ar = 301.2 ± 1.0
MSWD = 10.8
36Ar/ 40Ar
0.0030
0.0025
0.0020
0.0015
0.0010
0.0005
0.0000
0.00
0.05
0.10
0.15
0.20
0.25
0.30
39Ar/ 40Ar

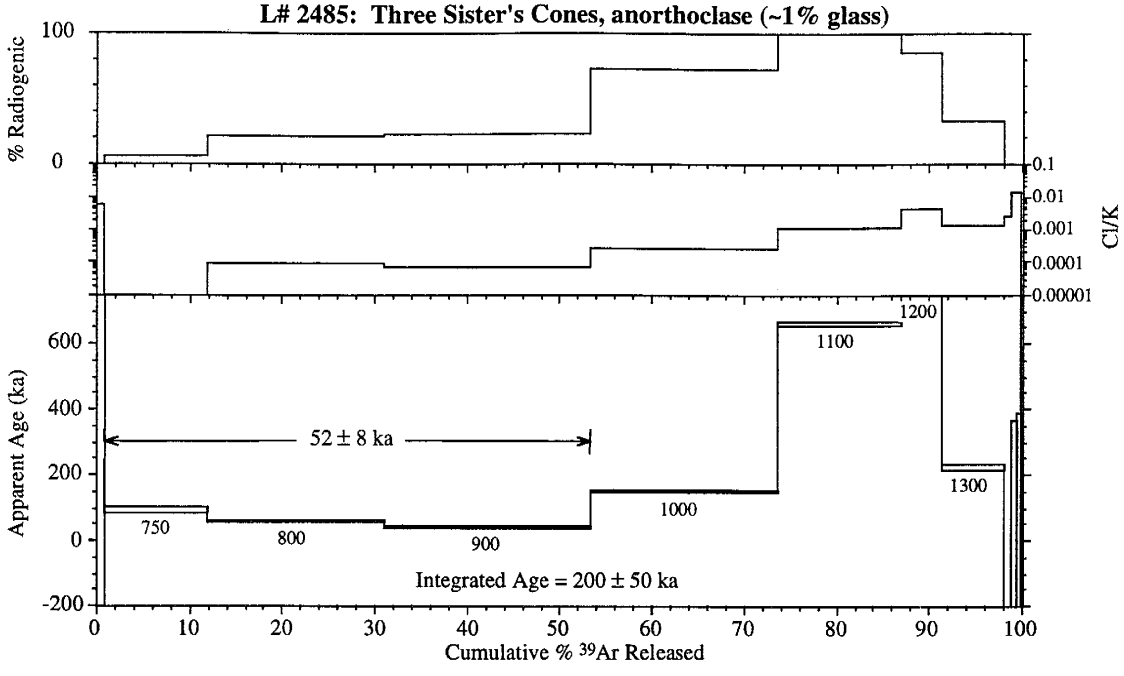
L# 2485: Three Sister's Cones, anorthoclase (~1% glass)
% Radiogenic
100
0
Cl/K
0.1
0.01
0.001
0.0001
0.00001
Apparent Age (ka)
600
400
200
0
-200
52 ± 8 ka
750
800
900
1000
1100
1200
1300
Integrated Age = 200 ± 50 ka
0
10
20
30
40
50
60
70
80
90
100
Cumulative % 39Ar Released

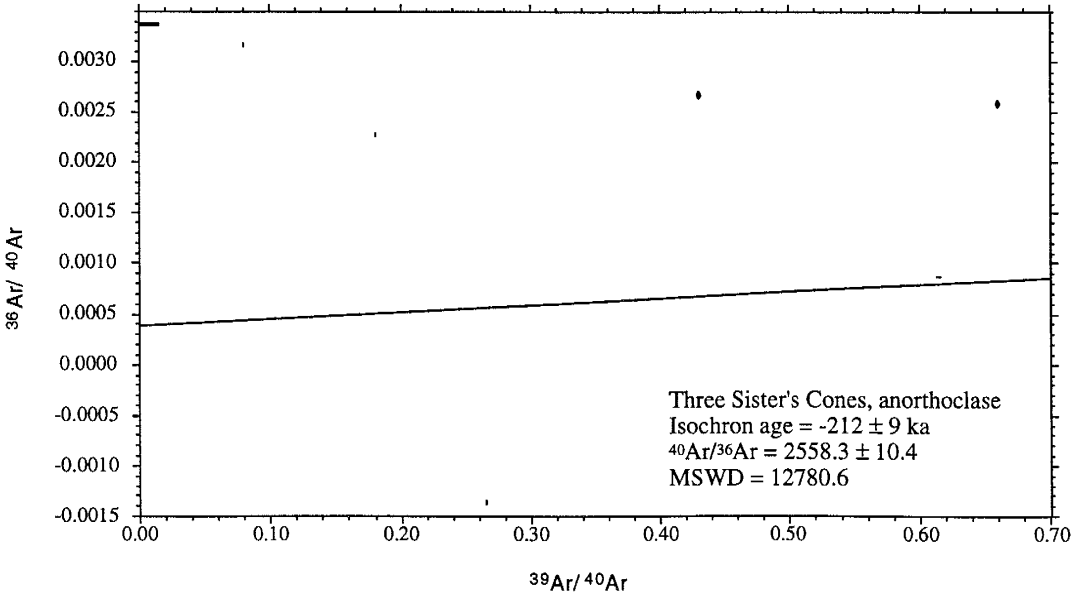
36Ar/ 40Ar
0.0030
0.0025
0.0020
0.0015
0.0010
0.0005
0.0000
-0.0005
-0.0010
-0.0015
0.00
0.10
0.20
0.30
0.40
0.50
0.60
0.70
39Ar/ 40Ar
Three Sister's Cones, anorthoclase
Isochron age = -212 ± 9 ka
40Ar/36Ar = 2558.3 ± 10.4
MSWD = 12780.6

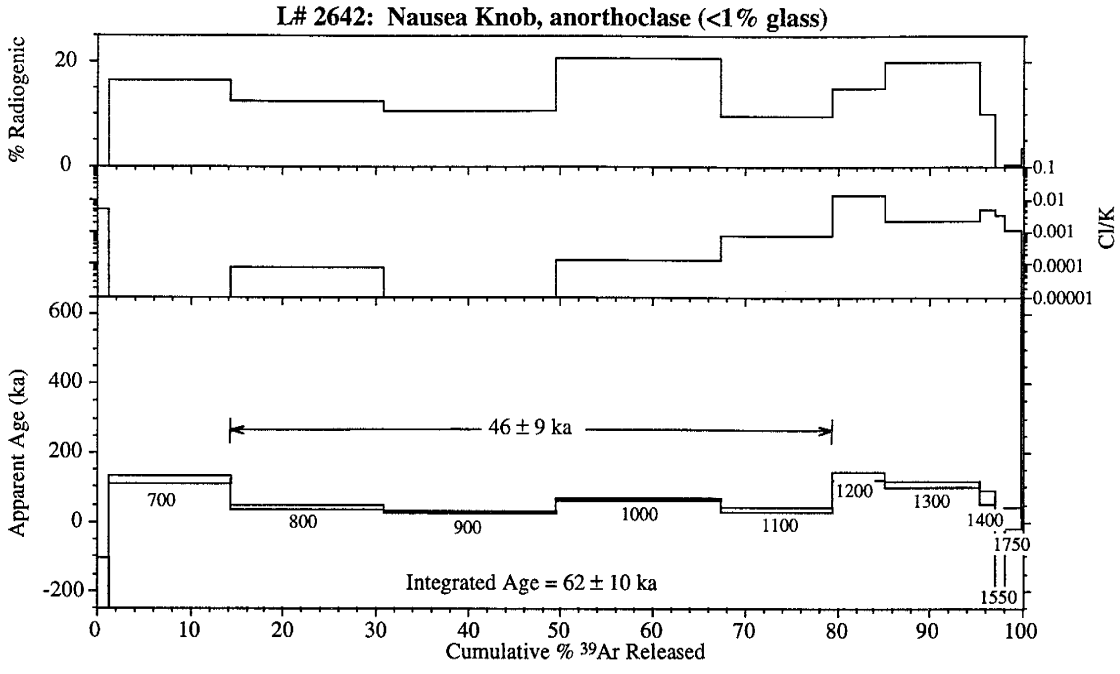
L# 2642: Nausea Knob, anorthoclase (<1% glass)
% Radiogenic
20
0
Cl/K
0.1
0.01
0.001
0.0001
0.00001
Apparent Age (ka)
600
400
200
0
-200
46 ± 9 ka
700
800
900
1000
1100
1200
1300
1400
1750
1550
Integrated Age = 62 ± 10 ka
0
10
20
30
40
50
60
70
80
90
100
Cumulative % 39Ar Released

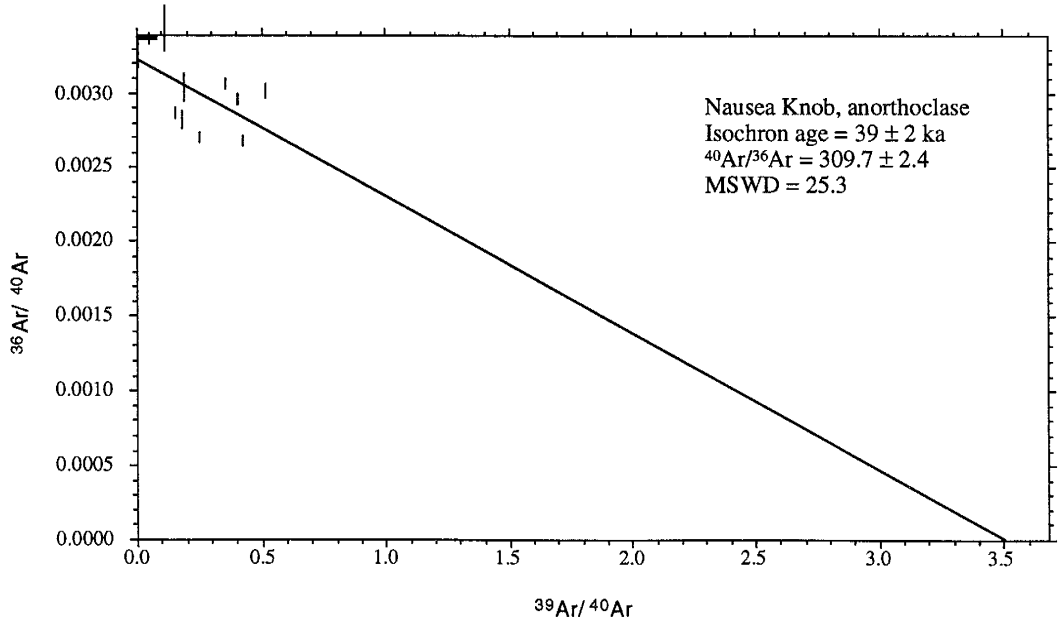
Nausea Knob, anorthoclase
Isochron age = 39 ± 2 ka
40Ar/36Ar = 309.7 ± 2.4
MSWD = 25.3
36Ar/ 40Ar
0.0030
0.0025
0.0020
0.0015
0.0010
0.0005
0.0000
0.0
0.5
1.0
1.5
2.0
2.5
3.0
3.5
39Ar/ 40Ar

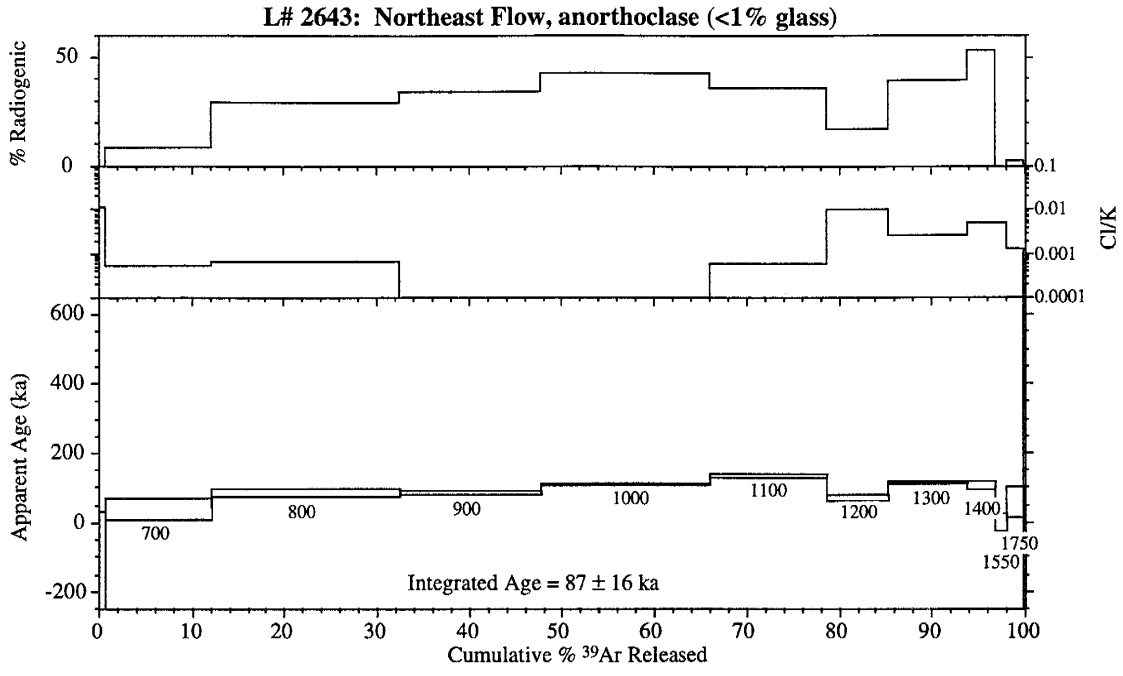
L# 2643: Northeast Flow, anorthoclase (<1% glass)
% Radiogenic
50
0
0.1
0.01
0.001
0.0001
Cl/K
600
400
200
0
-200
Apparent Age (ka)
700
800
900
1000
1100
1200
1300
1400
1750
1550
Integrated Age = 87 ± 16 ka
0
10
20
30
40
50
60
70
80
90
100
Cumulative % 39Ar Released

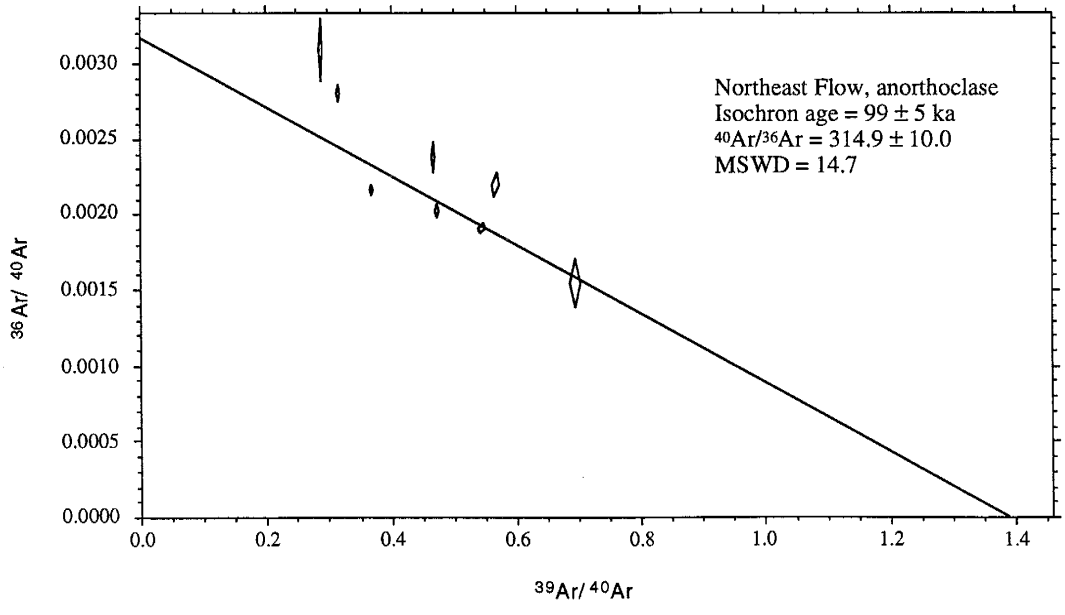
Northeast Flow, anorthoclase
Isochron age = 99 ± 5 ka
40Ar/36Ar = 314.9 ± 10.0
MSWD = 14.7
36Ar/ 40Ar
0.0030
0.0025
0.0020
0.0015
0.0010
0.0005
0.0000
0.0
0.2
0.4
0.6
0.8
1.0
1.2
1.4
39Ar/ 40Ar

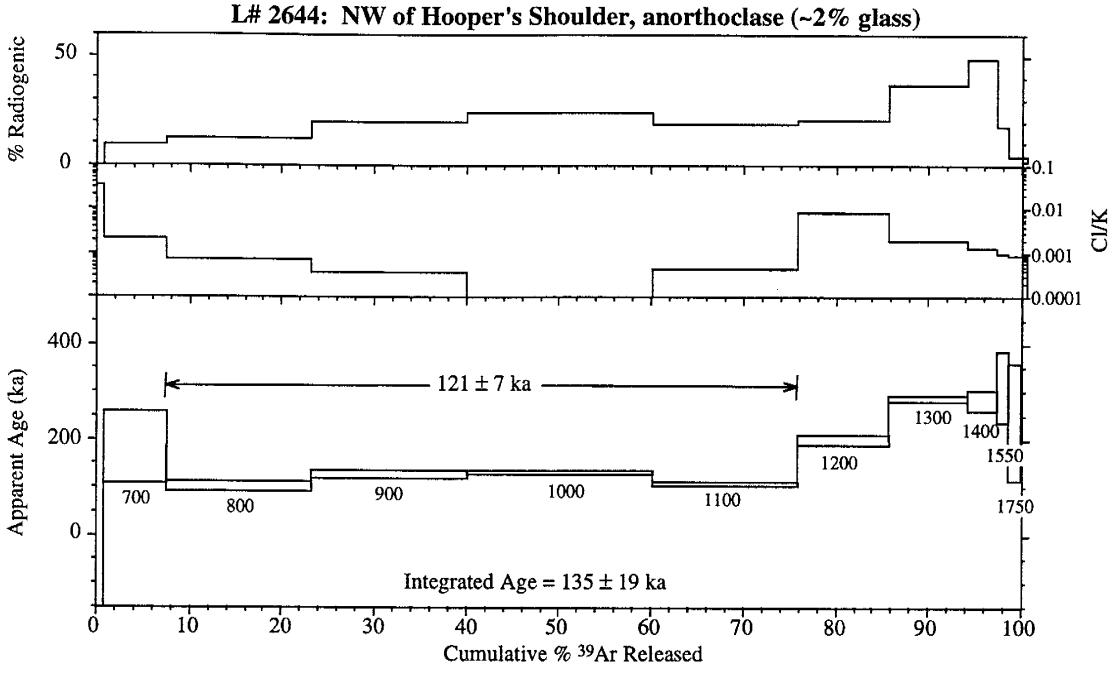
L# 2644: NW of Hooper's Shoulder, anorthoclase (~2% glass)
% Radiogenic
50
0
0.1
0.01
0.001
0.0001
Cl/K
400
200
0
Apparent Age (ka)
121 ± 7 ka
700
800
900
1000
1100
1200
1300
1400
1550
1750
Integrated Age = 135 ± 19 ka
0
10
20
30
40
50
60
70
80
90
100
Cumulative % 39Ar Released

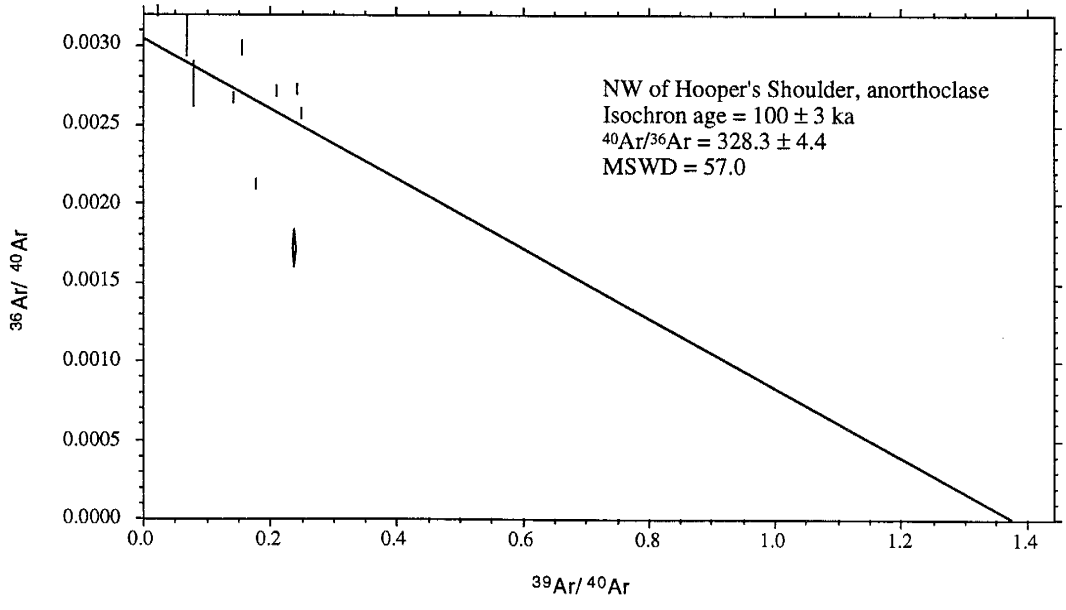
NW of Hooper's Shoulder, anorthoclase
Isochron age = 100 ± 3 ka
40Ar/36Ar = 328.3 ± 4.4
MSWD = 57.0
36Ar/ 40Ar
0.0030
0.0025
0.0020
0.0015
0.0010
0.0005
0.0000
0.0
0.2
0.4
0.6
0.8
1.0
1.2
1.4
39Ar/ 40Ar

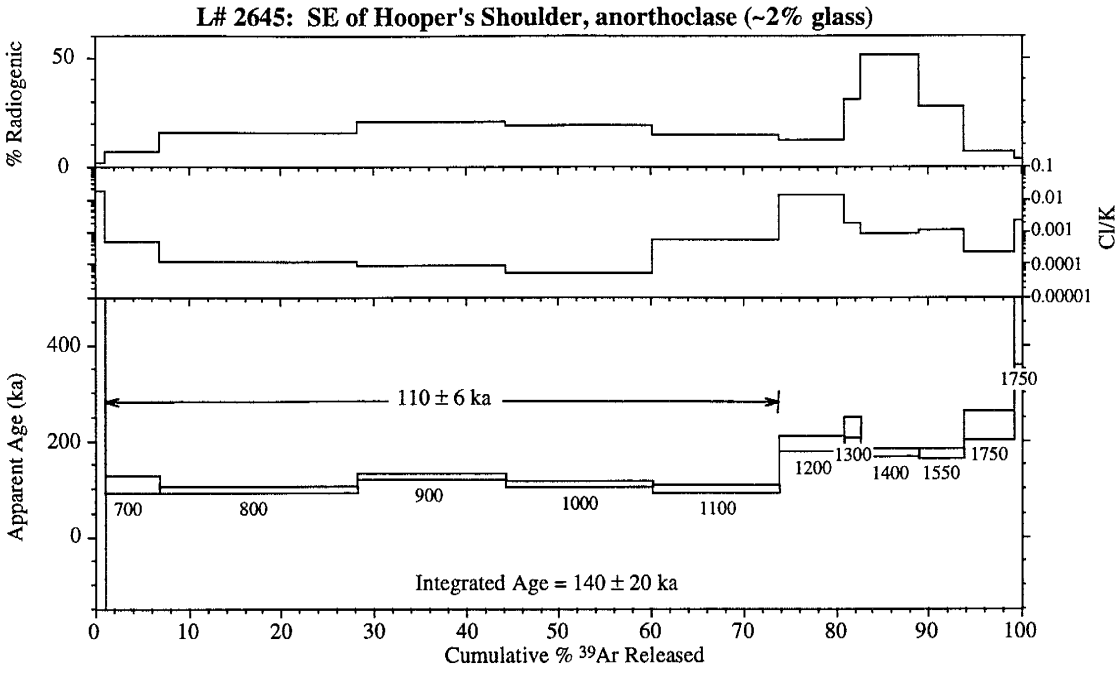
L# 2645: SE of Hooper's Shoulder, anorthoclase (~2% glass)
% Radiogenic
50
0
0.1
0.01
0.001
0.0001
0.00001
Cl/K
400
200
0
Apparent Age (ka)
110 ± 6 ka
1750
700
800
900
1000
1100
1200
1300
1400
1550
1750
Integrated Age = 140 ± 20 ka
0
10
20
30
40
50
60
70
80
90
100
Cumulative % 39Ar Released

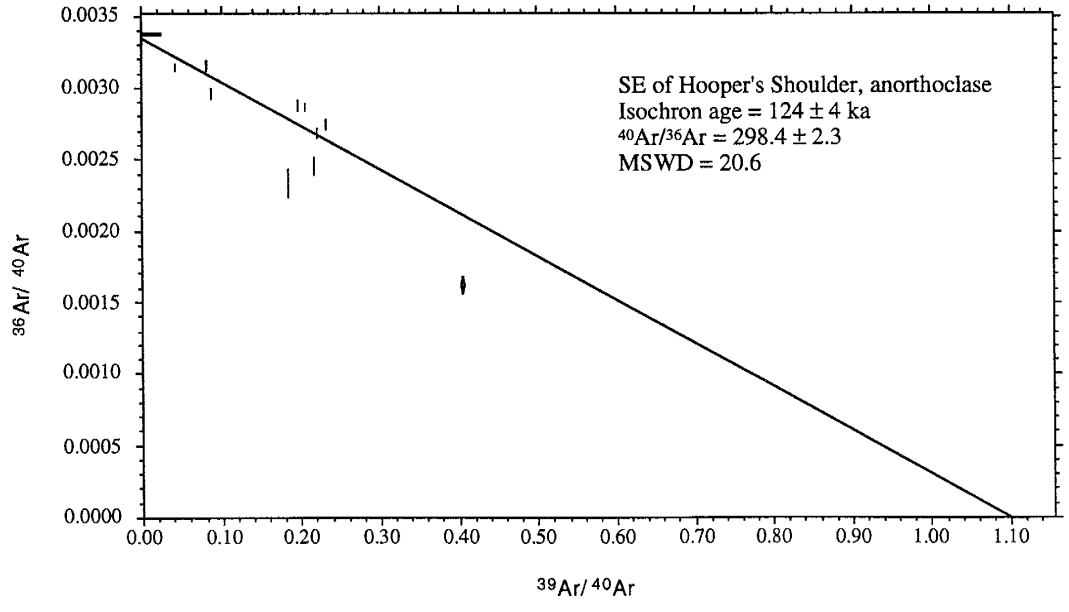
0.0035
0.0030
0.0025
0.0020
0.0015
0.0010
0.0005
0.0000
36Ar/ 40Ar
SE of Hooper's Shoulder, anorthoclase
Isochron age = 124 ± 4 ka
40Ar/36Ar = 298.4 ± 2.3
MSWD = 20.6
0.00
0.10
0.20
0.30
0.40
0.50
0.60
0.70
0.80
0.90
1.00
1.10
39Ar/ 40Ar

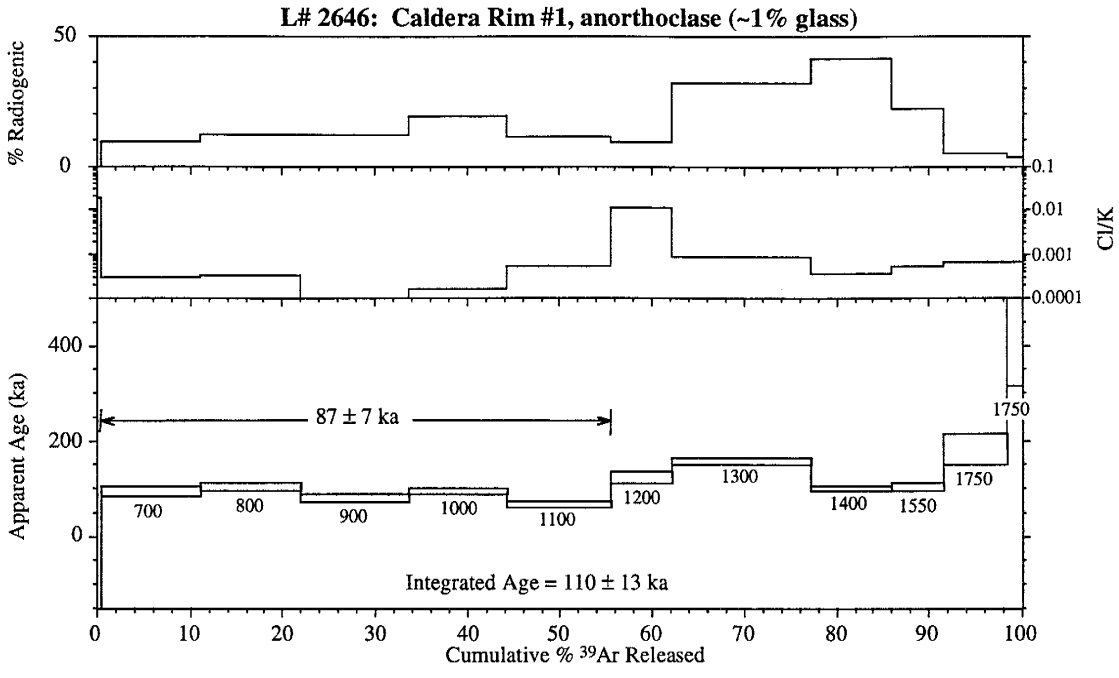
L# 2646: Caldera Rim #1, anorthoclase (~1% glass)
% Radiogenic
50
0
0.1
0.01
0.001
0.0001
Cl/K
400
200
0
Apparent Age (ka)
87 ± 7 ka
700
800
900
1000
1100
1200
1300
1400
1550
1750
1750
Integrated Age = 110 ± 13 ka
0
10
20
30
40
50
60
70
80
90
100
Cumulative % 39Ar Released

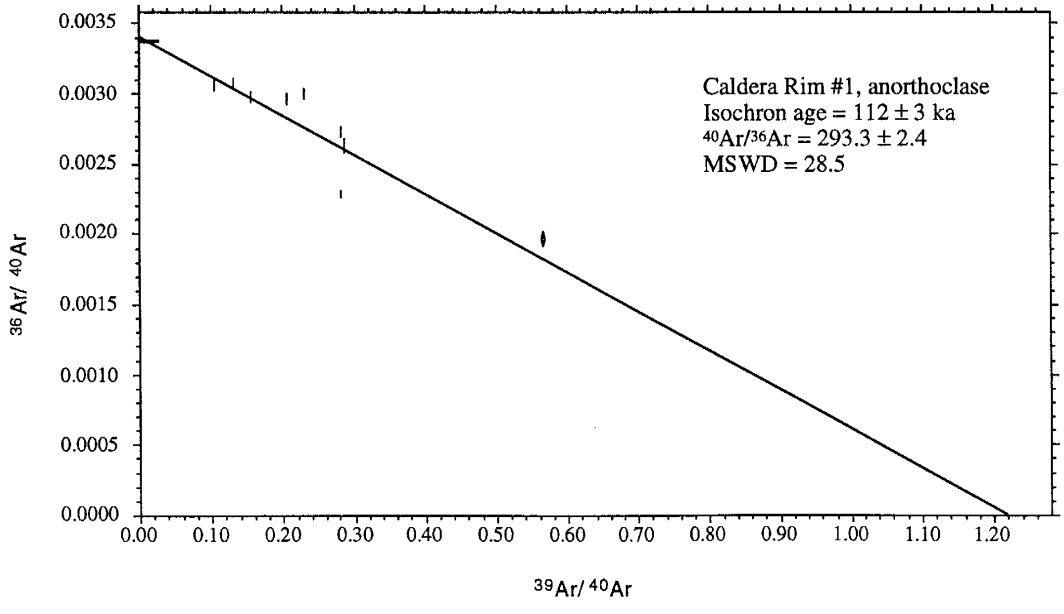
0.0035
0.0030
0.0025
0.0020
0.0015
0.0010
0.0005
0.0000
36Ar/ 40Ar
Caldera Rim #1, anorthoclase
Isochron age = 112 ± 3 ka
40Ar/36Ar = 293.3 ± 2.4
MSWD = 28.5
0.00
0.10
0.20
0.30
0.40
0.50
0.60
0.70
0.80
0.90
1.00
1.10
1.20
39Ar/ 40Ar

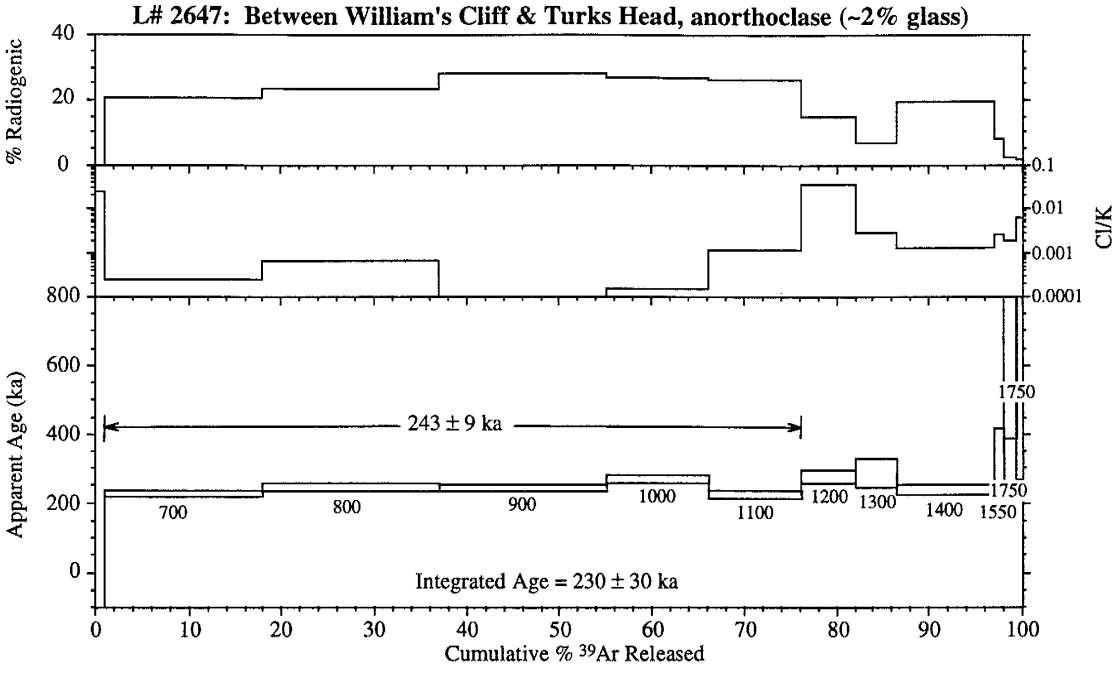
L# 2647: Between William's Cliff & Turks Head, anorthoclase (~2% glass)
% Radiogenic
Cl/K
Apparent Age (ka)
243 ± 9 ka
Integrated Age = 230 ± 30 ka
Cumulative % 39Ar Released

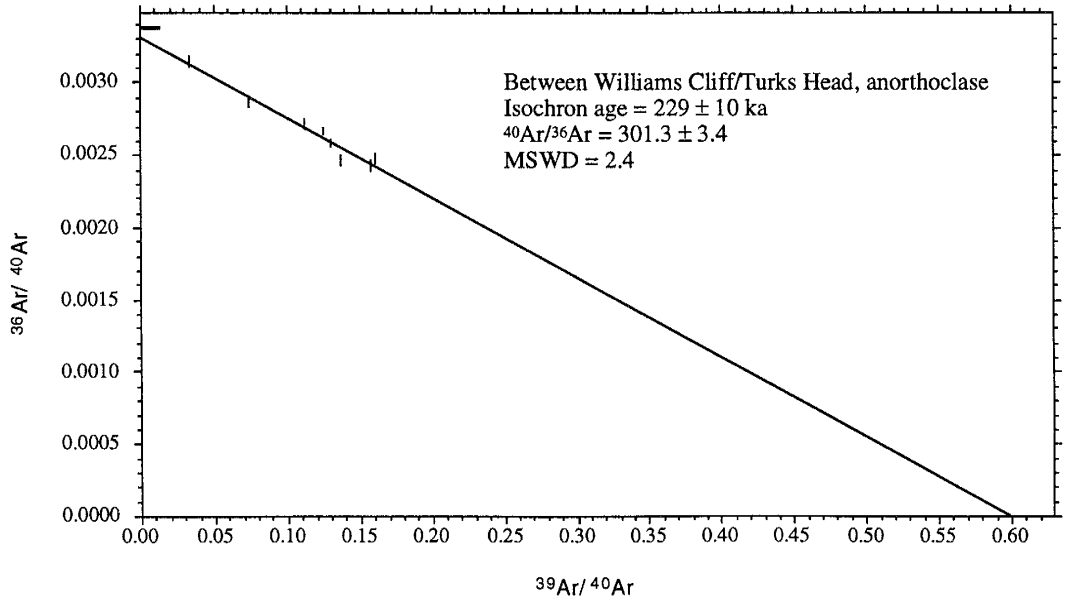
Between Williams Cliff/Turks Head, anorthoclase
Isochron age = 229 ± 10 ka
40Ar/36Ar = 301.3 ± 3.4
MSWD = 2.4
36Ar/ 40Ar
39Ar/ 40Ar

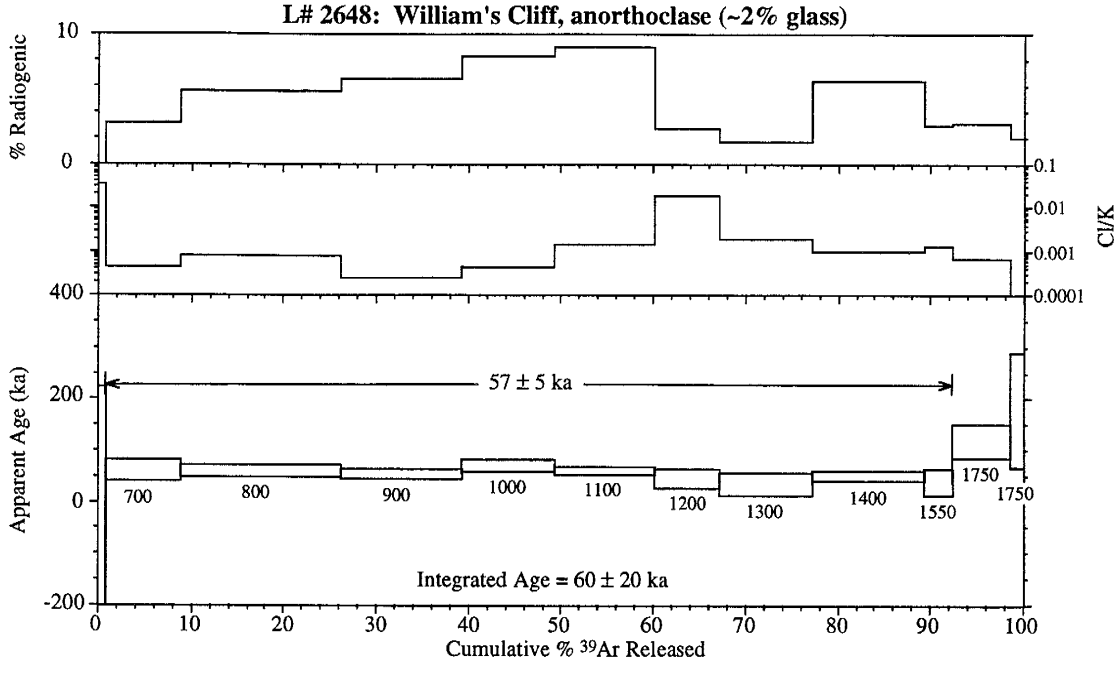
L# 2648: William's Cliff, anorthoclase (~2% glass)
% Radiogenic
10
0
0.1
0.01
0.001
0.0001
Cl/K
400
200
0
-200
Apparent Age (ka)
57 ± 5 ka
700
800
900
1000
1100
1200
1300
1400
1550
1750
1750
Integrated Age = 60 ± 20 ka
0
10
20
30
40
50
60
70
80
90
100
Cumulative % 39Ar Released

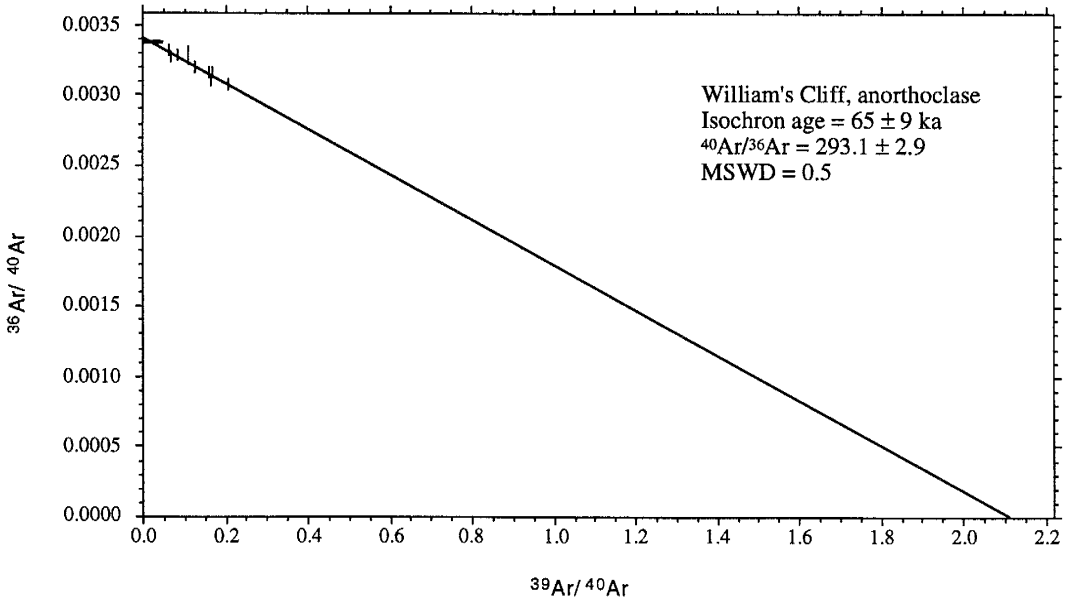
William's Cliff, anorthoclase
Isochron age = 65 ± 9 ka
40Ar/36Ar = 293.1 ± 2.9
MSWD = 0.5
0.0035
0.0030
0.0025
0.0020
0.0015
0.0010
0.0005
0.0000
36Ar/ 40Ar
0.0
0.2
0.4
0.6
0.8
1.0
1.2
1.4
1.6
1.8
2.0
2.2
39Ar/ 40Ar

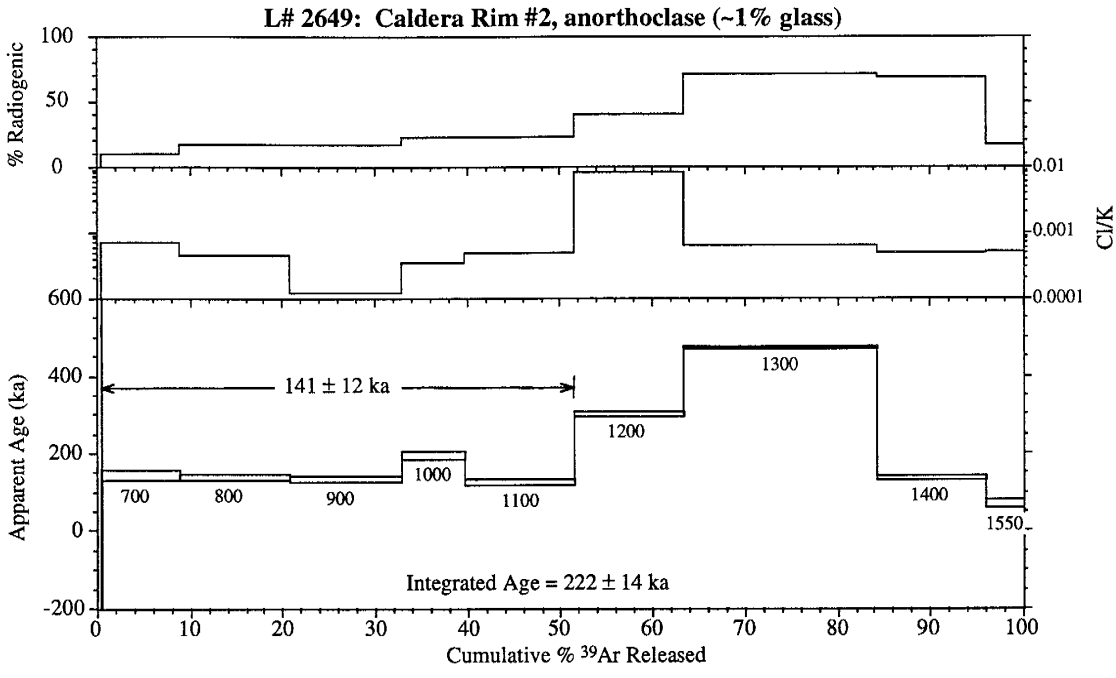
L# 2649: Caldera Rim #2, anorthoclase (~1% glass)
% Radiogenic
100
50
0
0.01
0.001
0.0001
Cl/K
600
400
200
0
-200
Apparent Age (ka)
141 ± 12 ka
700
800
900
1000
1100
1200
1300
1400
1550
Integrated Age = 222 ± 14 ka
0
10
20
30
40
50
60
70
80
90
100
Cumulative % 39Ar Released

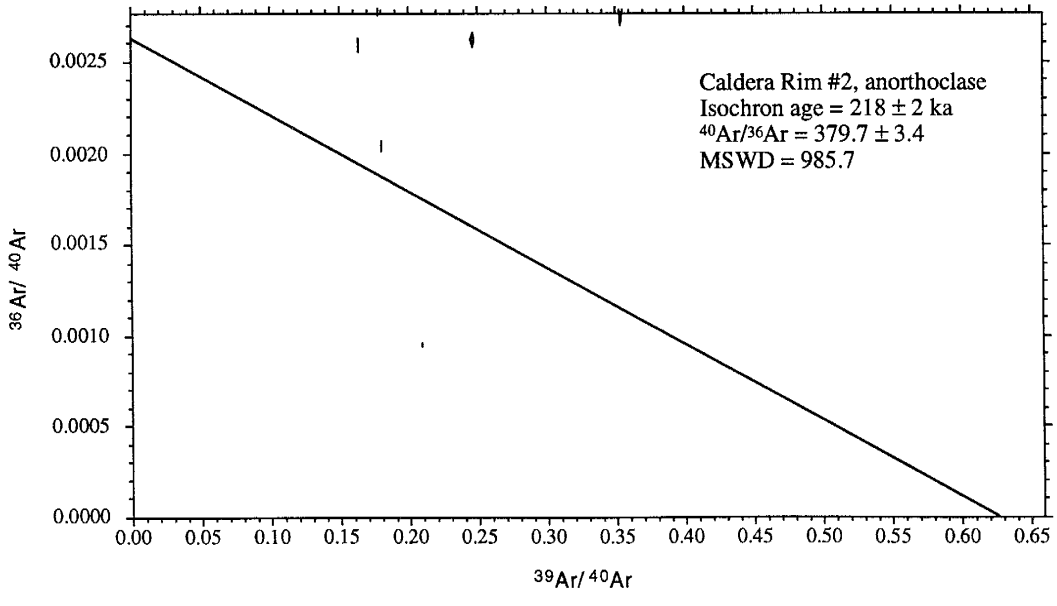
Caldera Rim #2, anorthoclase
Isochron age = 218 ± 2 ka
40Ar/36Ar = 379.7 ± 3.4
MSWD = 985.7
0.0025
0.0020
0.0015
0.0010
0.0005
0.0000
36Ar/ 40Ar
0.00
0.05
0.10
0.15
0.20
0.25
0.30
0.35
0.40
0.45
0.50
0.55
0.60
0.65
39Ar/ 40Ar

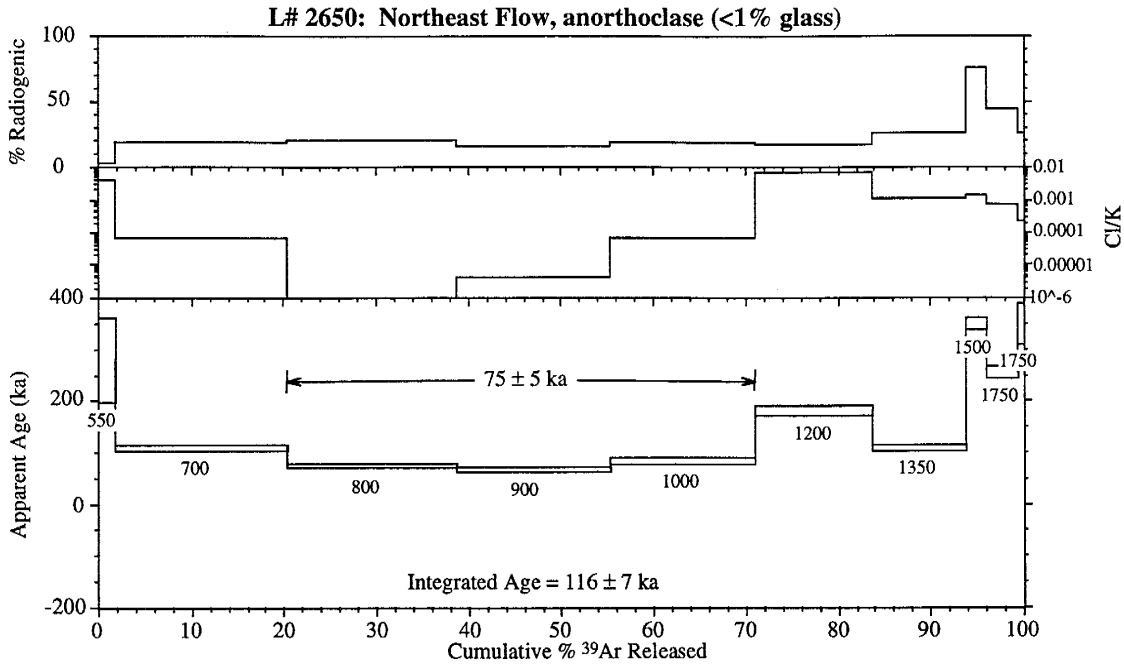
L# 2650: Northeast Flow, anorthoclase (<1% glass)
% Radiogenic
100
50
0
Cl/K
0.01
0.001
0.0001
0.00001
10^-6
400
200
0
-200
Apparent Age (ka)
75 ± 5 ka
550
700
800
900
1000
1200
1350
1500
1750
1750
Integrated Age = 116 ± 7 ka
0
10
20
30
40
50
60
70
80
90
100
Cumulative % 39Ar Released

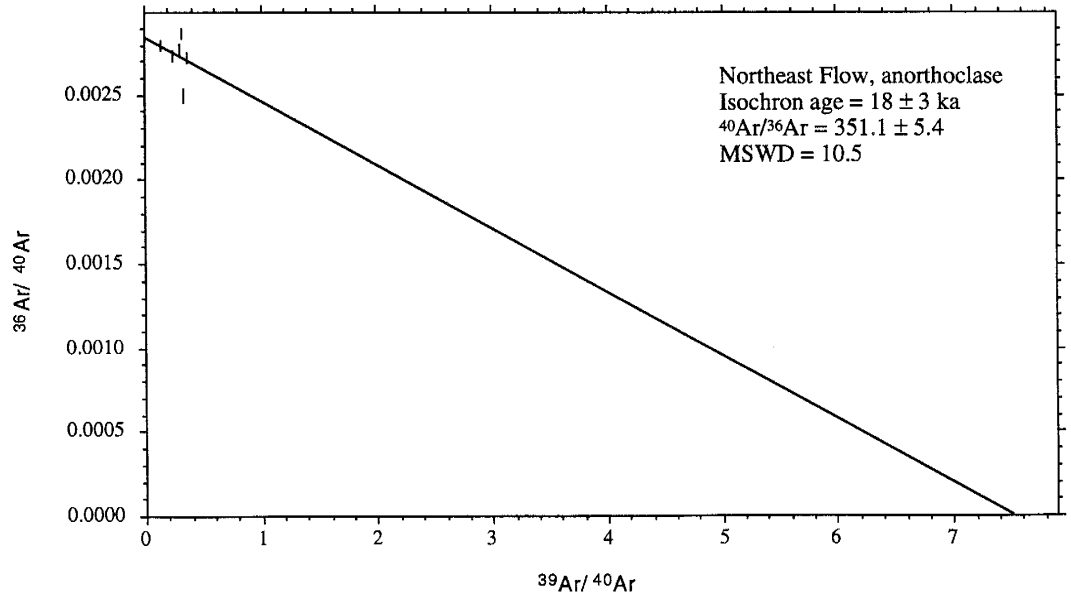
Northeast Flow, anorthoclase
Isochron age = 18 ± 3 ka
40Ar/36Ar = 351.1 ± 5.4
MSWD = 10.5
36Ar/ 40Ar
0.0025
0.0020
0.0015
0.0010
0.0005
0.0000
0
1
2
3
4
5
6
7
39Ar/ 40Ar

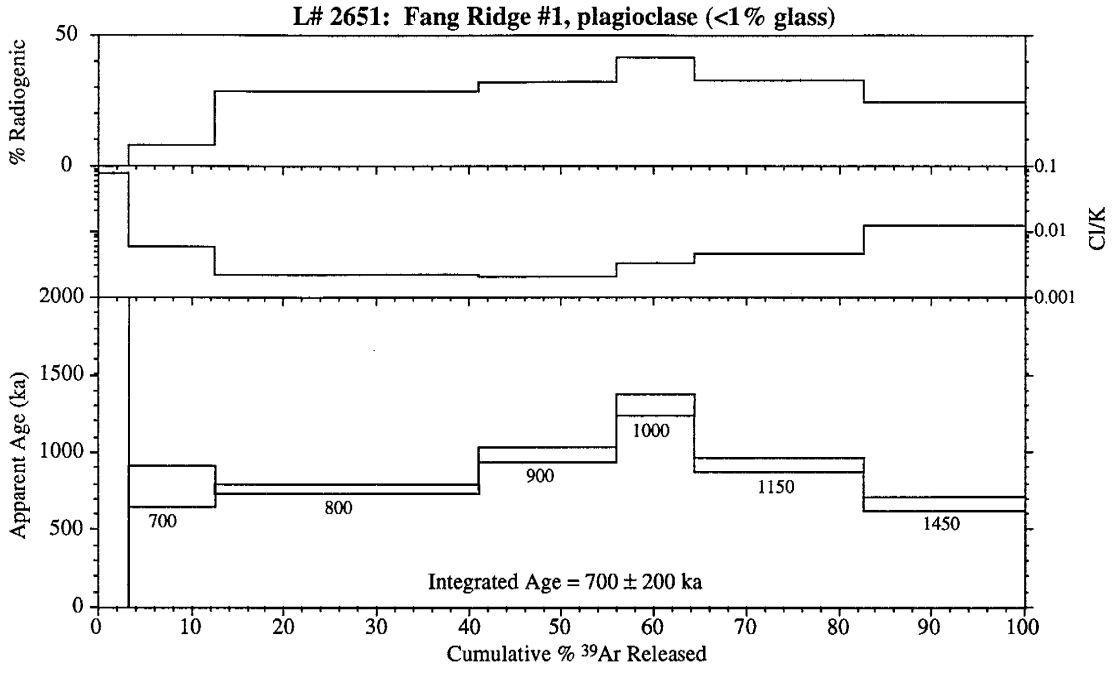
L# 2651: Fang Ridge #1, plagioclase (<1% glass)
% Radiogenic
50
0
0.1
0.01
0.001
Cl/K
2000
1500
1000
500
0
Apparent Age (ka)
700
800
900
1000
1150
1450
Integrated Age = 700 ± 200 ka
0
10
20
30
40
50
60
70
80
90
100
Cumulative % 39Ar Released

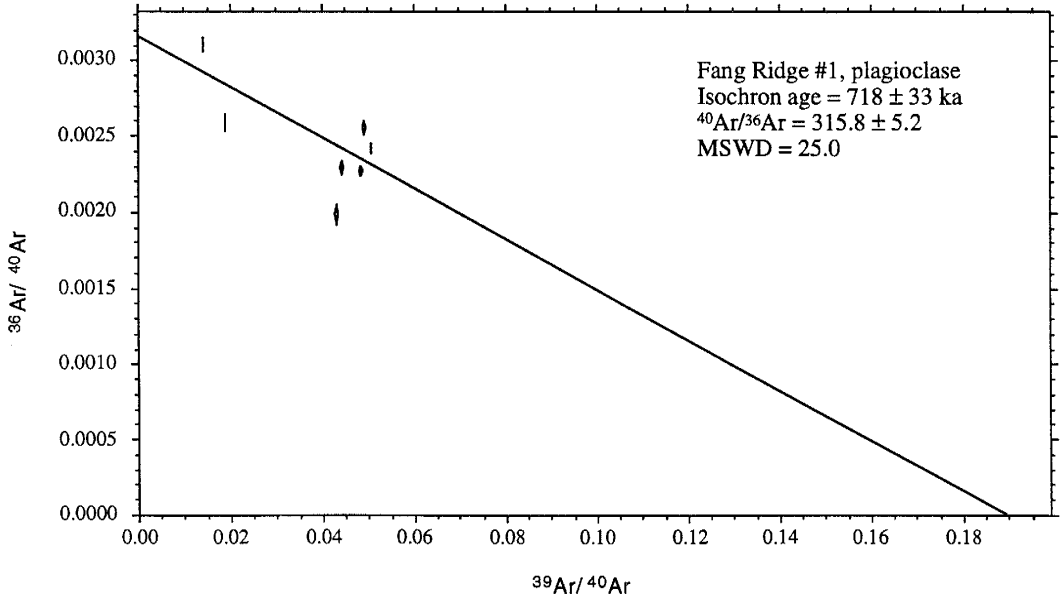
Fang Ridge #1, plagioclase
Isochron age = 718 ± 33 ka
40Ar/36Ar = 315.8 ± 5.2
MSWD = 25.0
36Ar/ 40Ar
0.0030
0.0025
0.0020
0.0015
0.0010
0.0005
0.0000
0.00
0.02
0.04
0.06
0.08
0.10
0.12
0.14
0.16
0.18
39Ar/ 40Ar

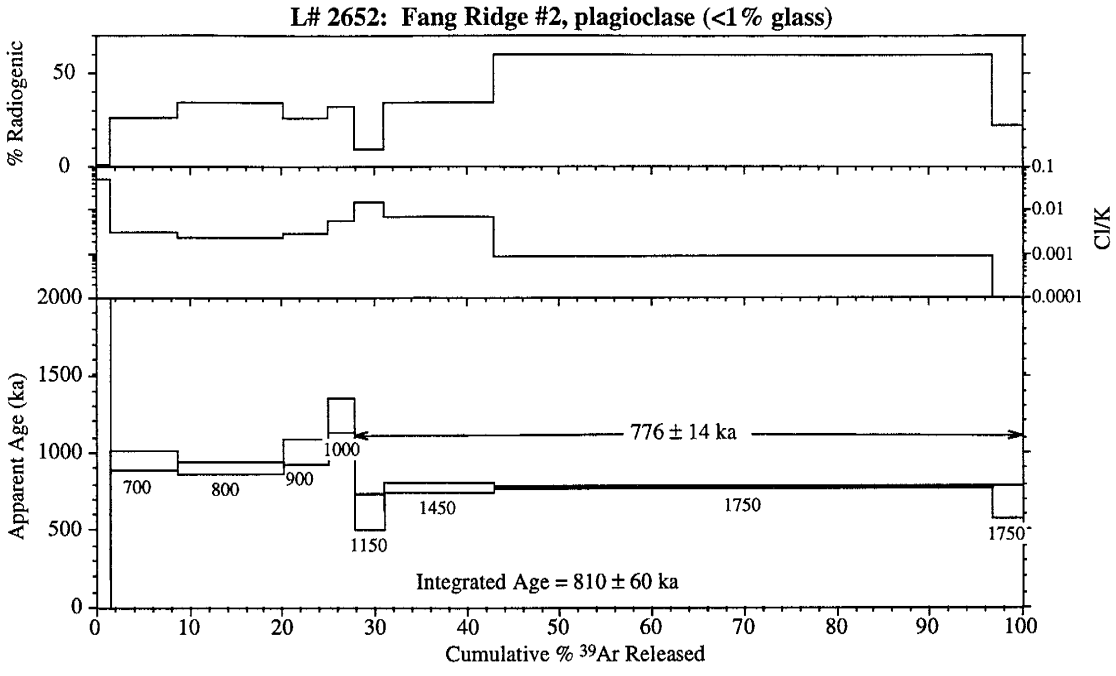
L# 2652: Fang Ridge #2, plagioclase (<1% glass)
% Radiogenic
50
0
0.1
0.01
0.001
0.0001
Cl/K
2000
1500
1000
500
0
Apparent Age (ka)
776 ± 14 ka
700
800
900
1000
1150
1450
1750
1750
Integrated Age = 810 ± 60 ka
0
10
20
30
40
50
60
70
80
90
100
Cumulative % 39Ar Released

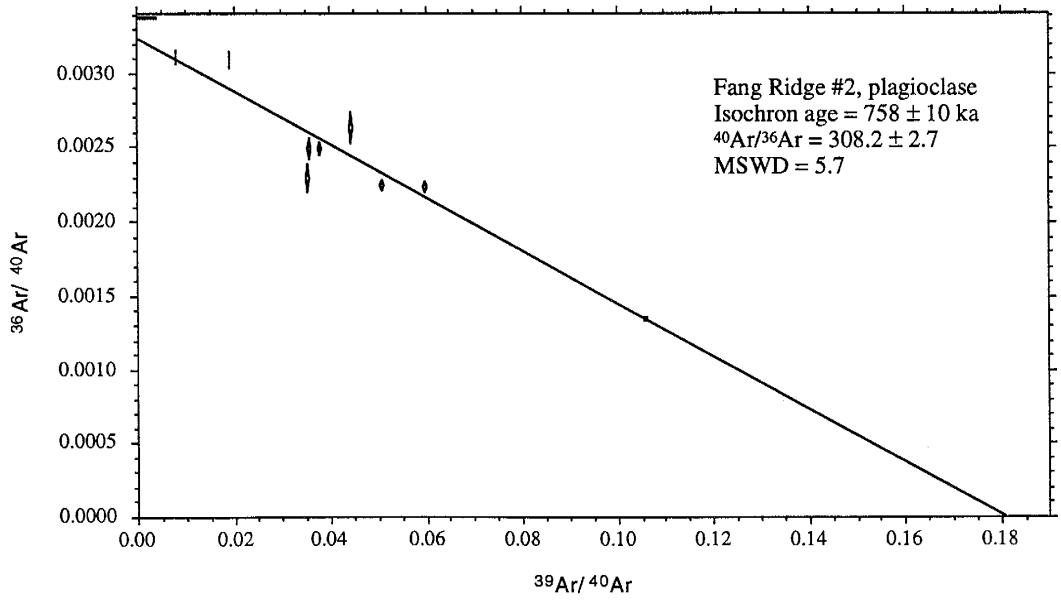
Fang Ridge #2, plagioclase
Isochron age = 758 ± 10 ka
40Ar/36Ar = 308.2 ± 2.7
MSWD = 5.7
0.0030
0.0025
0.0020
0.0015
0.0010
0.0005
0.0000
36Ar/ 40Ar
0.00
0.02
0.04
0.06
0.08
0.10
0.12
0.14
0.16
0.18
39Ar/ 40Ar

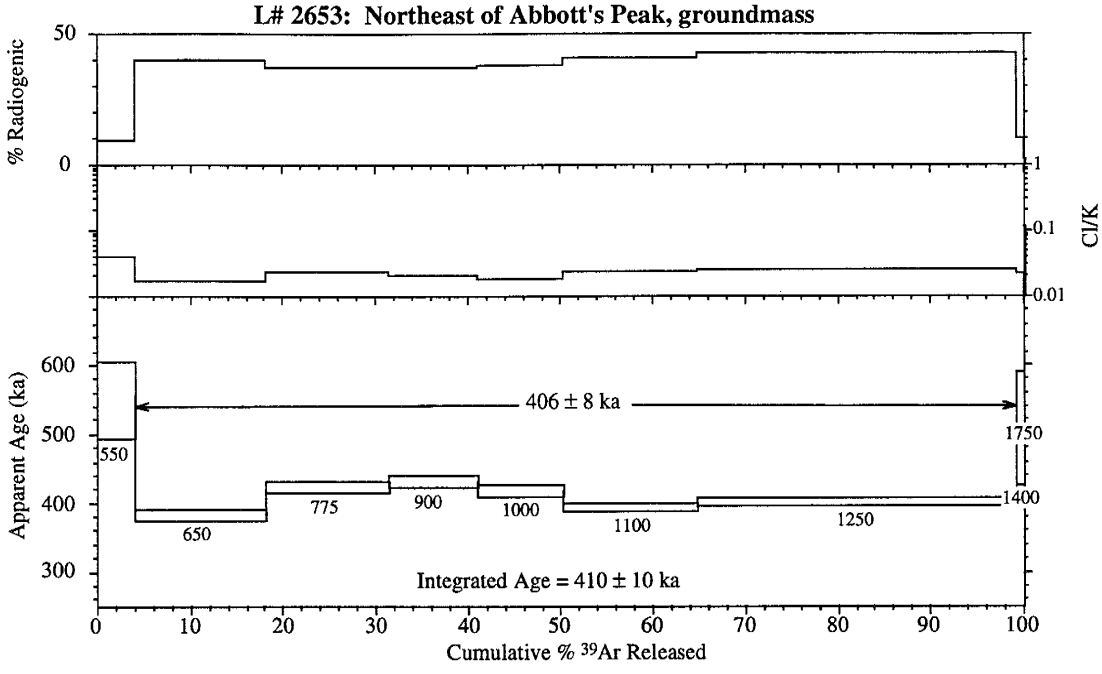
L# 2653: Northeast of Abbott's Peak, groundmass
% Radiogenic
50
0
Cl/K
1
0.1
0.01
Apparent Age (ka)
600
500
400
300
406 ± 8 ka
550
650
775
900
1000
1100
1250
1400
1750
Integrated Age = 410 ± 10 ka
0
10
20
30
40
50
60
70
80
90
100
Cumulative % 39Ar Released

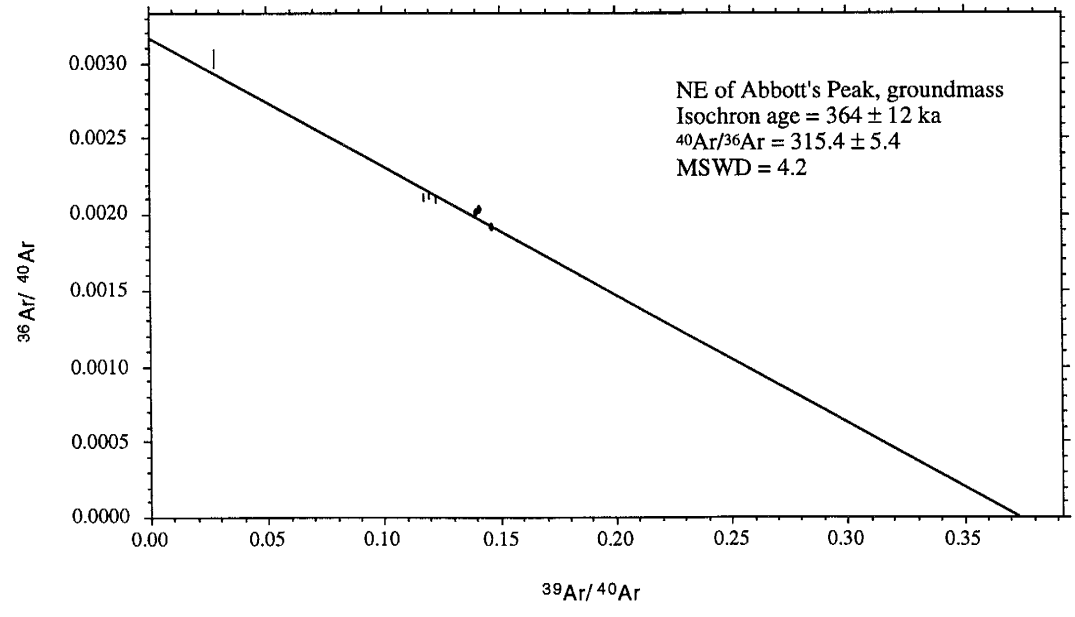
NE of Abbott's Peak, groundmass
Isochron age = 364 ± 12 ka
40Ar/36Ar = 315.4 ± 5.4
MSWD = 4.2
36Ar/ 40Ar
0.0030
0.0025
0.0020
0.0015
0.0010
0.0005
0.0000
0.00
0.05
0.10
0.15
0.20
0.25
0.30
0.35
39Ar/ 40Ar

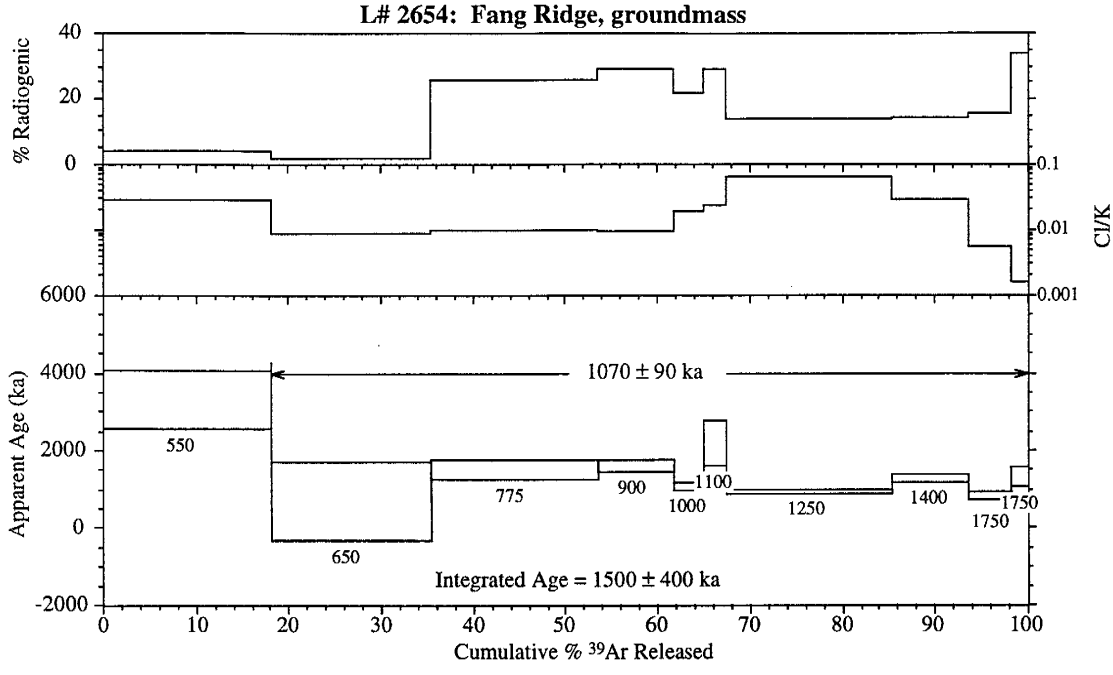
L# 2654: Fang Ridge, groundmass
% Radiogenic
40
20
0
0.1
0.01
0.001
Cl/K
6000
4000
2000
0
-2000
Apparent Age (ka)
1070 ± 90 ka
550
650
775
900
1100
1000
1250
1400
1750
1750
Integrated Age = 1500 ± 400 ka
0
10
20
30
40
50
60
70
80
90
100
Cumulative % 39Ar Released

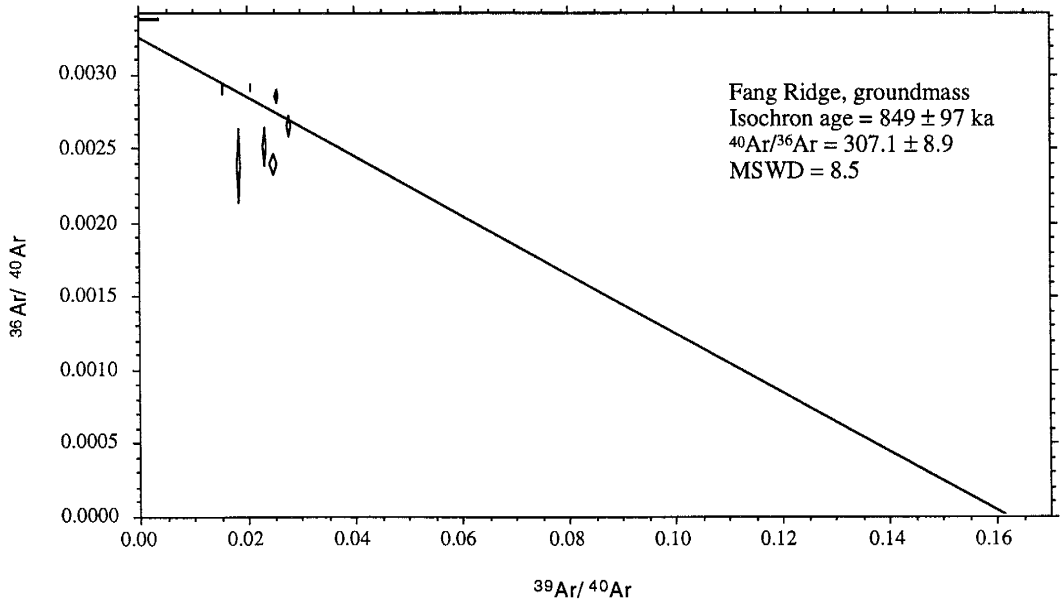
Fang Ridge, groundmass
Isochron age = 849 ± 97 ka
40Ar/36Ar = 307.1 ± 8.9
MSWD = 8.5
36Ar/ 40Ar
0.0030
0.0025
0.0020
0.0015
0.0010
0.0005
0.0000
0.00
0.02
0.04
0.06
0.08
0.10
0.12
0.14
0.16
39Ar/ 40Ar

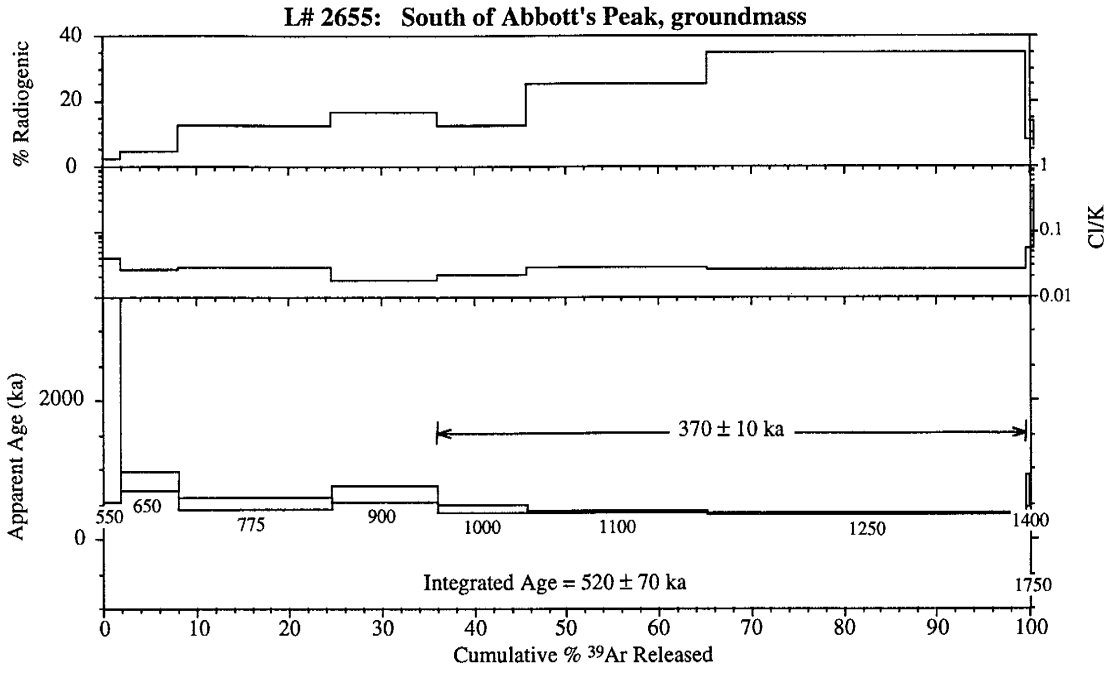
L# 2655: South of Abbott's Peak, groundmass
% Radiogenic
40
20
0
Cl/K
1
0.1
0.01
Apparent Age (ka)
2000
0
370 ± 10 ka
550
650
775
900
1000
1100
1250
1400
1750
Integrated Age = 520 ± 70 ka
0
10
20
30
40
50
60
70
80
90
100
Cumulative % 39Ar Released

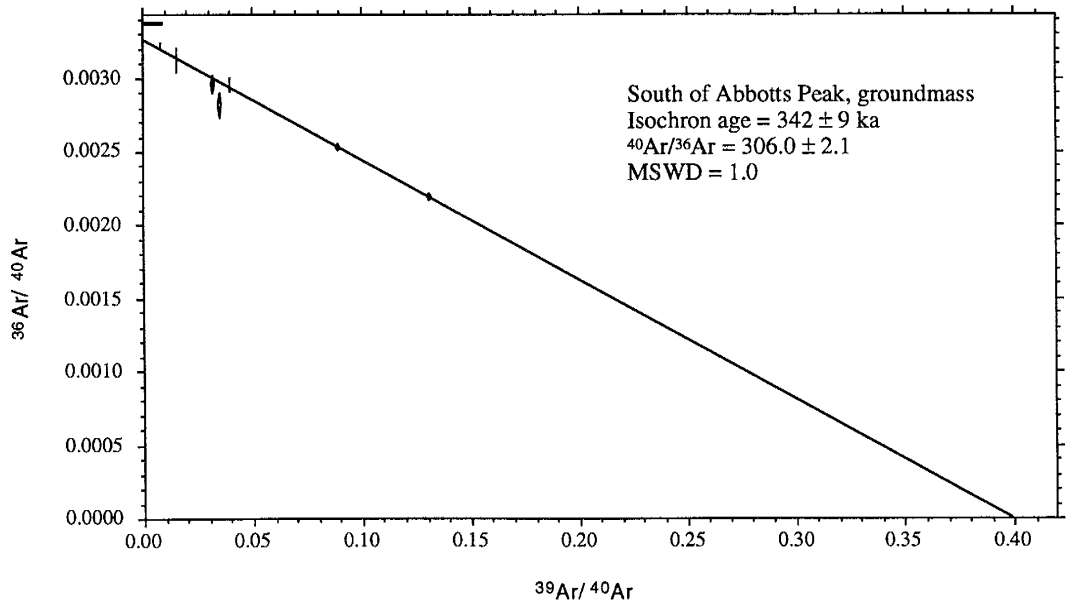
South of Abbotts Peak, groundmass
Isochron age = 342 ± 9 ka
40Ar/36Ar = 306.0 ± 2.1
MSWD = 1.0
36Ar/ 40Ar
0.0030
0.0025
0.0020
0.0015
0.0010
0.0005
0.0000
0.00
0.05
0.10
0.15
0.20
0.25
0.30
0.35
0.40
39Ar/ 40Ar

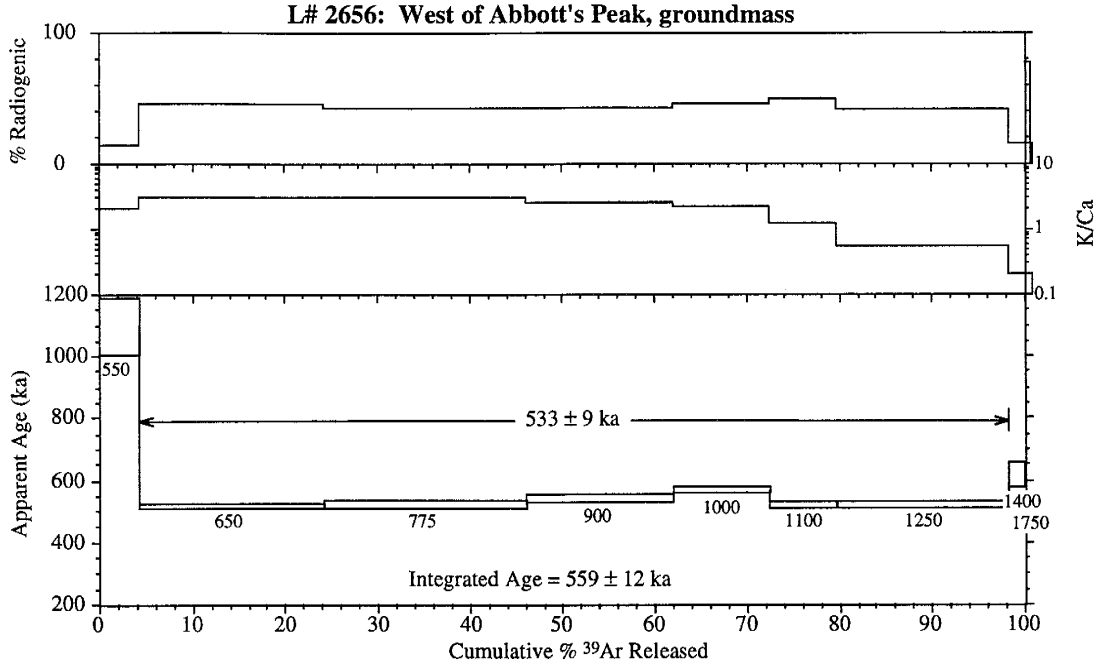
L# 2656: West of Abbott's Peak, groundmass
% Radiogenic
100
0
10
1
0.1
K/Ca
1200
1000
800
600
400
200
Apparent Age (ka)
550
533 ± 9 ka
650
775
900
1000
1100
1250
1400
1750
Integrated Age = 559 ± 12 ka
0
10
20
30
40
50
60
70
80
90
100
Cumulative % 39Ar Released

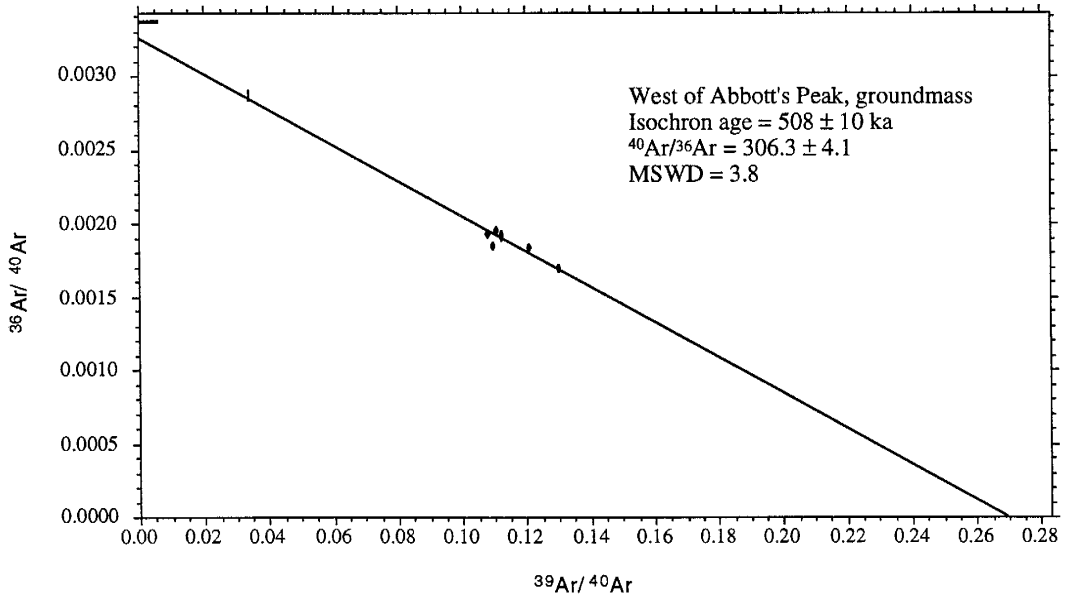
West of Abbott's Peak, groundmass
Isochron age = 508 ± 10 ka
40Ar/36Ar = 306.3 ± 4.1
MSWD = 3.8
36Ar/ 40Ar
0.0030
0.0025
0.0020
0.0015
0.0010
0.0005
0.0000
0.00
0.02
0.04
0.06
0.08
0.10
0.12
0.14
0.16
0.18
0.20
0.22
0.24
0.26
0.28
39Ar/ 40Ar

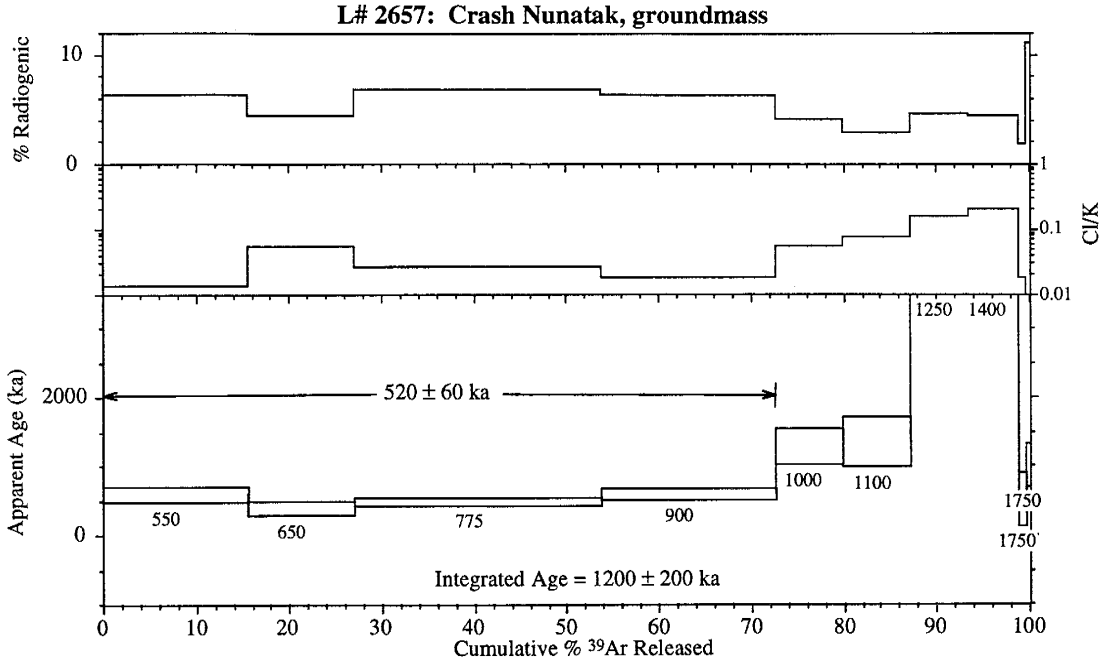
L# 2657: Crash Nunatak, groundmass
% Radiogenic
10
0
Cl/K
1
0.1
0.01
Apparent Age (ka)
2000
0
520 ± 60 ka
550
650
775
900
1000
1100
1250
1400
1750
1750
Integrated Age = 1200 ± 200 ka
0
10
20
30
40
50
60
70
80
90
100
Cumulative % 39Ar Released

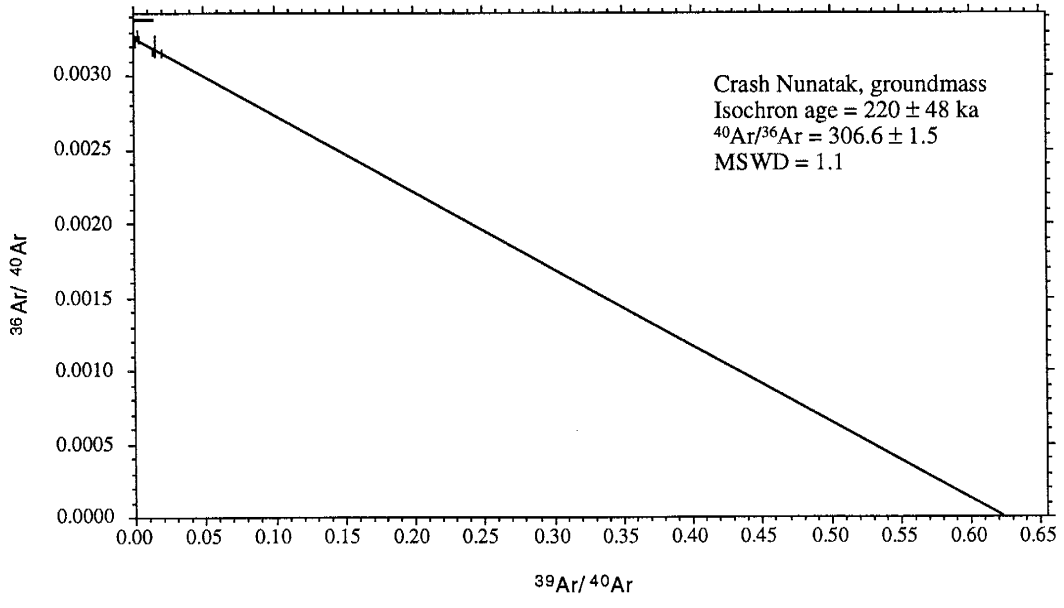
Crash Nunatak, groundmass
Isochron age = 220 ± 48 ka
40Ar/36Ar = 306.6 ± 1.5
MSWD = 1.1
36Ar/ 40Ar
0.0030
0.0025
0.0020
0.0015
0.0010
0.0005
0.0000
0.00
0.05
0.10
0.15
0.20
0.25
0.30
0.35
0.40
0.45
0.50
0.55
0.60
0.65
39Ar/40Ar

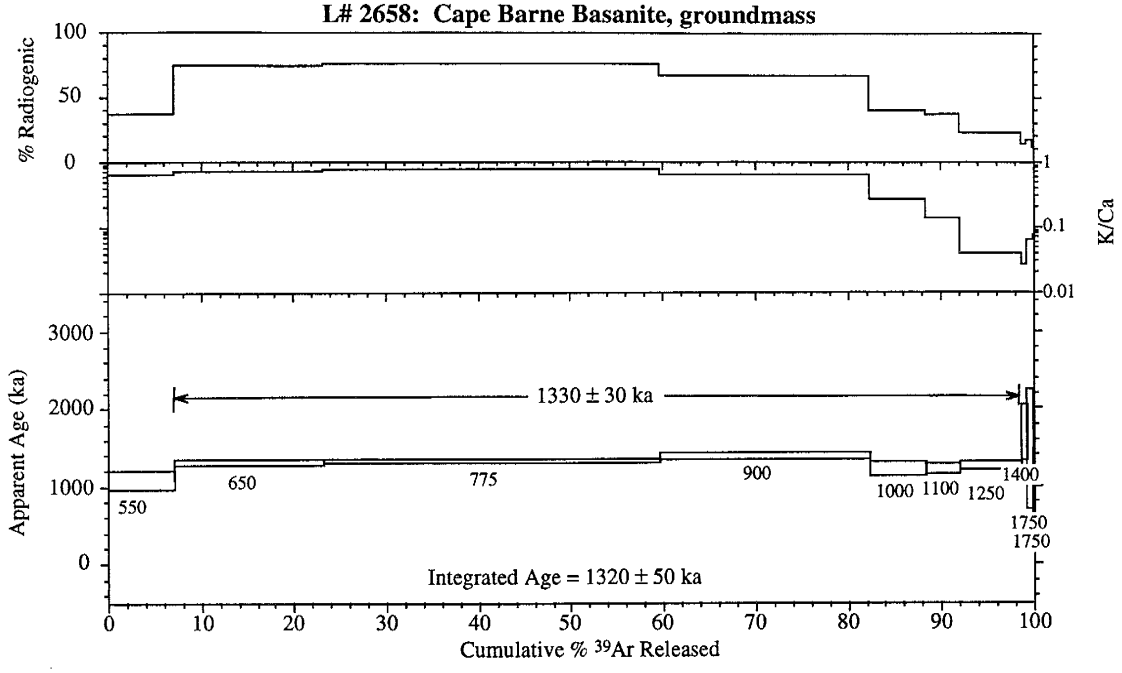
L# 2658: Cape Barne Basanite, groundmass
% Radiogenic
100
50
0
K/Ca
1
0.1
0.01
Apparent Age (ka)
3000
2000
1000
0
1330 ± 30 ka
550
650
775
900
1000
1100
1250
1400
1750
1750
Integrated Age = 1320 ± 50 ka
0
10
20
30
40
50
60
70
80
90
100
Cumulative % 39Ar Released

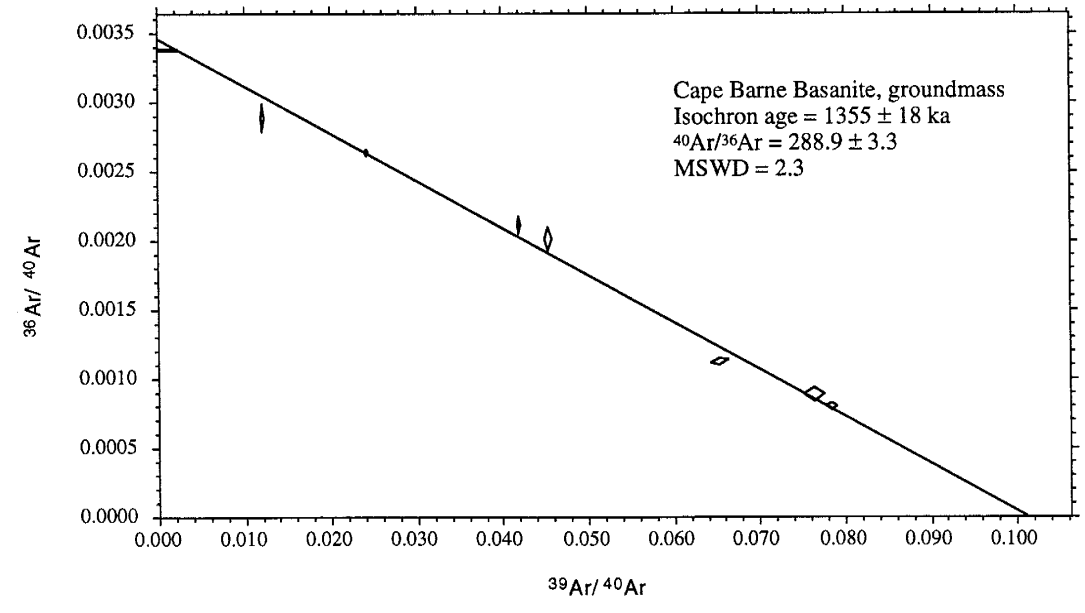
Cape Barne Basanite, groundmass
Isochron age = 1355 ± 18 ka
40Ar/36Ar = 288.9 ± 3.3
MSWD = 2.3
36Ar/ 40Ar
0.0035
0.0030
0.0025
0.0020
0.0015
0.0010
0.0005
0.0000
0.000
0.010
0.020
0.030
0.040
0.050
0.060
0.070
0.080
0.090
0.100
39Ar/ 40Ar

Appendix C-3. Paleomagnetic results on lavas from Mt. Erebus.

Sample	Sample #	Polarity	Inclination	Declination	no.	k	α_{95}	$^{40}Ar/^{39}Ar$ apparent age
Crash Nunatak	E93008	**N**	-80.2	203.5	7	1165.5	1.62	520 ± 60
Fang Ridge tephriphonolite	E93005	**N**	-72.4	350.8	8	105.7	5.90	718 ± 33
Fang Ridge tephriphonolite	E93007	**N**	-69.3	265.9	8	2130.6	1.20	758 ± 10
Fang Ridge tephrite	E93012	**R**	84.2	290.1	6	452.8	3.15	1070 ± 90

k = precision parameter
α_{95} = cone of confidence of 95% probability

Appendix C-4. Names, identification numbers and respective locations for all Mt. Erebus $^{40}Ar/^{39}Ar$ samples in this study.

Sample Name	Sample #	Latitude	Longitude	Source
Lower Hut Flow	E87034	77° 31.0' S	167° 06' E	Map
Three Sister's Cones	E80020	77° 34' S	166° 58' E	Gazetteer
Hooper's Shoulder	E81001	77° 32' S	166° 53' E	Gazetteer
Cape Evans	E83400	77° 38.5' S	166° 25.1' E	Map
Nausea Knob	E87035	77° 31.0' S	167° 06' E	Map
William's Cliff	E93020	77° 34.8' S	166° 48.1' E	GPS
Cape Royds	E83448	77° 33.4' S	166° 10.0' E	Map
Northeast Flow	E86026	77° 31.0' S	167° 06' E	Map
Caldera Rim #1	E93013	77° 30.8' S	167° 06' E	Map
Cape Barne	E83433	77° 34.9' S	166° 15.3' E	Map
SE of Hooper's Shoulder	E93021	77° 32.4' S	166° 51.3' E	GPS
NW of Hooper's Shoulder	E93011	77° 31.0' S	166° 48.0' E	GPS
Bomb Peak	E82405	77° 30.8' S	167° 28.6' E	Gazetteer
Aurora Cliffs	E83454	77° 39.0' S	167° 28.0' E	Map
Btwn Williams Cliff and Turks Head	E93019	77° 36.7' S	166° 46.1' E	GPS
Turks Head tephriphonolite	AW82015	77° 40' S	166° 46' E	Gazetteer
South of Abbott Peak	E93024	77° 28.6' S	166° 53.7' E	GPS
NE of Abbott's Peak	E93023	77° 25.8' S	167° 01.4' E	GPS
Tryggve Point dike	E77012	77° 39' S	166° 42' E	Gazetteer
Turks Head tephrite	AW82038	77° 40' S	166° 46' E	Gazetteer
SW of Abbotts Peak	E83453	77° 28.3' S	166° 49.5' E	Map
West of Abbotts Peak	E93010	77° 27.1' S	166° 48.8' E	GPS
Crash Nunatak	E93008	77° 26.7' S	167 ° 33.6' E	GPS
Inaccessible Island	E83407	77° 39' S	166° 21'E	Gazetteer
Abbott's Peak	E81002	77° 26' S	167° 00' E	Gazetteer
Fang Ridge #1	E93005	77° 29' S	167° 12' E	Gazetteer
Fang Ridge #2	E93007	77° 29' S	167° 12' E	Gazetteer
Fang Ridge #3	E93012	77° 29' S	167° 12' E	Gazetteer
Cape Barne	E83432/E93032	77° 34.9' S	166° 15.3' E	Map

Map: USGS 1:250,000 Map of Ross Island
Gazetter: Gazetter of the Antarctic (1989); NSF
GPS: Navy VXE-6 helicopters